THE UNIVERSITY OF MANITOBA

ENVIRONMENTAL ASSESSMENT OF THE AIR POLLUTANT EMISSIONS FROM THE MANITOBA HYDRO THERMAL GENERATING STATION AT BRANDON, MANITOBA

by

ANDRIAN DOUGLAS HOFFER

A THESIS

SUBMITTED TO THE FACULTY OF GRADUATE STUDIES

IN PARTIAL FULFILMENT OF THE REQUIREMENTS FOR THE DEGREE OF

MASTER OF SCIENCE

DEPARTMENT OF CIVIL ENGINEERING

WINNIPEG, MANITOBA

December, 1975

"ENVIRONMENTAL ASSESSMENT OF THE AIR POLLUTANT EMISSIONS FROM THE MANITOBA HYDRO THERMAL GENERATING STATION AT BRANDON, MANITOBA"

by

Andrian Douglas Hoffer

A dissertation submitted to the Faculty of Graduate Studies of the University of Manitoba in partial fulfillment of the requirements of the degree of

MASTER OF SCIENCE

UNIVERSITY OF MANITOBA

DEPARTMENT OF CIVIL ENGINEERING

This paper presents an evaluation of the air pollutant emissions from the Brandon Generating Station. Emission rates were estimated using a materials balance of the combustion products versus the fly ash retained in the boilers and the dust collectors. Dispersion analyses were performed to determine the corresponding ground-level pollutant concentrations for a variety of meteorological conditions.

The major air pollution problem was found to be high concentrations of suspended particulate matter in excess of the Manitoba and National Air Quality Maximum Acceptable levels. This problem exists under virtually all conditions at full load. A reduction of 90 to 95% in the particulate emissions is required to effect compliance with the air quality standards.

ENVIRONMENTAL ASSESSMENT OF THE AIR POLLUTANT EMISSIONS FROM THE MANITOBA HYDRO THERMAL GENERATING STATION AT BRANDON, MANITOBA

by Andrian Douglas Hoffer

ADVISOR: Professor A.B. Sparling

December, 1975

Winnipeg, Manitoba

TABLE OF CONTENTS

LIST OF TABLES

LIST OF FIGURES

PREFACE

Air pollution technology is a relatively new field, with most of the major advances in analysis and control having been made during the past decade. Hence, many people in the environmental engineering field who are not directly concerned with air pollution have only limited knowledge in this area. An extensive introduction has therefore been included with this paper to provide some general background information on this topic. This will allow those less knowledgeable in the air pollution field to better understand the work presented here.

The opinions, conclusions, and recommendations expressed in this report are those of the author only and in no way reflect the policies or judgements of Environment Canada.

ENVIRONMENTAL ASSESSMENT OF THE AIR POLLUTANT EMISSIONS FROM THE MANITOBA HYDRO THERMAL GENERATING STATION AT BRANDON, MANITOBA

1. INTRODUCTION

The practical assessment of an industrial air pollution problem is usually carried out in four major stages. These are: 1) source evaluation, 2) receptor evaluation, 3) dispersion analyses, and 4) abatement and control recommendations. These steps are briefly discussed below in order to give the reader an overview of the basic approach used in the Brandon evaluation. A more in-depth discussion of those fundamentals of each area applicable to the Brandon study then follows.

1.1 GENERAL APPROACH TO AIR POLLUTION ASSESSMENTS

1.1.1 Source Evaluation

The first step in evaluating an air pollution problem is an accurate assessment of the source or sources involved. This should include specification of the source parameters such as type and nature of pollutants, pollutant output rates, and the heights, temperatures, speeds, and volumes of the gas emissions.

1.1.2 Receptor Evaluation

The second step of the assessment is a receptor evaluation, wherein are specified those circumstances under which the pollutants could cause a problem. The receptor evaluation should also determine whether the effects of the air pollutants are likely to be dependent upon other variables, such as temperature, humidity, or time of day.

1.1.3 Dispersion Analyses

The third step involves the compilation and use of pertinent meteorological data in conjunction with the source information to arrive at a reasonable estimate of the dispersion patterns of the airborne effluents. The most suitable techniques now available for the quantitative approximation of air pollution problems emphasize ordinary, continuous stack emissions over relatively uncomplicated terrain. It must therefore be emphasized that dispersion calculations based on these techniques can only provide a first approximation in the analysis of a given situation.

The case of the worst conceivable conditions is usually considered first to determine whether any problem can possibly exist. A simple first approximation of this case is the calculation of the downwind pollutant concentration assuming the source to be a ground level under very stable atmospheric conditions (i.e. in a deep surface temperature inversion). If this first calculation does not indicate a problem situation, it can usually be assumed that no air pollution problem is ever likely to develop from the given source. If, however, the first estimate indicates potential trouble, then simulation of the stack effect is necessary. This is accomplished by calculating several cases

which include a stack height term, to determine whether the maximum ground level concentrations are within an acceptable range. These estimates may be based first on the actual stack height alone, without any allowance for the buoyancy and momentum of the plume. Should these calculations yield results that are acceptable by a wide margin, and if there is no evidence that the source is subject to unusual terrain or meteorological conditions, no problem should exist. This is particularly true where it is certain that the plume will remain well above sensitive receptors under inversion conditions.

Failure of the last step to produce acceptably low concentration estimates necessitates the incorporation of more detailed computations into the study. This involves the use of terms to account for the buoyancy and momentum of the actual stack plume to obtain effective stack heights, with subsequently lower estimates of the maximum ground level concentrations. Where such refined estimates are required, it is usually necessary to calculate fairly complete ground level concentration patterns, in order to define values for sensitive receptor areas and to determine the probable frequency of occurrence of adverse air quality conditions. A first approximation can be based on general meteorological data for the given area and consideration of peculiarities of the locality. The probable effects of terrain and nearby elevated structures should also be taken into account when the assessment has reached this degree of sophistication.

Wind tunnel and/or tracer studies simulating the anticipated effluent behaviour are normally considered for air pollution studies only when

the desired information cannot be determined by the previously outlined methods. Such sophisticated assessments are generally more expensive than calculated estimates and meteorological studies by about one order of magnitude.

1.1.4 Abatement and Control Recommendations

The final step in the analysis of an industrial air pollution problem concerns the recommendation of preventive or corrective measures which will ensure compliance of the pollutant source with regulatory air emission limits. The control of atmospheric emissions from a process may be effected by any of three general methods. These are: 1) process change, 2) fuel change, and 3) installation of control equipment.

A process change can be either a modification of the operating procedures for an existing process or the substitution of a completely different process. In some cases the least expensive control is achieved by completely abandoning the old process and replacing it with a new, less polluting process. A portion of the costs incurred in renovating an operation may be offset by any increased production and/or recovery of material.

For many operations the ideal solution to air emission problems is a change to a less polluting fuel. If, for example, a thermal power plant is emitting large quantities of sulfur dioxide and fly ash, conversion to natural gas may be cheaper than installing the necessary control equipment to reduce the pollutant emissions to acceptable levels. Fuel switching based upon meteorological or air pollution forecasts is practised in some areas as a means of reducing the air pollution load

at critical times (1). Many control agencies allow power plants to operate on residual oil during certain times of the year when pollution potential is low. Some large power utilities convert to a more expensive, but lower sulfur coal when a high air pollution potential is forecast, e.g. during stagnation conditions.

The third option is the removal of specific air contaminants from the exhaust gases by incorporating control equipment into the process stream. This method of reducing the pollutant emissions is required in a great number of situations where sufficient emission reduction cannot be obtained by a fuel or process change, necessitating the reduction of pollutant levels in the exhaust gases prior to their release to the atmosphere. The equipment for the pollutant removal system includes all hoods, ducting, fans, controls, and disposal or recovery systems that might be necessary. Maximum efficiency and economy are achieved by engineering the entire system as a unit. Many systems operate at less than maximum efficiency because a portion of the system was designed or adapted without consideration of the other portions (2).

1.1.5 Summary

Clearly, the decision to opt for one or more of the control measures previously described is based on a compromise between meeting the requirements of regulatory air emission standards and the economics of doing so. Furthermore, consideration must also be given to future changes in the governing parameters, e.g. changes in the availability of a chosen fuel or future increased restrictions on air pollutant emissions.

1.2 AIR POLLUTANT EMISSIONS FROM THERMAL GENERATING STATIONS

1.2.1 Introduction

Thermal generating stations rank third in their contribution to air pollution in the United States. These power plants emit approximately 25% of the particulates, 46% of the sulfur oxides, and 25% of the nitrogen oxides in the United States. They are relatively minor contributors of carbon monoxide and hydrocarbons (3). In Canada utilities and power generation account for only 9.7% of the particulates, 6.7% of the sulfur oxides, and 13.0% of the nitrogen oxides emitted into the atmosphere. Carbon monoxide and hydrocarbon emissions from these sources are relatively small in Canada, totaling only < 0.05% and 0.1%, respectively, of the total emissions for Canada of these contaminants (4). It can readily be seen from the above figures that power plants contribute a much smaller portion of the air pollution load in Canada than in the United States.

Power plants were recognized early to be sources of concentrated air pollutants, mainly because they are relatively few in number in comparison with other sources such as automobiles. Initially sulfur dioxide and particulate emissions were the items of primary concern, but more recently nitrogen oxide emissions have been given some consideration (2,3).

The different types of thermal power plants and their related air pollutant emissions are discussed in the section which follows. (Although the operation of nuclear power plants involves the production of heat to drive turbo-electric generators, the term "thermal power plants" as

used in this discussion refers only to those power plants which rely on the combustion of fossil fuels (coal, oil, and natural gas) for heat).

1.2.2 Sources of Electrical Power

Electrical power utilities may be classified according to the energy source used for the generation of electricity. The three major types of power utilities are thermal, hydroelectric, and nuclear, in order of decreasing generating capacity in the United States. Current and projected distributions of electrical energy sources are given in Table 1.1. The figures in Table 1.1 indicate a large forecast increase in the use of nuclear energy, favoured by the anticipated development of breeder reactors, but the absolute growth in the generating capacity of fossil fuel plants will exceed that for nuclear plants. Hydroelectric sources are very limited in their growth potential, an unfortunate situation in view of the fact that they are virtually air pollution-free

1.2.3 Types of Fossil Fuel Power Plants

Thermal generating stations may be further classified according to the type of fossil fuel or fuels utilized. The major energy sources are coal, oil, and natural gas, as shown in Table 1.2. The data given show a forecast increase in all three categories. No dramatic change is indicated in the percentage use of each fuel type with the exception of the recent shift from the use of oil to natural gas.

Practically all use of fossil fuels for electrical power generation involves the production of steam to drive turbo-electric generators.

Gas turbines are being used to a limited degree for handling peak operating loads, but they are not expected to represent a significant fraction of the total power generating capacity in the future (3). Tables 1.1 and 1.2 predict a continued increase in fossil fuel use for power generation, and hence without a corresponding reduction in combustion product emissions from thermal generating stations, the air pollution contribution of these plants will also continue to increase.

1.2.4 Thermal Power Plant Construction and Operation

1.2.4.1 Boiler Construction and Capacity

Most thermal power installations utilize relatively large furnace boilers capable of producing several hundred thousand pounds of steam per hour per unit.

A boiler consists basically of a burner, firebox, heat exchanger, and a means of creating and directing a flow of gases through the unit. All combustion equipment of this type includes these essentials. Most also include some auxiliary systems, the number and complexity of which increase with the size of the units. Larger combustion equipment often includes flame safety devices, soot blowers, air preheaters, economizers, superheaters, fuel heaters, and automatic flue gas analyzers.

The boiler units used in power plants are typically 20 to 30 feet square by 80 to 100 feet in height. A typical coal-fired unit is shown in Figure 1.1. Variations in design deal primarily with the type and location of the coal-firing equipment. Figure 1.2 shows a typical oil or natural gas fired boiler. The same unit may be used to burn fuel oil, natural gas, or both simultaneously.

TABLE 1.1

ANNUAL ELECTRIC UTILITY GENERATION IN THE UNITED STATES (3)

Power Source	1947		1965		1980	
	10^9 kw-hr	% total	10^9 kw-hr	% total	10^9 kw-hr	% total
Hydro	85	33	181	17	350	13
Nuclear	-	-	4	0.4	458-723	16-26
Fossil Fuel	173	67	872	83	1941-1676	71-61
TOTAL	258	100	1057	100	2739	100

TABLE 1.2

ANNUAL USE OF FOSSIL FUELS IN ELECTRIC

POWER GENERATION IN THE UNITED STATES (3)

Fossil Fuel	1947		1965		1980	
	10^{15} Btu	% total	10^{15} Btu	% total	10^{15} Btu	% total
Coal	2.1	70	6.0	67	11.1-13.4	74-78
Oil	0.5	17	0.6	7	0.9	6-5
Natural Gas	0.4	13	2.4	26	3.0	20-17
TOTAL	3.0	100	9.0	100	15.0-17.3	100

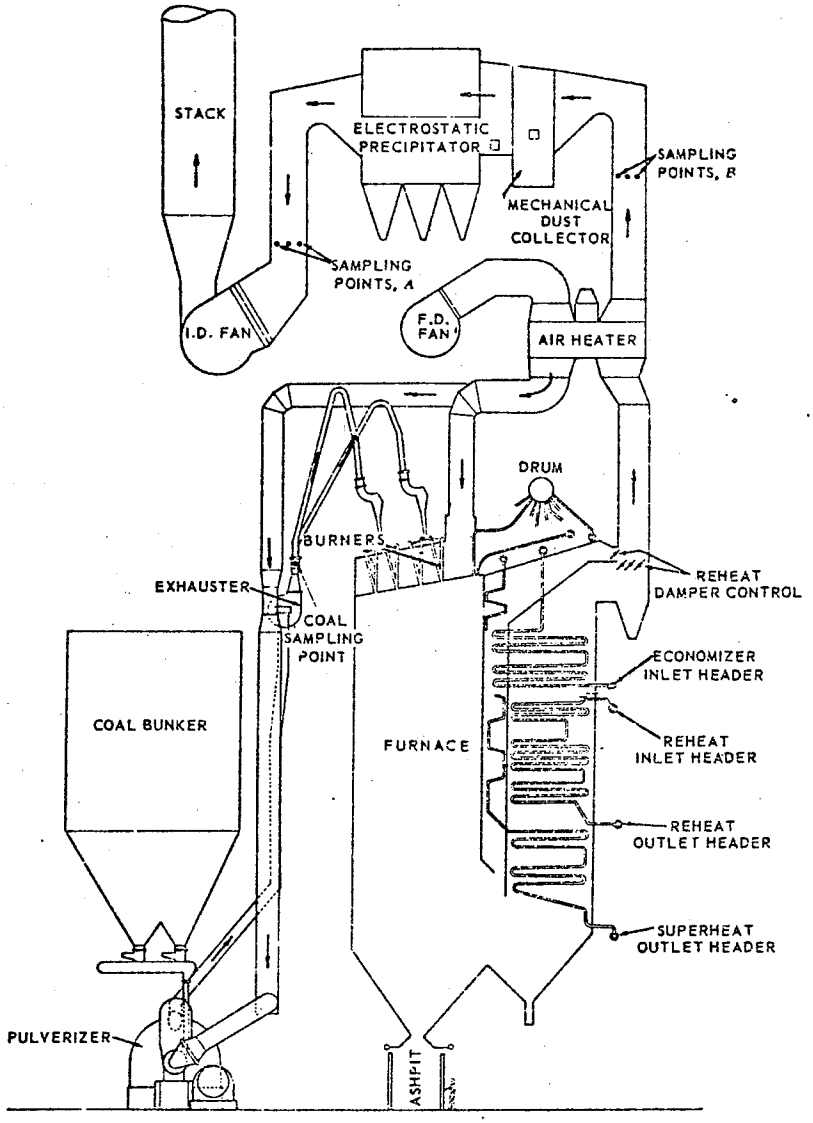

Figure 1.1. Coal fired steam generator, vertically fired (3).

Power plant furnace boilers (commonly referred to as steam generators), produce from 50,000 to 5,000,000 pounds of high-pressure, superheated steam per hour, at up to 2500 psig and 1000°F. A typical medium-sized power plant steam generator consumes 2,500,000 cubic feet of natural gas per hour or 450 barrels of fuel oil per hour, exhausting about 700,000

scfm of combustion products and producing all the steam required to drive a 310 megawatt turboelectric generator (2).

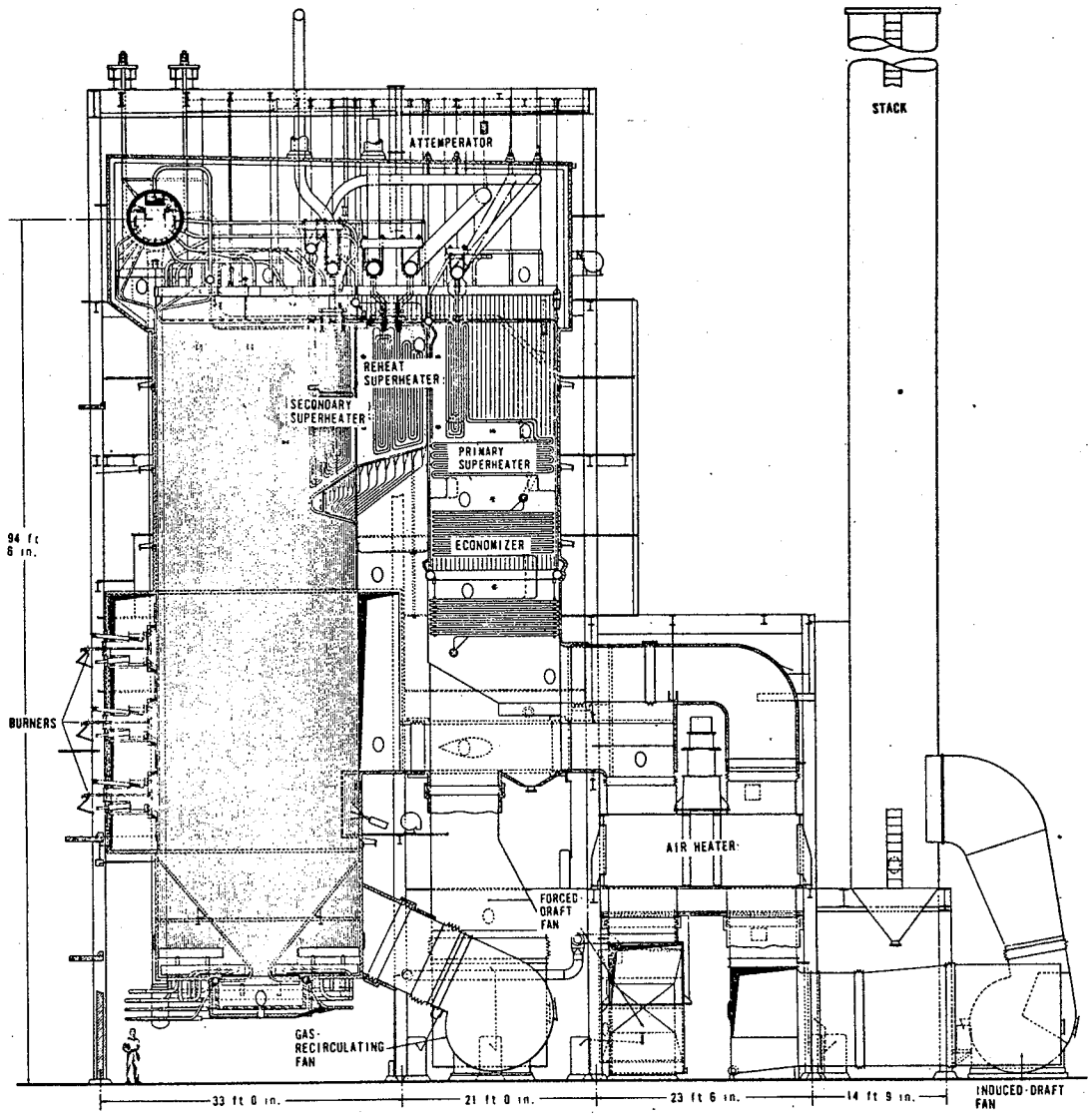

Figure 1.2. A front-fired power plant steam generator, oil or gas fired (2).

1.2.4.2 Basic Boiler Operation

The conventional steam generator unit shown in Figure 1.2 is equipped with the full line of auxiliary boiler systems, including an air preheater, oil heater, economizer, superheaters, and other equipment. Air, usually preheated, is forced into the furnace by large blowers. The pressure within the furnace is near atmospheric. As much heat as possible is extracted from the combustion products in order to maximize the thermal efficiency of the units, with stack temperatures as low as 225°F normally being maintained. Condensation and the resultant boiler tube corrosion are the major deterrents to lower power plant temperatures. When exhaust gas temperatures approach the dew point, condensation and visible stack plumes are encountered.

Steam generators operate with thermal efficiencies of about 90 percent (2), and their operating variables are more carefully controlled than those of any other type of combustion equipment. One of the most important factors is the excess air rate. Any air supplied in excess of the theoretical requirement causes a thermal loss, but the firebox oxygen concentration must nevertheless be high enough to provide near perfect combustion. Power plant operators hold excess air rates during fuel oil firing as low as feasible by providing strong mixing conditions and optimum fuel oil atomization at the burner. During gas firing, excess air rates are about 10% above theoretical requirements. When fuel oil is burned, the excess air is usually held below 15%. Attempts have been made to operate with excess air at rates as low as 1% (approximately 0.2% oxygen) with oil firing; the benefits from this practice are reduced corrosion, less air contaminants, and increased thermal efficiencies (2).

1.2.4.3 Soot Blowing

The burning of fuels with measurable ash content is accompanied by the deposit of some solids, including both carbon and inorganic ash, onto the heat transfer surfaces in the combustion equipment. In order to maintain adequate heat transfer rates, these deposits must be removed periodically. Common practice is to remove these deposits with jets of air or steam while the combustion equipment is in operation. The boiler of a large power plant is normally equipped with from 8 to 15 soot blowers which perform this function. The removed particulates are entrained in the combustion gases, and thus the particulate concentrations in the exhaust stream are considerably higher during soot blowing periods than during normal operation.

Whenever residual fuel oils or solid fuels are burned in large steam generators, tube cleaning is usually carried out at least once during every 24 hours of operation. When clean natural gas fuels are burned, the same boiler can be operated indefinitely without soot blowing, except possibly for the air preheater. In fact, the burning of natural gas gradually removes materials deposited during oil or coal firing. Many highly integrated power plants are equipped with automatic soot blowers which operate at 2- to 4-hour intervals. Many older installations use manual soot blowing equipment which makes the operation time-consuming, with comparatively longer intervals between blowings (usually one blowing per 24 hours of plant operation). In addition, the use of manual soot blowing equipment results in the emission of larger and more concentrated particulates during blowing than are encountered with automated systems (2).

1.2.5 Types of Pollutants

The air pollution contribution of thermal power plants is comprised mainly of particulates, sulfur oxides, and nitrogen oxides. As noted earlier, electric power plants in the United States are responsible for about half of the sulfur dioxide, one fourth of the nitrogen oxides, and one fourth of the particulate air contaminants discharged into the atmosphere annually (3). Carbon monoxide, hydrocarbons, and aldehydes are also emitted by thermal power plants, but the quantities of these pollutants are relatively low in comparison with those mentioned above.

Combustion-generated air contaminants fall into three categories: 1) carbon and the unburned and partially oxidized organic materials resulting from incomplete combustion, 2) sulfur oxides and ash directly attributable to fuel composition, and 3) nitrogen oxides formed at firebox temperatures from oxygen and nitrogen in the air. Products from incomplete combustion can usually be minimized through proper operation of modern burner equipment. Sulfur and ash emissions are governed by the fuel makeup. Nitrogen oxide concentrations are mainly functions of firebox design and operating temperatures.

1.2.5.1 Fly Ash

Fly ash is comprised of the incombustible portions of fuels which are too small to settle out in the combustion chamber of a furnace and escape suspended in the high-velocity exhaust stream. Fly ash is usually nonhomogeneous and is normally made up of a large number of widely occurring inorganic compounds found in the mineral matter of the earth's crust. In suspension burning, as occurs in furnaces fired with pulverized coal, the

high temperature often fuses the ash into rough, solid or hollow spheres called cenospheres. Fly ash from the burning of fossil fuels will often contain unburned carbon if the combustion is incomplete.

The range of chemical characteristics typical of fly ash from various power plants using pulverized coal is shown in Table 1.3. For a given thermal plant burning a relatively constant grade of coal from one producing area, the range of chemical compositions of the fly ash will likely be much narrower than that shown in Table 1.3. Fly ash has a mass-median diameter of 15μ, with 30%-40% being less than 10μ in diameter (5).

TABLE 1.3

TYPICAL RANGES OF CHEMICAL COMPOSITION OF FLY ASH FROM PULVERIZED COAL-FIRED PLANTS (5)

Constituent	Range % by wt.
Silica (SiO_2)	34-8
Alumina (Al_2O_3)	17-31
Iron oxide (Fe_2O_3)	6-26
Calcium oxide (CaO)	1-10
Magnesium oxide (MgO)	0.5-2
Sulfur trioxide (SO_3)	0.2-4
Loss on ignition (carbon)	1.5-20

The fly ash collected at large, efficient power plant boilers during oil burning usually contains less than 10% carbon and other combustibles

(2). Where oxidizable particulate concentrations are excessive, the problem can usually be traced to improper use of burner equipment, or an improper combination of fuel and combustion equipment.

The actual quantity of inorganic solid particulates in a power plant exhaust stream is entirely dependent upon the characteristics of the fuel being burned. Natural gas and other clean gaseous hydrocarbons contain no measurable inorganic ash; the only ash present in the exhaust gases from the combustion of such fuels is the small amount attributable to the dust usually present to some degree in the air used for combustion. Low-sulfur residual fuel oils contain very small amounts of ash, ranging from 0.007 to 0.20 percent by weight. Residual oils, however, may contain up to 0.1 percent (by weight) ash-forming materials, mostly in the form of long-chain organo-metallic compounds. The strong oxidation conditions present in most fireboxes convert these materials to metallic oxides, sulfates, and chlorides which show up in exhaust gases as finely divided particulates (2). Even so, the combined ash and unburned particulates in exhaust gases from gaseous and liquid fuel combustion are not likely to exceed air emission standards. For example, the efficient burning of a common heavey residual oil of 0.1% ash results in a stack gas particulate concentration of only 0.030 grains per scf (7 $\mu g/m^3$) at 12% carbon dioxide, as compared to the limiting value of 0.3 grains per scf (70 $\mu g/m^3$) specified by Rule 53b of the Los Angeles County Air Pollution Control District (2), and Chapter 130 of the Clean Air Act of Canada(6).

Fly ash is produced in much greater quantities in coal-fired power plants than in oil or gas-fired plants. This is due to the relatively high ash content of solid fuels. The typical ash content (% by weight)

of the solid fuels used in power plants ranges from 5% for lignite and subbituminous coals to 15% for coke. Anthracite coal has a typical ash content of 10% (5). In many cases the use of solid fuels necessitates the provision of fly ash collectors to keep the final solids emissions within the limits of local ordinances. Pulverized coal-fired furnaces, for example, emit 50% to 80% of the ash fired in the coal in the form of fine fly ash (5); hence, all modern power plants of this type are equipped with high-efficiency dust collectors.

1.2.5.2 Smoke

Smoke comprises the submicron portion of the particulate emissions from a combustion source. It is an aerosol which usually contains comparatively little particulate matter by weight, but by virtue of the light-scattering properties of materials in the 0.3 to 0.5 μ range, it obscures vision and may even appear to be an impenetrable mass. This opacity makes dense smoke plumes undesirable in populated areas.

Smoke is produced when hydrocarbon fuels are burned in an oxygen-deficient environment, resulting in the occurrence of carbon particles in the combustion products. Poor fuel atmoization, inadequate mixing of fuel and air, or a marked oxygen shortage all promote increased carbon concentrations in boiler exhaust gases, imparting to them a visible blackness. Black smoke is usually associated with the improper burning of solid fuels and viscous, heavy-crack residual oils, although it is not impossible to produce black smoke by burning gaseous fuels. Heavy, carbonaceous accumulations in exhaust stacks, referred to as soot, are attributable to the same cause as black smoke, i.e. poor combustion.

White smoke, which includes visible emissions ranging from grey through brown to white, can also be formed through the combustion of fossil fuels, especially liquid types. White smoke (non-black smoke) is attributable to finely divided particulates, usually liquid, in the gas stream. These pollutants are most often formed by the vaporization of hydrocarbons in the firebox, followed by condensation of droplets at 300° to 500°F stack temperatures. The occurrence of white smoke is often caused by excessive combustion air (cold fire) or loss of flame (gassing). Visible contaminants can also exist with optimum combustion and a minimum concentration of oxidizable materials, but this situation is normally limited to large power plant boilers where there is measurable sulfur trioxide in the exhaust stream.

Smoke and fly ash together comprise a source of large particle emissions from power plants. During boiler operation, as discussed earlier, fine particles of smoke and fly ash accumulate on boiler heating surfaces, and subsequently flake off as agglomerates. These deposits retard heat transfer to such an extent that within a few hours of operation they must be removed by sootblowing. Most of the agglomerates removed by this process are coarse and are readily collected in conventional collectors. Nevertheless, particulate emissions are greatly increased during sootblowing.

1.2.5.3 Sulfur Oxides

The sulfur oxides present in the exhaust gases from thermal power plants are formed by the oxidation of sulfur present in the fuel being burned. Most of the sulfur is converted to sulfur dioxide on combustion. A small fraction, about 5% or less, is further oxidized to form sulfur

trioxide. Where the fuel is coal or residual oil, a small amount of the sulfur (0.2%-4%) remains in the ash as sulfates (5).

As stated earlier, the quantities of sulfur oxides produced by a combustion source are a function of the sulfur content of the fuel. The coals utilized in power plants contain anywhere from 0.5% to 2% sulfur (5). Anthracite coals have a typical sulfur content of 0.5% by weight. Lignite, subbituminous, and low volatile bituminous coals contain about 1% sulfur. Medium- and high-volatile bituminous coals average about 2% sulfur (5). In liquid hydrocarbon fuels sulfur occurs in concentrations ranging from a trace to more than 5% by weight (2). Distillate oils normally have less than 0.3% sulfur, though some may contain as much as 1% sulfur. Heavy residual oils usually contain much more sulfur than distillates; most residual oils contain over 1% sulfur by weight, with a typical value of about 1.6% (2). Natural gas fuels contain only a trace of sulfur.

Despite the comparatively small amount of sulfur trioxide produced during fossil fuel combustion, its presence is very important. Sulfur trioxide is highly reactive and extremely hygroscopic in comparison with SO_2. It drastically raises the dew point of flue gas and hence is a major cause of the visible plume created by burning high-sulfur fuels in large power plant boilers. Furthermore, SO_3 readily forms sulfuric acid mist with atmospheric moisture, resulting in possible acid damage to vegetation and property in downwind areas (2,5).

The main mechanism of SO_3 formation is the oxidation of SO_2, catalyzed by the iron oxides formed on the various metal surfaces within the

boiler unit. The method of firing and the type of fuel also affect the production of SO_3; low quantities of fly ash, moderate amounts of excess air, and high-sulfur fuels all favour high SO_3 concentrations in flue gases (2,5). In oil-fired systems, for example, the ash content is relatively small, whereas the sulfur content of a residual oil is of the same order of magnitude as that in coal; consequently, the role of sulfur is accentuated in oil-fired systems. The SO_3 content of the exhaust stream increases with the sulfur content of the oil, the flame temperature, the rate of firing, and the amount of excess air (2,5).

The SO_3 content of flue gases is commonly measured by the acid dew point, which lies between 140° and 360°F, depending on the SO_3 concentration. The dew point has been shown to increase with the sulfur content of the fuel, the water vapour of the flue gases, and the amount of excess air (2,5).

1.2.5.4 Nitrogen Oxides

Nitrogen oxides, mainly nitric oxide (NO) and nitrogen dioxide (NO_2), are formed in every combustion process when atmospheric nitrogen and oxygen are heated to a high temperature in a flame. The rapid transfer of combustion heat effected in most furnaces prevents these products from decomposing back to nitrogen and oxygen, and the nitrogen oxides are thus fixed in the exhaust gases.

NO_x (nitrogen oxide) concentrations have been shown to be functions of flame and firebox temperature, flame location and direction, firebox design, and excess air rate (2,5). The highest concentrations are found in the exhaust gases of the largest combustion sources, e.g. steam power

plants, which are operated at high furnace temperatures (> 3200°F). NO_x concentrations from these sources range from 400-1000 ppm as NO_2 (2,5).

Nitrogen oxide emissions can be reduced by uniformly distributing the combustion process within the furnace. This minimizes the formation of hot spots and the subsequent formation of NO from overheating.

Mills et al. (1961) established a general relationship between NO_x emissions and gross heat input for a wide variety of combustion equipment, including large power plant steam generators (2). The data collected for both oil and gas-fired units plotted as straight lines on log-log coordinates, despite wide differences in firebox design, excess air, and flame temperature over the range of equipment tested. Figure 1.3 is a plot of the data compiled by Mills, and shows lower NO_x levels than the equivalent Btu gas firing; the literature indicates varying reports as to whether oil or gas produces the greatest NO_x emissions (2,5,7).

Within the limits of the curves given in Figure 1.3, the NO_x emissions from almost any oil or gas combustion source can be estimated. When combustion air is preheated, as is common practice in most large power plants, preheat must be added to the gross Btu input value.

1.2.5.5 Carbon Oxides

The stoichiometric burning of carbon in air produces a dry flue gas of about 21% CO_2 and 79% nitrogen, by volume. Since most fuels contain hydrogen, however, the resulting flue gas is a mixture of CO_2, water vapour, and nitrogen.

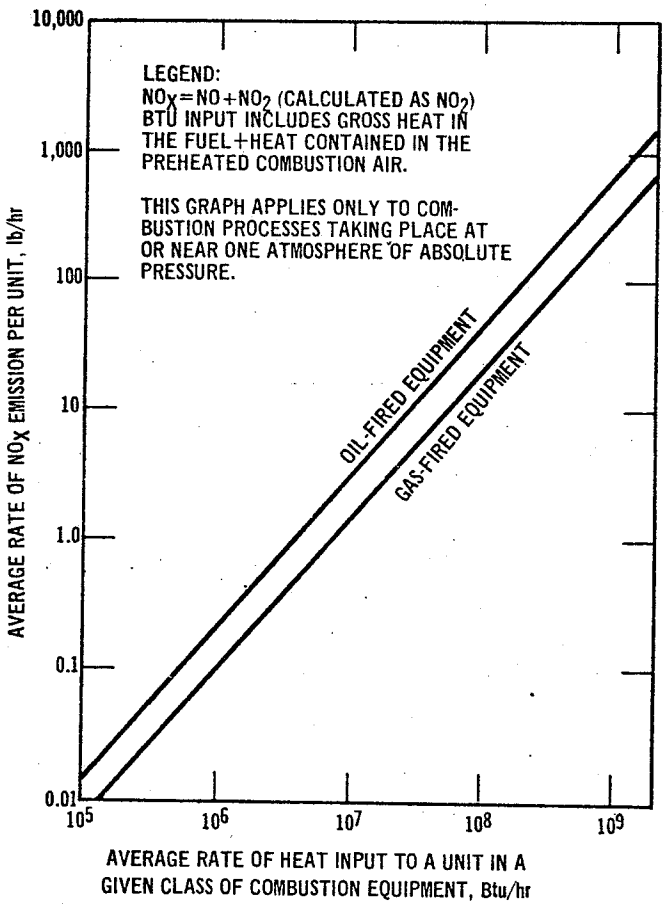

Figure 1.3. Estimation of average unit NO_x emissions from similar pieces of combustion equipment (Mills et al., 1961) (2).

Stationary fuel burners emit no carbon monoxide (CO) if combustion is at maximum efficiency. Since carbon monoxide is a fuel itself with a heat value of 4347 Btu/lb, it should be burned in the furnace if it does form. CO is usually produced where carbon is burning in an oxygen-deficient environment. Even if the total oxygen supply is sufficient, or even

excessive, poor mixing of the fuel and air may result in CO formation. From an air pollution standpoint, however, CO emissions from large stationary furnaces, including power plant boilers, are rarely a problem (5); because the losses in efficiency which accompany significant CO emissions are economically unacceptable to a plant owner, such emissions will normally elicit prompt corrective measures to optimize combustion.

1.2.6 Pollution Characteristics of Thermal Power Plants

The preceding discussion of pollutant types emphasized the dependence of power plant emissions upon the fuel burned and the furnace design. For purposes of comparison a summary of average emission values based on fuel type is given in Table 1.4. The emission characteristics of each type of power plant are now discussed in detail. It is important to remember that the values given in Table 1.4 are averages only, and that wide deviations from these values may be expected in specific cases. The assumptions made in calculating the values in Table 1.4 are referenced below:

Bituminous coal: ash = 10% (5)
sulfur = 2% (5)
gross heating value = 26.2×10^6 Btu/ton (1)

Anthracite coal: ash = 10% (5)
sulfur = 0.5% (5)
gross heating value = 25.4×10^6 Btu/ton (1)

Assumed Fuel Specifications (continued)

No. 6 fuel oil: sulfur = 1.6% (2)

gross heating value = 150,000 Btu/U.S. gallon (9)

Natural gas: gross heating value = 1054 Btu/cu fr (8)

Legend to subscripts used in Table 1.4:

a - expressed as nitrogen dioxide (NO_2)

b - expressed as methand (CH_4)

c - without flyash reinjection

d - based on average sulfur content of natural gas of 2000 grains per 10^6 cu ft (7)

e - tangentially-fired furnace units

1.2.6.1 Gas-Fired Power Plants

Gas-fired equipment generally produces a minimum of air pollution, although poor burning conditions may sometimes result in small but objectionable emissions of carbon monoxide, organic gases, and vapors. Solid particulate pollutants are produced with gaseous fuels only in two situations: 1) when combustion air supply to a high temperature zone is deliberately or inadvertently restricted, resulting in dense black smoke formation, and 2) when the fuel gas contains residual solids, which, if incombustible, will be emitted in solid form. The occurrence of these conditions is relatively low in modern gas-fired power plants, and average particulate emissions are only 15 lbs/10^6 cu ft of gas fired (7).

Unburned gas losses are normally negligible with virtually all of the gas burners and appliances used in modern power plants. This is a result of the rigid test requirements set by the American Gas Association (5).

TABLE 1.4

AVERAGE AIR POLLUTANT EMISSIONS FROM POWER PLANTS (7)

TYPE OF PLANT	PARTICULATES	SULFUR OXIDES	NITROGEN OXIDES[a]	CARBON MONOXIDE	HYDROCARBONS[b]
Coal-Fired					
Pulverized Bituminous					
general	6.11	2.90	0.687	0.038	0.011
wet bottom	4.96[c]	2.90	1.14	0.038	0.011
dry bottom	6.49	2.90	0.687	0.038	0.011
cyclone	0.76	2.90	2.10	0.038	0.011
Pulverized Anthracite					
dry bottom[c]	6.70	0.76	0.71	0.039	0.0012
Oil-Fired	0.053	1.70	0.70 0.33[e]	0.020	0.013
Gas-Fired	0.0142	0.00057[d]	0.57	0.016	0.00095

All values expressed as "lbs species/10^6 Btu gross heat input".

See preceding page for legend to subscripts.

The trace quantities of sulfur in natural gas result in only very small quantities of SO_2 and SO_3 when gas is burned. These emissions depend on the sulfur content of the gas, and average about 0.6 lb $SO_x/10^6$ cu ft of gas burned (7).

Nitrogen oxides are unavoidable and their levels depend on the combustion parameters discussed earlier, i.e. flame characteristics and firebox design. Typical NO_x emissions from gas-fired power plants are about 600 lb (as NO_2) per 10^6 cu ft of natural gas burned (7).

1.2.6.2 Oil-Fired Power Plants

Most of the ash and sulfur in fuel oil may be assumed to be emitted as pollutants from an oil-fired furnace. Ash in fuel oil ranges from 0.007 to 0.020% by weight in low-sulfur fuel oils to 0.1% in some residual fuel oils. This produces average particulate emissions of 8 lb per 1000 U.S. gallons fired (7). Even at 0.1% ash, the burning of fuel oil only produces a stack gas concentration of 0.030 grains of ash per scf at 12% CO_2, well below most control standards (2,6).

Sulfur content in fuel oils averages about 1.6% in residual oils, and less than 0.3% in distillate fuel oils (2). A fuel oil containing 1.6% sulfur by weight will yield about 250 lb of SO_2 and 3.2 lb of SO_3 per 1000 U.S. gallons fired (7).

One of the greatest causes of air pollution from oil burning is overloading, i.e. firing in excess of the design firing rate. Systems which have been chronically neglected often become gradually overloaded because of growing heat requirements and also because of more urgent plant problems taking precedence over heat loadings.

Impingement of an oil flame on a cool solid surface can partially quench the flame and cause incomplete combustion, accompanied by the release of hydrogen, hydrocarbons, carbon monoxide, and soot. This again can be the result of overloading, which may cause the flame envelope to become larger than that for which the combustion chamber was designed.

Acid smuts form by agglomeration of smoke particles on the inside surfaces of chimneys, especially when uninsulated or poorly designed chimneys are operated at low loads or below 275°F. This eventually forms a heavy layer, highly acidified by adsorption of the sulfur oxides present. When there is an increase in flue gas temperature or velocity, the deposits flake off and are carried out of the chimneys as large flakes and are deposited nearby.

Nitrogen oxide emissions are again unavoidable with oil burners, and are determined by combustion temperature and excess air. Average NO_x emissions from oil-fired power plants are about 105 lb NO_x (as NO_2) per 1000 U.S. gallons of fuel oil burned (7).

1.2.6.3 Coal-Fired Power Plants

Coal, of the three basic fossil fuels used in power plants, contains the largest amounts of ash; hence coal-fired plants produce the greatest quantities of particulate pollutants. Most coal-fired power plants are of the pulverized coal type. The coal is pulverized to a median size of 50 μ to permit rapid combustion, and is burned using an air suspension technique. The ash content of the commonly used coals ranges from 5% in lignite and subbituminous coals to 10% in anthracite and bituminous

coals (5). Pulverized coal furnaces characteristically emit about 50% to 80% of the ash fired in the coal, in the form of fine fly ash; this is equivalent to roughly 50-160 lbs of fly ash per ton of coal burned (7). Increasingly widespread enforcement of air pollution control regulations has caused most users of solid fuels to install dust collectors to control these emissions (5). The collection efficiencies of these units vary from 40-75% for cyclones to 80-99.5% for electrostatic precipitators when used in conjunction with pulverized coal-fired furnaces (5).

Sulfur dioxide emissions are again governed by the sulfur content of the fuel. Coals contain anywhere from 0.5% sulfur in anthracite varieties to 2+% in bituminous types (5). Nearly all of the sulfur in pulverized coal appears as SO_2 or SO_3 in the flue gases of coal-fired plants, giving rise to emissions of about 19-76 lbs of sulfur oxides per ton of coal fired (7). Attempts to reduce sulfur oxide emissions by coal desulfurization and stack gas scrubbing have thus far proven to be uneconomical (5). The most successful economic "solution" to this problem so far has been the use of tall stacks (5).

Nitrogen oxide emissions from pulverized coal furnaces range from 18 to 55 lbs/ton of coal burned (7). Cyclone furnaces produce the highest NO_x emissions, possibly due to the rapid cooling effect of the cyclone walls (5).

Excellent mixing and burning conditions in pulverized coal-fired furnaces result in almost complete combustion of volatile matter and produce very low hydrocarbon emissions, comparable to those of oil-fired furnaces. These emissions vary from 0.03-0.3 lb per ton of coal fired,

with bituminous coals producing the greater amounts (7). Carbon monoxide emissions are likewise very low for this type of furnace, typically about 1 lb of CO per ton of coal burned (7).

1.3 AIR SAMPLING

1.3.1 Source Sampling

Source sampling is one of the major methods commonly used in evaluating an air pollution source. The object of source sampling is to obtain as accurate a sample as possible, of the material being emitted to the atmosphere, at a minimum cost. The three basic requirements in source sampling are that the material collected be representative of that entering the atmosphere, that the sample accurately represent the total effluent, and that the sampling procedure used be economically justifiable.

A source test may be conducted for any of the following reasons: 1) to obtain data concerning the emissions for an emission inventory or to identify a predominant source in a given area, 2) to determine compliance of a source with air pollution regulations, 3) to gather information which will enable selection of appropriate control equipment, or 4) to determine the efficiency of control equipment installed to reduce emissions.

1.3.1.1 Gas Flow Measurement

Gas flow measurement is a very important part of source testing. The volume of gaseous effluent from a source must be determined in order to compute the total mass loading to the atmosphere. Measurement of the flow through the sampling train is needed to determine the volume of the

gas sample containing the pollutants of interest. Many of the sampling devices used for source testing have associated gas flow indicators; these must be continually checked and calibrated.

Measurement of gas flows is often accomplished by measuring the pressures associated with them. Several commonly used pressure measurements for gas systems are shown in Figure 1.4. Total gaseous effluent is usually calculated using the continuity equation:

$$Q = AV$$

where Q = flow at the specified temperature, pressure, and humidity conditions,

A = cross-sectional area of the gas flow,

V = velocity of effluent gas averaged over the area of the flow cross-section.

The cross-sectional area, A, is usually measured, V is determined by the test, and Q is then calculated as shown. The average effluent velocity, V, is determined by measuring the velocity at several points, in the center of equal duct areas, and then averaging the results. Traverses are made along two diameters at right angles to each other as shown in Figure 1.5. Rectangular ducts are similarly divided into the necessary number of equal areas and traversed lengthwise and widthwise as shown in Figure 1.6. Velocity measurements are usually made with devices called pitot-static tubes. Two commonly used types of pitot tubes are illustrated in Figure 1.7. The standard type requires no calibration but may plug easily in some situations; the opposite is true of the S-type tube. The velocity pressure of the flowing gas is read at each traverse point and the

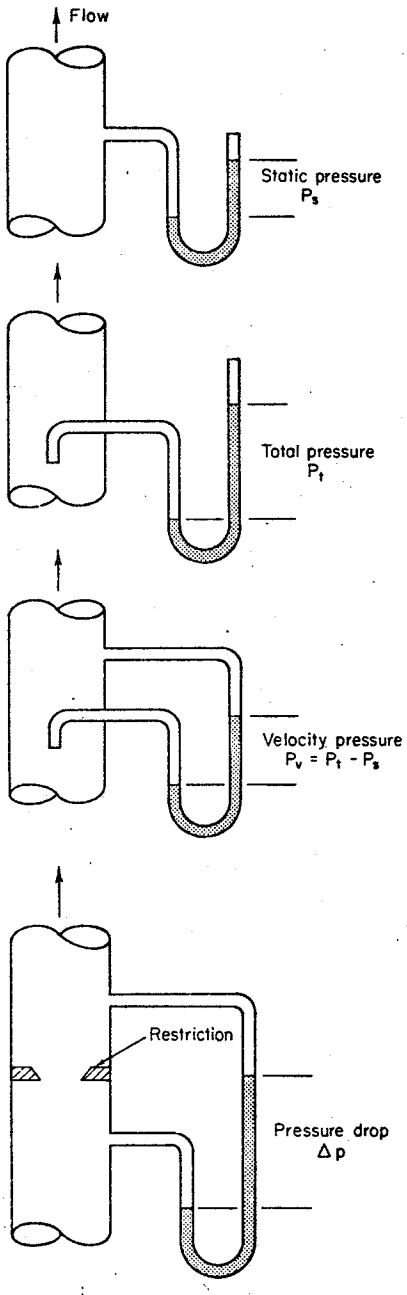

Figure 1.4. Common pressure measurements for gas flow systems (1).

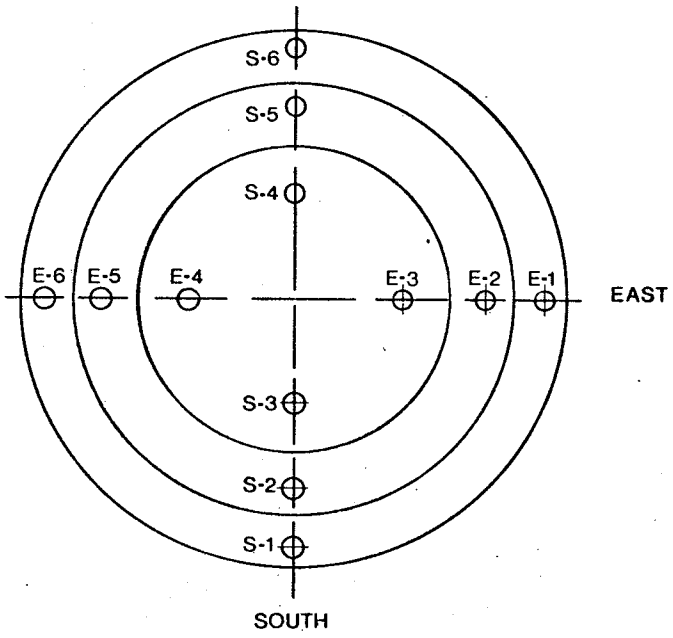

Figure 1.5. Traverse points for circular duct divided into three equal areas (1).

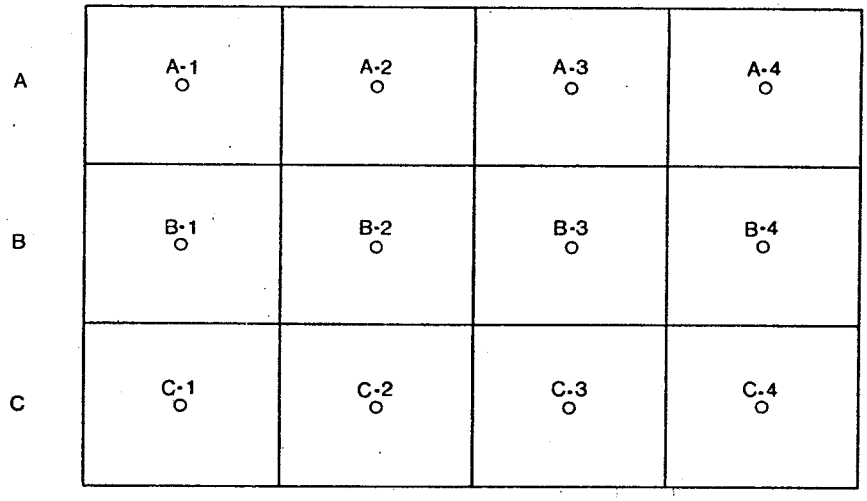

Figure 1.6. Traverse points for rectangular duct divided into twelve equal areas (1).

associated gas velocity is calculated from the equation:

$$V = 420.5 \ (P_v/\rho)^{\frac{1}{2}}$$

where V = velocity (meters/minute)

P_v = velocity pressure (millimeters of mercury)

ρ = gas density (kg/cubic meter)

The velocities for all traverse points are then averaged to give the average gas velocity.

Gas flow in the sampling train itself must be measured to determine the sample volume. This volume is used to compute the pollutant concentration of the sample in micrograms per cubic meter. Some sampling trains contain built-in flow meters, all of which must be calibrated to ensure accurate test readings.

1.3.1.2 Sample Collection

A typical sampling train is shown in Figure 1.8. Some systems may combine the components shown, but these constitute the minimum number of components for a sampling train. Extreme care must be taken to ensure that no leaks occur in the train and that the components are identical for both calibration and testing. In addition, the pumps used must be oilless and leakproof to avoid contamination or biasing of the sample. Operating curves are normally prepared prior to source testing. These include: 1) velocity versus velocity pressure at various temperatures, 2) probe tip velocity versus flow meter readings at various temperatures, and 3) flow meter calibration curves (flow versus pressure drop).

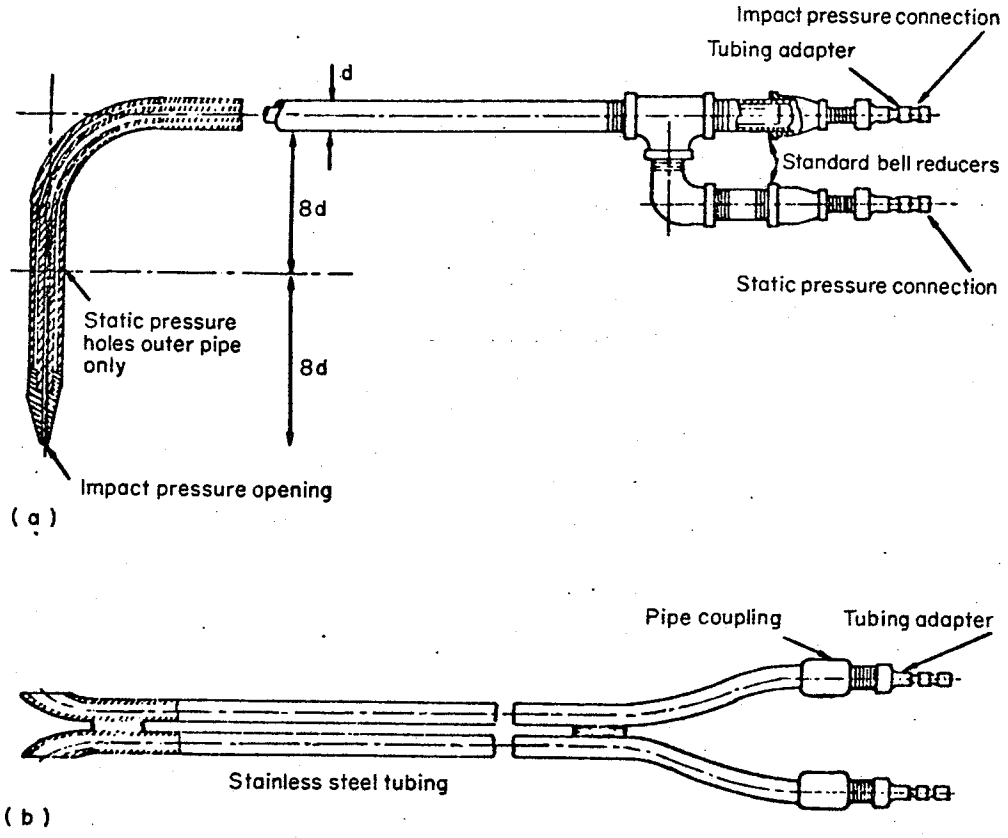

Figure 1.7. Standard and 'S'-type pitot tubes (1).

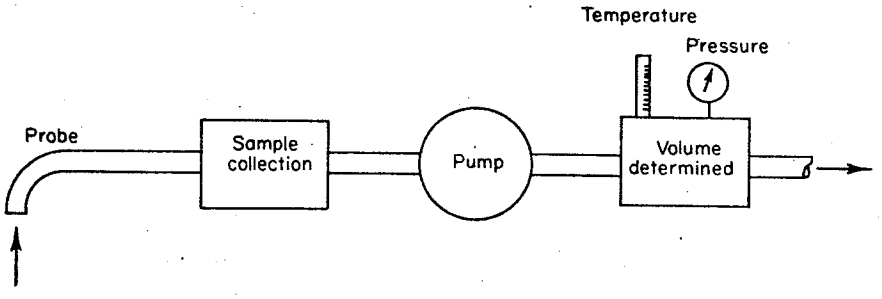

Figure 1.8. Sampling train (1).

Gaseous sample collection may be accomplished by any of several devices, including: 1) Orsat analyzers, 2) absorption systems, 3) adsorption systems, 4) bubblers, 5) reagent tubes, 6) condensers, and 7) traps. Continuous analyzers, which are seeing increased use in modern practice include: 1) infrared analyzers, 2) flame ionization detectors, 3) mass spectrometers, and 4) calorimetric systems.

Particulate sampling systems all effect a separation of the aerosol from the gas stream, sometimes using several types of collectors in series. In any of these systems the probe itself removes some particulate matter before the carrying gas reaches the first collection device, so the probe must be cleaned and the weight of the material added to that collected in the remainder of the sampling train. Particulate collectors include wet and dry impingers, filters, and electrostatic precipitators. Care must be taken when sampling for particulate matter to ensure that the same flow velocity is maintained in the probe tip as exists in the adjacent gas stream (isokinetic sampling). Inertial effects of the particulates will produce erroneously high or low values for the particulate load if the probe velocity is less or greater, respectively, than the effluent stream velocity.

Care should also be exercised when sampling for condensable aerosols. Some separating systems, such as wet impingers, may remove condensables from the gas stream, while others, such as electrostatic precipitators, will not. Of similar concern are possible reactions within the sampling train, with the resultant formation of precipitates or aerosols not normally found when the stack gases are vented directly to the atmosphere.

For example, SO_3 and other gaseous products may react in a water-filled impinger to form particulate matter not truly representative of normal SO_3 release.

Combustion processes, such as fuel burning at power plants, necessitate the measurement of CO_2 levels in the stack gases during particulate sampling. Emission standards often require that combustion stack gases be reported relative to either 12% CO_2 or 50% excess air (1). This adjustment to standard CO_2 or excess air values normalizes the emission base. In addition, emission standards require that the loadings be based on weight per standard cubic volume of air, normally at 20°C and 760 mm Hg.

1.3.2 Ambient Air Sampling

Ambient air sampling is used primarily to determine the severity of an air pollution problem through air-quality determinations at one or more receptor points. As is the case with source sampling, the complexity of the sampling system used is dependent upon the objectives of the test, the accuracy required, and the costs of labor and equipment. Relatively simple equipment is usually sufficient for determining background levels, pollution trends, odor levels, or local source nuisances; more elaborate systems are required for complete air quality evaluations, regulation control, legal action, operation of alert networks, and evaluation of in-plant equipment (1).

Ambient air quality may also be investigated by evaluating receptor effects such as metal corrosion, vegetation markings, and paint discoloration. These effects can be correlated with ambient air pollutant concentrations to give rough estimates of air quality.

1.3.2.1 Operation of Ambient Air Sampling Systems

The sampling train for ambient air testing is very similar to that used for source sampling, consisting of an inlet system, collection device, air flow measurement system, and an air mover. The inlet system brings air to a collection device where the pollutant is either analyzed, concentrated, or fixed (stabilized) for subsequent analysis. The volume of air sampled, corrected to a fixed temperature and pressure, is determined with the flow measurement system, while an air mover draws the air through the sampling train. Figure 1.9 illustrates a typical ambient air sampling system, and lists the more common types of equipment used.

1.3.2.2 Sampling Parameters

There are three basic sampling parameters which must be evaluated at the outset of an ambient sampling program. These are: 1) instrument adequacy, 2) instrument location, and 3) site evaluation. Each of these factors may influence the bias of results by yielding a range of concentrations which may not be representative of the pollutant sampled. The sampling systems must be calibrated and sufficiently sensitive at the anticipated pollutant concentrations. Then the equipment must be located such that the results are not consistently high or low. The use of several instruments or repeated samplings at different locations may be used to obtain average values. Finally, the measurements must be taken so as to best characterize the site conditions. This is an important consideration where emissions from the sampling site area vary cyclically or seasonally.

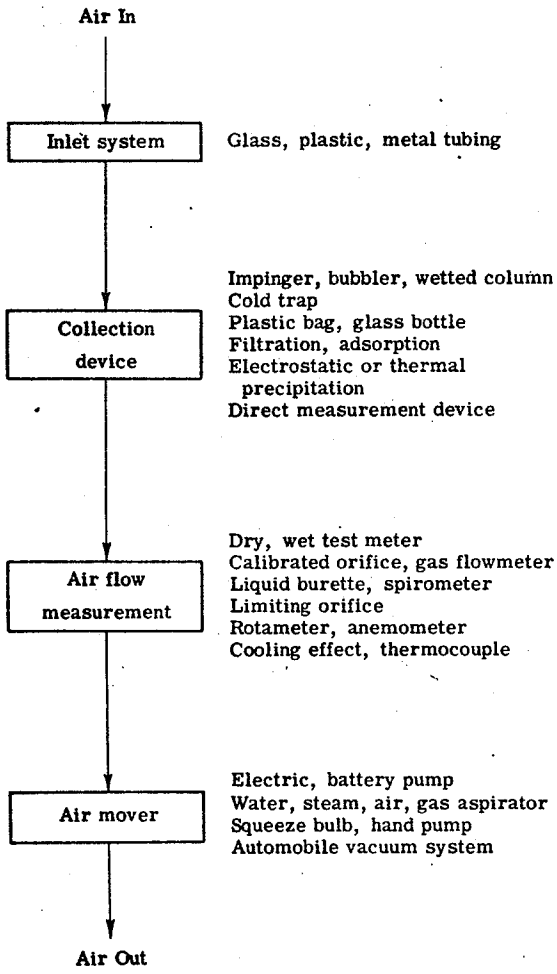

Figure 1.9. Typical ambient air sampling system (1).

1.3.2.3 Minimization of Sampling Error

Once again, steps should be taken to minimize sampling errors in order to maintain the integrity of the test results. Inlet tubes should be as short as possible and made of inert materials in order to minimize the reaction and sorption of pollutants with the inlet system. Inlet tubes should also be cleaned periodically to avoid interference from accumulated dirt and condensed water vapor.

The most commonly used collection devices are impingers, bubblers, and wetted columns, wherein a chemical solution is used to fix or stabilize the pollutant for subsequent analysis. These systems all require careful control of air flow rates which are limited by the reaction rate of the pollutant with the solution. Too high a flow rate will prevent complete fixing of the pollutant, or may even carry solution droplets from the collector, introducing a negative error into the test results. Interfering substances are also a source of error and must sometimes be removed from the inlet stream prior to absorption of the pollutant.

Air flow measuring devices must be calibrated and tested in order to provide accurate air flow measurements needed to determine pollutant concentrations.

Finally, the volume rate of air flow should be kept constant to provide accurate readings, and the air leaving the sampling train should not be exhausted close to or directly upwind of the inlet.

1.4 ANALYSIS OF AIR POLLUTANTS

Once an air pollutant has been collected or fixed by sampling, it must be analyzed. The analytical method used depends upon the type and

concentration of both the pollutant and any interfering substances present. Other considerations are: 1) the stability of reagents and reagent products, 2) the speed of chemical reactions, 3) temperature coefficients, 4) facility of calibration, and 5) the degree of simplicity, specificity, precision, and accuracy of the test method. The various methods commonly used to analyze emissions from thermal power plants are summarized below.

1.4.1 Analysis of Gaseous Pollutants

1.4.1.1 Sulfur Dioxide

Sulfur dioxide may be analyzed either by wet chemical or physical (spectrographic or spectroscopic) methods. The wet chemical methods vary in sensitivity, but are in the low range of 13-525 $\mu g/m^3$ SO_2 (0.005-0.2 ppm) found in ambient air (1). The West-Gaeke method is most specific for sulfur dioxide; the analysis is colorimetric, and entails the absorption of SO_2 in Na_2HgCl_4, followed by color development with p-rosaniline hydrochloride. These methods which involve an oxidizing agent, eg) the hydrogen peroxide methods, are least specific because other oxidizable materials in the air will be determined as sulfur dioxide.

Other wet chemical methods for SO_2 analysis are the hydrogen peroxide, iodine, fuchsin, iodine-thiosulfate, and barium sulfate methods. These involve either the oxidation or absorption of SO_2 by a chemical reagent, followed by a colorimetric or titrimetric analysis of the reagent products. The concentration of sulfur dioxide is based upon stoichiometric relationships, and the volume of air sampled, corrected to a standard temperature and pressure. When monitoring and calibration procedures are properly

carried out, the total error involved is about ± 10% below 260 $\mu g/m^3$ SO_2; accuracy increases up to 2620 $\mu g/m^3$ (1 ppm) SO_2 (1).

Sulfur dioxide can also be analyzed by spectrographic or spectroscopic methods which have the advantages of speed and low air volume requirements. These methods include mass spectrometry, flame photometry, infrared analysis, and atomic absorption analysis. Mass spectrometry involves the use of electron bombardment to ionize an air sample; the fragments of the sample components are then separated according to their mass/charge ratio. The current density, as measured by a detector, is proportional to the number of particles in each relevant class of components.

Infrared absorption analysis is based on the amount of infrared radiation (2-15 μ) absorbed by a gas sample. This absorption is characteristic of a given compound and may be used to identify it.

Atomic absorption is based on the measurement of light absorbed at the wavelength of a resonance line by the unexcited atoms of an element; emitted radiation, brought about by a transition from the ground state to a higher energy level, is a measure of the number of atoms of the element present in the gas sample.

Air samples analyzed by flame photometry must be in solution and sprayed into a flame under carefully controlled conditions. The flame excites samples with low excitation potentials; radiation from the flame is then isolated and determined by a suitable photosensitive device. This radiation is characteristic of the atoms sprayed into the flame.

1.4.1.2 Nitrogen Oxides

Wet chemical techniques for the analysis of nitrogen oxides include the Griess-Ilosvay, Saltzman, and phenoldisulfonic acid methods. The first two methods involve the oxidation of nitrogen oxide (NO) with $KMnO_4$, followed by volumetric analysis of the combined NO_2 by reaction with sulfanilic acid, acetic acid, and a naphthyl amine. The third method is colorimetric, and involves the formation of a yellow nitrate of phenoldisulfonic acid by reaction with the NO_2 in the sample (1).

The spectrographic and spectroscopic methods of physical analysis previously discussed are also applicable to determinations of nitrogen oxides.

1.4.2 Analysis of Particulate Pollutants

Particulate pollutants may be analyzed by any of several gravimetric or optical techniques, the choice of which is dependent upon the sampling method and the degree of analysis required. Filtration of the gases being sampled will normally suffice if the objective is to determine the weight of particulate matter present; subsequent chemical analysis of the particulates is also possible. If however, it is desired to determine particle size distribution or other physical characteristics, the inertial sampler, electrostatic collector, greased slide, or photometric methods should be considered.

1.4.2.1 Filtration Techniques

These methods involve the removal of particulate matter from the gas flow sampled using paper or glass filters. The simplest method is to dry the trapped particulates at constant temperature and weigh the

material. More definitive analysis of the filtered particulates is possible by determining the organic and inorganic fractions and/or the water-soluble and benzene-soluble components. The organic fraction may be further analyzed for carcinogenic compounds; the water-soluble fraction may be analyzed for sulfate, nitrate, or chloride pollutants.

An alternate method of measuring the filtered particulate matter involves determining the light reflected from or transmitted through the filter medium after filtration. Either of these two measurements may be related to the soiling characteristics of the sampled air. The filtered solids may then be identified by microscopic examination.

1.4.2.2 Inertial, Electrostatic, and Photometric Techniques

Inertial separators may be used to differentiate particles according to size, in the range of 0.5-50 μ. These devices rely on the tendency of large particles to maintain their original direction when the carrier gas changes its direction; this tendency is used to bring about the impingement of the particles on prepared surfaces. The slits or jets through which the airstream passes can be made progressively smaller, with consequent retention of correspondingly smaller particles. The particles captured at the various stages are counted and sized microscopically.

Electrostatic methods are used for special sampling for small quantities of dusts, and are most effective on particles less than 10 μ in size. These techniques involve the charging of the dust with ions, followed by the collection of the ionized particles on an oppositely charged surface. The particles may then be examined microscopically or

imbedded on an electron microscope grid for identification.

Photometric analysis involves measurement of the amount of light from a beam scattered by particles in the 0.3-10 μ size range. The amount of scattered light is roughly proportional to the projected particle surface area.

1.5 DETRIMENTAL EFFECTS OF POWER PLANT EMISSIONS

The possible adverse effects of air emissions upon receptors are an important ramification of thermal power plant operations. It is these effects which can render the emissions of an air pollution problem and therefore necessitate receptor evaluations.

The three major pollutants emitted by power plants, oxides of nitrogen and sulfur, and particulates, are reviewed below in terms of their detrimental effects upon human health, vegetation, property, and the aesthetic quality of the atmosphere.

1.5.1 Sulfur Oxides

Emissions of sulfur oxides may cause vegetation damage, adverse health effects, visibility reduction, corrosion of materials, and unpleasant odors. The extent of these effects is, of course, dependent upon the duration and intensity of the emissions to which receptors are exposed.

Gaseous oxides of sulfur are significant mainly because of their toxicity. Both SO_2 and SO_3 can produce illness and lung injury, even at low concentrations of 5 to 10 ppm. These oxides also act as irritants to the eyes and respiratory system in concentrations as low as 5 ppm (2). Individuals already suffering from pulmonary diseases such as asthma or

bronchitis are much more susceptible to inhaled sulfur oxide irritants, experiencing coughing and constriction of lung airways at doses which would normally have no noticeable effects upon healthy individuals (3). In addition, further narrowing of airways caused by inhaled irritants in patients who already have constricted airways may have more serious consequences than it would have in healthy persons. It has not been proven conclusively that sufficient exposure to sulfur oxide pollutants can cause lung diseases such as chronic bronchitis or emphyzema, but epidemiological studies have shown that it promotes or aggravates these conditions (3).

Chronic vegetation damage by sulfur oxides is characterized by distinctive yellowing of leaf tissue (chlorosis), resulting from exposure to relative low concentrations of a few tenths of a ppm over long periods of time (3). The typical symptom of acute injury from sulfur dioxide is a white to tan bleaching of leaf tissues, sometimes accompanied by the death of cells or tissues. This injury extends right through the leaf from one surface to the other. The susceptibility of plants to sulfur oxide damage varies with the species: alfalfa, barley, cotton and lettuce are among the most sensitive plants, while gladiolus, corn, citrus, and oak are among the most resistant. In foggy or misty weather, SO_2 and SO_3 emissions may form acid droplets which settle on leaves. As these droplets dehydrate with time, the acid becomes sufficiently concentrated to burn leaf tissues and cause small discrete spots, usually confined to the upper surfaces of the leaves (3).

The combination of sulfur oxide emissions with atmospheric moisture to form acid aerosols also results in property damage. These aerosols can produce extensive corrosion of metal surfaces and accelerated deterioration of fabrics and painted surfaces (2).

The presence of sulfur dioxide in photochemical smog reactions enhances the formation of visibility-reducing aerosols. In addition, sulfur trioxide condenses readily in humid weather to further obscure visibility.

Sulfur dioxide emissions have the added nuisance value of a sharp pungent odor and taste.

1.5.2 Nitrogen Oxides

The air pollution effects of nitrogen oxides include photochemical reactions, adverse health effects, vegetation damage, and atmospheric coloration. The most significant of these are the photochemical effects, induced by the sunlight-initiated reactions between certain hydrocarbons and oxides of nitrogen. Upon absorbing energy from sunlight, nitrogen dioxide undergoes several reactions, depending on the wavelength of the light. The near-ultraviolet wavelengths are the most effective in producing atomic oxygen from nitrogen dioxide; this oxygen reacts with a number of organic compounds to produce photochemical smog. Vegetation damage can result from only a few hours exposure to peroxyacetyl nitrate, an important photochemical product, at concentrations as low as 0.05 ppm (3). The vegetation effects include reduced growth and fruit yield, and glazing or metallic silvering of the lower leaf surfaces accompanied by a tendancy for the affected leaves to dry out and die. Photochemical

smog also produces eye, nose, and throat irritations, and causes noticeable reduction of visibility and accelerated aging (cracking) of rubber products.

In the absence of photochemical smog, oxides of nitrogen can produce deleterious effects by themselves. It has been found that plant growth can be reduced by as much as 35% after several weeks exposure to NO_x concentrations of only a few tenths of a ppm, with no acute symptoms on the leaves (3).

Nitrogen oxide is much less toxic than the dioxide form, acting as an asphyxiant only when in concentrations great enough to reduce the normal oxygen supply from the air. Nitrogen dioxide, on the other hand, can produce lung injury and edema after 8 hours exposure at about 10 ppm, and fatal lung damage after 8 hours at 20-30 ppm (2).

Nitrogen dioxide is an aesthetic problem in high concentrations because of its reddish-brown color and sharp odor, but these concentrations are not normally encountered in power plant emissions.

Nitrogen dioxide is thus seen to be a highly undesirable air pollutant. Nitrogen oxide is also undesirable because of its ability to produce the dioxide atmospheric by oxidation.

1.5.3 Particulates

The air pollution effects of particulate emissions are dependent upon particle size as well as concentration. Particles in the 0.1 to 1.0 μ range result in visible plumes, reduced visibility, and possible health effects due to deposition in the lungs. Particles greater than 10 μ in size are undesirable mainly because of their soiling characteristics as dustfall (3).

Aerosol particles are important sources of irritant materials, not only because of the nature of the particles, but also because of their ability to adsorb other contaminants on their surfaces. This property of particulates enhances the toxic effects of sulfur dioxide and sulfur trioxide pollutants by allowing them to come into contact with the inner surfaces of the lungs and mucous membranes in much greater concentrations than would otherwise be possible. In the absence of particulates, very little inhaled SO_2 penetrates beyond the larynx due to its high solubility and rapid removal from inspired air in the large conducting airways (2,3).

Particulate emissions are also associated with reduction of visibility and the soiling of materials. Visibility is reduced both through the obscuration of light by the interfering particles and by the refraction and scattering of light by smaller particles (< 1.0 μ). Maximum reduction of visibility is caused by 0.7 μ particles, and increases with the partic- loading of the emissions. Soiling is attributable mainly to particles greater than 10 μ which are deposited on exposed surfaces. This is simply a nuisance effect as it applies to property, but soiling may also interfere with normal photosynthesis in plants due to reduced light reaching the leaves (2,3).

1.5.4 Summary

It has been demonstrated in the preceding discussion that the effects of pollutants are very much dependent upon the length of exposure, the type and concentration of the contaminants, and the nature of the receptors themselves. Due consideration must therefore be given to the nature of the source (emission rates, operating patterns), the efficiency of control

equipment used, and the dispersive effects of atmospheric diffusion when attempting to forecast the possible effects of pollutant emissions upon a receptor or receptor area.

1.6 AIR POLLUTION METEOROLOGY

The fundamental method of predicting the concentrations of air pollutants downwind from emission sources is dispersion analysis. This analysis involves the compilation and use of pertinent meteorological and source data to estimate the dispersion patterns of air emissions. The first part of this section examines the basic meteorological phenomena which affect the transport and dilution of air contaminants; the second part deals with the fundamentals of dispersion analyses.

1.6.1 Meteorological Aspects of Air Pollution

The three major factors governing the dispersion of atmospheric pollutants are air temperature, wind, and topography. It is these determinants which give rise to the motions of the atmosphere which effect the vertical and horizontal mixing of gaseous effluents with the surrounding air.

1.6.1.1 Temperature Lapse Rate and Vertical Stability

Buoyancy effects are the basic cause of vertical mixing throughout the depth of the lower atmosphere, and are attributable to the vertical temperature gradients of the atmospheric layers.

The rate at which the air temperature decreases with height is known as the "lapse rate of temperature":

$$\gamma_e = -dT/dz$$

where z = vertical coordinate, T = temperature, and γ_e = lapse rate (1). The rate at which a parcel of dry air will cool if raised adiabatically is 1.0°C per 100 meters; this is referred to as the "dry adiabatic lapse rate", γ_d. It is the magnitude of the environmental lapse rate, γ_e, relative to the adiabatic lapse rate, γ_d, which determines how rapidly contaminants may diffuse through and become diluted by the layers of the atmosphere.

If the environmental lapse rate of an air layer is greater than adiabatic, i.e. superadiabatic, a parcel of air lifted through that layer will cool at a slower rate than its environment and will develop a positive buoyancy. This positive buoyancy tends to raise the air parcel even further from its initial position, increasing the buoyant force. Similarly, the temperature of an air parcel lowered through this layer will not increase as rapidly as that of the surrounding air, resulting in a negative buoyant force on the air parcel. This downward force causes further downward displacement of the air parcel, with a corresponding increase in negative buoyancy. Superadiabatic lapse rates thus promote vertical mixing and result in high atmospheric diffusion rates. Layers of the atmosphere exhibiting this characteristic are said to be unstable with respect to vertical displacements.

If an atmospheric layer has a lapse rate equal to the dry adiabatic rate of cooling (1°C/100 m), vertical displacements within it produce no buoyant forces. Such a layer is said to have neutral stability, and since vertical motions within it are unopposed by buoyant forces, diffusion rates within this layer are high, though not as high as in unstable layers.

A third situation arises when the atmospheric lapse rate is less than adiabatic, or subadiabatic. In this case a parcel of air raised adiabatically through the air layer will cool faster than the surrounding air and will develop a negative buoyancy. This force acts on the parcel in the opposite direction of the original displacement and will tend to return the air parcel to its original position. Similarly, a downward displacement of the air parcel will produce a positive buoyancy. Thus an air layer with a subadiabatic lapse rate is stable with respect to vertical displacements, opposing all vertical mixing motions. In such a thermally stable layer diffusion rates will be small due to the restoring buoyant forces opposing vertical motions. Of particular interest is the inversion condition in which the atmospheric lapse rate is negative, i.e. where the temperature actually increases with height. This represents the most stable atmospheric configuration. Vertical mixing is so greatly suppressed in inversion layers that in most cases the vertical transfers of pollution by eddy diffusion are effectively halted. This results in higher local concentrations of atmospheric pollutants due to greatly reduced dispersion rates.

Figure 1.10 illustrates the comparative thermal stability of atmospheric layers as a function of their lapse rates.

1.6.1.2 Wind Effects on Pollutant Dispersion

Horizontal air motions and topography are the main determinants affecting the horizontal transport and diffusion of pollutants. The most important effect of horizontal air movements is to introduce unpolluted air into a source area, while simultaneously removing an equal volume of

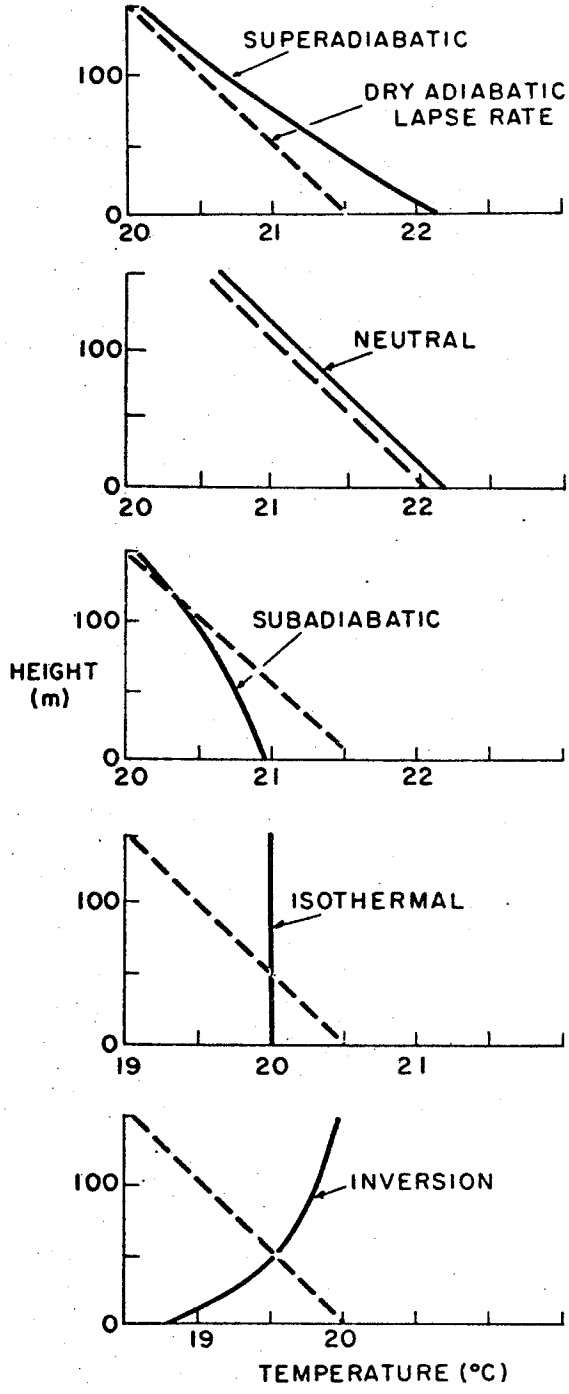

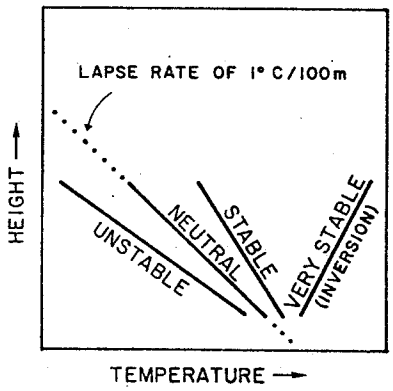

Figure 1.10. Stability of atmospheric layers as a function of typical environmental lapse rates (10,11).

polluted air on the downwind side of the area. This reduces the pollutant concentration in the air layer over the source area. For any given wind speed and time interval, with a given atmospheric mixing height (determined by temperature lapse rates), there is a prescribed volume of air into which the sources of an area inject contaminants. Doubling the wind speed doubles the volume, while halving the pollutant concentration. The blanket of polluted air over the source area is usually able to widen under the influence of horizontal eddy diffusion; this additional dilution, however, is normally considered to be secondary relative to that provided by the bulk horizontal transport of new air past the source area. Vertical mixing of the pollutants would be governed by the lapse rates of the atmospheric layers over the area. Unstable conditions would allow vigorous vertical diffusion as discussed earlier; a low, strong inversion over the source area, however, would place an upper limit on eddy diffusion, preventing contaminants introduced below the inversion layer from penetrating vertically beyond the sub-inversion layer.

1.6.1.3 Topography

The previous descriptions of horizontal and vertical air flow fields were greatly simplified for illustrative purposes. The unwarranted assumptions were made that the contaminants being transported were not removed or altered either chemically or mechanically. Such is not the case, however, as demonstrated in earlier discussions of photochemical and other atmospheric reactions involving air pollutants. Furthermore, local terrain usually imparts significant diurnal fluctuations to air motions and places a variety of constraints upon them. This complicates the

horizontal and vertical air motions, necessitating the consideration of topographical effects in evaluating the dispersion patterns of air pollutants.

The most obvious effect of terrain upon horizontal air movements is the steering and channeling of the air flow. The degree to which this occurs depends upon the stability or instability of the atmospheric layers involved. If, for example, the layer of air covering the terrain has an unstable lapse rate, air encountering a mountain will find it much easier to move up and over the obstacle than to change its direction horizontally; this is due to the positive buoyant forces caused by positive vertical displacements under unstable conditions. A very stable layer, on the other hand, would oppose movement of the air over the mountain; in this case the obstacle would redirect the air flow horizontally.

Terrain also plays a part in determining the rate at which fresh air is introduced over a source area. Winds usually exhibit a diurnal fluctuation caused by differences in the heating and cooling of different terrain surfaces. The greater the temperature differential between the surfaces, the greater will be the convection regime set up in the air over them, and the greater will be the induced air flow. The greatest diurnal variations in ventilation occur over coastlines, with ground level sea-breezes (winds directed from the sea toward land) being set up during the day, and off-shore land-breezes being set up at night. Diurnal variations also occur over valley-mountain regimes due to alternate heating and cooling of mountain slopes. This thermal contrast results in up-valley and up-slope air flows during the day, and down-valley and down-slope winds during the night.

It is important to realize that in areas where the large scale pressure patterns induce only a weak flow, it is these diurnal wind fluctuations which provide whatever horizontal ventilation an area receives. Furthermore, each locality, with its own unique topographical characteristics, has its own varying potential for receiving clean air, depending on both general wind conditions and locally generated winds.

1.6.2 Atmospheric Dispersion of Stack Effluents

The analysis of plume behaviour in the atmosphere comprises the major method used to predict pollutant concentrations downwind of continuous point sources. This subject will be dealt with extensively in the literature search section of this paper, but is presented here by way of introduction.

Figure 1.11 shows the instantaneous and time-averaged boundaries of a pollutant plume. The mean concentration of pollutants within any vertical cross section approximates a Gaussian (normal) distribution (1,11). Since the amount of contaminant material passing through any vertical cross section at any moment equals the emission rate of the source, the area under the Gaussian curve must remain constant downstream. This results in reduced mean concentrations downstream as shown in Figure 1.11.

Plume behaviour is sensitive to the combined effects of sunlight, temperature structure, and wind movements. Plumes are normally categorized according to the stability of the atmosphere above and below the stack height. The five basic types (fanning, coning, lofting, fumigating, and looping) are illustrated in Figure 1.12. In the figure, stability above the stack decreases from left to right; stability below stack height

decreases from top to bottom. Coning plumes are most probable under strong winds, or under overcast skies when surface heating is moderate. A fanning is most often observed under strong inversion conditions, usually just before sunrise after a calm, clear night. After sunrise the lower temperature structure is altered by surface heating and the plume begins to fumigate. If the sun is bright and the winds light, the plume will then tend towards looping behavior (1).

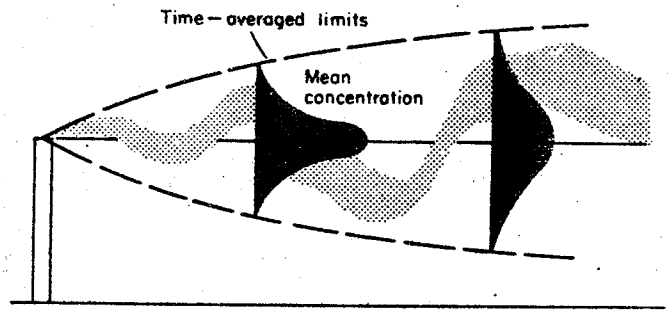

Figure 1.11. Instantaneous and time-averaged limits of a pollutant plume, showing cross sections of the Gaussian distribution of mean concentration (1).

The most common approach to modeling the plume from a continuous point source is to assume Gaussian behaviour, as mentioned earlier. This assumption implies that each contaminant particle exhibits random motion through continuous time and space, independent of any other particles present (1). When the plume is not constrained, the double normal probability (Gaussian) surface can be used to approximate the rando diffusion of the contaminants in the plume. The concentration of these contaminants at a downwind point (x,y,z) can be described by the equation:

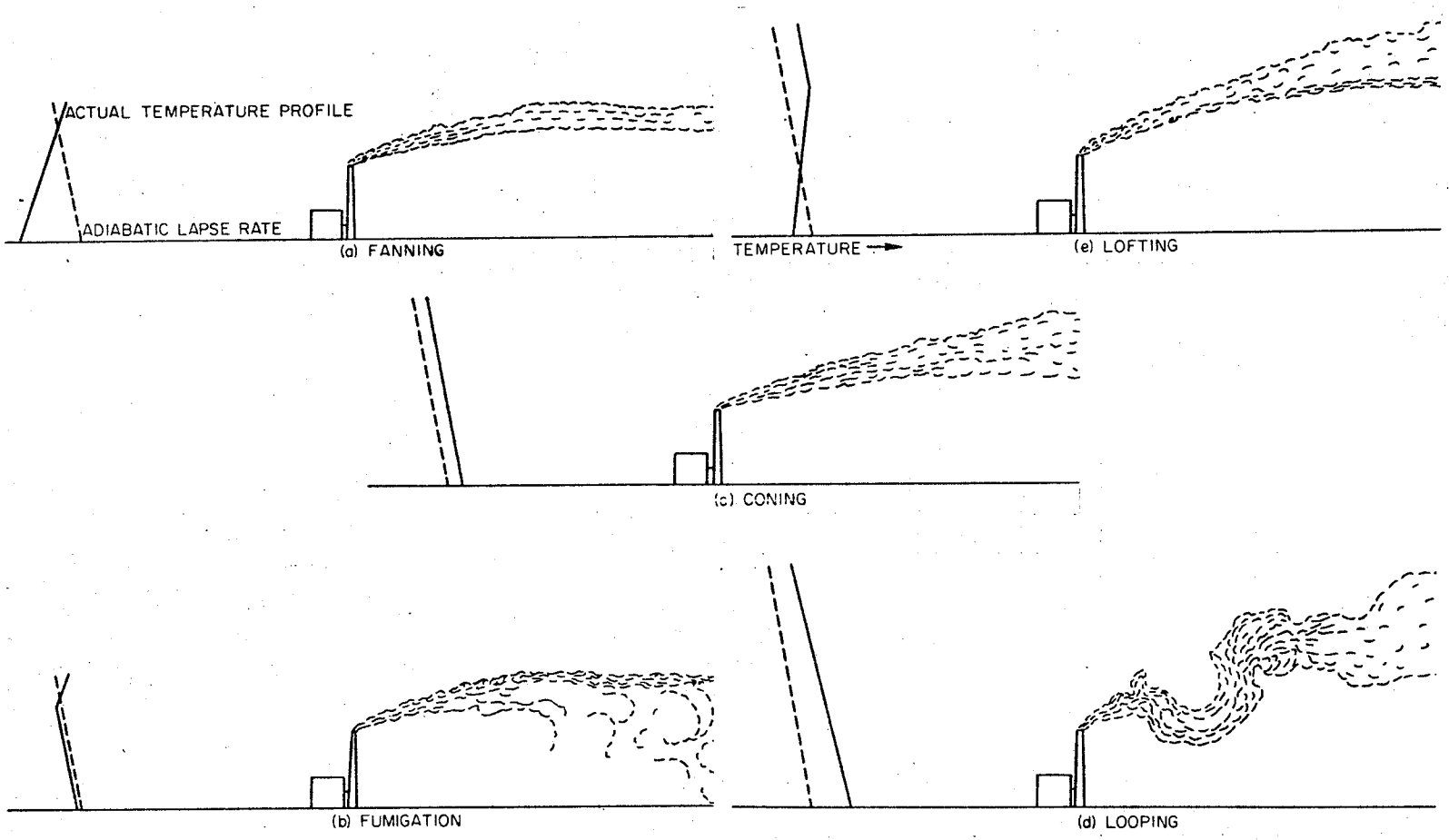

Figure 1.12. Plume nomenclature related to thermal stability of the atmosphere above and below the source height. Above- and below-source stability decrease from left to right and from top to bottom, respectively (1).

$$\chi(x,y,z) = (Q/2\pi\sigma_y\sigma_z U)\ \exp((-y^2/2\sigma_y^2) + (-1(z-H)^2/2\sigma_z^2))$$

where Q = pollutant emission rate

H = stack height, or effective source height above the ground

U = mean wind speed

σ_x = diffusive function in the x-direction (mean wind direction)

σ_y = diffusive function in the y-direction (crosswind)

σ_z = diffusive function in the z-direction (vertical)

Reflection of pollutants from the ground surface is accounted for by including the contribution from an imaginary "mirror image" source and plume at a distance H below the surface, and adding the two equations - that given above plus another identical except for the replacement of H by -H. The result after addition is the "Gaussian plume model":

$$\chi(x,y,z) = \left(\frac{Q}{2\pi\sigma_y\sigma_z U}\right)\left(\exp\frac{-y^2}{2\pi_y^2}\right)\left(\exp\frac{-(z-H)^2}{2\sigma_z^2} + \exp\frac{-(z+H)^2}{2\sigma_z^2}\right)$$

Here x enters functionally since σ_y and σ_z are both increasing functions of the downwind distance, x.

The elements of the Gaussian plume, as related to the above equation, are illustrated in Figure 1.13 below. Because the actual plume meanders within the envelope described by the figure and the model equation, the model describes the time-averaged concentrations in the plume. The averaging time is typically about 10 minutes (1).

The Gaussian plume model has the advantages of modest data requirements and being simple enough to use in manual calculations. It fails to give a realistic indication of plume behavior, however, when the

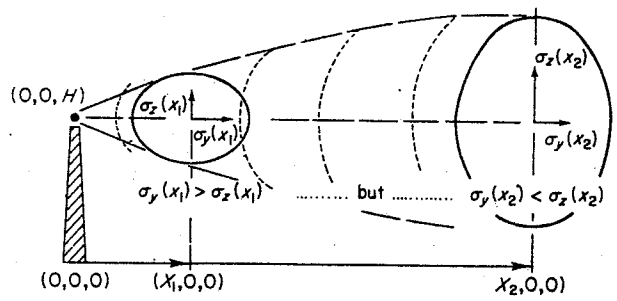

Figure 1.13. Schematic diagram of the Gaussian plume from a continuous elevated point source. Origin of coordinates is at the base of the stack. Crosswind diffusion exceeds vertical diffusion at downwind distance x_1. Vertical exceeds crosswind at downwind distance x_2 in the case depicted (1).

surrounding terrain is complex or when meteorological conditions are changing over short periods of time (an hour or less).

When a plume leaves a stack with significant momentum and/or buoyancy, due respectively to a rapid exit velocity and excess temperature relative to the ambient air, a correction must be made for the additional rise of the plume before calculations with analytical models produce reasonable results. Two of the many plume rise equations which have been proposed are the Davidson-Bryant and Briggs formulae. The Davidson-Bryant equation is empirically derived; it is given below:

$$\Delta H = 2r_{st}(V_{st}/U)^{1.4} \ (1 + (\Delta T/T_s))$$

where ΔH = adjustment to stack height (m)

r_{st} = inside radius of stack (m)

V_{st} = stack exit velocity (m/sec)

U = mean wind speed at stack height (m/sec)

ΔT = (stack gas temperature) - (ambient air temperature)

^{o}K

T_s = stack gas temperature (^{o}K)

The term involving V_s represents the allowance for plume momentum, while the term $(\Delta T/T_s)$ allows for buoyancy.

The Briggs formula represents a theoretically based plume rise equation; the equation is given as:

$$\Delta H = 2.6(F_p/Us)^{1/3}$$

where $F_p = gV_s r^2(\Delta T/T_s)$, and the stability parameter making allowance for the thermal structure of the atmosphere is $s = (g/T)(\partial\theta/\partial z)$. Here g is the acceleration due to gravity (m/sec^2), and θ is the potential temperature of the ambient air. Potential temperature is given as:

$$\theta = T(1000/p)^{0.288}$$

where T = absolute air temperature (^{o}K)

p = air pressure

The plume rise may be related to downstream distance x for neutral conditions where s = 0, and the theoretical plume rise would be infinite. The relationship is given as:

$$\Delta H_x = 2.0(F_p x^2/U^3)^{1/3}$$

The effective maximum rise will be near $\Delta H_{max} = 10^3(F_p/U^3)$. The Briggs forumlae appear to be the most reliable over a wide range of conditions, although they require a temperature sounding whenever the lower atmosphere is not neutral.

All of the equations presented for the Gaussian plume model and the Davidson-Bryant and Briggs plume rise formulae were abstracted from reference (1). These and other dispersion equations will be discussed further in the literature search.

1.6.3 Downwash and Aerodynamic Effects

Plume distortion may result from a low exit velocity, from buildings near the stack, and from terrain irregularities. The conditions which promote such distortion are discussed below.

Aerodynamic effects at the lee of a stack produce eddies and a region of reduced pressure that draws the effluent down along the side of the stack. This phenomenon is known as "downwash". The beneficial effect of a significant exit velocity is primarily to prevent this downwash from occurring. Figure 1.14a illustrates stack downwash; Figure 1.14b shows the effect of exit velocities great enough to prevent this phenomenon. Aerodynamic problems of this type are well suited to wind tunnel modeling, and it has been found in such studies that a V_s/u ratio of 1.0 is marginal with respect to stack downwash, where V_s is the stack gas exit velocity and u is the mean wind speed at the top of the stack (11).

A study of wind speed climatology of a proposed stack location will permit the choice of a stack exit velocity which will insure against downwash for any desired fraction of time.

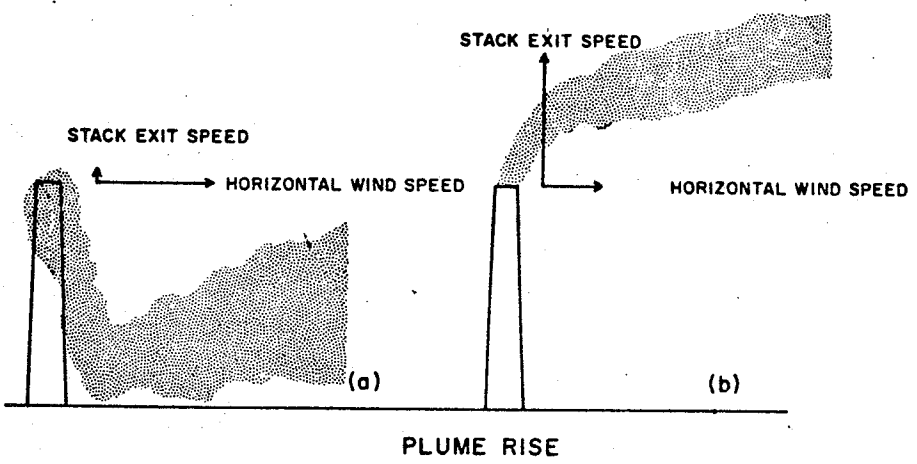

Figure 1.14. Stack aerodynamics: a) downwash resulting from a relatively low exit velocity ($V_s/u < 1$); b) downwash prevented by a sufficiently large exit velocity ($V_s/u > 2$). (11).

The presence of buildings and irregular terrain can influence wind behavior for considerable distances and therefore affect plume behavior. When a large building is situated in the vicinity of a conventional stack, the plume becomes distorted even if it does not contact the building. This effect occurs because the plume is carried in an airstream that accommodates itself to the shape of the building. If the airflow is disturbed locally, that portion of the plume which penetrates the disturbed flow region will also become distorted (11,20).

Figure 1.15 shows the characteristic flow zones around a sharp-edged cubical building with one wall normal to the wind direction. The main characteristic of the flow disturbance is the highly turbulent wake. Within the upwind portion of the wake, adjacent to the ground and lee

walls and the roof of the building lies a roughly ellipsoidal region called a cavity. Flow in the cavity is torroidal, moving in the direction of the background flow in the outer portion, and opposite to the background flow in the inner portion. Cavity dimensions are governed by changes in building shape and orientation of the wind, but the gross dimensions of the displacement zone and wake for sharp-edged buildings appear to be a function primarily of the frontal area normal to the wind flow.

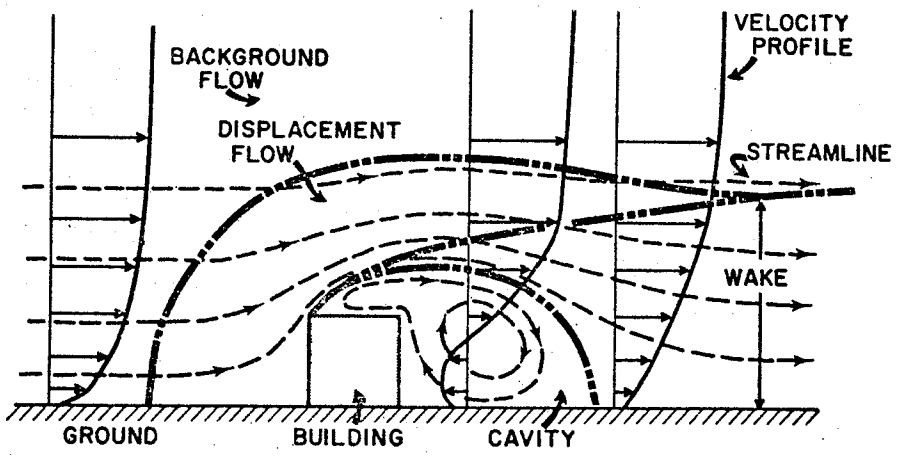

Figure 1.15. Mean flow around a cubical building (11).

A plume which lies above the displacement zone and wake will not be affected by the presence of the building. Those plumes which come into contact with the region of disturbed flow, however, will be affected as shown in Figures 1.16, 1.17, and 1.18. Plume intersection with the wake produces more rapid downward diffusion due to the increased turbulence. If the plume centerline falls in the vicinity of the cavity

boundary, the plume will descend rapidly in the lee of the building, producing high ground level concentrations in the cavity.

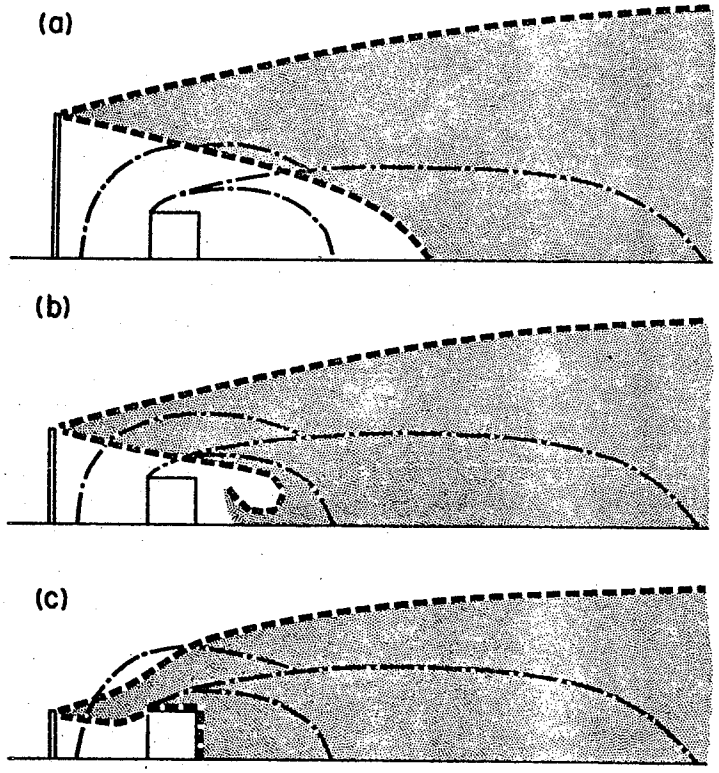

Figure 1.16. Aerodynamic effects on plume dispersion, stack located upwind of building (11).

Building-supported tall stacks are more effective in clearing the wake than upwind stacks of the same height, as shown in Figure 1.17. Stacks of medium height will clear the cavity, while short stacks result in thorough mixing of the effluent within the cavity, producing a high

concentration. The gas subsequently diffuses through the cavity boundary and is carried through the wake boundary into the background flow, finally producing concentration distributions resembling those from a point source located on the ground upwind of the building.

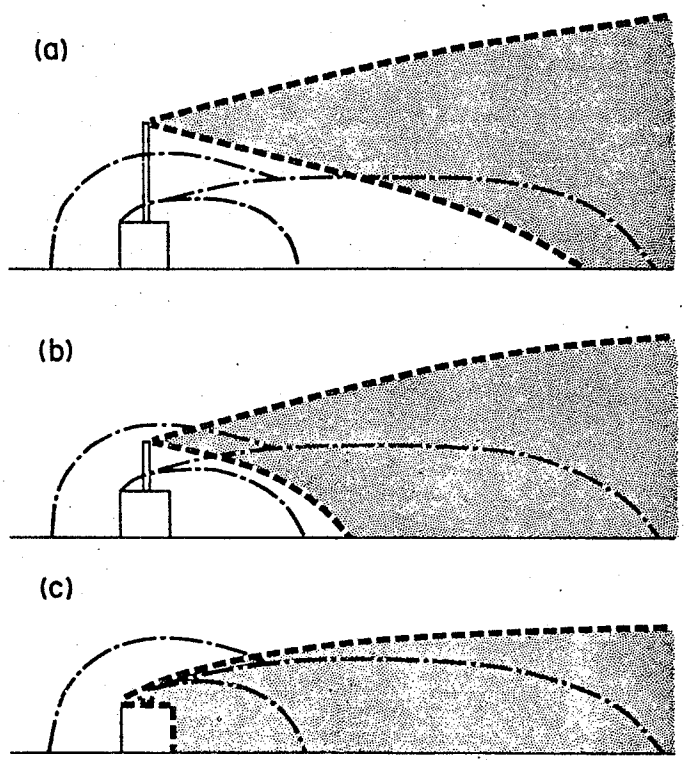

Figure 1.17. Aeordynamic effects on plume dispersion, stack located on top of building (11).

The ideal location for a tall stack is at the downwind end of the cavity. A shorter stack will result in buffeting of the plume by wake gusts, and a very short stack will result in very pronounced downwash effects, as shown in Figure 1.18. In no case will the cavity be contaminated, but the short stack will produce high ground-level concentrations in the wake.

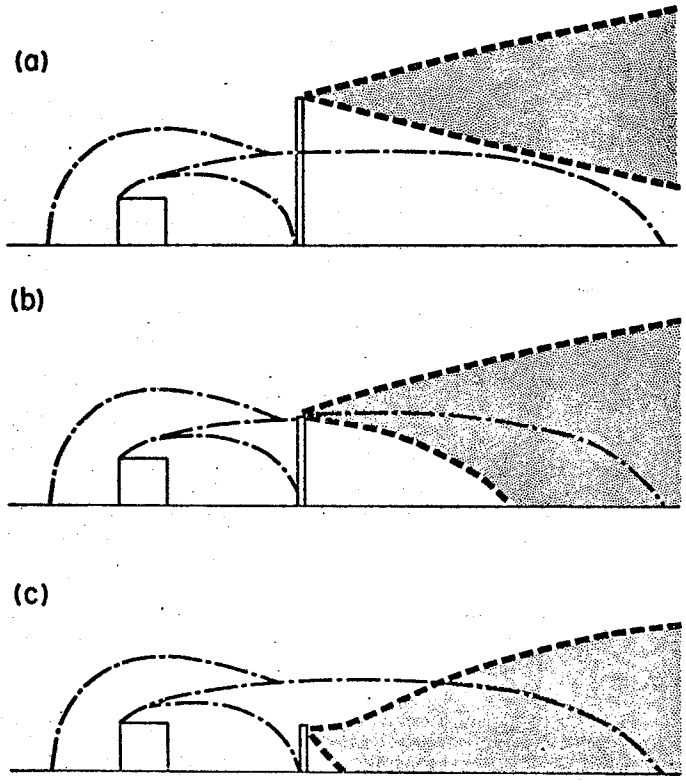

Figure 1.18. Aerodynamic effects on plume dispersion, stack located downwind of building (11).

The third major source of plume distortion is natural terrain irregularities, eg. valleys and hills. Figure 1.19 illustrates two cases of plume dispersion in a deep valley with a cross wind. With the wind direction from high ground towards the center of the valley (section "a"), the stack is in the cavity and the plume may be brought quickly to ground level by the aerodynamic eddies. The effluent becomes thoroughly diffused before passing downwind. Turbulence is high and the plume is distributed vertically through much of the valley depth.

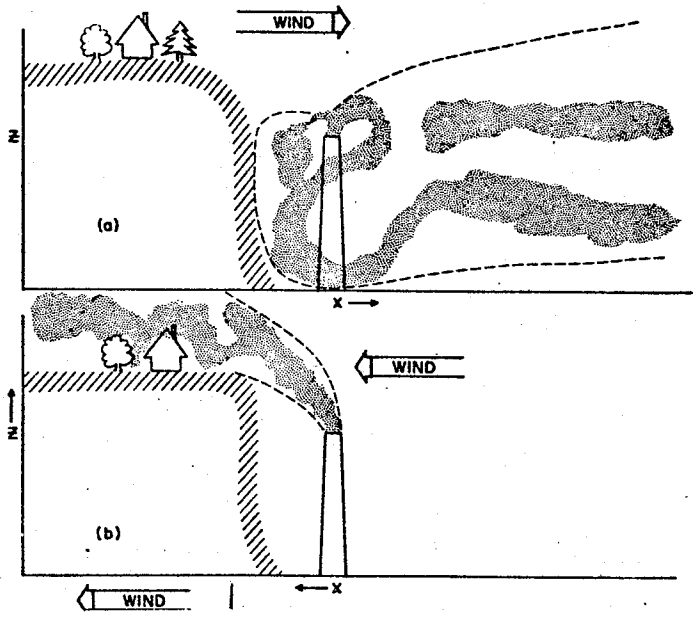

Figure 1.19. Plume dispersion in a deep valley with a crosswind (11).

In the second case (section "b"), the stack is upwind of the valley side. The plume is thus deflected along with the airstream up over the edge of the hill; this may produce high concentrations on the higher ground.

Figure 1.20 shows a stack in a valley with the wind along the axis of the valley. In this case, dispersion tends to occur fairly normally until the plume is confined by the valley walls. This results in an abrupt increase in concentrations along the walls as more and more of the of the available valley volume is filled with stack effluent.

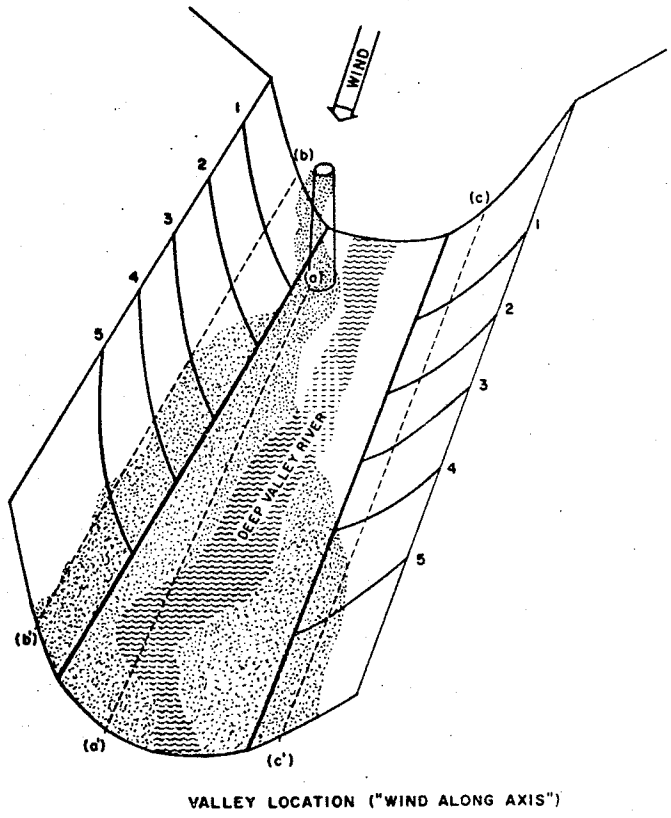

Figure 1.20. Plume dispersion in a deep valley with a parallel wind (11).

If both the stack and land formations are very high, aerodynamically-generated air motions may be modified by vertical stability effects as illustrated in Figures 1.21 and 1.22. Figure 1.21 shows a plume being carried over a tall hill under unstable conditions. Figure 1.22 shows the possible diversion of the air flow and the plume around the hill under stable conditions, where plumes tend to follow terrain contours and resist being forced over obstacles (11). Unfortunately little or no quantitative data are available concerning the impingement concentrations resulting when such plumes contact the obstructing landform.

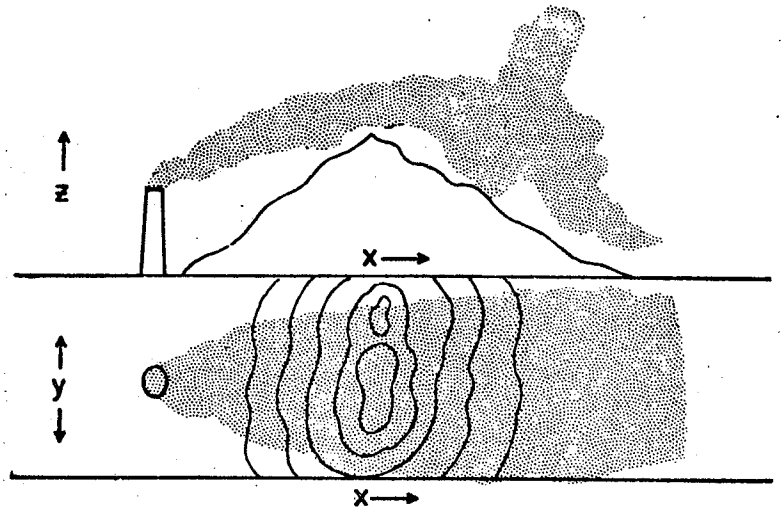

Figure 1.21. Plume dispersion near very large obstacles - unstable atmosphere (11).

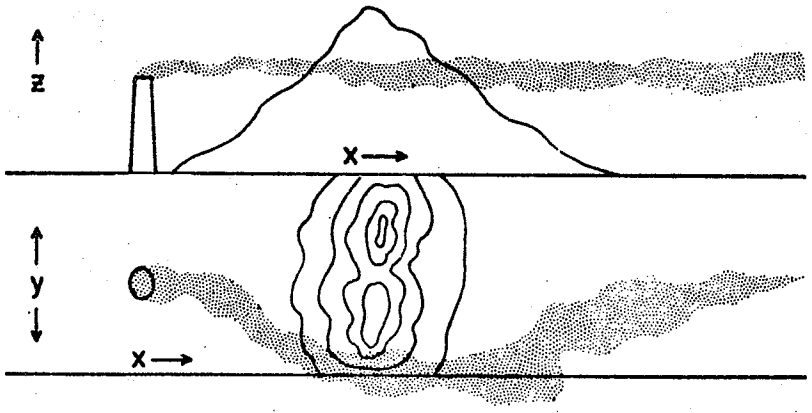

Figure 1.22. Plume dispersion near very large obstacles - stable atmosphere (11).

1.7 AIR POLLUTION ABATEMENT AND CONTROL

1.7.1 Air Emission Standards and Regulations

The abatement and control of air pollution are usually initiated by the governmental imposition of limits on air emissions from sources. Such regulations quantitatively specify the allowable emissions from stacks, chimneys, and vents. In addition, limits may be placed on the quantity or quality of fuel or raw material to be used, on the design or size of the equipment or process in which it may be used, on the heights of stacks, chimneys, and vents, on the location of sites from which emissions are permitted or prohibited, or on the times when emissions are or are not permitted. Regulations usually also prescribe the acceptable methods of test or measurement to be used for air quality determinations.

Stack emission limits may be either subjective or objective. Subjective limits may be based upon the visual appearance of an emission (eg. color, opacity) or its odor. The most common form of subjective limit is that which regulates the optical density (opacity) of a stack plume.

Objective limits fall into one of two categories: those which limit the emission of a specific contaminant irrespective of the type of source; and those which limit the emissions of a specific contaminant from a specific process or type of equipment. Air pollution standards may specify the same emission limit for all sources, or they may vary the allowable emission according to the size or capacity of the source. Emission limits may absolute, i.e. they may specify a mass of pollutant per unit of time; or they may be stated in relative terms, i.e. they may

specify an allowable mass of pollutant per unit mass of fuel burned, material processed, product produced, or per unit of heat released in a furnace. Emission limits for gaseous pollutants are normally stated in volumetric rather than gravimetric terms. In this case the limits are usually stated as a mass of pollutant per unit volume of effluent or per unit volume of ambient air. Since effluent volume is a function of gas temperature and pressure and the amount of diluting air present, volumes must be reduced to their equivalent at a specified temperature, pressure, and percent dilution air. Dilution is usually expressed as percent excess air or percent carbon dioxide in the flue gas in the case of fuel combustion.

Air emission standards may apply either to new installations only, existing installations only, or to all installations. In many cases new installations are required to comply with more stringent regulations than existing installations.

Table 1.5 lists the air quality objectives for the Province of Manitoba. Table 1.6 lists the air quality objectives promulgated by the Canadian Department of the Environment.

TABLE 1.5

MANITOBA AIR QUALITY OBJECTIVES (89)

Air contaminant	Maximum acceptable	Maximum desirable
Sulfur dioxide	900 $\mu g/m^3$ (0.34 ppm) 1-hr avg concentration	450 $\mu g/m^3$ (0.17 ppm) 1-hr avg concentration
Nitrogen dioxide	380 $\mu g/m^3$ (0.14 ppm) 1-hr avg concentration	190 $\mu g/m^3$ (0.07 ppm) 1-hr avg concentration
Suspended particulate matter	120 $\mu g/m^3$ 24-hr avg concentration	100 $\mu g/m^3$ 24-hr avg concentration

TABLE 1.6

NATIONAL AIR QUALITY OBJECTIVES (12)

Air contaminant	Maximum acceptable level	Maximum desirable level
Sulfur dioxide	60 $\mu g/m^3$ (0.02 ppm) Annual arithmetic mean	30 $\mu g/m^3$ (0.01 ppm) Annual arithmetic mean
	300 $\mu g/m^3$ (o.11 ppm) Average concentration over a 24 h period	150 $\mu g/m^3$ (0.06 ppm) Average concentration over a 24 h period
	900 $\mu g/m^3$ (0.34 ppm) Average concentration over a 1 h period	450 $\mu g/m^3$ (o.17 ppm) Average concentration over a 1 h period
Suspended particulate matter	70 $\mu g/m^3$ Annual geometric mean	60 $\mu g/m^3$ Annual geometric mean
	120 $\mu g/m^3$ Average concentration over a 24 h period	
Carbon monoxide	15 mg/m^3 (13 ppm) Average concentration over a 8 h period	6 mg/m^3 (5 ppm) Average concentration over a 8 h period
	35 mg/m^3 (30 ppm) Average concentration over a 1 h period	15 mg/m^3 (13 ppm) Average concentration over a 1 h period
Nitrogen dioxide	100 $\mu g/m^3$ (.053 ppm) Annual arithmetic mean	60 $\mu g/m^3$ (.032 ppm) Annual arithmetic mean
	200 $\mu g/m^3$ (.106 ppm) Average concentration over a 24 h period	
	400 $\mu g/m^3$ (.213 ppm) Average concentration over a 1 h period	

All measurements of air quality are corrected to a reference temperature of 25°C and to a reference pressure of 760 millimeters of mercury. Average concentrations are arithmetic averages.

1.7.2 Alternatives in Control

Air pollutant emissions can be controlled by modifying the contributing process, by changing the fuel used at the source, or by installing air pollution control equipment. An obvious fourth alternative is not to have any pollutant sources in the first place, or to have fewer of them. This latter method of control manifests itself through zoning regulations and the establishment of air-quality control regions, within which the number and type of pollutant sources are restricted. The following discussion, however, will be limited to the first three alternatives as they apply to the three major pollutants emitted by thermal power plants i.e. sulfur dioxide, nitrogen oxides, and particulates.

1.7.2.1 Control of Sulfur Dioxide

The major alternatives for the control of sulfur dioxide emissions from power plants are: 1) the use of low sulfur fuels, 2) stack gas scrubbing to remove SO_2, 3) fluidized-bed combustion, and 4) tall stacks to promote effluent dispersion.

Low sulfur fuels, when available and economical to use, can be utilized either full time or in a fuel switching program to reduce SO_2 emissions. Fuel switching may be used where supplies of low-sulfur fuels are insufficient to support their full time use. These approaches, and the use of tall stacks, are considered to have only intermediate term applications due to the shortage of low-sulfur fuels and increasingly more stringent air quality requirements (13).

Due to the increasing consumption of fuels bearing relatively large amounts of sulfur, stack gas cleaning has gained increased importance in

controlling SO_2 emissions. The SO_2 removal systems are of two basic types: those which recover the SO_2 in a useful form and those which result in the formation of a solid or liquid waste. The latter methods, often referred to as throwaway methods, may convert an air pollution problem to a water-pollution or solid-waste disposal problem, while recovery processes necessitate the marketing of a chemical product. Both the throwaway and recovery methods can be carried out in either wet or dry systems. Dry removal systems do not usually require stack gas reheating, while wet systems normally do. In some cases, dry-removal systems can also remove particulate matter. Wet systems can usually remove particulates and sulfur dioxide simultaneously.

Figure 1.23 summarizes the existing technologies for SO_2 removal. Six of these have gained some degree of user acceptance in the United States (14). Thses are:

1) wet lime/limestone scrubbing
2) alkali scrubbing without regeneration
3) alkali scrubbing with calcium regeneration
4) alkali scrubbing with thermal regeneration
5) magnesium oxide scrubbing
6) catalytic oxidation.

All of the above processes, except catalytic oxidation, employ a wet scrubber. Catalytic oxidation is difficult to retrofit as it is a high-temperature process; the other processes can usually be added on to an existing system easily.

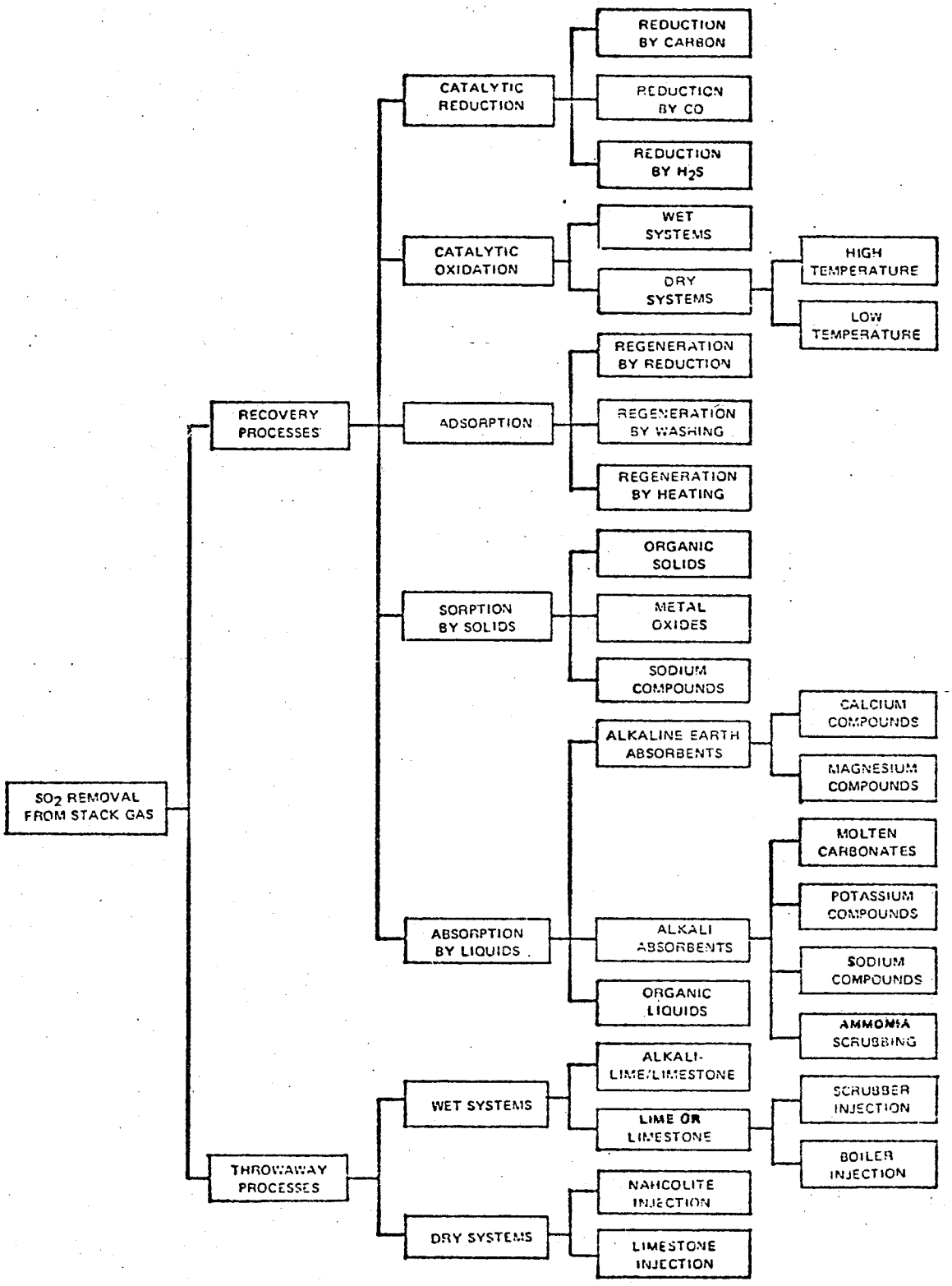

Figure 1.23. Technologies for the removal of SO_2 from stack gas (14).

The major problem associated with the SO_2 scrubbing systems is the demonstration of continuous, long-term reliability. Other problems of stack gas cleaning technology are stack gas reheating, sludge disposal for throwaway systems, marketing of by-products for recovery systems, and the availability of appropriate grades of limestone and lime.

Removal efficiencies for available SO_2 removal systems range from 70-90% (14), but poor system reliability and associated down time result in lower overall efficiencies.

Fluidized-bed combustion, though still in the experimental stages, has been demonstrated to be a potentially efficient and economically attractive process for steam and power generation. In a fluidized-bed combustor, crushed coal is burned in a dense air suspension of granular crushed limestone or dolomite. The crushed limestone is fed continuously to the bed where it calcines and reacts with sulfur oxides (SO_2 and SO_3) to form calcium sulfate. This process results in greatly reduced emissions of sulfur oxide pollutants, and in many cases greatly reduced NO_x and fine particulate emissions (15).

1.7.2.2 Control of Nitrogen Oxides

The formation of nitrogen oxides increases with increased excess air, flame temperature, fuel nitrogen content, and time at temperature. It is therefore necessary to control these variables in order to lower NO_x emissions from stationary combustion sources (16).

There are five major approaches to reducing NO_x emissions from power stations. These are:

1) lowering combustion temperature

2) use of low excess air combustion

3) stack gas treatment to remove NO_x from flue gases

4) flue gas recirculation

5) catalytic decomposition of NO_x (13).

Carrying out the combustion process at a lower temperature suppresses the high temperature reaction of atmospheric nitrogen and oxygen that forms nitrogen oxides. Several approaches can be utilized to effect this reduction of combustion temperature. One solution is to reduce the firing rate, but this may not always be compatible with the load demands of the power plant (17).

Staged combustion offers another method of reducing NO_x emissions. This consists of firing all of the fuel with substoichiometric quantities of primary air in the first stage and injecting secondary air in the second stage to complete burnout of the fuel. In the first stage, NO formation is limited by the unavailability of oxygen. Removal of heat between stages reduces the temperatures achieved when excess air is added in the second stage, thereby kinetically limiting NO formation. NO_x reductions as high as 90% have been achieved by combining this technique with low overall excess air firing in large gas-fired power plants (18).

Burner configuration also affects NO_x emissions. Cyclone furnaces, for example, which are characterized by high turbulence, result in high levels of NO_x emissions in coal-fired plants. Tangential firing, on the other hand, results in NO_x reductions as great as 60%. In tangential firing, the furnace itself acts as the burner, which results in a more

spread out flame front and correspondingly lower peak flame temperatures (18).

Lower flame temperatures are also a basis for considering fluidized bed combustion for low NO_x emission boilers. This technique, previously discussed with reference to SO_2 control, is characterized by high heat transfer rates which allow low average combustor bed temperatures of 1500-1800^{o}F to be maintained. The oxidation of chemically bound nitrogen in the fuel, however, may result in NO_x emissions exceeding those formed by the fixation of atmospheric nitrogen in conventional combustion (18).

Flue gas recirculation to the combustion zone has the principal effect of lowering peak flame temperature. The oxygen concentration is also lowered. Both of these factors favor reduced NO_x formation; reductions of 35% on oil and 60% on gas firing have been achieved with 30% gas recirculation (15,16,18).

NO_x formation increases as excess air is increased with all fuels, making low excess air firing desirable in terms of controlling emissions. However, other factors which must be considered in establishing minimum excess air levels in a given application are emissions of CO, smoke and solid combustibles, and flame stability. Furnace slagging is an additional consideration for coal-fired plants. Operating at 10% higher excess air than the established minimum will usually increase NO_x emissions by 20% for all fuels (16).

Utilities burning natural gas have been the most successful in reducing NO_x emissions, with oil-fired plants next, and coal-fired plants last. This results from the greater facility of limiting excess air

and flame temperature with gas and oil. It is a great deal more difficult to reduce flame temperature and excess air in coal-fired plants because of the secondary effects mentioned above. In addition, coal, as well as oil, contains chemically bound nitrogen which oxidizes to form additional NO_x; this reaction is more difficult to suppress than atmospheric nitrogen fixation (13).

The remaining alternatives for NO_x control are stack gas treatment and catalytic decomposition of NO_x, both of which have met with little success in power plant applications. The problems of removing NO_x from stack gases are similar to those of removing SO_2 and SO_3, i.e. the concentrations are low (up to 1000 ppm or possibly higher), the flue gas quantities are very large, and the presence of other constituents in the gas complicates the problem. Presently no proven process is currently available which can effect substantial removal of NO_x from combustion stack gases. Catalytic decomposition of NO_x at elevated temperatures has been achieved in laboratories, but conversion of this process to an industrial scale is complicated by the constituents of power plant flue gases (ash and sulfur oxides), which may inactivate or poison the catalyst, even after the stack gases have been scrubbed (13).

17.2.3 Control of Particulate Emissions

The prevailing method for removal of particulates from flue gas in coal-fired power plants is the installation of electrostatic precipitators on the flue gas exit side of the air preheater. However, results from the commercial operation of these units have not been successful in all applications, despite the simplicity of the concept and the theorectically

attainable removal efficiencies. Many problems have been due to the failures of parts of the precipitators or of associated equipment, e.g. wire breakages (13). Other problems include optimizing power input and collection efficiency. Design efficiencies for electrostatic precipitators range from 99.0-99.8%, depending on operating conditions (17). A schematic diagram of an electrostatic precipitator is shown in Figure 1.24.

Baghouse filters have only been used for demonstration and test purposes on thermal power plants. Even though baghouses are recognized as being potentially very effective in particulate removal and may be able to operate at elevated temperatures, they have not yet shown the long-term reliability and availability required for power plants without incurring excessive maintenence costs (13).

A third alternative to particulate control is the use of wet scrubbers. These are now gaining increased acceptance by the power industry. By incorporating a high energy wet scrubber stage in a SO_2 scrubbing system, both flyash and SO_2 can be removed simultaneously (13).

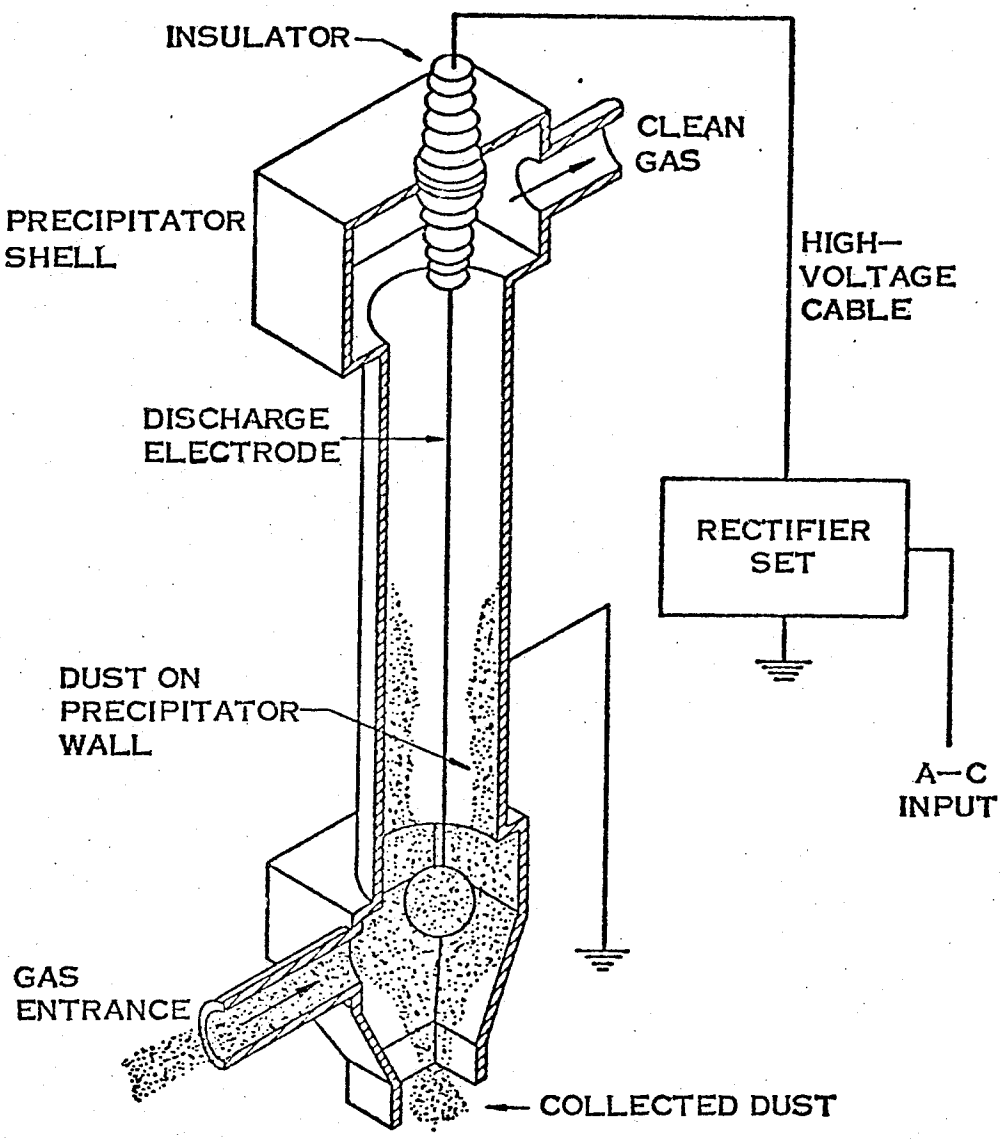

Figure 1.24. Schematic diagram of an electrostatic precipitator (19).

2. LITERATURE REVIEW

The analysis of plume behaviour in the atmosphere comprises the major method used to predict the contributions of continuous point sources to downwind pollutant concentrations. The literature pertaining to the various aspects of plume analysis has been reviewed extensively and is discussed in this section.

2.1 PLUME RISE EQUATIONS

Plume rise, the rise of a continuous emission of gaseous effluent above its source height, is often the most influential single factor affecting the effluent concentration at ground level. Ironically, its prediction is subject to more controversy than other factors contributing to the dispersion of effluents.

Several equations, both empirical and theoretical, have been proposed to account for the plume rise induced by plume buoyancy and/or plume momentum. This plume rise is added to the physical stack height to obtain the effective height of emission, required in order to obtain reasonable results with analytical dispersion models. Six of the more noteworthy plume rise equations in the literature are compared below. Most authors use their own notation in presenting their formulae. To facilitate comparison of these equations, a uniform set of symbols has been adopted for use in this paper. These symbols are based upon the notation used by Strom (20), Moses et al. (21), and Briggs (32), and are listed in Appendix 8.1.

2.1.1 Davidson-Bryant Plume Rise Equation (1949)

Davidson's formula (23) is based upon wind tunnel data compiled by Bryant (23). Any consistent system of units may be used in the Davidson-Bryant equation:

$$\Delta h = \left(\frac{V_s}{u}\right)^{1.4} (d)\left(1 + \frac{\Delta T}{T_s}\right) \qquad (2.1)$$

Davidson stated that the factor $(V_s/u)^{1.4}$ is in fair agreement with Bryant's experimental data on plume rise due to momentum. To account for rise due to buoyancy, Davidson proposed the use of the multiplying factor, $(1 + (\Delta T/T_s))$. He further indicated that this formula should be applied to "stacks of moderate or great height", but he failed to define these terms.

2.1.2 Bosanquet, Carey, and Halton Plume Rise Equation (1950)

Bosanquet, Carey, and Halton (24) published their technique for calculating plume rise in a paper on estimating dust deposition from stacks. This technique has experienced extensive use for gas plume analysis. It was developed theoretically and utilizes some fundamental experimental constants of diffusion. In the procedure by Bosanquet et al. momentum rise and buoyancy rise are calculated separately as functions of downwind distance and are added to yield the total plume rise. These calculations are based on a neutral atmosphere.

The momentum rise, Δh_v, is given by:

$$\Delta h_v = \Delta h_{v_{max}}\left(1 - 0.8\ \frac{\Delta h_{v_{max}}}{x}\right) \qquad (2.2)$$

when $x > 2\Delta h_{v_{max}}$ (x is measured downwind of stack)

and
$$\Delta h_{v_{max}} = \frac{4.77}{1 + 0.43\ u/V_s}\ (\sqrt{Q_{v_1} V_s}/u) \tag{2.3}$$

The buoyancy rise, Δh_b, is given by:

$$\Delta h_b = \frac{6.37\ g\ Q_{v_1}\ \Delta T_1\ Z}{u^3 T_1} \tag{2.4}$$

and
$$X = \frac{ux}{3.57\ \sqrt{Q_{v_1} V_s}} \tag{2.5}$$

when $u^2 > (\Delta T_1 g/T_1) \cdot (Q_{v_1}/V_s)^{\frac{1}{2}}$, and where the values of X and Z are related by the curve given in Figure 2.1:

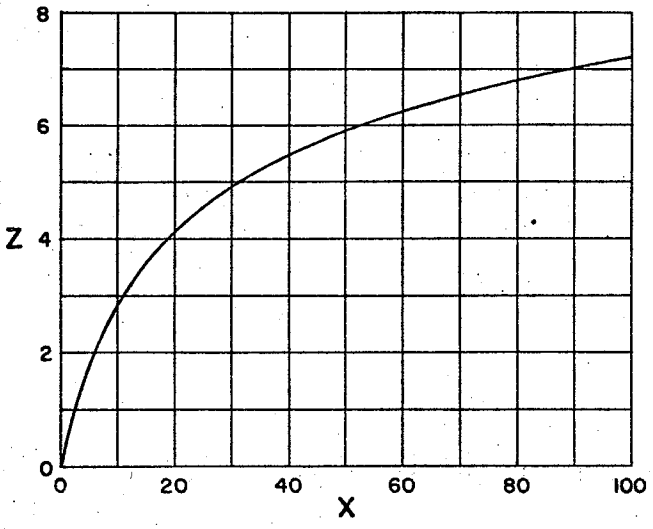

Figure 2.1. Z as a function of X for use in the buoyancy rise equations of Bosanquet et al. (20,24).

The preceding equations by Bosanquet et al. (24) are valid in any consistent units. Total rise is given by:

$$\Delta h = \Delta h_v + \Delta h_b \tag{2.6}$$

Bosanquet et al. state that the above equations for plume rise in a neutral atmosphere may be applied to other stability classes for short downwind distances as used in dust deposition calculations.

Bosanquet et al. also give the following equation for maximum plume rise in a stable atmosphere:

$$\Delta h_{max} = \frac{4.77}{1 + 0.43\ u/V_s} \cdot \frac{\sqrt{Q_{v_1} V_s}}{u} + 6.37\ g\ \frac{Q_{v_1}\ \Delta T_1}{u^3 T_1} \{\ln\ (J^2 + \frac{2}{J} - 2)\} \tag{2.7}$$

$$\text{where}\quad J = \frac{u^2}{\sqrt{Q_{v_1} V_s}} \left(0.43 \sqrt{\frac{T_1}{g(d\theta/dz)}} - 0.28 \frac{V_s}{g} \frac{T_1}{\Delta T_1} \right) + 1 \tag{2.8}$$

This gives a limit to the previous equations for this atmospheric condition. Consistent units must be used.

2.1.3 Holland Plume Rise Equation (1953)

Holland (25) used photographs of plumes at three power stations near Oak Ridge, Tennessee to modify the momentum rise relationship given by Rupp, Beall, Bornwasser, and Johnson (26). Rupp et al. gave the height of rise of a chimney effluent with buoyance as:

$$\Delta h = 1.5 \frac{V_s}{u} d \tag{2.9}$$

This formula was based on wind-tunnel experiments with ammonium chloride as a tracer. Holland added to this equation a term for buoyancy rise based on the plume observations, giving the following

empirical plume rise formula for neutral stability:

$$\Delta h = \frac{1.5\ V_s d + 3 \times 10^{-4}\ Q_h}{u} \qquad (2.10)$$

where Δh and d are in feet, u and V_s in mph, and Q_h in calories per second.

Holland's field data cover a range of stability conditions and indicate that plume height increases with instability. Holland suggests that stability be taken into account by adding 10-20% to the plume rise determined with the above equation for unstable conditions, and by subtracting the same amount for stable (inversion) conditions.

Strom (20) and Moses et al. (21) note that Q_h may be evaluated in terms of other effluent variables with the following equation wherein consistent units must be used:

$$Q_h = Q_m\ C_p\ \Delta T \qquad (2.11)$$

Hawkins and Nonhebel (27) found that the rise obtained with Holland's formula was not the maximum rise but rather the rise occurring at a downwind distance equal to two or three stack heights. Holland, however, makes no mention of this point in (25).

2.1.4 Bosanquet Plume Rise Equation (1957)

Moses et al. (21) note that the Beaver Committee in England applied the plume rise formula of Bosanquet, Carey, and Halton (24) to stack data and found that it gave too high a thermal rise for large plants. Bosanquet was asked to reexamine his original calculations; he later published the revised technique (28) described below.

Bosanquet, again basing his development on certain fundamental principles of the dilution of a gas plume in the atmosphere, gave a theoretical formula for plume rise which included the effects of relative motion of plume and surrounding atmosphere as well as ambient atmospheric turbulence. These effects are introduced with dilution coefficients. The equations presented by Bosanquet are based on the assumption of equal values for the dilution coefficients; therefore only one coefficient is given in the equations below. (Bosanquet demonstrated in his discussion that the plume rise is relatively insensitive to inequalities of the coefficients.) All of the following equations were developed for a neutral atmosphere, with the exception of the last equation which applies to a stable atmosphere.

Bosanquet gave the following plume rise formula for an effluent with a density less than that of the ambient air:

$$\Delta h = Au \left[f_I(X') + f_{II}(X'_o) - \frac{0.615\ X_o^{\frac{1}{2}}}{\left(\left(\frac{V_s}{u} \right)^2 + 0.57 \right)^{\frac{1}{2}}} \right] \tag{2.12}$$

where

$$A = \frac{1}{2\pi\ C^2} \frac{g Q_{v_1} \Delta T_1}{T_1 u^4} \tag{2.13}$$

$$X' = \frac{t + t_o}{A} \tag{2.14}$$

$$X'_o = \frac{t_o}{A} \tag{2.15}$$

$$t_o = \frac{4}{3} \frac{V_s T_1}{g \Delta T_1} \tag{2.16}$$

$$t = \frac{x}{u} \tag{2.17}$$

The above equations must be used with consistent units.

Bosanquet has presented tables of $f_I(X')$ and $f_{II}(X'_o)$, where the quantities of X' and X'_o are calculated from the stack and meteorological measurements. Tables 2.1 and 2.2 are taken directly from Bosanquet's paper (26). The plume rise may be determined using these tables and Equation 2.12. For values of X' and X'_o outside the limits of Tables 2.1 and 2.2, Bosanquet gives the following expressions:

when X' is very large: $f_I(X') = \ln X' - 0.12$

when X' is very small: $f_I(X') = 1.054 \times X'^{3/4}$

when X'_o is very large: $f_{II}(X'_o) = 1.311\, X_o'^{\frac{1}{2}} - \frac{1}{2} \ln X'_o - 1$

when X'_o is very small: $f_{II}(X'_o) - -0.527\, X_o'^{3/4}$

Bosanquet recommended that the dilution coefficient, C, be given the value 0.13. He also placed a limit on plume rise by not exceeding the value of Δh at $t + t_o = 200$ seconds.

For a non-buoyant plume subject to momentum rise only, the maximum plume rise is given by:

$$\Delta h_{max} = \frac{\left(\frac{2Q_{v_1} V_s}{3}\right)^{\frac{1}{2}}}{C\pi^{\frac{1}{2}} u} \left[1.311 - \frac{0.615}{\left((V_s/u)^2 + 0.57\right)^{\frac{1}{2}}}\right] \tag{2.18}$$

when $V_s/u > 0.5$. For small values of V_s/u,

TABLE 2.1

VALUES OF $f_I(X)$ FOR USE IN EQUATION 2.12, BOSANQUET (28)

VALUES OF $f_I(X)$													
X	$f_I(X)$	X	$f_I(X)$	X	$f_{I(X)}$	X	$f_I(X)$	X	$f_I(X)$	X	$f_I(X)$	X	$f_I(X)$
0.0010	0.0059	0.010	0.0323	0.10	0.170	1.0	0.767	10	2.33	100	4.50	1,000	6.79
0.0012	0.0067	0.012	0.0370	0.12	0.193	1.2	0.852	12	2.49	120	4.68	1,200	6.97
0.0014	0.0075	0.014	0.0414	0.14	0.215	1.4	0.930	14	2.64	140	4.83	1,400	7.13
0.0016	0.0083	0.016	0.0456	0.16	0.235	1.6	1.00	16	2.75	160	4.97	1,600	7.26
1.0018	0.0091	0.018	0.0497	0.18	0.255	1.8	1.07	18	2.86	180	5.08	1,800	7.38
0.0020	0.0098	0.020	0.537	0.20	0.274	2.0	1.13	20	2.95	200	5.19	2,000	7.48
0.0025	0.0116	0.025	0.0632	0.25	0.319	2.5	1.27	25	3.16	250	5.41	2,500	7.71
0.0030	0.0133	0.030	0.0721	0.30	0.360	3.0	1.39	30	3.33	300	5.59	3,000	7.89
0.0035	0.0149	0.035	0.0806	0.35	0.398	3.5	1.50	35	3.48	350	5.74	3,500	8.04
0.0040	0.0164	0.040	0.0887	0.40	0.434	4.0	1.59	40	3.61	400	5.88	4,000	8.18
0.0045	0.0179	0.045	0.0965	0.45	0.469	4.5	1.68	45	3.72	450	5.99	4,500	8.29
0.0050	0.0194	0.050	0.104	0.50	0.501	5.0	1.76	50	3.82	500	6.10	5,000	8.40
0.0060	0.0222	0.060	0.119	0.60	0.562	6.0	1.90	60	4.00	600	6.28	6,000	8.58
0.0070	0.0249	0.070	0.132	0.70	0.619	7.0	2.03	70	4.15	700	6.43	7,000	8.74
0.0080	0.0274	0.080	0.145	0.80	0.617	8.0	2.14	80	4.28	800	6.57	8,000	8.97
0.0090	0.0299	0.090	0.158	0.90	0.720	9.0	2.24	90	4.40	900	6.69	9,000	8.99
0.0100	0.0323	0.100	0.170	1.00	0.767	10.0	2.33	100	4.50	1,000	6.79	10,000	9.09

TABLE 2.2

VALUES OF $f_{II}(X_o)$ FOR USE IN EQUATION 2.12, BOSANQUET (28)

VALUES OF $f_{II}(X_o)$													
X	$f_{II}(X_o)$	X	$f_{II}(X_o)$	X	$f_{II}(X_o)$	X	$f_{II}(X_o)$	X	$f_{II}(X_o)$	X	$f_{II}(X_o)$	X	$f_{II}(X_o)$
0.0010	-0.0028	0.010	-0.0138	0.10	-0.044	1.0	0.155	10	1.99	100	9.9	1,000	37.0
0.0012	-0.0032	0.012	-0.0156	0.12	-0.045	1.2	0.212	12	2.28	120	11.1	1,200	40.9
0.0014	-0.0036	0.014	-0.0172	0.14	-0.046	1.4	0.269	14	2.58	140	12.2	1,400	44.5
0.0016	-0.0039	0.016	-0.0186	0.16	-0.046	1.6	0.380	16	2.88	160	13.2	1,600	47.8
0.0018	-0.0043	0.018	-0.0200	0.18	-0.045	1.8	0.325	18	3.15	180	14.1	1,800	50.9
0.0020	-0.0046	0.020	-0.0213	0.20	-0.043	2.0	0.43	20	3.41	200	15.0	2,000	53.8
0.0025	-0.0054	0.025	-0.0242	0.25	-0.037	2.5	0.56	25	4.01	250	17.1	2,500	60.6
0.0030	-0.0061	0.030	-0.0268	0.30	-0.030	3.0	0.69	30	4.56	300	19.0	3,000	66.8
0.0035	-0.0068	0.035	-0.0291	0.35	-0.020	3.5	0.80	35	5.07	350	20.7	3,500	72.4
0.0040	-0.0075	0.040	-0.0312	0.40	-0.010	4.0	0.91	40	5.54	400	22.3	4,000	77.7
0.0045	-0.0081	0.045	-0.0331	0.45	0.002	4.5	1.02	45	6.00	450	23.9	4,500	82.6
0.0050	-0.0087	0.050	-0.0347	0.50	0.014	5.0	1.12	50	6.43	500	25.3	5,000	87.4
0.0060	-0.0099	0.060	-0.0375	0.60	0.041	6.0	1.32	60	7.24	600	28.0	6,000	96.1
0.0070	-0.0110	0.070	-0.040	0.70	0.068	7.0	1.50	70	7.98	700	30.5	7,000	104.1
0.0080	-0.0120	0.080	-0.042	0.80	0.096	8.0	1.67	80	8.68	800	32.8	8,000	111.6
0.0090	-0.0129	0.090	-0.043	0.90	0.125	9.0	1.84	90	9.33	900	35.0	9,000	118.6
0.0100	-0.0138	0.100	-0.044	1.00	0.155	10.0	1.99	100	9.95	1,000	27.0	10,000	125.3

$$\Delta h_{max} = \frac{\left(\frac{2Q_{v_1} V_s}{3}\right)^{1/2}}{C\pi^{1/2} u} \times 0.9 \left(\frac{V_s}{u}\right)^{1/2} \qquad (2.19)$$

The two equations yield the same result when $V_s/u = 0.48$. Equations 2.18 and 2.19 are approximate empirical solutions of the differential equations for plume growth, and according to Bosanquet, are within 1% of the exact solution found by numerical integration.

The maximum rise of a buoyant plume in a stable atmosphere is found from Equation 2.12, using the following expression for $t + t_o$, or a value of 200 seconds, whichever is smaller:

$$t + t_o = 1.527 \left(\frac{2T}{g(d\theta/dz)}\right)^{1/2} \qquad (2.20)$$

where $d\theta/dz$ is the gradient of potential temperature in degrees Kelvin per meter.

2.1.5 Lucas, Moore, and Spurr Plume Rise Equation (1963)

The plume rise formula of Lucas, Moore, and Spurr (29) was developed on the basis of extensive plume rise measurements from two moderately large power plants using neutral buoyancy balloons as tracers. Strom (20) cites other studies of the Lucas et al. equation using data from other power plants; these studies confirmed the equation in regard to its functional form. Values of the numerical constant in the formula have been obtained for various plants. The formula gives maximum plume rise as follows:

$$\Delta h_{max} = \frac{\alpha Q_h^{1/4}}{u} \qquad (2.21)$$

where Δh max is in feet, Q_h in calories/second, and u in meters/second. (1 MW = 9.96 x 10^3 calories/second). α is dimensional and will, therefore, change with units. Lucas et al. found values of 150 and 190 for α at the two plants under neutral conditions. Maximum plume rise was largely achieved at a downwind distance of 3,600 feet. This value is supported by studies at other power plants.

The value of α is found to vary with stack height, stack diameter, exit velocity, and atmospheric stability. A tentative expression for the effect of stack height is given by Lucas (30):

$$\alpha = 135 + 0.067\ h_s \qquad (2.22)$$

This is considered to apply in the height range 160-400 feet.

It is to be noted that the Lucas, Moore, and Spurr formula does not take into account the contribution to plume rise due to momentum.

2.1.6 Briggs Plume Rise Equations (1965)

Briggs (31) used dimensional analysis to develop several plume rise equations for both stable and neutral air under calm or windy conditions. Numerical constants were evaluated with test data from various published sources. Briggs assumes wind speed, plume buoyancy, heat emission rate, and atmospheric stability to be the dominant parameters in his analyses omitting momentum rise as a negligble.

The early stage of plume rise, where dependence on downwind distance is significant, is given by:

$$\Delta h = \frac{(2.0F^{1/3}x^{2/3})}{u} \qquad (2.23)$$

where $$F = \frac{gQ_h}{\pi C_{pa} \rho T} \quad (2.24)$$

An appropriate value for F is given by:

$$F = \frac{g \Delta T V_s d^2}{4 T_s} \quad (2.25)$$

when the stack gas has an average molecular weight and heat capacity similar to that of air.

2.1.7 Briggs Plume Rise Equations (1969)

In 1969, Briggs (32) published a critical review of the plume rise observations and formulas in the literature. The discussion included the development of a relatively simple theoretical model which Briggs compares with other models. Briggs found the inverse wind speed relation, $\Delta h \propto u^{-1}$, to be generally valid for the rise of a hot plume at a fixed distance downwind in near-neutral conditions. Nine formulas of this type were compared with data from sixteen different sources, and the best agreement was obtained using the "2/3 law", $\Delta h = (1.6F^{1/3}x^{2/3})/u$, modified by the assumption that a ceiling height is reached at a downwind distance of ten stack heights. The "2/3 law" of plume rise is so called because it states that the rise is proportional to the two-thirds power of distance downwind. The term F is proportional to the heat emission. For conditions of uniform atmospheric stratification, Briggs found that buoyant plumes follow the "2/3 law" until a ceiling height of $2.9\,(F/us)^{1/3}$ is approached, where "s" is the restoring acceleration per unit vertical displacement in a stable atmosphere; $s = (g/T)\,(d\theta/dz)$, where $d\theta/dz = dT/dz + 5.4^{o}F/1{,}000$ ft, i.e. the potential temperature gradient of ambient air

(atmospheric lapse rate). For calm conditions, the formula $\Delta h = 5.0F^{\frac{1}{4}} s^{-3/8}$ was found to be in excellent agreement with a wide range of data. Formulas of a similar type were recommended for nonbuoyant plumes on the basis of much more limited data.

Briggs (32) developed his simplified theory of plume rise based on assumptions common to most of the theories, i.e. treating the stack as a point source, treating the plume as being nearly vertical or nearly horizontal (thus avoiding the complicated bending-over stage), neglecting wind shear, assuming the wind speed to be constant, and assuming that either the initial vertical momentum or the buoyancy dominates the rise. (In the case where vertical momentum dominates the plume is called a jet, and the buoyancy flux parameter F is set equal to zero. Most hot plumes, on the other hand, are dominated by buoyancy, and the initial vertical momentum flux, given by the term F_m, is neglected).

Briggs (32) gives approximations for plume rise into stable air, developed from the simplified theory, as shown in Table 2.3. In the calm case, Equation 2.26 gives the height at which buoyancy goes to zero. The plume will penetrate a ground-based inversion or a stable layer if the preceding formulas predict a rise higher than the top of the stable air. If the air is neutrally stratified above this level, a buoyant plume will continue to rise since it still has some buoyancy. A jet will fall back and level off near the top of the stable air because it becomes negatively buoyant as it rises.

Briggs' equations for unstable and neutral conditions are given in Table 2.4.

TABLE 2.3

PLUME RISE INTO STABLE AIR, BRIGGS (32)

For rise into stable air:		
(2.26)	$\Delta h = 5.0 F^{1/4} s^{-3/8}$	buoyant plume, vertical (calm conditions)
(2.27)	$\Delta h = 2.4 \left(\frac{F}{us}\right)^{1/3}$	buoyant plume, bent-over (windy)
(2.28)	$\Delta h = 4 \left(\frac{F_m}{s}\right)^{1/4}$	jet, vertical
(2.29)	$\Delta h = 1.5 \left(\frac{F_m}{u}\right)^{1/3} s^{-1/6}$	jet, bent-over

The buoyancy flux parameter, F, is given in Equations 2.24 and 2.25.

The momentum flux parameter, F_m, is given by:

$$F_m = \frac{\rho_o}{\rho} V_s^2 r^2 \qquad (2.29a)$$

TABLE 2.4

PLUME RISE IN UNSTABLE AIR, BRIGGS (32)

First stage of rise:		
(2.30)	$\Delta h = 1.8 F^{1/3} u^{-1} x^{2/3}$	buoyant plume, wind
(2.31)	$\Delta h = 2.3 F_m^{1/3} u^{-2/3} x^{1/3}$	jet, wind

For the buoyant plume in neutral conditions, the first stage of rise is given by Equation 2.30 up to the distance, x*, at which atmospheric turbulence begins to dominate entrainment. The complete plume rise is given by Equation 2.30 when $x < x^*$, and by the following equation when $x > x^*$:

$$\Delta h = 1.8F^{1/3}u^{-1}x^{*2/3}\left[\frac{2}{5} + \frac{16}{25}\frac{x}{x^*} + \frac{11}{5}\left(\frac{x}{x^*}\right)^2\right]\left(1 + \frac{4}{5}\frac{x}{x^*}\right)^{-2} \qquad (2.32)$$

Briggs gives the following formulas as conservative approximations of x*:

$$x^* = 0.52\left(\frac{\sec^{6/5}}{ft^{6/5}}\right)F^{2/5}h_s^{3/5} \qquad (2.33)$$

(for $h_s < 1{,}000$ ft.)

$$x^* = 33\left(\frac{(\sec)^{6/5}}{(ft)^{6/5}}\right)F^{2/5} \qquad (2.34)$$

(for $h_s > 1{,}000$ ft.)

Briggs cautions that Equation 2.32 should not be applied beyond $x = 5x^*$, since very few data go beyond this distance. He then suggests a rule of thumb for sources $\geq$ 20 MW heat emission at full load, whereby Equation 2.32 can be approximated by the "2/3 law", Equation 2.30, up to a distance of 10 stack heights, beyond which further plume rise is neglected, i.e.:

$$\Delta h = 1.8F^{1/3}u^{-1}x^{2/3} \qquad (x < 10h_s) \qquad (2.35)$$

$$\Delta h = 1.8F^{1/3}u^{-2}(10h_s)^{2/3} \qquad (x > 10h_s) \qquad (2.36)$$

For sources < 20 MW heat emission, Equation 2.30 gives a conservative approximation of Equation 2.32 up to a distance of $x = 3x^*$. The rise at this distance is considered to be the final rise, i.e.:

$$\Delta h = 1.8F^{1/3}u^{-1}(3x^*)^{2/3} \qquad (2.37)$$

Finally, Briggs optimizes Equations 2.30, 2.32, 2.35, 2.36, and 2.37 for the best fit to the data covered by his survey (32). This was accomplished by dividing these formulas by 1.09; readjustment of the constants in the previously given equations is indicated by primes on the equation numbers. Table 2.5 summarizes Briggs' optimized equations and the range of their applicability.

Equations 2.30',2.32',2.35' and 2.36'are also recommended for the mean rise in unstable conditions, although larger fluctuations about the mean center line should be expected. No enhancement of plume rise over that of a single plume was found when two stacks in close vicinity were operating in neutral conditions.

In stable stratification, Equation 2.30' holds to a distance $x = 2.4\ us^{-\frac{1}{2}}$, beyond which the plume levels off at about

$$\Delta h = 2.9\left(\frac{F}{us}\right)^{1/3} \qquad (2.38)$$

Briggs notes that even though Equation 2.32' is the best of the dozen or so formulas evaluated, the average plume rise at a given plant may deviate from the value given by Equation 2.32' by ± 10% if the site is flat and uniform and by ± 40% if a substantial terrain step or a large body of water is nearby. He also states that normal variations in the intensity of turbulence at plume heights at a typical site cause x^* to vary by about ± 20% on the average, with corresponding variations in Δh.

TABLE 2.5

OPTIMIZED PLUME RISE EQUATIONS, BRIGGS (32)

Eqn. No.	Plume Rise Formula	Range of Applicability
2.30'	$\Delta h = 1.6F^{1/3}u^{-1}x^{2/3}$	- buoyant plume, wind - neutral stratification $x < x^*$
2.32'	$\Delta h = 1.6F^{1/3}u^{-1}x^{*2/3}\left(\frac{2}{5} + \frac{16}{25}\frac{x}{x^*} + \frac{11}{5}\left(\frac{x}{x^*}\right)^2\right)\left(1 + \frac{4}{5}\frac{x}{x^*}\right)^{-2}$	- buoyant plume, wind - neutral stratification $5x^* > x > x^*$
2.33	$x^* = 0.52\left(\frac{\sec^{6/5}}{ft^{6/5}}\right)F^{2/5}h_s^{3/5}$	$50 \text{ ft.} < h_s < 1{,}000 \text{ ft.}$
2.34	$x^* = 33\left(\frac{\sec^{6/5}}{ft^{6/5}}\right)F^{2/5}$	$h_s > 1{,}000$ ft.
2.24	$F = \frac{gQ_h}{\pi C_{pa}\rho T}$	
2.25	$F = \frac{g\Delta T V_s d^2}{4T_s}$	(continued on page)

TABLE 2.5 (CONTINUED)

OPTIMIZED PLUME RISE EQUATIONS, BRIGGS (32)

Eqn. No.	Plume Rise Formula	Range of Applicability
2.35'	$\Delta h = 1.6F^{1/3}u^{-1}x^{2/3}$	- heat emission $\geq$ 20 MW (fossil fuel plants) $x < 10\ h_s$ - neutral stratification (good working approximation to Equation 2.21')
2.36'	$\Delta h = 1.6F^{1/3}u^{-1}(10h_s)^{2/3}$	- heat emission $\geq$ 20 MW (fossil fuel plants) $x > 10h_s$ - neutral stratification (good working approximation to Equation 2.21')
2.30'	$\Delta h = 1.6F^{1/3}u^{-1}x^{2/3}$	- heat emission < 20 MW $x \leq 3x^*$ - neutral stratification
2.37'	$\Delta h = 1.6F^{1/3}u^{-1}(3x^*)^{2/3}$	- heat emission < 20 MW $x > 3x^*$ - neutral stratification

2.1.8 Comparison of Plume Rise Equations

There are over 30 plume rise formulas in the literature, and new ones appear at the rate of about two per year (32). All require empirical determination of one or more constants, and some formulas are totally empirical. However, the plume rises predicted by various formulas may differ by a factor of 10 or greater (32). This is attributable to the differing types of analysis, data selection, and data weighting used by various investigators.

Comparison of the plume rise equations presented earlier show that they differ in functional form. Hence good agreement for one application is not likely to be found for another. Strom (20) points out the danger of extending the application of a procedure to ranges outside of those of the field data on which it is based or outside of the field examples used to show its accuracy in the case of the theoretically derived forms. Thomas et al. (33) illustrated this point by applying the Holland and Lucas et al. formulas in determining ground-level concentrations. Substantial agreement was found for power plants of less than 400 MW capacity, but disagreement increased with power plant capacity for larger plants. The Holland equation, developed on using data from smaller plants, gave overly conservative plume rise values, while the Lucas et al. formula, based on recent data from large power plants (20), yielded much more accurate estimates.

Another example is found in the case of low-buoyancy plumes. The formulas of Briggs (31) and Lucas et al. do not include momentum rise. They must therefore not be applied to cases where there is substantial momentum rise in relation to buoyancy rise. This condition may exist

where the gas effluent temperature is relatively low (20). Selection of a plume rise formula for a given problem should therefore be based, at least in part, upon the data used in developing the formula.

The choice of a plume rise formula is further complicated by the fact that the leveling off of a plume is brought about in different ways by different meteorological conditions, and thus no one equation applies to all cases (34).

The plume rise formulas previously given are compared below with the purpose of qualifying the selection of the plume rise formula used in this research. They have been grouped according to their performance in estimating actual plume rise:

The formulas of Bosanquet et al. and Lucas, Moore, and Spurr (29) have both been found to overestimate plume rise (20, 21, 32, 36), while those of Davidson (23), Holland (25), Bosanquet (28), and Briggs (31) tend to give predictions which are low (20, 21, 32, 35, 36).

The formula of Bosanquet et al. (24) tends to give an excessive buoyancy rise for large plants (20, 21). Thomas, Carpenter and Colbaugh (36) also found that this formula induces a large scatter of plume center lines as compared with observed values.

The formula of Lucas, Moore, and Spurr (29) includes both a transitional and a final-rise stage, and gives better agreement with the data than the Holland formula (32). When the empirical stack height factor by Lucas (30) is applied to Equation 2.21, the agreement is considerably improved (32). Briggs (32), however, advises caution in applying the Lucas et al. formula to plants with heat emission < 10 MW (eg. the

Manitoba Hydro plant at Brandon) because it predicts continued plume rise to almost 1 km. downwind, regardless of source size. In addition, Moses, Strom, and Carson (21) note that the Lucas et al. formula does not take into account the contribution due to momentum. Thomas et al. (36) also found that this formula has a tendancy to overestimate plume rise and induces a moderate scatter in the predicted plume center lines.

Briggs (32) points out that the Davidson-Bryant prediction of $\Delta h \propto u^{-1.4}$ does not fit most of the data and is therefore invalid for most sources. In most cases, $\Delta h \propto u^{-1}$ is the best elementary wind speed vs. plume rise relation. Furthermore, Davidson's formula is physically over-simplified in that the buoyancy term ($\Delta T/T_s$) does not take into consideration the total heat emission or the effect of gravity, without which buoyancy would not exist. The main weakness of Equation 2.21 is that it is based on data obtained only seven stack diameters downwind, and often greatly underestimates observed rises, as demonstrated by Briggs (32), Moses and Strom (35), and Thomas et al. (36).

The Holland formula (25) has had extensive use but is known to give very conservative estimates of plume rise, lower than those given by most formulas (20, 21, 32, 35). Furthermore, Holland's equation is completely empirical and does not allow for the effect of distance of measurement on plume rise as do the formulas of Lucas et al. (29) and Briggs (32); consequently Holland's formula gives poorer agreement with the data. The Holland formula also shows a particularly high percentage of scatter, according to Briggs (32).

Bosanquet's formula (28) underestimates plume rise at large values of x/L (i.e. $x/L > 10^3$) as shown by Briggs (32). Moses and Strom (21)

also found Bosanquet's rise predictions to be too low. Moses, Strom, and Carson (21), however, found that Bosanquet's formula yields excessive rise values when modified by Stumke's correction factor K. Moses and Strom (35) cite Bosanquet's questionable assumption of a constant diffusion coefficient equal to 0.13 for all meteorological conditions; this assumption fails to account for possible differences between horizontal and vertical diffusion rates.

Briggs' first equation (31) showed substantial agreement over the wide range of data examined, but these data do not include the more recent large power plants. Briggs' first equation underestimates plume rise at large values of x/L ($> 10^4$), the nondimensional downwind distance used by Briggs in a later work (32).

Briggs' Equation 2.30 (the "2/3 law") is a transitional rise formula, and agrees with the data as well as the Lucas modification (30) of the Lucas et al. (29) formula. Equation 2.32, which includes both a transitional-rise stage (where plume rise is influenced mainly by plume momentum and self-induced, turbulent mixing with the air), and a final rise stage (where entrainment is dominated by atmospheric turbulence), gives both improved numerical agreement and much less percentage of scatter than Equation 2.30 (32). The fit to observed plume center lines can be even further optimized by dividing through by 1.09, yielding Equation 2.32'. Of the formulas examined, Briggs' Equation 2.32' gives the best results, and is the one recommended for buoyant plumes in neutral and near-neutral conditions (32).

2.2 DOWNWASH AND AERODYNAMIC EFFECTS

The influence of mechanical turbulence around a building or stack can significantly alter the effective stack height through its effect on plume rise. This is especially true with high winds, when the beneficial effect of high stack gas velocity is minimized and the plume is emitted nearly horizontally.

2.2.1 Stack Downwash

Downwash of the plume into the low-pressure region in the wake of a stack can occur if the exit velocity is too low relative to the wind speed. In addition, if the stack is too low, the plume can be caught in the wake of associated buildings, where it will produce high ground-level concentrations of the effluent.

Sherlock and Stalker (37) studied the phenomenon of stack downwash in a wind tunnel. Their results are summarized in Figure 2.2. This chart shows the relation between wind velocity and stack effluent velocity and stack effluent velocity and the occurrence of downwash. This chart indicates that downwash will be minimized if $V_s/u > 1.5$, where V_s is the exit velocity and u is the average wind speed at the top of the stack. Briggs (32) confirms the results of Sherlock and Stalker by demonstrating their consistency with elementary theoretical considerations: when $V_s/u > 1.8$, the upward momentum of the stack gases should overcome the downwash pressure gradient produced by wind blowing around the stack; when $V_s/u < 0.8$, the effluent can be drawn down into the lower pressure region across the entire back of the chimney.

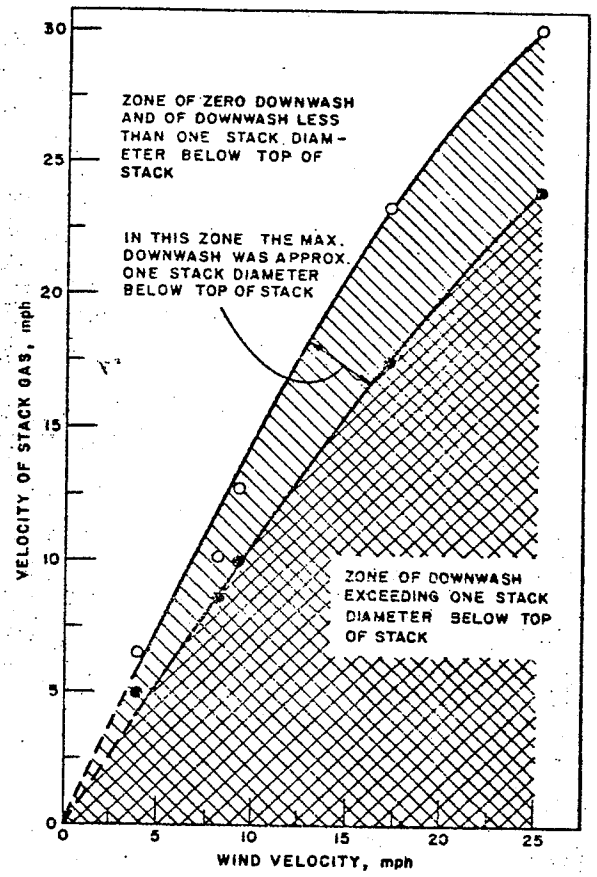

Figure 2.2. Critical relations between wind speed and stack-gas velocity in the control of downwash (37).

Briggs (32) further states that if the plume is very buoyant, the buoyancy forces are sufficient to counteract some of the adverse pressure forces and the preceding criterion for V_s could be relaxed. He cites the need for quantitative data on the effect of plume buoyancy on the abatement of downwash, noting that buoyancy was not a significant factor in the Sherlock and Stalker experiments.

Nonhebel (38) recommends that V_s be at least 20 - 25 ft/sec for small plants (heat emission < 10^6 cal/sec) and that V_s be about 50 - 60 ft/sec for larger plants (heat emission > 10^7 cal/sec). Larger effluent

velocities are not necessary since such high winds occur very rarely; furthermore, much higher velocities may be detremental to the rise of a buoyant plume due to more rapid entrainment of ambient air into the plume (32).

Scorer (39) reports that when stack gas velocity must be low, downwash may be prevented by placing a horizontal disk, about one stack diameter in breadth, around the rim of the chimney top.

Briggs (32) has shown that an effluent emitted vertically from a stack can rise due to its momentum or can be brought downward by the low pressure in the wake of the stack. In a later paper (70), Briggs accounts for the aerodynamic effect of the stack with an adjustment to the effective stack height given by $2(V_s/u - 1.5)D$, where V_s is the stack exit velocity, u is the wind speed, and D is the stack diameter. The critical ratio is $V_s/u = 1.5$, as given by Sherlock and Stalker (37). A value of V_s/u greater than 1.5 produces an increase in effective stack height, while $V_s/u < 1.5$ reduces the effective stack height. The adjusted stack height, accounting for stack aerodynamics is given by:

$$h' = h_s + 2(V_s/u - 1.5)D \qquad (2.38a)$$

2.2.2 Building Downwash and Terrain Downwash

The region of disturbed flow surrounding an isolated building generally extends upwards to at least twice its height and downwind 5 to 10 times its height (22). Hawkins and Nonhebel (26) proposed, as a general rule, that chimneys should be at least 2½ times the height of adjacent buildings, but in a factory or built-up area with many high

buildings, or in a valley, or where the ground is uneven, it is highly desirable to ensure by means of a wind-tunnel test that the stack is of sufficient height to avoid building downwash. If such a stack is designed with sufficient effluent velocity to avoid stack downwash, the plume is normally carried above the region of downflow in the wake of the building. If the stack height or effluent velocity is slightly lower, in high winds the plume will be caught in the downflow and be efficiently mixed to the ground by the increased turbulence in the wake of the building. If the stack is less than twice the building height, at least part of the plume is likely to be caught in the cavity of air circulating in the lee of the building, bringing high concentrations of effluent to the ground near the building and possible into the building (32). Figure 2.3 illustrates the advantage of using a stack height of 2½ times the height of the surrounding buildings; it also demonstrates the advantage of constructing a stack on the side of the building downwind of the prevailing wind, where the air is still rising.

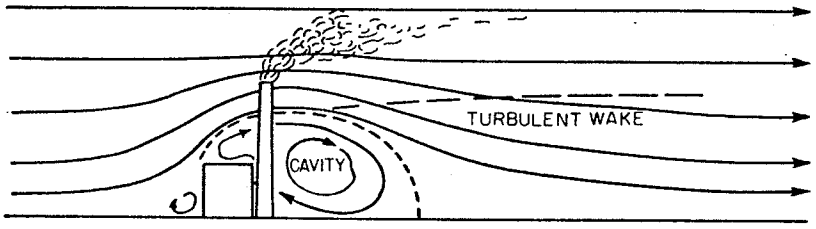

Figure 2.3. Flow past a typical power plant (32)

The stack vs. building height factor of 2.5 is still only a rough rule, because the air-flow pattern around a building depends on the

particular shape of the building and on the wind direction (32). Through wind tunnel studies, the critical wind speeds that will cause donwwash from various directions can be determined for a given set of plant factors (size and shape of building; shape, height, and diameter of stack; emission rate; exit velocity). Sherlock and Lesher (40) demonstrated the use of climatological data for determining the average number of hours of downwash per year for a given site. Sherlock and Lesher (40) also showed that maximum downwash about a rectangular structure occurs when the direction of thw wind is at an angle of 45 degrees from the major axis of the structure; minimum downwash occurs with the wind flow parallel to the major axis of the structure.

Briggs (70) defines three regions of building influence on the flow regime around a structure: 1) $z \geq h_b + 1.5\ L_b$, 2) $h_b + 0.5\ L_b \leq z < h_b + 1.5\ L_b$, and 3) $z < h_b + 0.5\ L_b$, where L_b is equal to the lesser of the building height, h_b, or the building width normal to the wind direction, w_b. These regions are shown in Figure 2.3a. If h' (as defined in Equation 2.38a) is greater than $h_b + 1.5\ L_b$, the plume will not be affected by the flow around the building. In this case h", the effective stack height after building aerodynamics are accounted for, is set equal to h'.

If h' falls within region 2, the flow disturbance will exert a definite influence on dispersion. In this case the stack effluent is not necessarily trapped within the turbulent cavity zone, but the plume will be drawn down by the flow, thus reducing the effective stack height. Briggs accounts for this by further adjustment of the effective stack

height as follows:

$$h'' = 2h' - (h_b + 1.5\ L_b) \tag{2.38b}$$

If the effluent is released into region 3, the emissions will concentrate within the cavity. Briggs gives the concentration within the cavity for u > 5m sec as:

$$\chi = \frac{KQ}{uL_b^2} \tag{2.38c}$$

where K is typically 1-1.5. For lower wind speeds Equation 2.38c is invalid since the cavity does not develop fully at wind speeds less than 5 m/sec. The ground level concentration downwind of the cavity is determined by applying one of two equations for reducing the effective stack height:

if $h' > h_b$: $h'' = 2h' - (h_b + 1.5\ L_b)$ (2.38d)

if $h' < h_b$: $h'' = h' - 1.5\ L_b$ (2.38e)

If the value of h" determined for region 2 or region 3 is less than $L_b/2$, the plume is treated as a ground source with an initial cross-sectional area $A = L_b^2$. If $h'' > L_b/2$, the plume remains an elevated source.

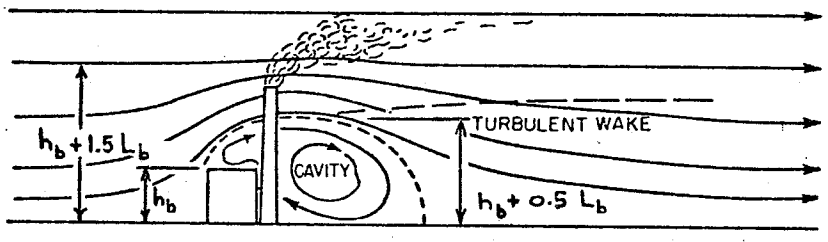

Figure 2.3a. Regions of building influence on flow regime (70).

No specific rules can be given about the effect of terrain features, partly because of the great variety of possibilities (32). Problems of

this nature can only be solved by wind tunnel modeling or on-site observations. Modeling is usually the best method. (21, 32, 41).

2.3 ATMOSPHERIC DISPERSION EQUATIONS

2.3.1 Introduction

The preceding discussions provided a qualitative description of plume behaviour and presented several mathematical formulations for calculating the effective height of a stack. This section outlines the fundamentals of estimating plume dispersion in the atmosphere.

The two basic parameters of atmospheric flow important in the short-term dispersion of stack gases from a continuous source are 1) the wind speed, and 2) the thermal and mechanical turbulence characteristics of the flow (11,22). An increase in wind speed has the direct effect of introducing the effluent gases from a continuous source into a greater volume of air per unit time interval, thus reducing the concentration. The wind turbulence serves to spread the effluent normal to the mean direction of transport, mixing it with ambient air from the surroundings.

The complexity of the variables involved in diffusion is such that no rigorous mathematical solution to dispersion problems has yet been developed. It has been found, however, that a statistical representation of the problem is often satisfactory if the governing parameters are chosen carefully. Particular attention must be paid to time and distance scales to ensure that they are not extended to such a degree that the dispersion conditions change significantly (11).

Once again, to facilitate comparison of the formulations which follow, a uniform set of symbols has been adopted. These symbols are

based upon the notation used by the American Society of Mechanical Engineers (11), Strom (20), and Turner (22), and are listed in Appendix 8.2.

2.3.2 Bosanquet and Pearson Diffusion Equation (1936)

One of the first equations to be applied to specific problems of gas plume diffusion was that of Bosanquet and Pearson (42). The Bosanquet and Pearson formulation is based on eddy diffusion theory, and neglects the comparatively small effects of kinetic diffusion and Brownian motion.

Bosanquet and Pearson (42) commence their development of a point source diffusion equation by solving for an elevated line source. The source is assumed to be at a height h above the ground, emitting a mass Q of some pollutant per unit time, with a constant wind velocity u at all points. The ground-level concentration produced by this source is given by:

$$\chi(x,y,o) = \frac{Q}{pux} \exp\left(-\frac{h}{px}\right) \qquad (2.39)$$

where p is a numerical constant. $\chi(x,y,o)$ is a maximum when $x = h/p$; when $x >> h/p$, the exponential term becomes unity, and χ decreases inversely with increasing distance.

Bosanquet and Pearson (42) then extend their solution for the elevated line source to the point source case, taking into account the additional factor of lateral diffusion. Solutions are given for estimating annual average and short term concentrations.

The annual average concentration due to a point source of strength Q and height h is given by:

$$\chi = \frac{Qa}{pux^2} \exp\left(-\frac{h}{px}\right) \qquad (2.40)$$

where u is the mean wind velocity and $a\theta$ is the fraction of the year during which the wind direction falls within an arc θ. The mean value of "a" is $1/2\pi$, and the variation of "a" with direction can be obtained from meteorological records.

For determining short term concentrations, Bosanquet and Pearson (42) specify an effective sampling period of the order of a few minutes to an hour, i.e. a period during which the mean wind direction is not likely to change appreciably. σ is given as the standard deviation referred to a vertical plane through the mean axis of the cloud, and is proportional to the downwind distance, x. In the case of gas emission, the mass m over a unit area of the earth's surface at a distance x downwind and a lateral distance y relative to the mean path of the plume is given by:

$$m = \frac{Q}{\sqrt{2\pi}\,\sigma u} \exp\left(-\frac{y^2}{2\sigma^2}\right) \qquad (2.41)$$

σ is related to downwind distance with a numerical constant q as follows:

$$\sigma = qx \qquad (2.42)$$

Substitution for σ in Equation 2.41 gives m in terms of downwind distance:

$$m = \frac{Q}{\sqrt{2\pi}\,qux} \exp\left(-\frac{y^2}{2q^2x^2}\right) \qquad (2.43)$$

This value of m is then substituted for Q in Equation 2.39 to give the ground level concentration due to a continuous point source:

$$\chi(x,y,o) = \frac{Q}{\sqrt{2\pi}\ pqx^2u} \exp\left[-\tfrac{1}{2}\left(\frac{y}{qx}\right)^2\right] \exp\left[-\frac{h}{px}\right] \qquad (2.44)$$

The concentration is at a maximum when $y = o$, and decreases to zero when $y >> \sigma$.

Bosanquet and Pearson (42) use a similar development for the case of dust with a free falling speed of f, emitted from a point source. The ground level concentration is given by:

$$\chi(x,y,o) = \frac{Q\left[1.78\ \frac{h}{p}\right]^{f/pu}}{\sqrt{2\pi}\ pqx\left(2 + \frac{f}{pu}\right)} \exp\left[-\tfrac{1}{2}\left(\frac{y}{qx}\right)^2\right] \exp\left[-\frac{h}{px}\right] \qquad (2.45)$$

Bosanquet and Pearson (42) discuss several empirical methods for determining the values of p and q, including smoke cloud observations and measurements of atmospheric eddy viscosity. An average value of $p = 0.005$ is given, with possible variations by a factor of at least 3 in either direction. This corresponds to the occurrence of the maximum ground level concentration, allowing for lateral diffusion, at a downwind distance of ten stack heights. A mean value of $q = 0.08$ is given, based on experiments with balloons. Bosanquet and Pearson give the relationship $q = \sqrt{2}\ p$ for plumes with roughly circular cross-sections, i.e. where σ is the same in the horizontal and vertical directions. In reference to Equation 2.45, the value of f for a 20 micron diameter coal particle in air is 1.5 cu/sec (42).

2.3.3. Sutton's Diffusion Equations (1947)

Reference to Sutton's original text (43) will reveal his use of the physical source height, h_s, in his diffusion equations, instead of the more accurate effective source height, h_e, used in the discussion which follows. In his paper, Sutton makes the unwarranted assumption that there is no significant rising of gas plumes because of their own buoyancy. He further states that such plumes attain ambient air temperature after travelling only a short distance downwind and that any errors introduced by neglecting plume rise are not likely to be serious. The literature on plume rise reviewed in section 2.1 proves that Sutton's assumptions regarding the significance of plume rise in diffusion analyses are invalid. Since the maximum ground level concentration produced by a dispersing gas plume is inversely proportional to the square of the stack height (or more accurately: <u>effective</u> stack height) as shown by Sutton (43) in Equation 2.50, it is evident that even a relatively small increase in the effective height of emission will in fact result in a significant reduction of the maximum ground level concentration. Therefore, in order to present a more valid representation of Sutton's diffusion equations, the author has followed the example of Strom (22) in substituting h_e for h_s in the discussion of Sutton's paper.

Sutton's diffusion equation for elevated point sources (43) is based on the approximate theory of eddy diffusion developed by Sutton for chemical warfare purposes (43). Sutton gives the following formula for gas concentration at any location downwind of a continuous point source:

$$\chi(x,y,z) = \frac{Q \exp(-y^2/C_y^2 x^{2-n})}{\pi C_y C_z u x^{2-n}} \left[\exp\left(- \frac{(z-h_e)^2}{C_z^2 x^{2-n}} \right) + \exp\left(- \frac{(z+h_e)^2}{C_z^2 x^{2-n}} \right) \right] \qquad (2.46)$$

where the variables are used with consistent units. Sutton assumes the ground to be an inert surface which does not absorb or capture the diffusing gas, and therefore allows for complete reflection of the plume by the plane z = o. The effect of plume reflection is given by the second exponential term of Equation 2.46. At ground level (z=0), Equation 2.46 reduces to:

$$\chi(x,y,0) = \frac{2Q}{\pi C_y C_z u x^{2-n}} \exp\left(- \frac{1}{x^{2-n}} \left(\frac{y^2}{C_y^2} + \frac{h_e^2}{C_z^2} \right) \right) \qquad (2.47)$$

Where the concentration is to be calculated along the centerline of the plume, Equation 2.46 may be further simplified to:

$$\chi(x,0,0) = \frac{2Q}{\pi C_y C_z u z^{2-n}} \exp\left(- \frac{h_e^2}{C_z^2 x^{2-n}} \right) \qquad (2.48)$$

Equation 2.48 can be differentiated with respect to the downwind distance x to give the point of maximum ground-level concentration along the plume centerline. The resulting expression is:

$$\chi_{max} = \left(\frac{h_e^2}{C_z^2} \right)^{\frac{1}{2-n}} \qquad (2.49)$$

The corresponding maximum ground-level concentration at y=0, $x=x_{max}$ is given by:

$$\chi_{max} = \frac{2Q}{e\pi u h_e^2}\left(\frac{C_z}{C_y}\right) \tag{2.50}$$

This equation shows that the maximum ground-level concentration varies inversely with the square of the plume height. Sutton (43) notes that Equation 2.50 is independent of the turbulence index, n.

For negligible ground effect (valid for relatively large values of h_e), maximum gas concentration at a given x occurs on the axis of the plume, a horizontal line through the virtual source at $z=h_e$, y=0, in the direction of the mean wind. Strom (20) gives the following expression for axial concentration based on Sutton's equation (43):

$$\chi_{axial} = \frac{Q}{\pi C_y C_z u x^{2-n}} \tag{2.51}$$

Axial concentration is the greatest at the source; it is infinite for the point source assumed in the above equations. In all cases, the concentration varies inversely with the wind speed.

The quantities C_y and C_z are virtual diffusion coefficients for the crosswind (y) and vertical (z) directions, respectively, with values given by:

$$C_y^2 = \left(\frac{4\nu^n}{(1-n)(2-n)u^n}\right)\left(\frac{\overline{v'^2}}{u^2}\right)^{1-n} \tag{2.52}$$

$$C_z^2 = \left(\frac{4\nu^n}{(1-n)(2-n)u^n}\right)\left(\frac{\overline{w'^2}}{u^2}\right)^{1-n} \qquad (2.53)$$

The quantity n is a dimensionless number between 0 and 1, related to the diffusing power of the turbulence. In the development of Equation 2.46 it is assumed that the wind speed and diffusion coefficients are constant with height, even though a gradient of wind speed is needed to produce mechanical turbulence over flat ground (22). Since these parameters usually do vary with height in the real atmosphere, however, specific values must be chosen. For axial concentrations, values of u, C_y, and C_z at plume level are appropriate (22). For computing ground-level concentrations, mean values over the height of the stack may be used (43).

The value of n can be determined by measuring the vertical transfer of momentum as indicated by the wind shear near the surface (43), but this is a difficult procedure according to Strom (20). Sutton (43) gives an alternate method of obtaining n by relating it to the mean wind velocity profile using the following power law:

$$u = u_1(z/z_1)^{\frac{n}{2-n}} \qquad (2.54)$$

where u is the wind velocity at elevation z and u_1 is the velocity at the reference level z_1.

Sutton's relationship for the diffusion coefficients in terms of turbulence characteristics (43) are given in Equations 2.52 and 2.53. These equations show that C_y and C_z depend primarily upon the value of n and the magnitude of the "gustiness factors" $\overline{v'^2}/u^2$ and $\overline{w'^2}/u^2$ and only slightly upon u, the mean wind speed. Due to the extreme variability

of the gustiness factors, it is difficult to choose representative mean values for C_y and C_z (43). Therefore, the practice in field experiments has been to determine the coefficients from measurements of concentration distribution by applying Equation 2.46. Sutton (43) gives surface values of C_y and C_z taken to agree with data obtained at Porton, England;these values, listed in Table 2.6, are based on conditions of small lapse rate, with gustiness appropriate to winds over relatively smooth, rolling terrain and u=5m/sec. The diffusion coefficients were determined for a 3-minute sampling period.

TABLE 2.6

VALUES OF DIFFUSION COEFFICIENTS ADOPTED

FOR EQUATIONS 2.38 TO 2.44, SUTTON (43).

HEIGHT OF SOURCE ABOVE GROUND (m)	C_y $(m^{n/2})$	C_z $(m^{n/2})$
0	0.21	0.12
10	0.21	0.12
25	0.12	0.12
50	0.10	0.10
75	0.09	0.09
100	0.07	0.07

Near the ground C_y tends to be greater than C_z due to the suppression of the vertical component of the turbulence, but with an increase in elevation turbulence becomes more nearly isotropic (22). Sutton (43) gives equal values of C_y and C_z for heights greater than or equal to 25 meters, as shown in Table 2.6. Suttton also gives values of n, u, and

w'/u for various atmospheric lapse rates, but no observational data are quoted to support them.

2.3.4 Gaussian Diffusion Equations

Many widely-used dispersion equations are based on the concept that the concentration distribution of a dispersing plume or cloud is Gaussian. Most of the practical dispersion formulations are comprised of the Gaussian, or normal distribution function, plus an expression for the mean-square particle diffusion (44). During recent years these formulas have undergone considerable revision, primarily due to the results of experimental measurements by Hay and Pasquill (45,49), Cramer (46,47,48), Pasquill (50), Gifford (51,52), Carpenter et al. (53), and Montgomery et al. (54). Several of the better-known formulas and their modifications applicable to continuous elevated point sources are presented in the subsequent sections.

2.3.4.1 Gaussian Form of Sutton's Diffusion Equation

The Gaussian diffusion equation is based on the assumption that the spread of a plume can be represented by a Gaussian distribution in both the horizontal and vertical planes, with standard deviations of the plume concentration distribution given by σ_y and σ_z respectively. Further assumptions include (22,44): a mean wind velocity, u, with the mean direction specifying the x-axis and the mean wind speed representative of the diffusing layer chosen;a uniform pollutant emission rate, Q; total reflection of the plume at the earth's surface, i.e. no reaction or deposition of pollutants at the surface;and values of σ_y and σ_z representative of approximately 10-minute sampling periods.

The Gaussian form of Sutton's diffusion equation (43) is easily obtained by substituting σ_y and σ_z for Sutton's parameters in Equation 2.46. The resulting equation is:

$$\chi(x,y,z) = \frac{Q}{2\pi\sigma_y\sigma_z u} \exp\left[-\tfrac{1}{2}\left(\frac{y}{\sigma_y}\right)^2\right]\left[\exp\left[-\tfrac{1}{2}\left(\frac{z-h_e}{\sigma_z}\right)^2\right] + \exp\left[-\tfrac{1}{2}\left(\frac{z+h_e}{\sigma_z}\right)^2\right]\right] \qquad (2.55)$$

where σ_y and σ_z are related to Sutton's parameters as given in Equations 2.56 and 2.57 by Turner (22):

$$\sigma_y = \frac{1}{\sqrt{2}} C_y x^{(2-n)/2} \qquad (2.56)$$

$$\sigma_z = \frac{1}{\sqrt{2}} C_z x^{(2-n)/2} \qquad (2.57)$$

Equation 2.55 is valid where diffusion in the x-direction (direction of plume travel) can be neglected. This assumption can be made if the release is continuous or if the duration of release is equal to or greater than the travel time (x/u) from the source to the location of interest (22).

For concentrations calculated at ground level, i.e. z=0, Equation 2.55 simplifies to:

$$\chi(x,y,0) = \frac{Q}{\pi\sigma_y\sigma_z u} \exp\left[-\tfrac{1}{2}\left(\frac{y}{y}\right)^2\right] \exp\left[-\tfrac{1}{2}\left(\frac{h_e}{z}\right)^2\right] \qquad (2.58)$$

For ground-level concentrations along the plume centerline (y=0), Equation 2.58 reduces to:

$$\chi(x,0,0) = \frac{Q}{\pi\sigma_y\sigma_z u} \exp\left[-\tfrac{1}{2}\left(\frac{h_e}{\sigma_z}\right)^2\right] \qquad (2.59)$$

Strom (20) points out that when Equations 2.56 and 2.57 are applied to field concentration data, the values of n for the two equations may differ. When σ_y and σ_z have the same functional form with respect to downwind distance, the maximum ground-level concentration on the plume centerline is given by:

$$\chi_{max}(x,0,0) = \frac{2Q}{\pi e u h_e^2} \frac{\sigma_z}{\sigma_y} \qquad (2.60)$$

The empirical coefficients σ_y and σ_z are evaluated in terms of the downwind distance, x. Values for these parameters are discussed in section 2.3.5.

2.3.4.2 Concentrations During Inversion Break-Up Fumigations

A ground-based inversion may be dissipated by the upward transfer of sensible heat from the ground surface when the ground is warmer than the overlying air. This situation occurs when the ground is being warmed by solar radiation or when air flows from a cold to a relatively warm surface. In either case, pollutants previously emitted above the surface into the stable inversion layer will be mixed rapidly downward to the ground when they are reached by the thermal eddies of the unstable layer developing upward from the ground (22,44). This process, referred to as "fumigation" by Hewson and Gill (55), commonly occurs in the morning after a night of marked stability, and may produce high ground-level

concentrations for a period on the order of one-half to two hours, depending on the season and local conditions (20,44).

Equations for estimating concentrations under fumigation conditions have been given by Holland (25), Hewson (56), Gifford (51), Bierly and Hewson (57), and Pooler (58).

Holland's equation for concentration along the plume centerline during fumigation, χ_F, is given by (25):

$$\chi_F(x,0,z) = \frac{Q}{\sqrt{\pi}\, C_y u h_i x^{(2-n)/2}} \qquad (2.61)$$

This equation is obtained by integrating Equation 2.46 (Sutton's diffusion equation) with respect to z from 0 to ∞ and distributing the result uniformly over the layer depth, h_i, which at the onset of fumigation is equal to the effective source height, h_e. The values of C_y, u, and n should be those appropriate to the inversion prior to fumigation (20).

Hewson (56) bases his fumigation equation on the assumption that the inversion plume before break-up has the form of a pie-shaped wedge of 5^o included angle and constant thickness. During fumigation the plume is treated as diffusing downward uniformly throughout a volume determined by the plume dimensions before break-up. Hewson gives the following equation for estimating the ground-level concentration during fumigation (56):

$$\chi(x_1 \to x_2,0,0) = \frac{36Q}{\pi u h_e (x_1+x_2)} \qquad (2.62)$$

χ, Q, u, and h_e are defined as they were for Equation 2.46, and x_1 and x_2

are the downwind distances to two locations between which the concentration is desired. For the concentration at a location x, (x_1+x_2) is replaced by 2x, giving the result:

$$\chi(x,0,0) = \frac{18Q}{\pi u h_e x} \tag{2.63}$$

Gifford's formula for the fumigation condition (51) is simply the Gaussian equivalent of Holland's formula (Equation 2.61), using the standard deviation σ_y in place of Sutton's parameters C_y and $x^{(2-n)/2}$. Gifford's equation for the fumigation concentration, χ_F, at y=0, is given by:

$$\chi_F = \frac{Q}{\sqrt{\pi}\,\sigma_y u h_i} \tag{2.64}$$

where h_i is the height of the base of the inversion.

The equation given by Bierly and Hewson (57) is based on the assumption that the plume is initially emitted into the inversion layer. Therefore, values of σ_y and σ_z characteristic of stable condtions must be selected for the downwind distance being examined. Bierly and Hewson give the following equation for the ground-level concentration when the inversion has been eliminated to a height h_i:

$$\chi_F(x,y,0) = \frac{Q \int_{-\infty}^{p} \frac{1}{\sqrt{2\pi}} \exp(-0.5\, p^2)\, dp}{\sqrt{2\pi}\,\sigma_{y_F}\, u\, h_i} \exp\left[-\tfrac{1}{2}\left(\frac{y}{y_F}\right)^2\right] \tag{2.65}$$

where $p = \dfrac{h_i - h_e}{\sigma_z}$.

The factor given by the integral in Equation 2.65 accounts for the portion of the plume that is mixed downward. If the inversion is eliminated up to the effective stack height, half of the plume is considered to be mixed downward, while the other half remains in the stable air above. Turner (22) gives the following approximation to Equation 2.65 when the fumigation concentration is near its maximum:

$$\chi_F(x,y,0) = \frac{Q}{\sqrt{2\pi}\, u\, \sigma_{y_F} h_i} \exp\left[-\tfrac{1}{2}\left(\frac{y}{\sigma_{y_F}}\right)^2\right] \qquad (2.66)$$

where $$h_i = h_e + 2\sigma_z \qquad (2.67)$$

Turner (22) points out the difficulty encountered in estimating a reasonable value for the horizontal dispersion during fumigation. This is due to the additional horizontal spreading which occurs when the stable plume is mixed through the vertical depth h_i. Neglect of this spreading while using the σ_y for the stable conditions tends to produce estimated concentrations higher than those actually observed. This effect may be compensated for by using an approximation for σ_{y_F} given by Bierly and Hewson (57). Bierly and Hewson assume that the edge of the plume is defined by the point at which the concentration equals one-tenth of the centerline concentration (i.e. at a distance of $2.15\sigma_y$ from the plume axis). It is further assumed that the edge of the plume spreads outward at an angle of 15^o. The resulting approximation for σ_{y_F} is given by:

$$\sigma_{y_F} = \frac{2.15\, y_{(stable)} + h_e \tan 15^o}{2.15} \qquad (2.68)$$

A Gaussian distribution in the horizontal is assumed as shown in Figure 2.4.

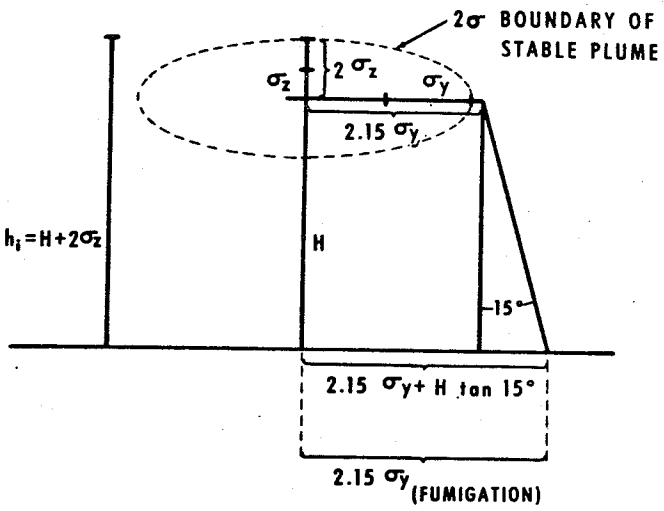

Figure 2.4. Diagram showing assumed height, h_i, and σ_y during fumigation;for use in Equation 2.66 (22).

Equation 2.68 should not be applied near the stack since the emission will be taking place under unstable not stable conditions if the inversion has been eliminated to a height sufficient to include the entire plume (22). Therefore the nearest downwind distance to be considered for an estimate of fumigation concentrations must be great enough, based on the time required to eliminate the inversion, that the portion of the plume considered was initially emitted into stable air. This distance is $x=ut_m$, where u is the mean wind speed in the stable layer and t_m is the time required to eliminate the inversion from h_s, the physical stack height, to h_i. The value of t_m is dependent upon both the strength of the inversion and the rate of heating at the surface. Pooler (58) gives the following expression for estimating t_m:

$$t_m = \frac{\rho_a c_p}{R} \frac{\partial\theta}{\partial z} (h_i - h_s) \left(\frac{h_s + h_i}{z} \right) \tag{2.69}$$

The term $(h_i - h_e)$ is the thickness of the layer to be heated and $(h_e + h_i)/z$ is the average height of the layer (22). Although R is dependent upon the season and cloud cover, Pooler (58) uses a value of $R = 67$ cal/m^2/sec as an average value for fumigation conditions.

Hewson (60) also gave a method for estimating t_m:

$$t_m = \frac{h_i^2 - h_s^2}{4K} \tag{2.70}$$

Hewson suggests a value of 3 m^2/sec for K, the eddy diffusivity for heat.

2.3.4.3 Limited Mixing

Limited mixing occurs when the plume is trapped between the ground surface and an elevated inversion layer. Bierly and Hewson (57) give the following equation that accounts for the multiple eddy reflections from both the ground and the stable layer aloft under trapping conditions:

$$\chi(x,o,z) = \frac{Q}{2\pi u \sigma_y \sigma_z} \left[\exp\left(-\tfrac{1}{2} \left(\frac{z-h_e}{\sigma_z} \right)^2 \right) + \exp\left(-\tfrac{1}{2} \left(\frac{z+h_e}{\sigma_z} \right)^2 \right) \right.$$

$$+ \sum_{N=1}^{N=J} \left[\exp\left(-\tfrac{1}{2} \left(\frac{z-h_e-2NL}{\sigma_z} \right)^2 \right) + \exp\left(-\tfrac{1}{2} \left(\frac{z+h_e-2NL}{\sigma_z} \right)^2 \right) \right.$$

$$\left. \left. + \exp\left(-\tfrac{1}{2} \left(\frac{z-h_e+2NL}{\sigma_z} \right)^2 \right) + \exp\left(-\tfrac{1}{2} \left(\frac{z+h_e+2NL}{\sigma_z} \right)^2 \right) \right] \right] \tag{2.71}$$

where L is the height of the stable layer and J=3 or J=4 is sufficient to include the important reflections. Turner (22) approximates Equation 2.71 by assuming that the concentration is not affected by the stable layer until $\sigma_z = 0.47L$. It is assumed that at this distance, x_L, the stable layer begins to affect the vertical distribution so that at the downwind distance $2x_L$, uniform vertical mixing has taken place and the following equation can be used:

$$\chi(x,y,z) = \frac{Q}{\sqrt{2\pi}\sigma_y LU} \exp\left[-\tfrac{1}{2}\left(\frac{y}{\sigma_y}\right)^2\right] \qquad (2.72)$$

For distance between x_L and $2x_L$ the best estimate to the ground level centerline concentration is that read from a straight line drawn between the concentrations at x_L and $2x_L$ on a log-log plot of ground level centerline concentration as a function of distance (22).

2.3.4.4 Effects of Extended Sampling Times on Concentration Estimates

Concentrations directly downwind from a source decrease with increased sampling time mainly because of a larger σ_y due to increased meander of wind direction (22). Several investigators have given relationships for the variation of maximum mean concentration with sampling period, for sampling periods ranging from a few minutes to an hour (20). These are summarized in Table 2.7.

The relationships of Stewart et al. (61) and Cramer (48) are both based on observations taken near the height of release. Nonhebel's relationship is based upon published dispersion coefficients rather than upon sampling results.

TABLE 2.7

SUMMARY OF RELATIONSHIPS FOR VARIATION OF MAXIMUM MEAN CONCENTRATION WITH SAMPLING PERIOD

Investigators	Sampling Period	Relationship for χ_t vs. t_s
Stewart, Gale, and Crooks (61)	3 - 30 minutes	$\chi_2 = \chi_1 \left(\frac{t_1}{t_2}\right)^{.2}$
Cramer (48)	3 seconds - 10 minutes	$\chi_2 = \chi_1 \left(\frac{t_1}{t_2}\right)^{.2}$
Nonhebel (38)	3 minutes - 24 hours	$\chi_2 = \chi_1 \left(\frac{t_1}{t_2}\right)^{.17}$

Gifford (62) indicates that the ratios of peak to mean concentrations are much higher than those given by the power laws in Table 2.7 where the observations of concentrations are made at heights considerably different from the height of release or considerably removed from the plume axis. He also shows that for increasing distances from an elevated source, the ratios of peak to average concentrations observed at ground level approach unity.

Singer (63) and Singer, Imai, and Del Campo (64) have shown that the ratios of peak to mean concentrations also depend on atmospheric stability and the type of terrain beneath the plume. Singer et al. (64) found reduced changes in peak concentration versus sampling period for

sampling times less than 5 minutes. They also found that increased surface roughness reduces the effect of sampling period on peak concentrations.

Turner (22) notes that complexity of sampling time effects given in the literature, and gives the following equation as the best estimate of concentrations from a single source for time intervals greater than a few minutes:

$$\chi_s = \chi_k \left(\frac{t_k}{t_s} \right)^p \qquad (2.73)$$

where χ_s is the desired concentration for the sampling time, t_s; χ_k is the concentration for the shorter sampling time, t_k, (probably about 10 minutes); and p should be between 0.17 and 0.2. Equation 2.73 would be most appropriate for sampling times less than 2 hours.

The curves of Figure 2.5 given by Briggs (65) show the approximate ratios of peak or longer term ground concentrations to 30 minute average ground concentrations. Briggs cautions that on infrequent occasions the values of χ might be twice as great as those computed using Figure 2.5.

2.3.4.5 Long-Term Average Concentrations

Estimates of seasonal or annual average concentrations can be made for any distance in any direction if stability wind "rose" data are available for the period under study, provided that the source emits at a constant rate from hour to hour and day to day (22). A wind rose gives the frequency of occurrence for each wind direction section (usually for 16 sectors of $22\frac{1}{2}^o$ width) and wind speed class (9 classes in standard

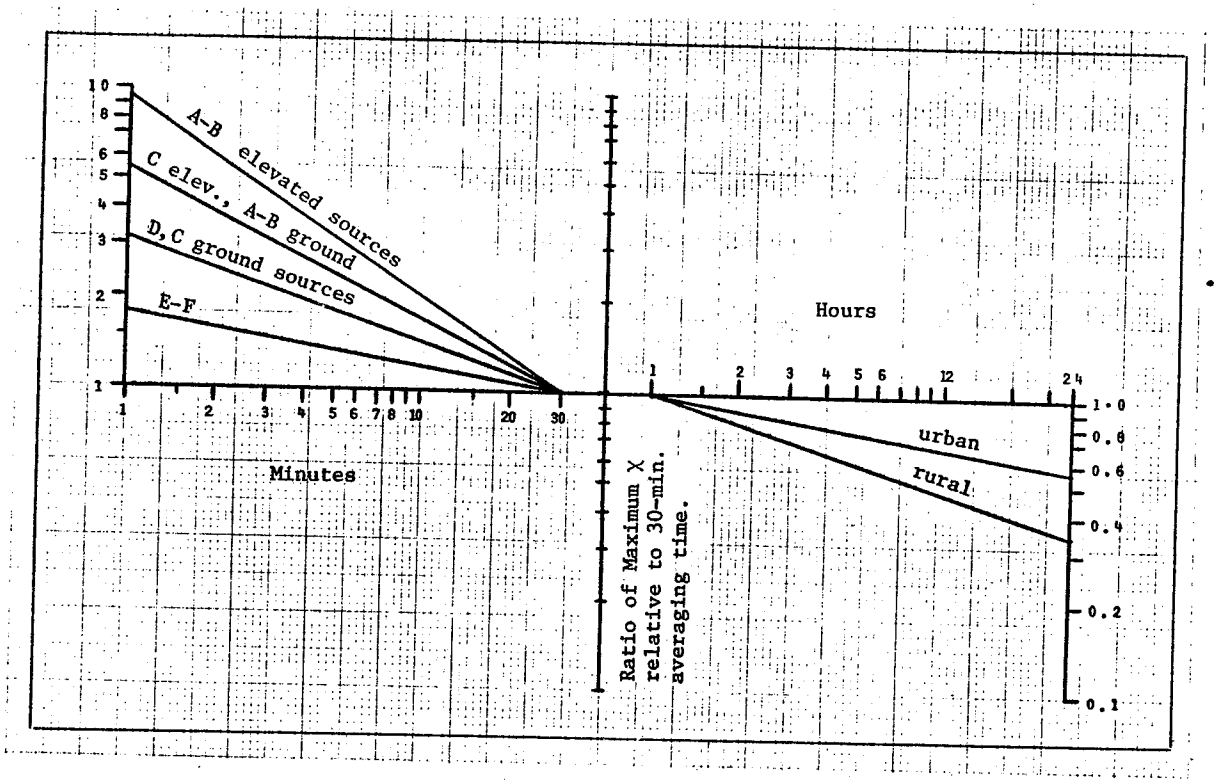

Figure 2.5. Maximum χ (relative to 30-minutes) versus averaging time, Briggs (65).

meteorological tabulations) for the period under consideration. A stability wind rose gives the same type of information for each stability class.

In determining long term average concentrations it is assumed that the wind directions within each sector are randomly distributed over a period of a month or a season (22). It is further assumed that the effluent is uniformly distributed horizontally within the sector (25).

Gifford (51) gives the following equation for the long-term average concentration at a given location:

$$\chi_{avg} = \frac{2Q(f/100)}{\sqrt{2\pi}\sigma_z u} \exp\left[-\tfrac{1}{2}\left(\frac{h_e}{\sigma_z}\right)^2\right] \qquad (2.74)$$

where f is the frequency in percent per radian with which the wind blows toward the chosen location.

Turner (22) gives two equations for the average concentration within a $22\tfrac{1}{2}^{o}$ wind direction sector, the latter (Equation 2.76) being applied where an elevated stable layer affects the distribution. The equations are as follows:

$$\chi_{avg} = \frac{2Q}{\sqrt{2\pi}\sigma_z u\left(\frac{2\pi x}{16}\right)} \exp\left[-\tfrac{1}{2}\left(\frac{h_e}{\sigma_z}\right)^2\right] \qquad (2.75)$$

$$\chi_{avg} = \frac{Q}{Lu\left(\frac{2\pi x}{16}\right)} \qquad (2.76)$$

χ_{avg} for a particular direction and downwind distance can be estimated by choosing a representative wind speed for each speed class and solving the appropriate equation (2.75 or 2.76) for all wind speed classes and stabilities. The resulting concentrations are weighted, each according to its frequency for the particular stability and wind speed class. The weighted concentrations are then summed to yield the long-term average

concentration for the chosen direction and distance. Different effective stack heights may be used for various wind speeds. The average concentration can be expressed by (22):

$$\chi_{avg} = \sum_S \sum_N \left[\frac{2Qf(\theta,S,N)}{\sqrt{2\pi}\sigma_{zS} u_N \left(\frac{2\pi x}{16}\right)} \exp\left(-\tfrac{1}{2} \left(\frac{h_{eN}}{\sigma_{zS}} \right)^2 \right) \right] \qquad (2.77)$$

where $f(\theta,S,N)$ = frequency during the period of interest that the wind is from the direction θ, for the stability condition S, and the wind speed N.

σ_{zS} = vertical dispersion parameter evaluated at the distance x for the stability condition S.

u_N = representative wind speed for class N.

h_{eN} = effective height of release for the wind speed u_N.

Where stability wind rose information cannot be obtained, a first-order approximation of seasonal or annual average concentrations may be made by using the appropriate wind rose in the same manner given above, and assuming the neutral stability class, D, only (22).

2.3.4.6 Multiple Sources

In cases where it is desired to determine the concentration at a receptor point resulting from several sources, the normal procedure is to consider the receptor as being at the origin of the diffusion coordinate system. Sutton (43) and Gifford (66) have both shown that the concentration at this point (0,0,0) due to a source at (x,y,h_e) on a coordinate system

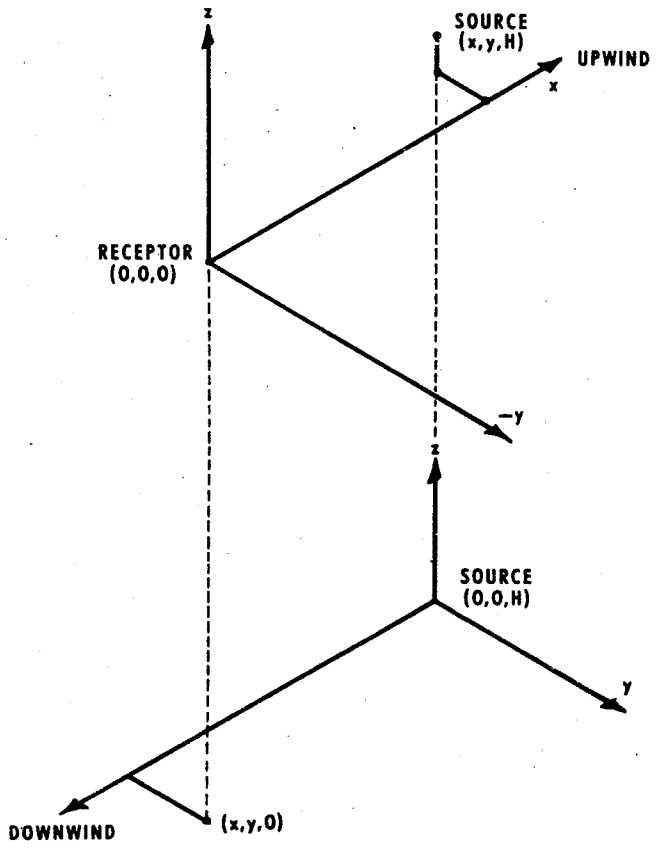

Figure 2.6. Comparison of source-oriented and receptor-oriented coordinate systems (22).

with the x-axis oriented upwind is the same as the concentration at (x,y,o) from a source at $(0,0,h_e)$ on a coordinate system with the x-axis oriented downwind. These two coordinate systems are compared in Figure 2.6. The total concentration at the receptor is thus obtained by summing the individual contributions from each source (22,44).

Turner (22) points out the difficulty of determining the atmospheric conditions of wind direction, wind speed, and stability which will result in the maximum combined concentrations from two or more sources; he recommends the drawing of concentration isopleths for various wind speeds and stabilities and orienting these according to the wind direction as a solution to this problem.

2.3.5 Comparison of Atmospheric Dispersion Equations

Bosanquet and Pearson (42) used dimensional analysis to develop a theoretical formulation for calculating the spreading of a smoke plume from a chimney. They have shown their results to agree reasonably well with experimental data. The average value of the vertical diffusion coefficient, $p \simeq 0.05$, varies from experimental values by a maximum factor of 3. The mean value of the horizontal diffusion coefficient, q, is given as 0.08, as determined experimentally (42); for plumes of roughly circular cross-section, the corresponding theoretical value of p is 0.057, which agrees with the mean value of p given above.

Sutton's diffusion model (43) has been widely proven in practice. The work of Bosanquet and Pearson (42) discussed above has been shown to be in general qualitative agreement with Sutton's equations, but Sutton's expressions have the advantages of greater accuracy and a development

based on both theoretical and empirical considerations (44). Sutton's model should not be applied universally since it has only been verified over a limited range of distance and meteorological conditions. Good correlations between diffusion predictions by Sutton's model and actual downwind concentrations have been obtained for distances of the order of several kilometers under neutral or unstable conditions (44). The theoretical concentrations are likely to be accurate within a factor of 2 over flat terrain within about 10 km of the source, and within a factor of 5 at greater distances (43).

The Gaussian form of Sutton's diffusion equation agrees well with much of the presently available atmospheric data, and Gaussian plume models (sections 2.3.4.1 to 2.3.4.6) have proven to be reasonably successful in providing a practical mathematical description of observed concentration patterns (22,44). The Gaussian model has several advantages: 1) only two dispersion parameters, σ_y and σ_z, are required; 2) the Gaussian form of the concentration equation is more flexible than Sutton's original expression in that the standard deviations, σ_y and σ_z, are not restricted to a power-law relationship with distance, as are Sutton's coefficients C_y and C_z; 3) the results of most diffusion experiments are now being reported in terms of the standard deviations of plume, spread, σ_y, and σ_z, required by the Gaussian model. These advantages, combined with previous successful applications of the Gaussian models to diffusion problems provide the rationale for the use of the Gaussian equations in the evaluation presented in this paper.

2.4 ESTIMATION OF HORIZONTAL AND VERTICAL DIFFUSION COEFFICIENTS

2.4.1 Introduction

For practical use to be made of diffusion formulas numerical values for the diffusion coefficients σ_y and σ_z must be determined. These parameters depend on ground roughness, atmophseric stability and turbulence, height above the ground, sampling time over which the concentration is to be estimated, wind speed, and distance from the source (22). The results of various field-diffusion experiments have been given in diffusion parameter form by several authors. Among the better known investigations are those of Hay and Pasquill (45,49), Cramer (46,47,48), Sutton (43), Pasquill (50), and Gifford (51,52).

2.4.2 Sutton's Diffusion Coefficients (1947)

The diffusion coefficients used by Sutton have been discussed at length in section 2.3.3. The quantities C_y and C_z are virtual diffusion coefficients for the crosswind and vertical directions, respectively. Their values are given by Equations 2.52 and 2.53. The turbulence index, n, used in computing C_y and C_z, is a dimensionless number, varying from almost zero for very turbulent air to an upper limit of unity for conditions of low turbulence.

The value of n can be determined by measuring the vertical momentum shear at the surface (43), but this is a difficult procedure (22). Sutton gives an alternate method of determining n by relating it to the mean wind velocity profile in terms of the power law given in Equation 2.54.

Equations 2.52 and 2.53 also show the values of C_y and C_z to be dependent upon the magnitude of the "gustiness factors" $\overline{v'^2}/u^2$ and $\overline{w'^2}/u^2$,

respectively. These factors are extremely variable, however, making the choice of representative mean values for C_y and C_z difficult (43). The practice in field experiments has therefore been to determine the coefficients C_y and C_z by applying Sutton's diffusion equation (Equation 2.46) to measurements of concentration distribution.

2.4.3 Hay and Pasquill Diffusion Coefficients

2.4.3.1 Hay and Pasquill (1957)

Hay and Pasquill (45,49) were two of the first investigators to relate plume dispersion to wind direction fluctuations. Their first paper (45) is based on a continuous source dispersion experiment carried out at Porton Downs, England. This paper presents evidence that the vertical distribution of spreading particles from an elevated point source is related to the standard deviation of the wind elevation angle, σ_e, at the point of release. In the experiment a continuous source of Lycopodium spores was generated at 150 m above the ground and sampled at downwind distances of 100-500 m by a series of samplers suspended along the cable of a barrage balloon. Hay and Pasquill give the results of 10 trials, each lasting approximately 30 minutes. It was found that σ_e, measured in degrees at the height of the source, was very similar to σ_z, the standard deviation of the vertical spread of particles, also measured in degrees, to distances of 500 m. The ratio σ_z/σ_e varied from 0.94 to 1.25 in eight of the trials; the other two trials yielded values outside this range as a result of marked inhomogeneity in the turbulence. The average arc value of σ_z for slightly unstable to slight inverstion conditions was $\simeq 3.9^{o}$.

2.4.3.2 Hay and Pasquill (1959)

In a later paper published in 1959, Hay and Pasquill (49) presented a method of estimating the lateral plume spread from measurements of wind-direction fluctuations made with a suitably responsive wind vane. In this case, a source height of 2 m and a sampling period of 3 minutes were used. Lycopodium spores were again released continuously from a mechanical dispenser, and samples of the resulting plume were collected on small adhesive cylinders along an arc 100 m downwind of the source. The basis of the experiment was the theoretical expression for the spread of serially released particles, given by Pasquill (68) as follows:

$$\overline{Y^2} = \overline{v'^2_{\tau,s}}\ t^2 \qquad \text{for } \tau > t \tag{2.78}$$

where $v'^2_{\tau,s}$ = variance of the lateral component of the eddy velocity, for the time parameters τ and s.

$s=t/\beta$ = averaging time of the variance $\overline{v'^2_{\tau,s}}$

τ = sampling time, equal to the duration of release of particles (or to the duration of the sampling of the distribution of particles)

β = ratio of the Lagrangian time-scale of turbulence to the time-scale deduced from(Eulerian) measurements of the turbulent fluctuations at a fixed point.

$\overline{Y^2}$ = variance of the wind-direction fluctuation

t = time of travel of plume.

Hay and Pasquill (49) converted Equation 2.78 into angular form for small angles:

$$\sigma_p^2 = \sigma_{\theta_{\tau,s}}^2 \qquad (2.79)$$

where $\sigma_{\theta_{\tau,s}}^2$ = variance of wind direction for sampling time τ and averaging time s.

σ_p^2 = variance of bearings of the particles from the point of release.

The ultimate goal of the Hay and Pasquill experiment (49) was to determine the values of β (and therefore the values of the averaging time s) required to satisfy Equation 2.79, thereby allowing the use of wind-direction records for estimating plume diffusion.

The values of β for each of 8 trials were obtained by first evaluating the standard deviation of the wind direction record over the 3-minute duration of release and for various averaging times, and then selecting the averaging time s at which this standard deviation was equal to the observed value of σ_p. This gave $s = t/\beta = x/u\beta$, with x = 100 m and u the mean wind speed during the time of release. The values of β obtained range from 1.1 to 8.5, with a mean value of about 4. Figure 2.7 demonstrates the practical acceptability of a constant value of β equal to the mean. The observed and computed values of σ_p are compared; for $\beta = 4$ the two worst discrepancies are only 10% and 30%.

Hay and Pasquill (49) also examined the variation of the computed value of cloud spread with downwind distance. A power-law relationship is given:

$$\sigma_p \propto x^q \qquad (2.80)$$

with q = -0.21 (for angular measure) corresponding to near-neutral conditions.

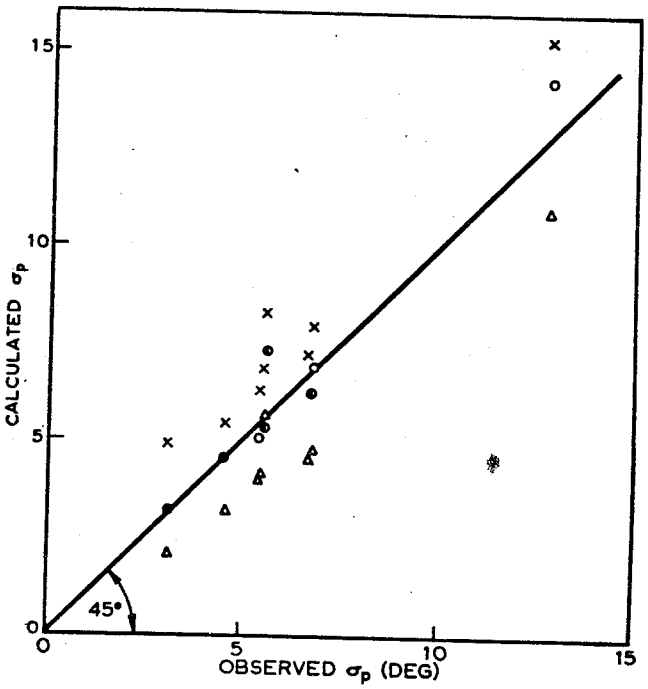

Figure 2.7. Comparison of observed and calculated angular values of cross-wind spread σ_p, at 100 meters from a continuous point source, Hay and Pasquill (49).

2.4.4 Cramer Diffusion Coefficients (1957-1959)

In 1957, Cramer (46) published a set of three graphs. σ_y and σ_z or the concentration $\bar{\chi}$, for distances up to 1.6 km could be determined directly from a knowledge of the horizontal wind-direction standard deviation, σ_θ. The curves in these graphs were based on data from the Round Hill Field Station at the Massachusetts Institute of Technology and from the Project Prairie Grass site at O'Neill, Nebraska (46). A sulfur dioxide tracer was used at both locations, with a source height of 0.5 in. The tracer was sampled along semicircular arcs at 50-800 m from the source, 1.5 m above the ground. Vertical concentration distributions were sampled from 6-20 m towers along the 100 m arc.

A sampling period of 10 minutes was used in measuring both wind fluctuations and ground-level tracer concentrations downwind. An important feature of these investigations was the use of fast-response instruments to give accurate observations of the lateral and vertical wind fluctuations.

In 1958 and 1959, Cramer published several comprehensive studies of the variations in basic diffusion parameters in all thermal stratifications (47,48), providing a method for estimating atmospheric dispersion using direct meteorological indicators.

The revised graphs given by Cramer (48) allow the determination of small-scale diffusion parameters using either wind records or atmospheric stability measurements. These graphs are shown in Figures 2.8 to 2.10. Cramer's stability classes are given in Tables 2.8 and 2.9.

TABLE 2.8

SMALL-SCALE DISPERSAL PARAMETERS FOR

VARIOUS THERMAL STRATIFICATIONS, CRAMER(48)

THERMAL STRATIFICATION	σ_θ (deg)	σ_e (deg)	b	a
Extremely unstable	25 - 30	8 - 30	1.1	0.9
Moderately unstable	15 - 20	6 - 8	1.1	0.9
Near-neutral	6 - 15	3 - 5	1.0	0.85
Moderately stable	5 - 15	2 - 4	0.8*	0.8*
Extremely stable	2 - 15	0 - 2	0.6*	0.7*

(Entries marked with an asterisk apply strictly at travel distances of the order of 0.5 miles and should not be used for appreciably longer or shorter distances.)

Cramer (48) describes the distance dependence of σ_y and σ_z by two simple power-law equations:

$$\sigma_y = \sigma_\theta x^a \tag{2.81}$$

$$\sigma_z = \sigma_e x^b \tag{2.82}$$

where σ_θ and σ_e are in radians and a and b are constants, as given in Table 2.8. Cramer limits the applicability of these equations to maximum travel distances of the order of one mile in all stability conditions except for extreme instability or stability.

TABLE 2.9

VALUES OF THE STANDARD DEVIATIONS OF AZIMUTH ANGLE σ_θ AND ELEVATION ANGLE σ_e ASSOCIATED WITH THE THERMAL STRATIFICATIONS OF FIGURES 2.8, 2.9, AND 2.10, CRAMER (48)

THERMAL STRATIFICATION	σ_θ (deg)	σ_e (deg)
Extremely unstable	30	10
Near-neutral (rough surface)	15	5
Near-neutral (smooth surface)	6	2
Extremely stable	3	1

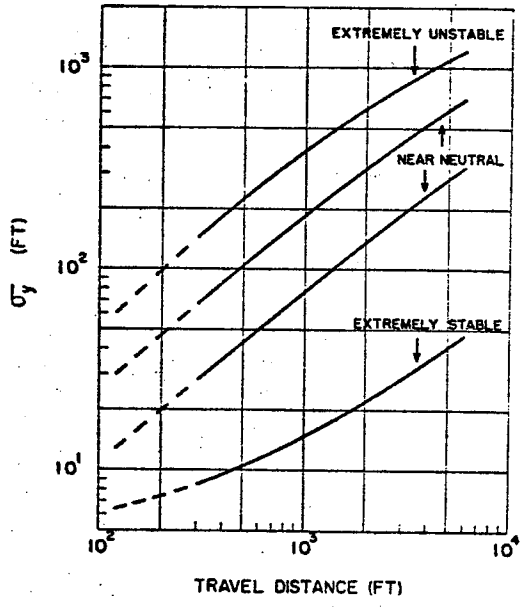

Figure 2.8. Estimates of crossplume standard deviation of concentration downwind from a continuous elevated point source in various thermal stratifications. Dashed lines indicate minimum values for area source. Estimates refer to ten-minute sampling time. Cramer (48).

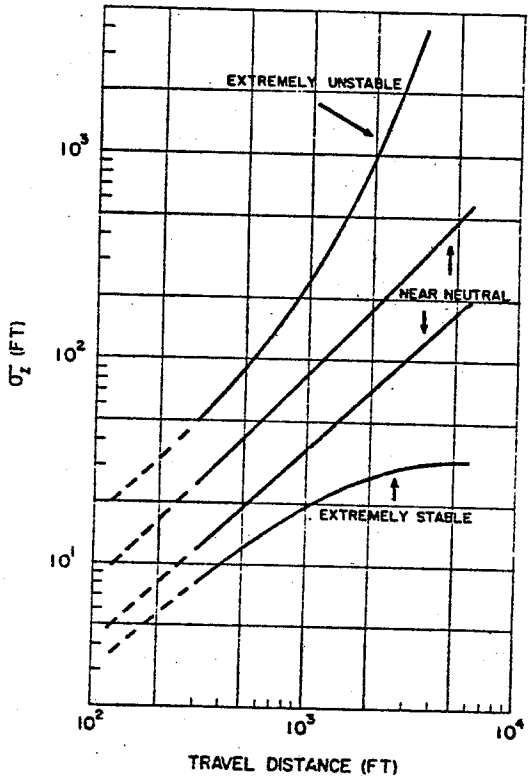

Figure 2.9. Estimates of vertical standard deviation of concentration downwind from a continuous elevated point source in various thermal stabilities. Dashed lines indicate minimum values for area source. Cramer (48).

Cramer states that the entries for σ_θ in stable stratifications account for the long-term meandering frequently observed during inversions. Exclusion of this factor would place an upper limit for σ_θ of $\simeq 4^o$ for extremely stable conditions. Cramer also cites the need for a satisfactory empirical determination of the exponent p for continuous elevated sources in the presence of extreme instability (48).

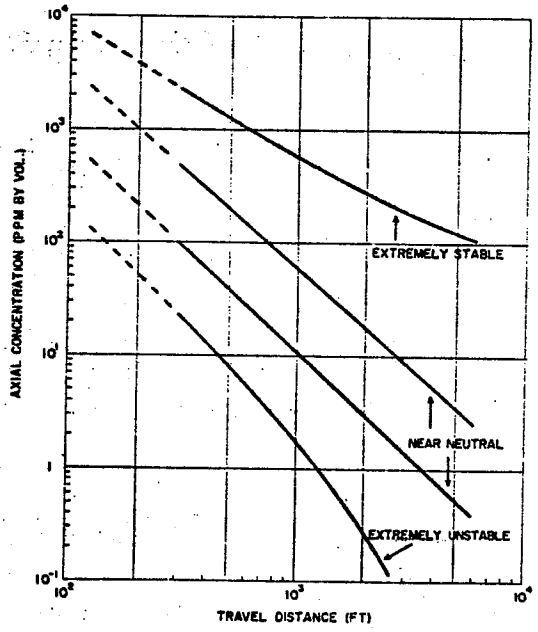

Figure 2.10. Axial concentration downwind from a continuous elevated point source in various thermal stratifications. Concentrations refer to ten-minute sampling interval and are adjusted for ratio of unity between emission rate and wind speed. Cramer (48).

The σ_z estimates given in Figure 2.9 have been altered to conform, at short and intermediate distances, to the rectilinear vertical spread ($p \simeq 1$) anticipated for elevated sources (48).

Two sets of values are given for near-netural atmospheric conditions to provide for differences in surface roughness. This factor is minimized under other stability conditions, since in lapse (unstable) conditions, mechanical turbulence associated with roughness elements is dominated by convective turbulence; and in stable atmospheres, mechanical turbulence

is rapidly damped with increasing height. The larger σ_y and σ_z values for near-neutral conditions correspond to a rough surface, while the smaller values correspond to a relatively flat surface with few obstructions (48).

Cramer (48) has also given a relationship between σ_θ and σ_e based on the Prairie Grass data. This is illustrated in Figure 2.11.

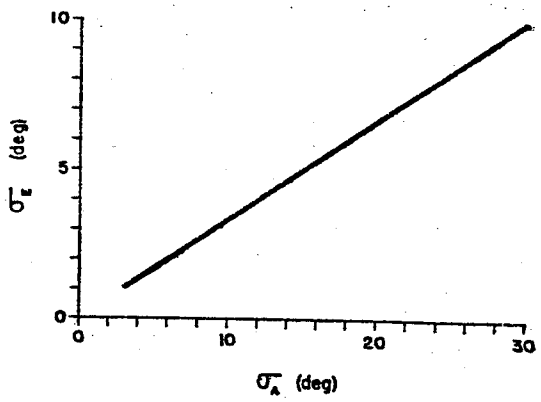

Figure 2.11. Relationship between standard deviations of azimuth angle σ_θ and elevation angle σ_e near ground level. Cramer (48).

The solid line is based on a regression analysis of the Prairie Grass measurements. These data indicate a σ_e/σ_θ ratio of 0.33. This ratio is larger at heights several hundred feet above ground level during extremely unstable conditions; smaller values will usually be found at these elevations for stable conditions.

2.4.5 Pasquill Diffusion Coefficients (1961)

On the basis of available data, including the Prairie Grass experiments discussed in section 2.4.4, Pasquill (50) developed a simple system of

estimating downwind effluent concentrations. Pasquill suggested that both σ_y and σ_z be estimated in accordance with the suggestions of Hay and Pasquill (45,49). The Hay and Pasquill papers presented a method of estimating both vertical and lateral cloud spread from measurements of wind-direction fluctuations made with a suitable instrument. Pasquill recognized that the data on vertical wind-direction fluctuation required by this method were not generally available, and therefore suggested values for the appropriate degree of vertical spreading which could be estimated from stability considerations. He also indicated how the lateral spreading of the plume could be estimated from the range of the wind-direction trace for long ($\simeq$1 hr.) pollutant releases and suggested a series of wind-direction-range values to be used in lieu of actual wind measurements for short releases during steady wind-direction conditions. These direction range values were related to the same estimates of stability used to infer the vertical spreading.

Pasquill's curves for obtaining tentative estimates of vertical spread, h, in the absence of wind fluctuation data, are given in Figure 2.12 for six categories of stability (in the surface layer) in open country. Estimates of lateral spread, θ, for different stability classes may also be obtained from Figure 2.12 for short releases (a few minutes). Greater uncertainty in the data of Figure 2.12 is implied by the thinner and broken lines for h and the addition of brackets to the numerical values for θ.

No attempt is made by Pasquill to give statistical estimates of θ for longer releases; instead, Pasquill (50) gives the following rough

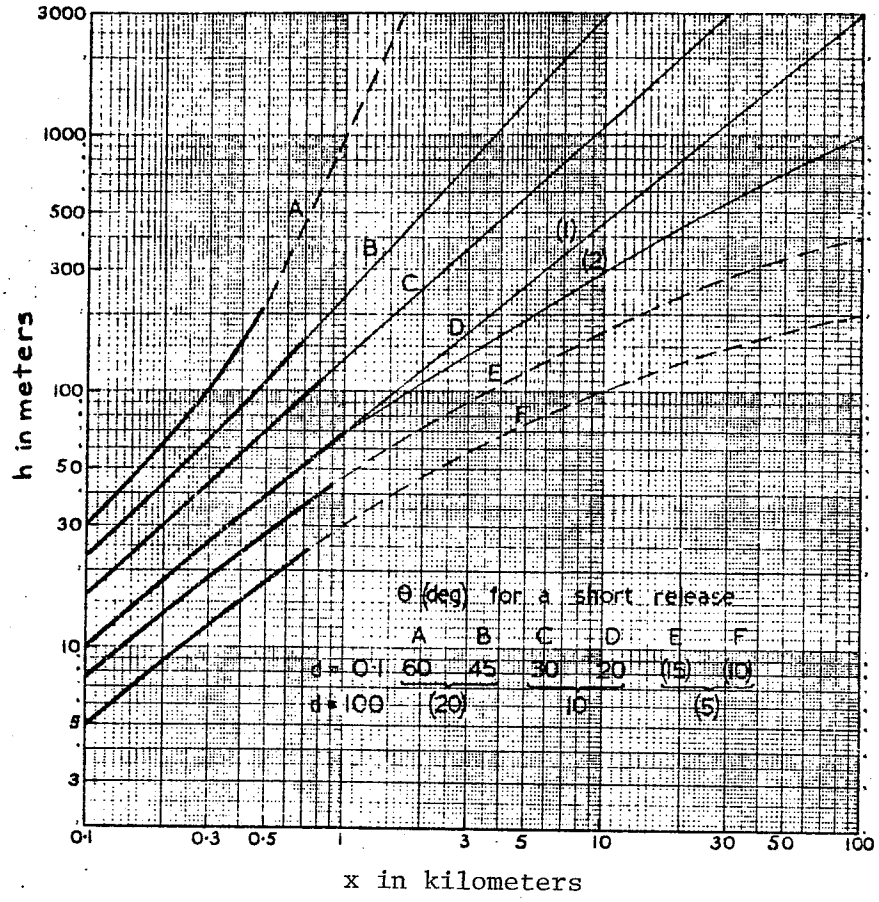

Figure 2.12. Tentative estimates of vertical spread (h) and lateral spread (θ), Pasquill (50).

estimates of θ for a long release (≥ 1 hour) derived from routine wind-direction traces:

x = 0.1 km : θ = difference between extreme maximum and minimum of trace over period of release,

x = 100 km : θ = difference between maximum and minimum "15-minute averages" of wind direction.

Pasquill's diffusion curves are accompanied by a table of stability categories (50) which are specified qualitatively in terms of wind speed, insolation, and cloud cover. These stability classes, used in selecting the appropriate curves from Figure 2.11, are given in Table 2.10.

TABLE 2.10

RELATION OF PASQUILL STABILITY CATEGORIES

TO WEATHER CONDITIONS (50)

A—Extremely unstable conditions
B—Moderately unstable conditions
C—Slightly unstable conditions
D—Neutral conditions*
E—Slightly stable conditions
F—Moderately stable conditions

Surface wind speed, m/sec	Daytime insolation			Nighttime conditions	
	Strong	Moderate	Slight	Thin overcast or ≥ 4/8 cloudiness†	≤ 3/8 cloudiness
<2	A	A-B	B		
2	A-B	B	C	E	F
4	B	B-C	C	D	E
6	C	C-D	D	D	D
>6	C	D	D	D	D

*Applicable to heavy overcast, day or night.
†The degree of cloudiness is defined as that fraction of the sky above the local apparent horizon that is covered by clouds.

"Strong" insolation in Table 2.10 refers to sunny midday conditions in midsummer in England, and "slight" insolation refers to similar conditions in midwinter. "Night" refers to the period from one hour before sunset to one hour after dawn. The neutral category D should also be assumed, irrespective of wind speed, for overcast conditions during day or night, and for any sky conditions during the hour preceding or following night as defined above. The D (1) curve should be followed to the top of the dry adiabatic layer; thereafter, in subadiabatic conditions, the D (2) curve or a curve parallel to it should be followed (50).

2.4.6 Gifford Modification of Pasquill's Diffusion Coefficients (1961)

As pointed out by Pasquill (50) and Gifford (52), the values of plume height (h) and width (θ) described by Pasquill can be expressed in terms of the diffusion coefficients σ_y and σ_z for use with the Grussian plume models given in section 2.3.4. Gifford performed this conversion and presented the resulting curves shown in Figures 2.13 and 2.14. Gifford (52) used the following expressions for h and θ in terms σ_y and σ_z to carry out the conversion:

$$h = 2.15\sigma_z \tag{2.83}$$

$$\tan(\theta/2) = 2.15\ \sigma_y/x \tag{2.84}$$

where the plume height, h, and the angular plume width, θ (in radius) are defined by the plume boundaries such that the concentration at the edge of the plume equals 10% of its axial concentration, as given by Pasquill (50).

Gifford (52) estimates effluent dispersion by estimating both σ_y and σ_z from the appropriate curves representing the various thermal stability values as specified by Pasquill in Table 2.10.

2.4.7 Comparison of Diffusion Coefficients

Ultimately it is desired to relate diffusion parameters to objective meteorological measurements. This is necessary in order to allow the direct utilization of meteorological data to estimate atmospheric diffusion without further laborious and expensive diffusion experiments.

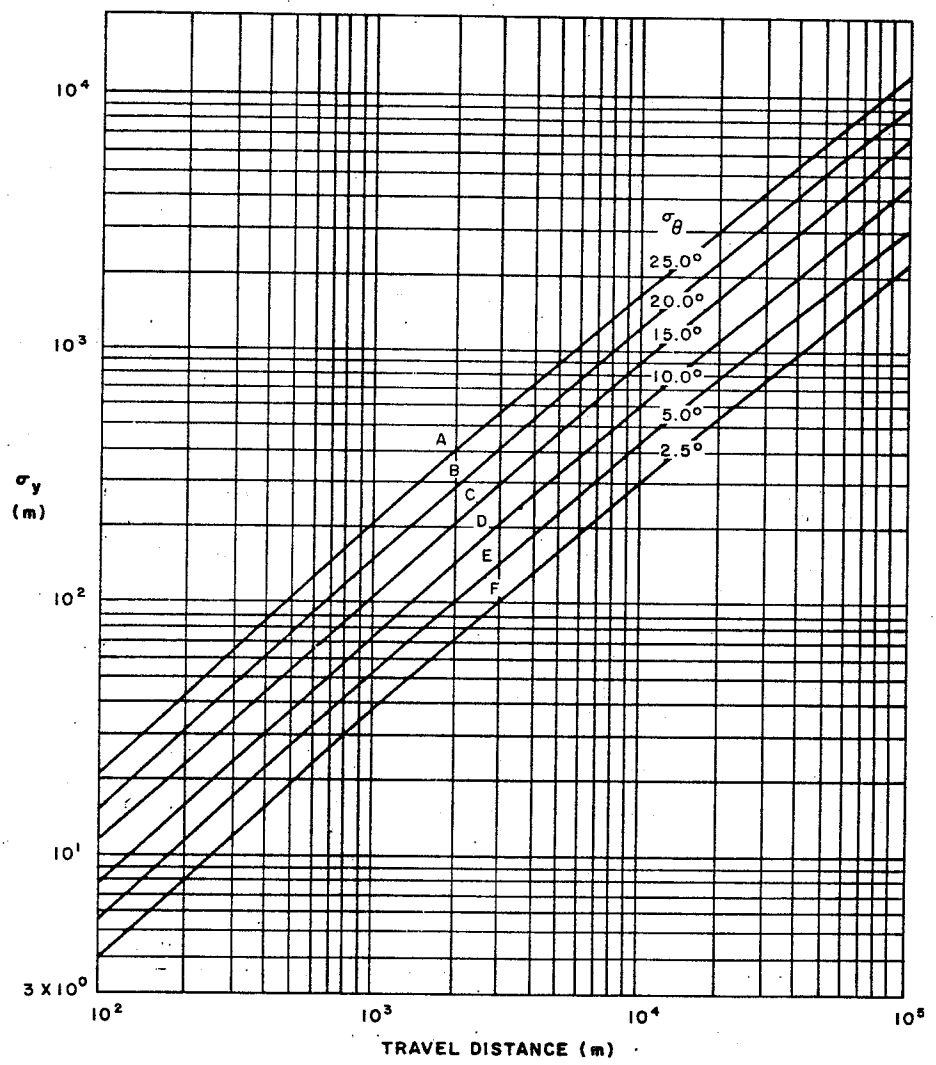

Figure 2.13. Standard deviation of the lateral concentration distribution, σ_y, as a function of travel distance from a continuous source, Gifford (52).

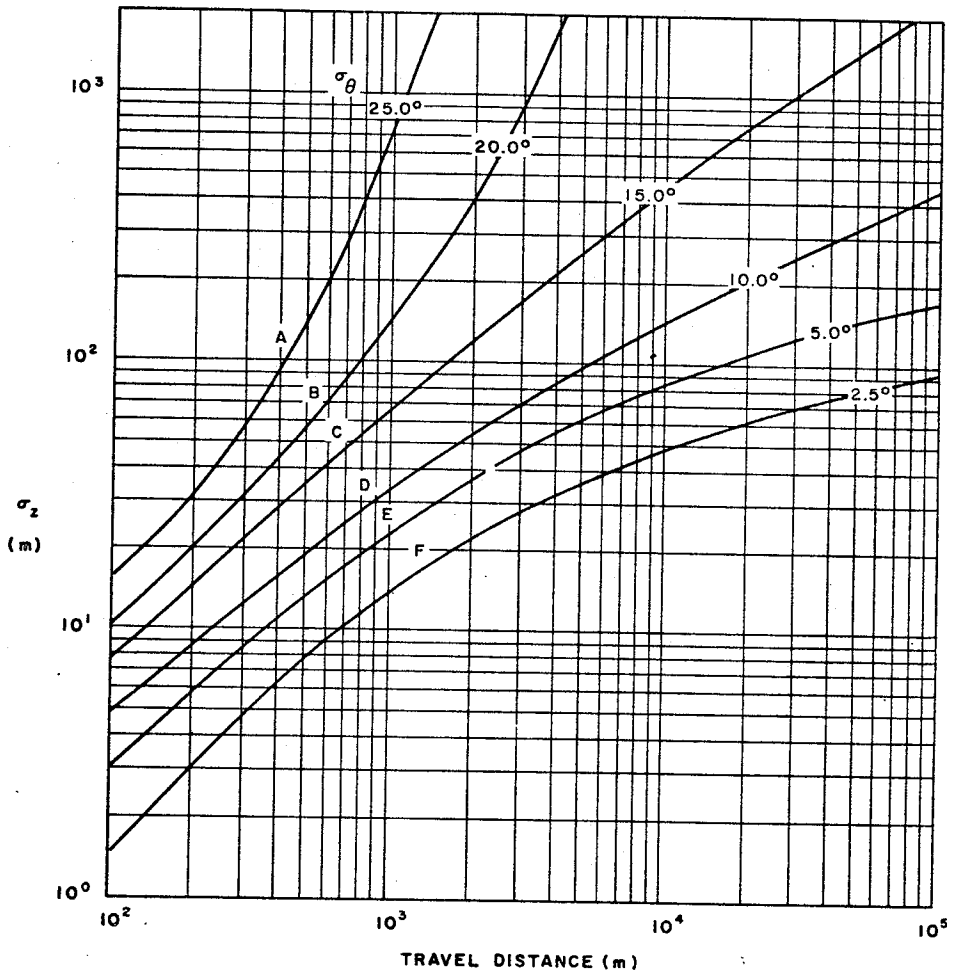

Figure 2.14. Standard deviation of the vertical concentration distribution, σ_z, as a function of travel distance from a continuous source, Gifford (52).

Sutton (43) has given values of n,u, and w'/u for various atmospheric lapse rates. He does not, however, present any observational data to substantiate them. Furthermore, Barad and Hauger (67) have shown that the slopes of the C_y versus x and C_z versus x curves cannot be obtained from the wind profiles as claimed by Sutton. Slade (44) states that there has been growing recognition of this deficiency in dealing with many practical problems. Barad and Hauger (67) also showed that in many cases the values of n are not the same for the y and z directions, i.e. $n_y \neq n_z$. This necessitates the awkward use of four variable diffusion parameters ($\overline{v'^2}/u^2$, $\overline{w'^2}/u^2$, n_y, and n_z) in obtaining an adequate fit of measured diffusion data to Sutton's diffusion equation.

The Hay and Pasquill method (45) for determining vertical diffusion coefficients has the obvious shortcoming of requiring extensive wind-direction fluctuation measurements. Such measurements are not generally available in meteorological records, thereby reducing the facility of using the Hay and Pasquill techniques.

Cramer (48) and Pasquill (50) have both presented good working methods for obtaining the diffusion parameters σ_y and σ_z from routine meteorological wind records, a marked improvement over the Sutton (43) and Hay and Pasquill (45,49) methods. In spite of the fact that Cramer's figures are based on ground-level measurements of ground-level sources, they appear to be consistent with observations reported for elevated sources (48,61,69). Cramer predicts that the values of effluent concentrations calculated using Figures 2.8 to 2.10 should be within a factor of 2 of the actual observed values.

Pasquill (50), however, has improved upon the work of Hay and Pasquill even further by providing a set of specified stability classes, related to wind speed, insolation, and cloud cover, and a corresponding set of stability curves from which the vertical and horizontal plume spread may be estimated. This method greatly facilitates the estimation of atmospheric dispersion where wind-fluctuation data are not readily available.

Finally, Gifford (52) expressed Pasquill's coefficients h and θ in terms of the dispersion coefficients, σ_y and σ_z, used in the Gaussian plume model, and converted Pasquill's curves to the Gaussian form. The use of σ_y and σ_z, rather than θ and h, is desirable in view of their expression of the standard deviations of the plume concentration distribution, and in view of their increasing widespread use in summarizing atmospheric dispersion data (51,52).

In the unstable, and stable cases, errors up to an order of magnitude in estimating σ_z can occur for the longer travel distances. In many cases, however, the σ_z values obtained from the Gifford curves may be expected to be correct within a factor of 2. These cases are: 1) all stabilities for distance of travel out to a few hundred meters, 2) neutral to moderately unstable conditions for distances out to a few kilometers, and 3) unstable conditions in the lower 1000 meters of the atmosphere with a marked inversion above for distances out to 10 km or more (22). Uncertainties in the estimates of σ_y are generally less than those of σ_z. The ground-level centerline concentrations for these three cases (where σ_z can be expected to be within a factor of 2) should be correct within a factor of 3, including errors in σ_y and u.

The Pasquill-Gifford curves given in Figures 2.13 and 2.14 thus represent the best currently available method of estimating σ_y and σ_z and will be used in the dispersion analysis of this paper.

3. RESEARCH OBJECTIVES AND BACKGROUND INFORMATION

3.1 RESEARCH OBJECTIVES

The operation of a coal-fired power plant results in the release of particulate and gaseous contaminants into the atmosphere. The purpose of this study was to prepare a primary environmental assessment of the air pollutant emissions from the Manitoba Hydro thermal generating station at Brandon, Manitoba.

3.2 BACKGROUND INFORMATION

3.2.1 Description of Receptor Area

3.2.1.1 Land Use and Population

The area surrounding Brandon Generating Station is primarily agricultural farmland except for the city of Brandon which is situated approximately 1½ miles due west of the power plant.

Brandon is located on the Assiniboine River, approximately 130 miles west of Winnipeg, and is bounded by N49°49'13" and N49°52'18" latitude and W99°54'57" and W99°59'04" longitude. The city has a population of 31,150 (71) and serves as the regional agricultural center for about 180,000 people.

Commercial and industrial enterprises include several feed mills, mean packing plants, dairies and farm equipment and supply dealerships. The Simplot Chemical Company has a multimillion dollar fertilizer plant located just east of Brandon and the Canadian Department of Agriculture operates an experimental farm and research station in the northwest corner of the city (72).

3.2.1.2 Terrain

The terrain in the Brandon area is relatively flat, rising very gradually from an elevation of 1175 ft. (above mean sea level) in the northeast corner of the city near the Assiniboine River to an elevation of approximately 1300 ft. at the southwest city limits. The river flows from west to east through the Brandon area.

Ground elevation varies from about 1200 to 1250 ft. in the East End section of Brandon, adjacent to the east city limits, and drops to 1179 ft. at the Brandon Generating Station. This is equivalent to an average ground slope between the power plant and the city of 36 ft./mile, or about 0.7%. The average east-west ground slope across the city is slightly less than one-half of this value, 0.32%.

The ground surface in the area surrounding Brandon is primarily cleared farmland with the exception of wooded areas along the banks of the Assiniboine River and widely-scattered stands of trees, many of the latter serving as windbreaks for farm homes.

The only prominent terrain feature in the area is a relatively steep slope which runs along the north city limits. This slope reaches a maximum grade of roughly 30%, with an average grade of about 15%. The slope varies from about 160 to 500 ft. in width, and flattens out one-third of a mile east of the east city limits.

A map of the Brandon area showing the Brandon Generating Station, contours, and wooded areas is given in Figure 3.1.

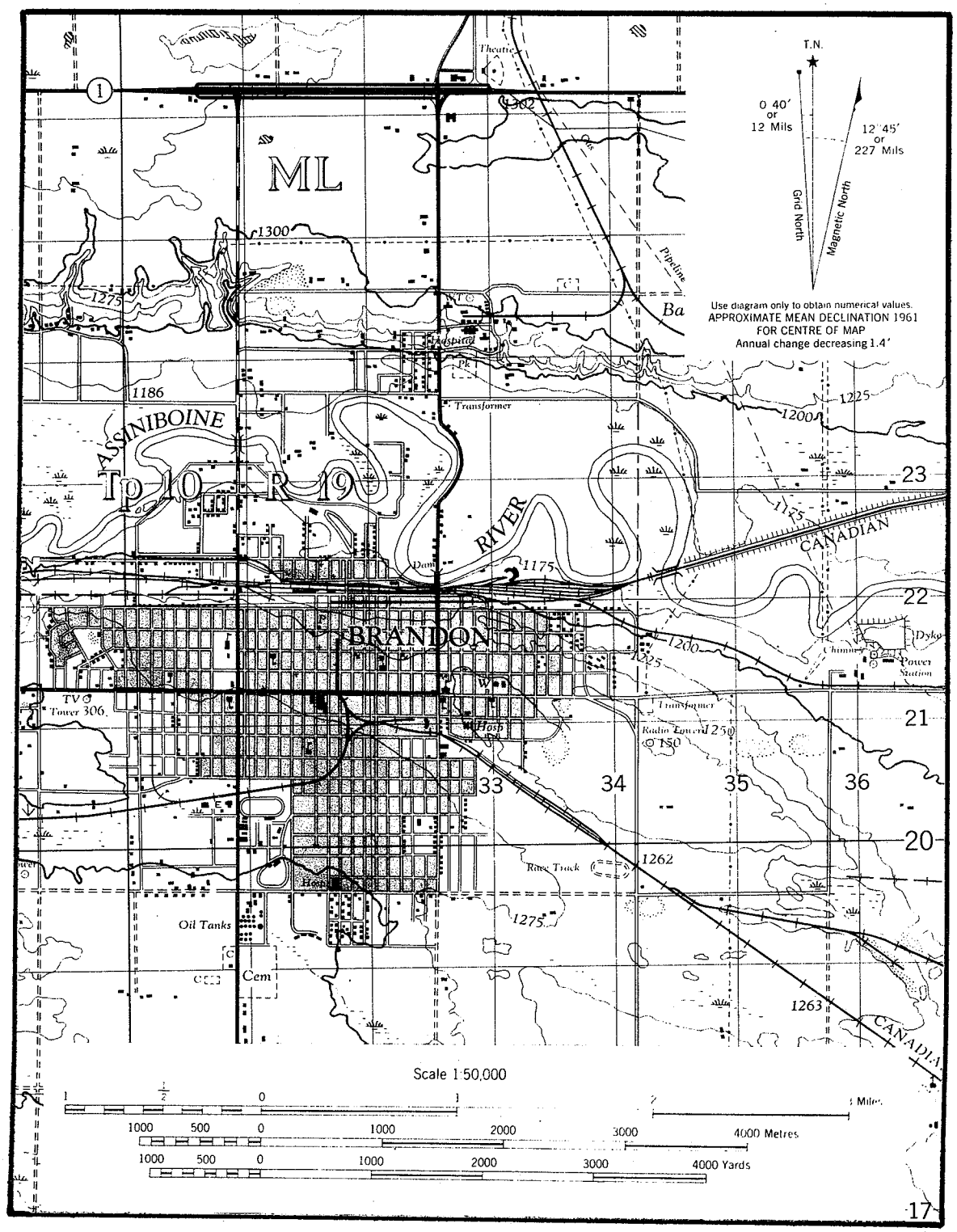

Figure 3.1. Map of Brandon Area (73)

3.2.1.3 Climatology

The Brandon study area has a continental climate typical of Manitoba and Saskatchewan (74). This is characterized by relatively long cool summers and precipitation throughout the year (75). The average mean daily temperature is 17.4°C during the summer months (June, July, and August), and -15.9°C during the winter (December, January, and February). The mean annual number of days with frost is 207. Measurable precipitation occurs an average of 8 days per month during the year; mean annual precipitation is comprised of 34.57 centimeters of rain and 124.71 centimeters of snow (76).

The Brandon area experiences prevailing westerly winds from July to March, and prevailing easterly winds during the balance of the year (77). Detailed wind data for Brandon are given in Appendix 8.4.3.

Munn et al. (74) give climatological estimates of inversion frequencies for Manitoba, based on data from the Canadian network of rawinsonde stations and the Canadian tower network. These values are listed in Table 3.1. They are applicable to the Brandon area and indicate that inversions occur on most nights, especially during the summer, with lapse conditions developing during the day. The annual mean maximum mixing height in the Brandon area is about 1000 m (78). Because the underlying surface is relatively uniform, there are few local effects. The most serious pollution potential occurs in autumn and winter when a stagnant continental arctic airmass lies over the region.

TABLE 3.1

CLIMATOLOGICAL ESTIMATES OF INVERSION

FREQUENCIES FOR MANITOBA (74)

SEASON	Inversion Frequency (%)	
	Day	Night
Winter	30*	55
Spring	5	60
Summer	5	70*
Autumn	20*	50

*Estimated from tower data

3.2.2 Description of Brandon Generating Station

3.2.2.1 Location

Brandon Generating Station is located 1.14 miles east of the Brandon city limits, 750 ft. southeast of the Assiniboine River. The approximate map coordinates of the station are N49°50'41", W99°53'22". Grade elevation at the site is 1179'-0".

3.2.2.2 Function and Operating Pattern

Brandon Generating Station supplements and complements the hydro-electric generating capability of Manitoba Hydro's power system. The station is required to operate, as dictated by local requirements and hydraulic capability, at times of peak power demand on the system, at times of low inflows to reservoirs, and at times when it is prudent to increase the rate of storage in the reservoirs. The operating pattern

of Brandon Generating Station may therefore vary from zero or intermittent output to continuous operation at high loads over several months.

The maximum monthly power output at the Brandon plant usually occurs during the month of January, with an average gross generation of approximately 80,000,000 kilowatt-hours. Power generation is at a minimum during the summer months with typical gross outputs of 2-5 million kilowatt-hours per month. Monthly gross power generation figures for Brandon Generating Station are given in Appendix 8.3.1.

3.2.2.3 Boiler Equipment and Fuel

Five high pressure steam generators comprise the main boiler equipment at the Brandon station. Units 1,2,3 and 4 were designed and constructed by Combustion Engineering-Superheater Limited and commissioned during 1957 and 1958. All four units are natural circulation water tube boilers with tangentially-fired furnaces as illustrated in Figure 3.2. Each unit has a maximum continuous rating of 325,000 lbs/hr of steam at 625 psig and 825^{o}F measured at the superheater outlet. Lignite, oil, and natural gas may be burned in all four units.

Boiler Unit No. 5 was designed and constructed by Babcock-Wilcox/ Goldie-McCullough Limited and commissioned in November 1969. It has the same circulation and firing characteristics as Units 1-4. Unit No. 5 has a maximum continuous rating of 875,000 lbs/hr of steam at 1250 psig and 950^{o}F measured at the superheater outlet. It is presently equipped to burned lignite and oil.

Each of the five power boilers provides steam to drive its own turbo-generator. The turbo-generators on Units No. 1-4 and Unit No. 5

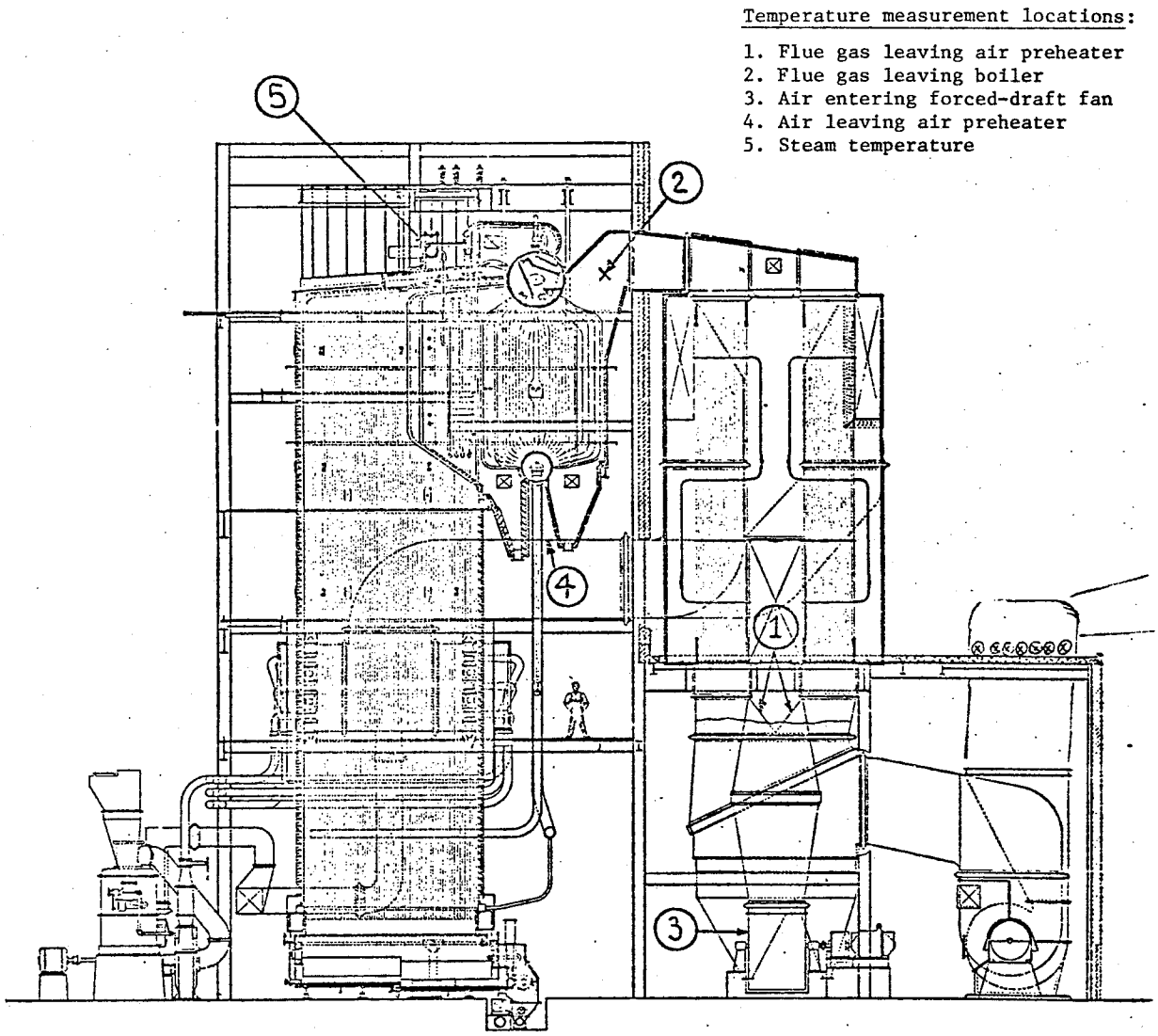

Figure 3.2. Steam generator. Units No. 1,2,3 and 4 (79).

have maximum continuous ratings of 33,000 kw and 105,000 kw, respectively, for a total generating capacity of 237,000 kilowatts. Detailed performance data for all five boilers and the main auxiliary systems are given in Appendix 8.3.2.

A low pressure hot water heating boiler rated at 16.5×10^6 Btu/hr may be fired with natural gas at 20 MCF maximum or with No. 2 fuel oil at 115 IGPH maximum by means of a horizontal rotary cup combination burner. This boiler provides heat for the plant when there is no power generation.

Saskatchewan Beinfait lignite, the primary fuel, is pulverized before burning. No. 2 fuel oil is used for ignition, light-off, flame stabilization and standby heating purposes. Natural gas, when it is economically available, may also be used in Units 1-4 for light-off, flame stabilization, standby heating and full load purposes; gas may also be burned simultaneously with lignite in any proportion. Typical analyses of the fuels used at Brandon Generating Station are given in Appendix 8.3.3. The maximum firing rates for Units 1-5 and the auxiliary heating boiler are given in Appendices 8.3.4 and 8.3.5, respectively. Fuel consumption tabulations for the years 1970-1974 are given in Appendix 8.3.6.

3.2.2.4 Superheater Blow-Off and Blow-Down Tank

In order to prevent overheating of the superheaters when the main steam supplies to the turbines are valved off (i.e. at boiler startup and shutdown) a flow of steam of 30,000 lbs/hr for each 33 MW boiler and about 45,000 lbs/hr for the 105 MW boiler is permitted to flow through

them to the atmosphere. The blow-off time may be about one hour if the boiler is warm or three hours if the boiler is cold.

All condensate and boiler system drainage is collected in a blow-down tank. Units No. 1 and No. 2 share a common blow-down tank as do Units No. 3 and No. 4; Unit No. 5 employs a tank of its own. The condensate is emptied from the blow-down tank into the station drains and is discharged into the Assiniboine River. Since the high pressure drainage entering the blow-down tank expands and partially evaporates, the flash steam blows to atmosphere via a vent line. A total of 7,000 lbs/hr of flash steam may be vented to the atmosphere in this manner.

3.2.2.5 Soot Blowers

Soot blowers are used to remove slag and ash deposits from the furance walls, tube banks, air heaters and dust collectors in order to maintain a clean heating surface with maximum heat transfer capability. Steam generators No. 1-4 (33 MW units) are equipped with a total of 18 soot blowers each and No. 5 (105 MW unit) is equipped with 67.

The soot blowing schedule depends upon the loading, operating conditions, and the fuel used. When any of Units 1-4 is operating at full load, a 2-hour blowing cycle, using 10,000 lbs/hr of steam, is required every 4 hours. The total amount is limited to a maximum of 20,000 lbs/hr of steam. Unit No. 5 operating at full load requires a 3-hour blowing cycle, using 10,000 lbs/hr of steam, every 8 hours.

A 15-minute blowing cycle every 4 hours, using 8,000 lbs/hr of stea, is required for the dust collectors.

The steam used in soot blowing is discharged to the atmosphere along with the flue gases.

3.2.2.6 Pollution Control Equipment

Flyash emissions are controlled by inertial type cyclone dust collectors. The collectors are designed to handle approximately 75% by weight of the particulate matter in the combustion products. The remaining 25% (estimated quantity) is retained in the boilers and collected in the ash hoppers. The dry ash from the ash hoppers and dust collectors is periodically sluiced to an ash lagoon along with the wet ash from the boiler wet bottom. An analysis of the lignite ash is given in Appendix 8.3.7.

The dust collectors on Units No. 1-3 are rated at 197,000 cfm each at 340^{o}F and 2.5" water gauge pressure drop; design efficiency of these units is 79% when normal lignite is being burned. The cyclone separators have been removed from Unit No. 4.

Unit No. 5 is equipped with two dust collectors with a total capacity of 423,000 cfm at 305^{o}F and 2.5" water gauge pressure drop. These collectors have a design efficiency of 79% when burning normal lignite.

Performance data for the dust collectors are given in Appendix 8.3.8.

Sulfur dioxide and NO_x emissions from Brandon Generating Station are uncontrolled.

3.2.2.7 Chimneys

Flue gases are emitted to the atmosphere via three reinforced concrete chimneys. Units No. 1-4 are served by two 250 ft. (76.2 m) stacks with a top inside liner diameter of 13' -0' (3.96 m). Unit No. 5 is served by one 350 ft (106.6 m) stack with a top inside liner diameter of 12' -0' (3.66 m). The two shorter stacks, Chimneys 1S and 2N, operate at temperatures of 295°F to 375°F (145°C to 190°C); the tall stack, Chimney 3, operates at 250°F to 350°F (120°C to 175°C), with a typical operating temperature of about 300°F (150°C).

Stack gas exit velocities at maximum rating are 17.1 m/sec for Chimneys 1S and 2N and 25.4 m/sec for Chimney 3.

4. METHOD

The methodology used in this assessment is basically that described in section 1.1 of the introduction. It is comprised of the following: 1) source evaluation, 2) receptor evaluation, 3) dispersion calculations, and 4) abatement and control recommendations. The methods used in the first three analyses are described in this section; abatement and control recommendations are given in section 7.

4.1 ESTIMATES OF STACK EMISSIONS

Sulfur dioxide and particulate emission rates for selected operating loads were estimated by performing a materials balance of the combustion products versus the flyash retained in the boilers and dust collectors. Emissions of nitrogen oxides (NO_x) were estimated using the emission factors published by the United States Environmental Protection Agency (7).

Operating loads were selected on the basis of the fuel consumption data (Appendix 8.3.6) in order to be representative of the monthly variations in load demand. Mean monthly emission rates for the three months of maximum power generation were computed for use in the dispersion calculations. Emissions at full load conditions were also computed for use in determining the "worst case" ground-level concentrations.

Emission calculations were based upon the following assumptions:

1. fuel and ash analyses as given in Appendices 8.3.3 and 8.3.7, respectively.

2. amount of ash retained in boilers and collected in the ash hoppers equal to 25% by weight of the ash in the combustion products.
3. amount of particulate matter going to dust collectors equal to 75% by weight of the ash in the combustion products.
4. collection of efficiency of dust collectors equal to 70%.
5. retention of sulfate in ash as given by lignite ash analysis, Appendix 8.3.7.
6. particle size distribution of particulate emissions as given by cyclone efficiency curves and performance data, Appendix 8.3.8.
7. sulfur emitted as SO_2.

4.2 ANALYSIS OF METEOROLOGICAL DATA

Monthly wind roses for the three months of maximum power generation were constructed from the Brandon wind frequency data (Appendix 8.4.1). Each wind rose provides a graphic representation of the monthly mean percent frequencies and wind speeds of winds from each of the 16 major compass directions. The orientations of the radial bar lines on the wind roses indicate the directions from which the wind is blowing. The percent frequency of a given wind direction is indicated by the length of the corresponding bar line; the mean wind speed for the given direction is denoted at the end of the bar line. The frequency of calms is given in the central circle of each rose.

Monthly mean maximum mixing heights for Brandon were extrapolated from mixing heights for The Pas, Manitoba (Appendix 8.4.3). The extrapolated values were used in the limited mixing calculations.

The frequency of nocturnal ground-based inversions was determined by analyzing the surface and 950 mb temperature data for Shilo, Manitoba published by the Canadian Department of Transport (80).

4.3 DISPERSION ANALYSES

Dispersion analyses were performed to determine the ground-level concentrations of SO_2, NO_x and suspended particulates downwind of the Brandon Generating Station during each of the three months of maximum power generation. One-hour concentrations under unlimited mixing, limited mixing and fumigation conditions were calculated for monthly mean and maximum emission rates. Monthly mean ground-level concentrations were also computed.

Unlimited mixing calculations were based on the Gaussian diffusion equation (22) and the Pasquill-Gifford diffusion coefficients (50,52). Calculations were performed with the aid of the Environment Canada Multiple Source Computer Program (81).

Limited mixing and fumigation calculations were based on Turner's simplifications of the Bierly and Hewson equations (22,57).

Monthly mean ground-level concentrations were computed using Turner's equation for long-term average concentrations (22) and the National Oceanic and Atmospheric Administration (NOAA) multiple source computer model (82).

Plume rise and downwash calculations were based on the equations given by Briggs (32,70). Downwash effects were considered first to yield preliminary stack heights. Plume rise effects were then calculated,

using the preliminary stack height in place of the physical stack height terms, yielding effective stack heights. Briggs' plume rise equations have been incorporated into both multiple source computer programs.

The following assumptions were made in performing the plume rise, downwash, and dispersion analyses:

1. mean wind speeds and wind frequency distributions as given by Brandon wind frequency data (77), Appendix 8.4.1.
2. stability classes based on mean monthly wind speeds, calculated insolation (83) and Pasquill's stability categories.
3. operating parameters as given in Appendix 8.3.2
4. mean ambient temperatures as given in temperature data (76), Appendix 8.4.2.

5. RESULTS

The results of the Brandon Generating Station air pollution study are presented below in tabular and graphic forms. They have been divided into two sections: 1) meteorological analyses, and 2) ground-level concentrations.

5.1 METEOROLOGICAL ANALYSES

5.1.1 Wind Roses

Monthly wind roses for December, January and February are presented in Figures 5.1, 5.2 and 5.3, respectively.

5.1.2 Inversion Frequencies

TABLE 5.1

FREQUENCY OF NOCTURNAL INVERSIONS

SHILO, MANITOBA

MONTH	FREQUENCY
December	52%
January	61%
February	68%

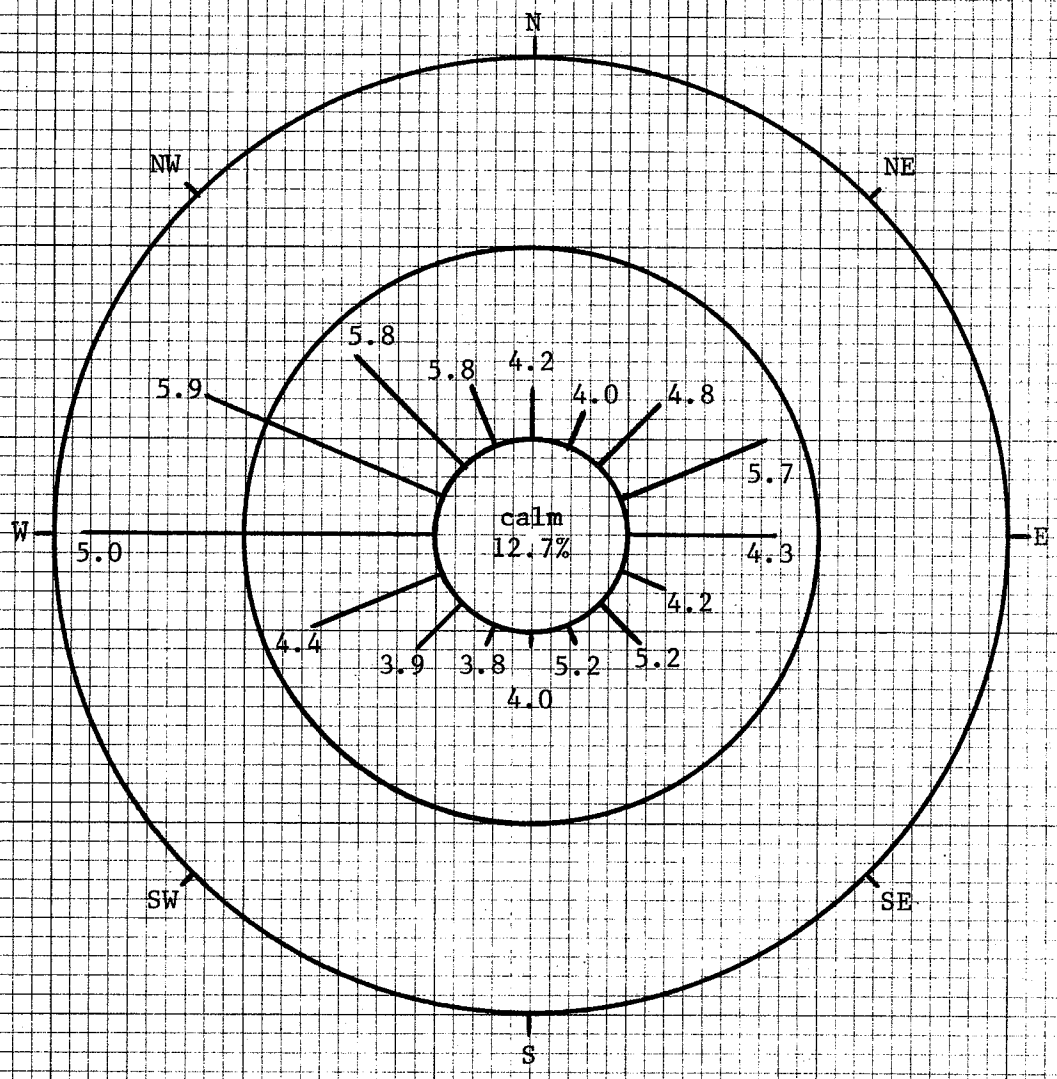

Frequency Scale:

0 5 10 15 20%

$\bar{u}$ = 4.4 m/sec

Figure 5.1. Monthly wind rose - December.

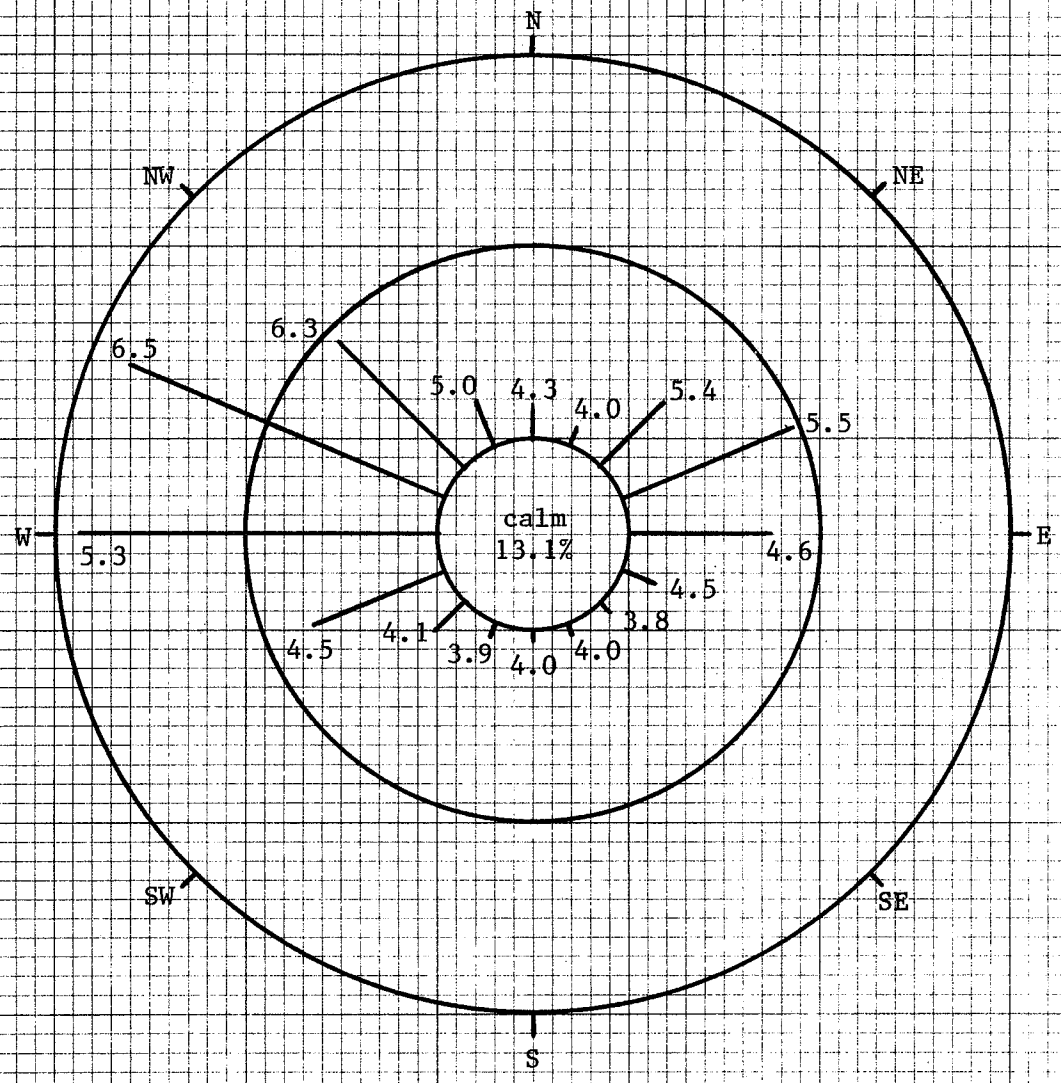

Frequency Scale:

0 5 10 15 20%

$\bar{u}$ = 4.7 m/sec

Figure 5.2. Monthly wind rose - January.

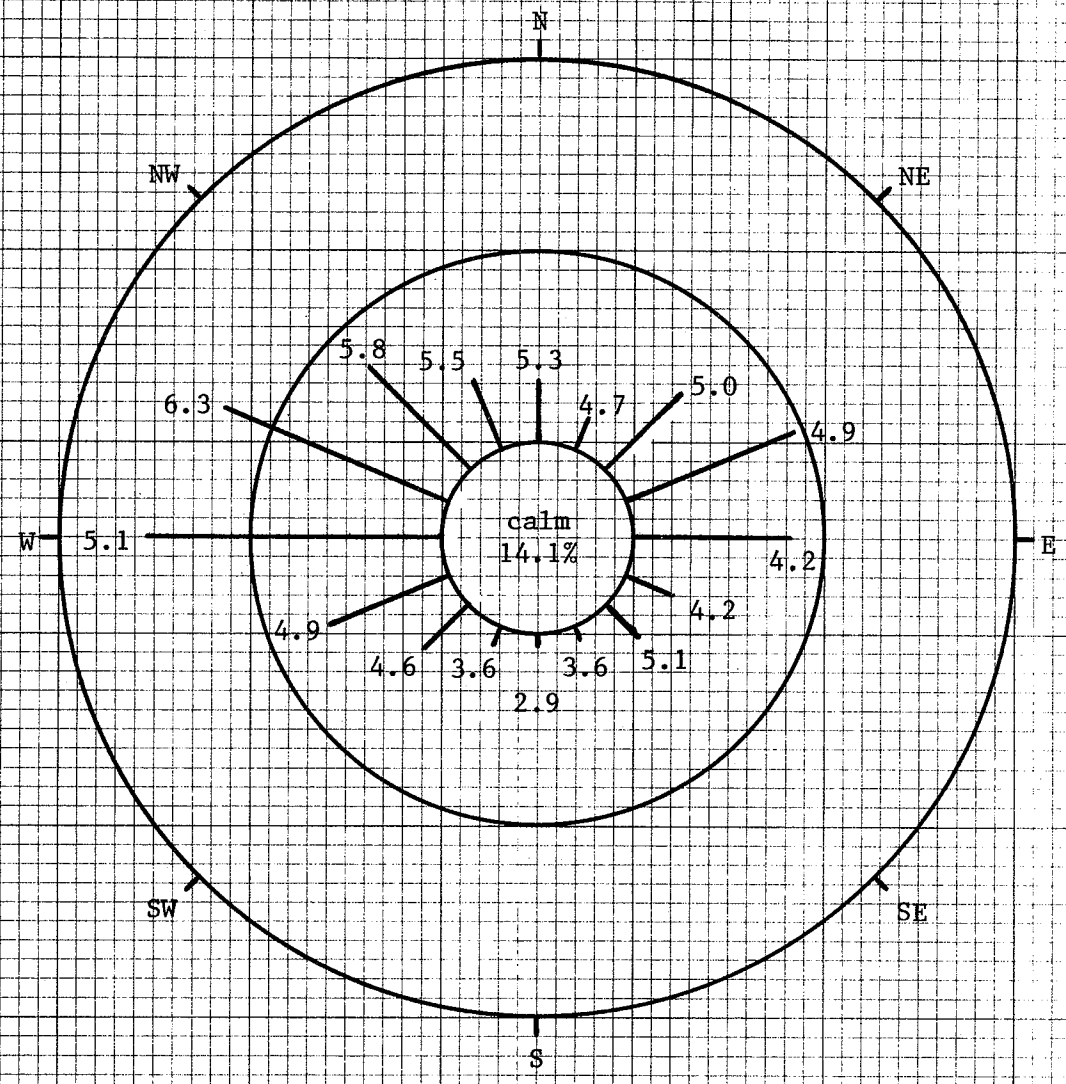

Frequency Scale:

0 5 10 15 20%

$\bar{u}$ = 4.4 m/sec

Figure 5.3. Monthly wind rose - February.

5.2 GROUND-LEVEL CONCENTRATIONS

5.2.1 Unlimited Mixing - Critical Wind Speed

Maximum ground-level SO_2 concentrations (unlimited mixing) are plotted in Figure 5.4 for several values of surface windspeed, u. The critical windspeed, u_{cr}, with respect to the ultimate maximum ground-level concentration is shown to be 11.0 m/sec. This is also the critical windspeed for the ultimate maximum ground-level NO_x and suspended particulate concentrations.

5.2.2 Monthly Mean Maximum Ground-Level Concentrations

Table 5.2 lists the monthly mean maximum 1-hour SO_2, 1-hour NO_x and 24-hour suspended particulate ground-level concentrations for unlimited and limited mixing conditions. These are based on the monthly mean emission rates (Table 8.18), windspeeds (Table 8.20), mixing heights (Figure 8.4) and ambient temperatures (Table 8.15), and class C stability (Table 2.10).

5.2.3 Ultimate Maximum Ground-Level Concentrations

Table 5.3 lists the maximum 1-hour SO_2, 1-hour NO_x and 24-hour suspended particulate ground-level concentrations for unlimited and limited mixing conditions and maximum emission rates. These are based on the critical windspeed for unlimited mixing, the mean winter windspeed (December, January and February), the mean daily maximum temperature for the warmest winter month (Table 8.15) and class C stability (Table 2.10).

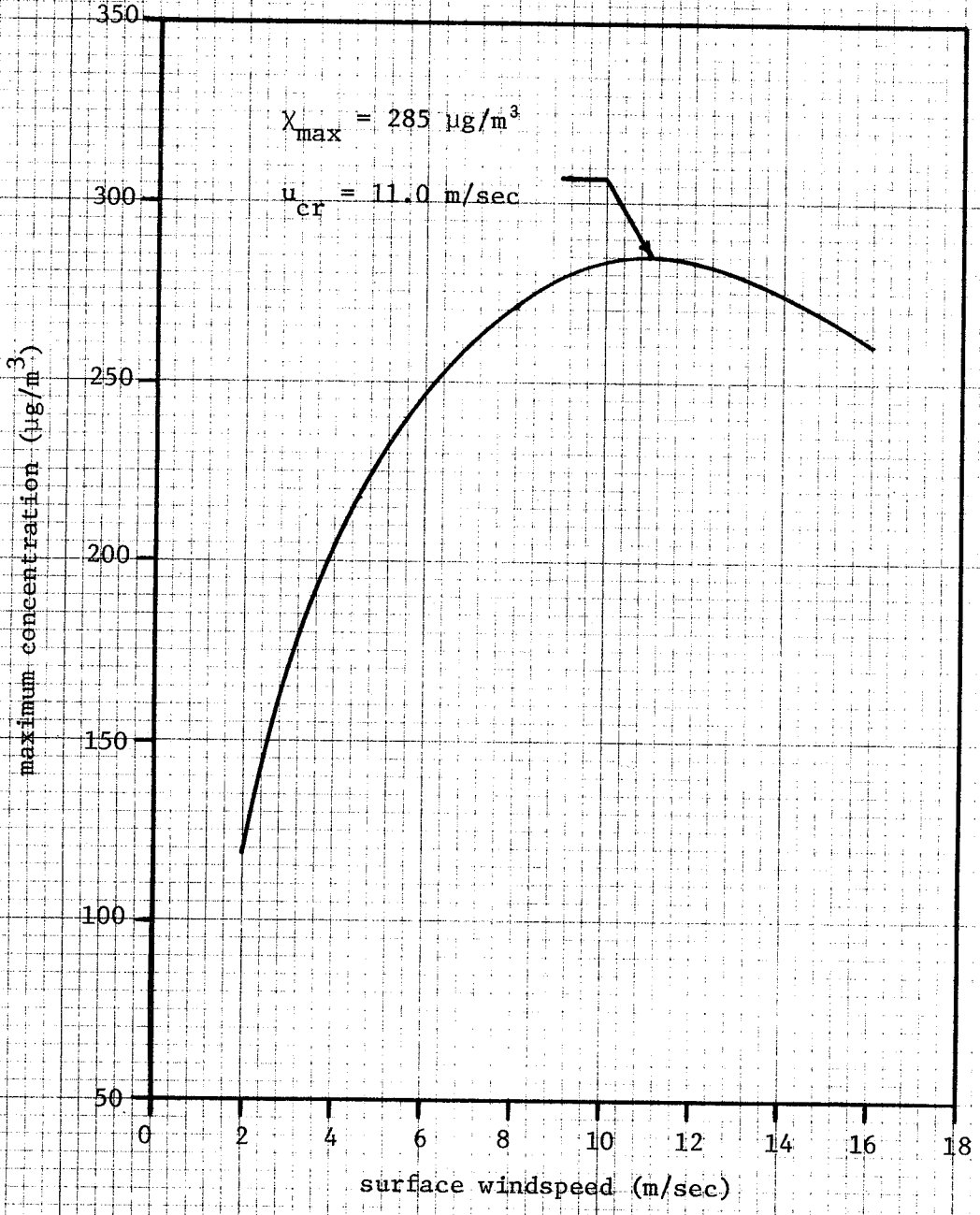

Figure 5.4. Unlimited Mixing Conditions. Maximum 1-hour ground-level SO_2 concentrations versus windspeed. Maximum emission rate.

TABLE 5.2

MONTHLY MEAN MAXIMUM GROUND-LEVEL CONCENTRATIONS

MONTH	SO_2 1-hour concentration ($\mu g/m^3$)		NO_x 1-hour concentration ($\mu g/m^3$)		SUSPENDED PARTICULATES 24-hour concentration ($\mu g/m^3$)	
	unlimited mixing	limited mixing	unlimited mixing	limited mixing	unlimited mixing	limited mixing
December	39	50	124	157	72	91
January	41	47	129	147	74	85
February	26	16	82	52	48	30

TABLE 5.3

ULTIMATE MAXIMUM GROUND-LEVEL CONCENTRATIONS

(MAXIMUM EMISSION RATE)

POLLUTANT	MAXIMUM CONCENTRATION ($\mu g/m^3$)							
	$u = u_{cr} = 11.0$ m/sec				$u = \bar{u} = 4.5$ m/sec			
	unlimited mixing	limited mixing			unlimited mixing	limited mixing		
		L=200m	L=277m	L=400m		L=200m	L=277m	L=400m
SO_2 (1-hour concentration)	285	197	97	43	217	482	240	105
NO_x (1-hour concentration)	389	267	132	58	296	653	325	143
Suspended Particulates (24-hour concentration)	429	297	146	64	327	727	361	159

5.2.4 Concentration Isopleths for Unlimited Mixing Conditions

Figures 5.5, 5.6 and 5.7 show the 1-hour SO_2, 1-hour NO_x and 24-hour suspended particulate concentration isopleths, respectively, for the January mean emission rates and an east wind with a speed of 4.7 m/sec (January mean).

Figures 5.8, 5.9 and 5.10 show the 1-hour SO_2, 1-hour NO_x and 24 hour suspended particulate concentration isopleths, respectively, for the maximum emission rates and an east wind with a speed of 11.0 m/sec (worst case conditions).

5.2.5 Limited Mixing Curves

Figures 5.11, 5.12 and 5.13 show the maximum 1-hour SO_2, 1-hour NO_x and 24-hour suspended particulate ground-level concentrations, respectively, for a range of windspeeds and mixing heights under limited mixing conditions. These curves are based on the January mean emission rates and stability class C.

Figures 5.14, 5.15 and 5.16 show the maximum 1-hour SO_2, 1-hour NO_x and 24-hour suspended particulate ground-level concentrations, respectively, for the maximum emission rates and limited mixing conditions. These curves are based on class C stability.

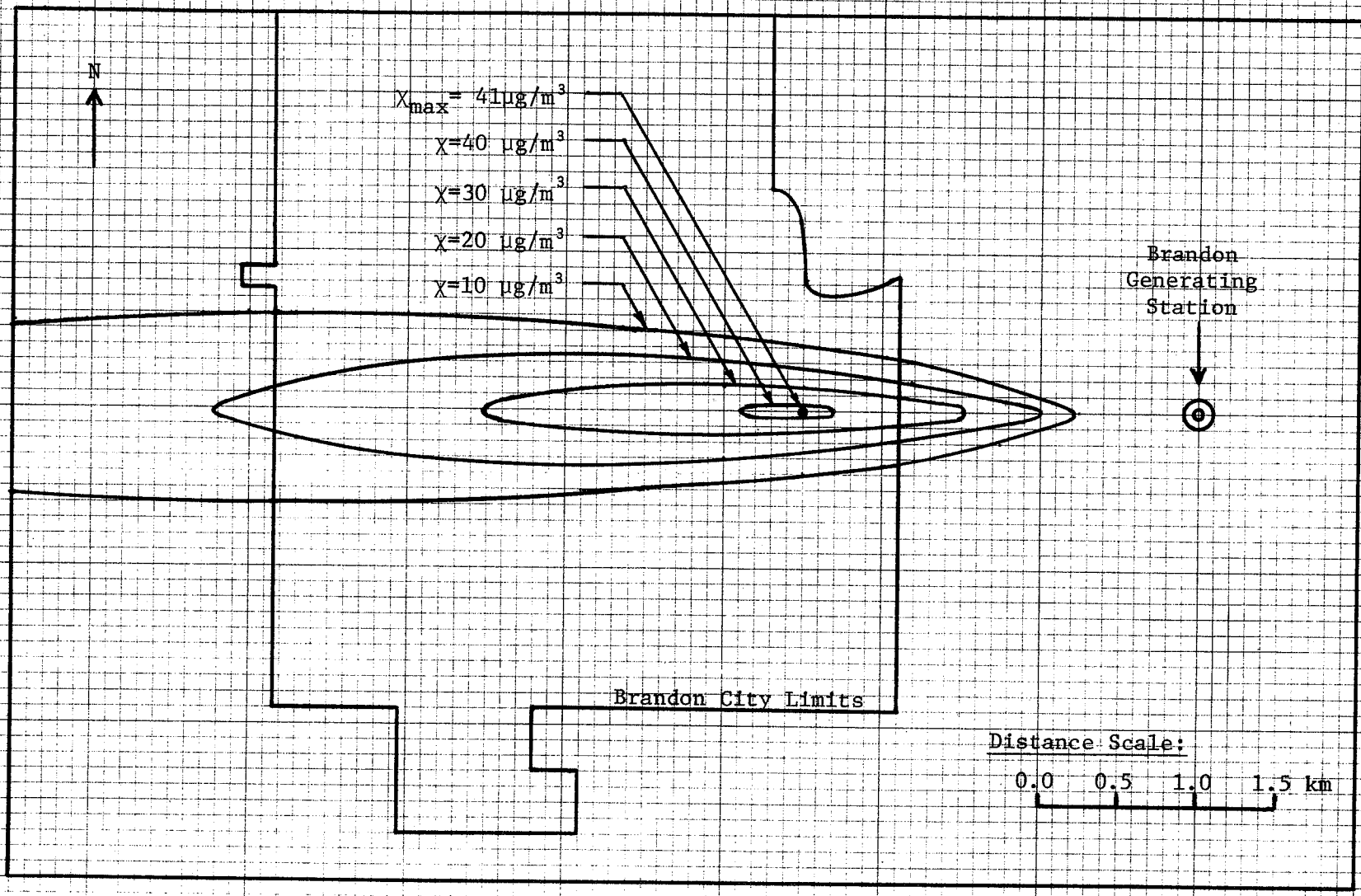

Figure 5.5. Ground-level 1-hour SO_2 concentration isopleths. January mean emission rate.

Windspeed = 4.7 m/sec. Stability class C.

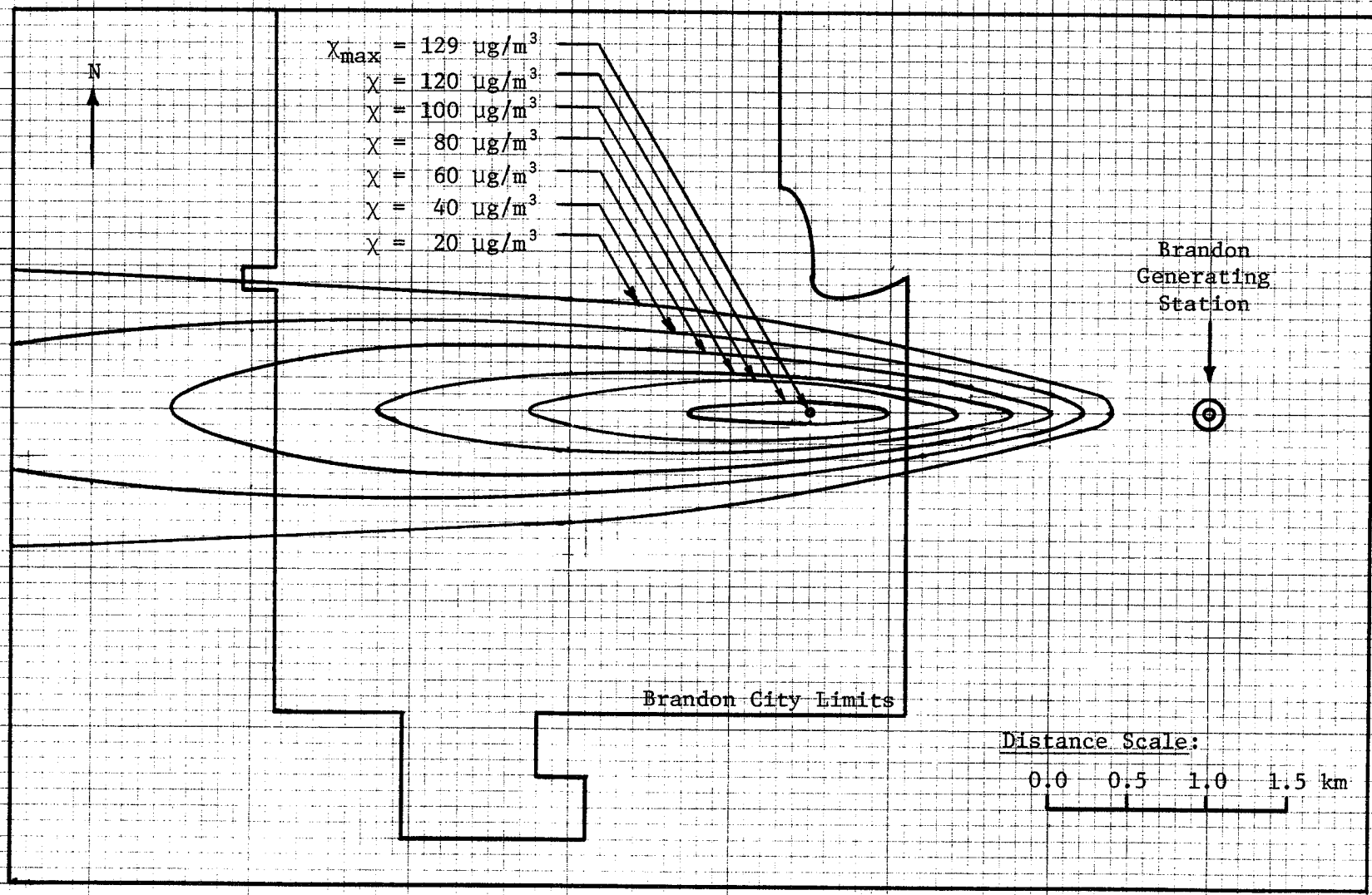

Figure 5.6. Ground-level 1-hour NO_x concentration isopleths. January mean emission rate. Windspeed = 4.7 m/sec. Stability class C.

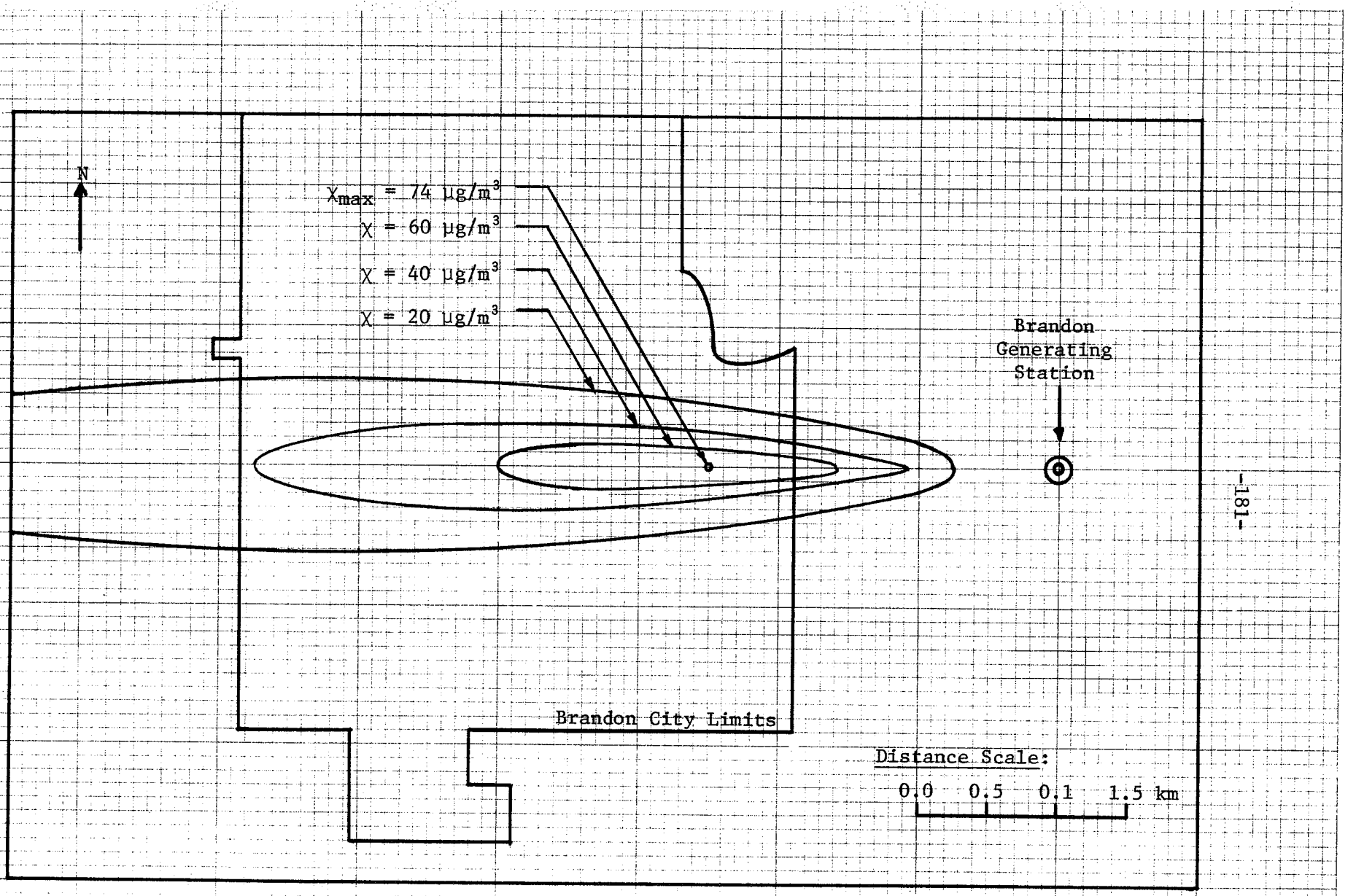

Figure 5.7. Ground-level 24-hour suspended particulate concentration isopleths.

January mean emission rate. Windspeed = 4.7 m/sec. Stability class C.

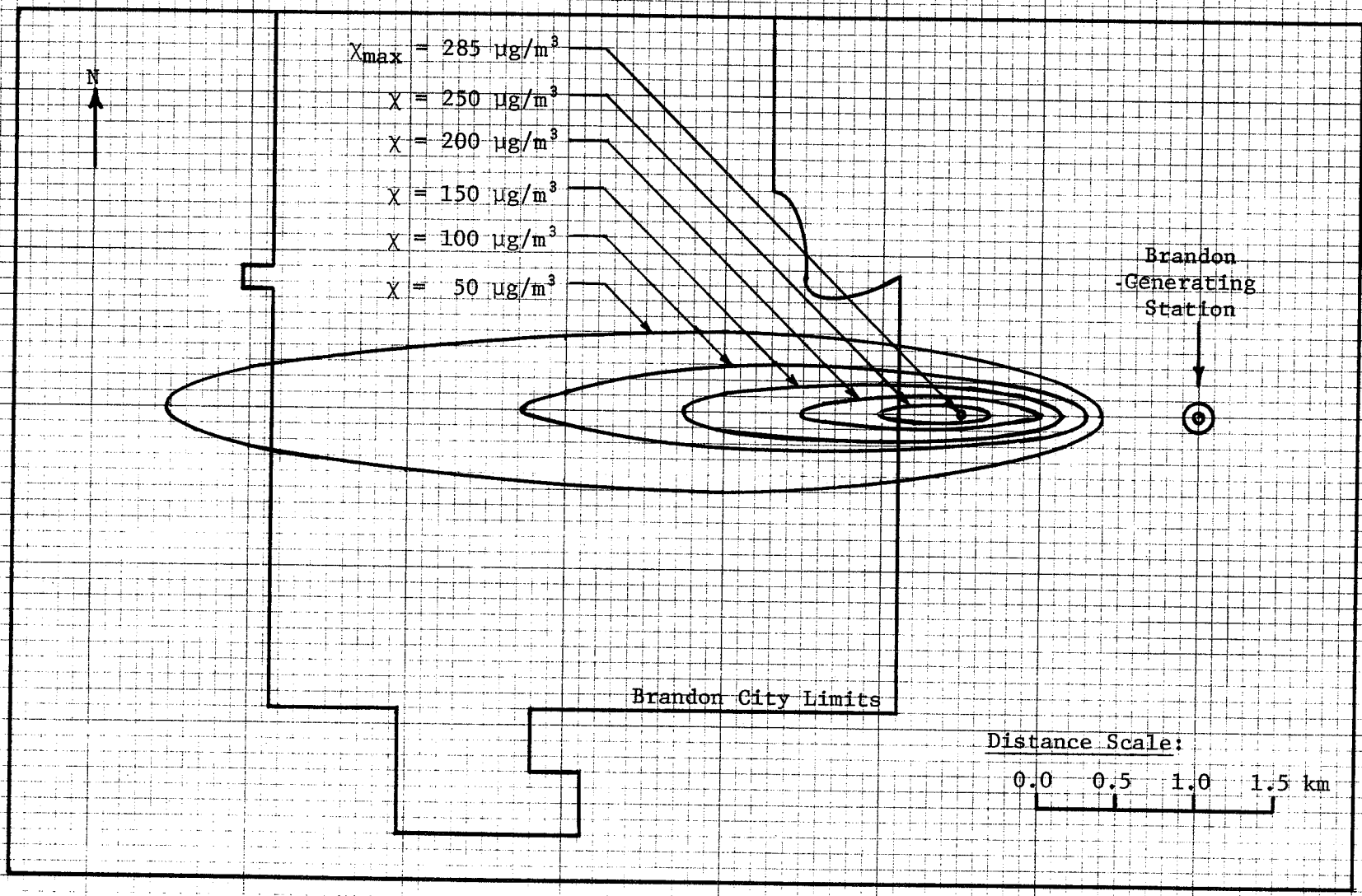

Figure 5.8. Ground-level 1-hour SO_2 concentration isopleths. Maximum emission rate. Critical windspeed = 11.0 m/sec. Stability class C.

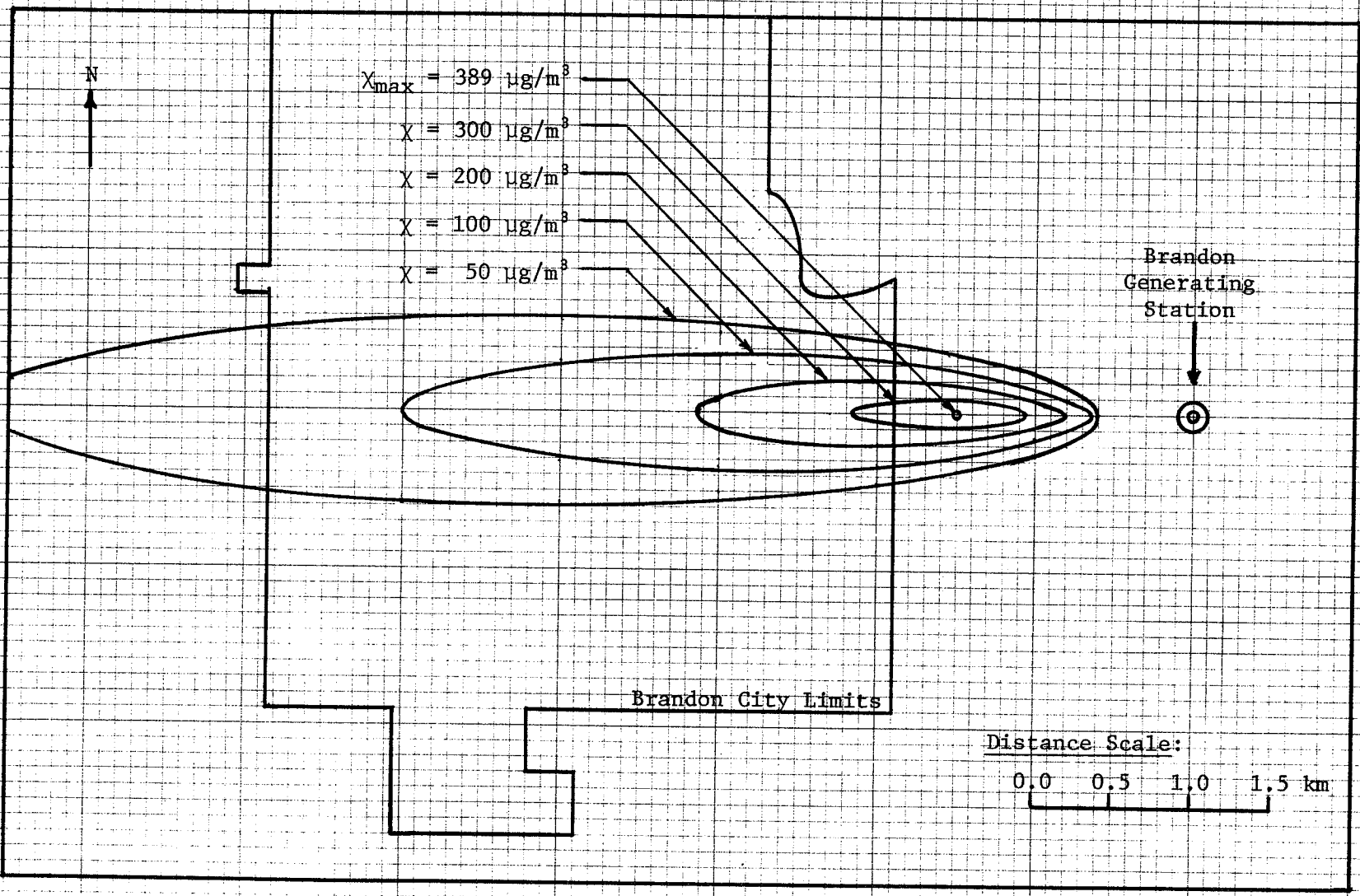

Figure 5.9. Ground-level 1-hour NO_x concentration isopleths. Maximum emission rate. Critical windspeed = 11.0 m/sec. Stability class C.

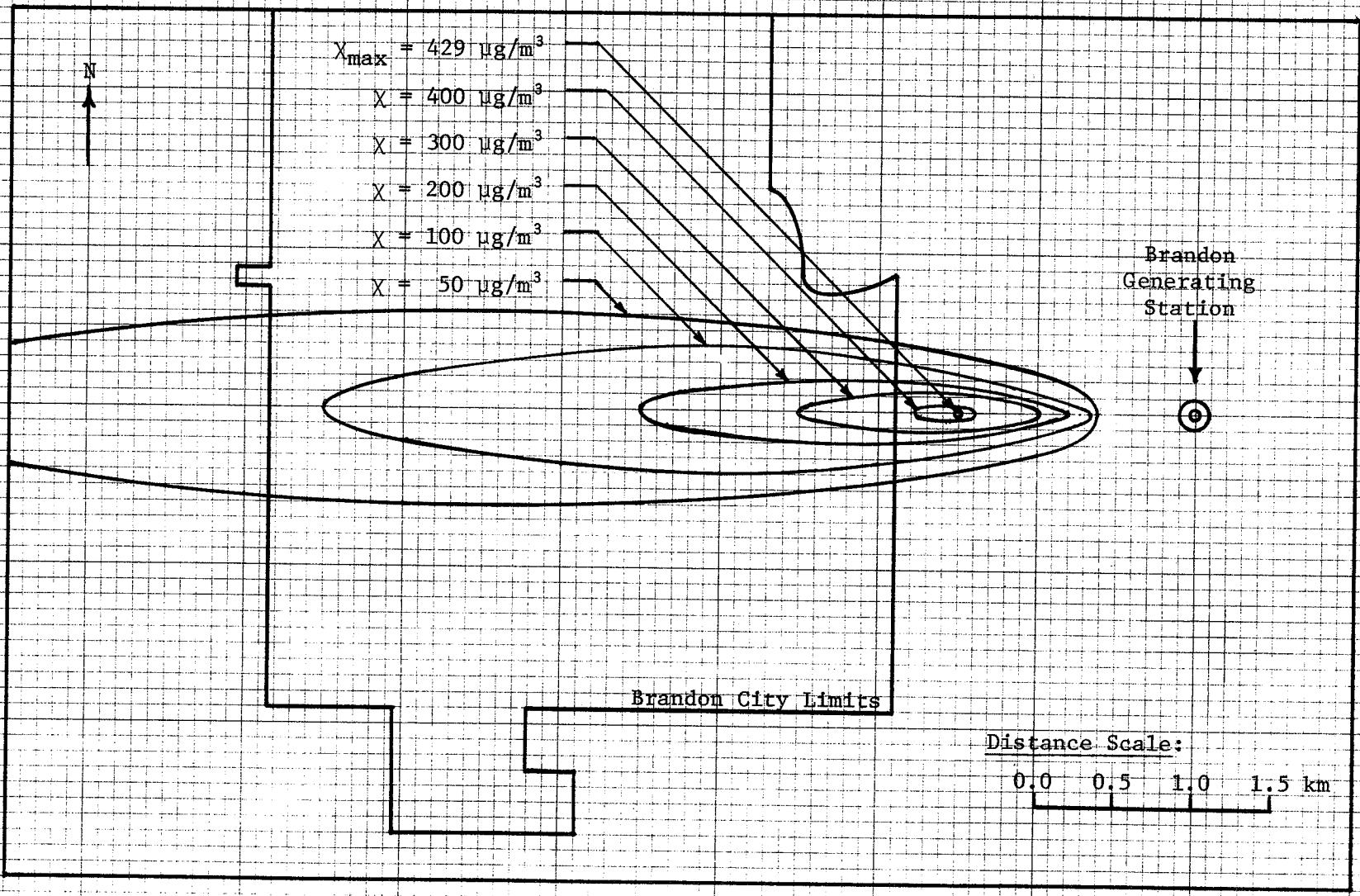

Figure 5.10. Ground-level 24-hour suspended particulate concentration isopleths.

Maximum emission rate. Critical windspeed = 11.0 m/sec. Stability class C.

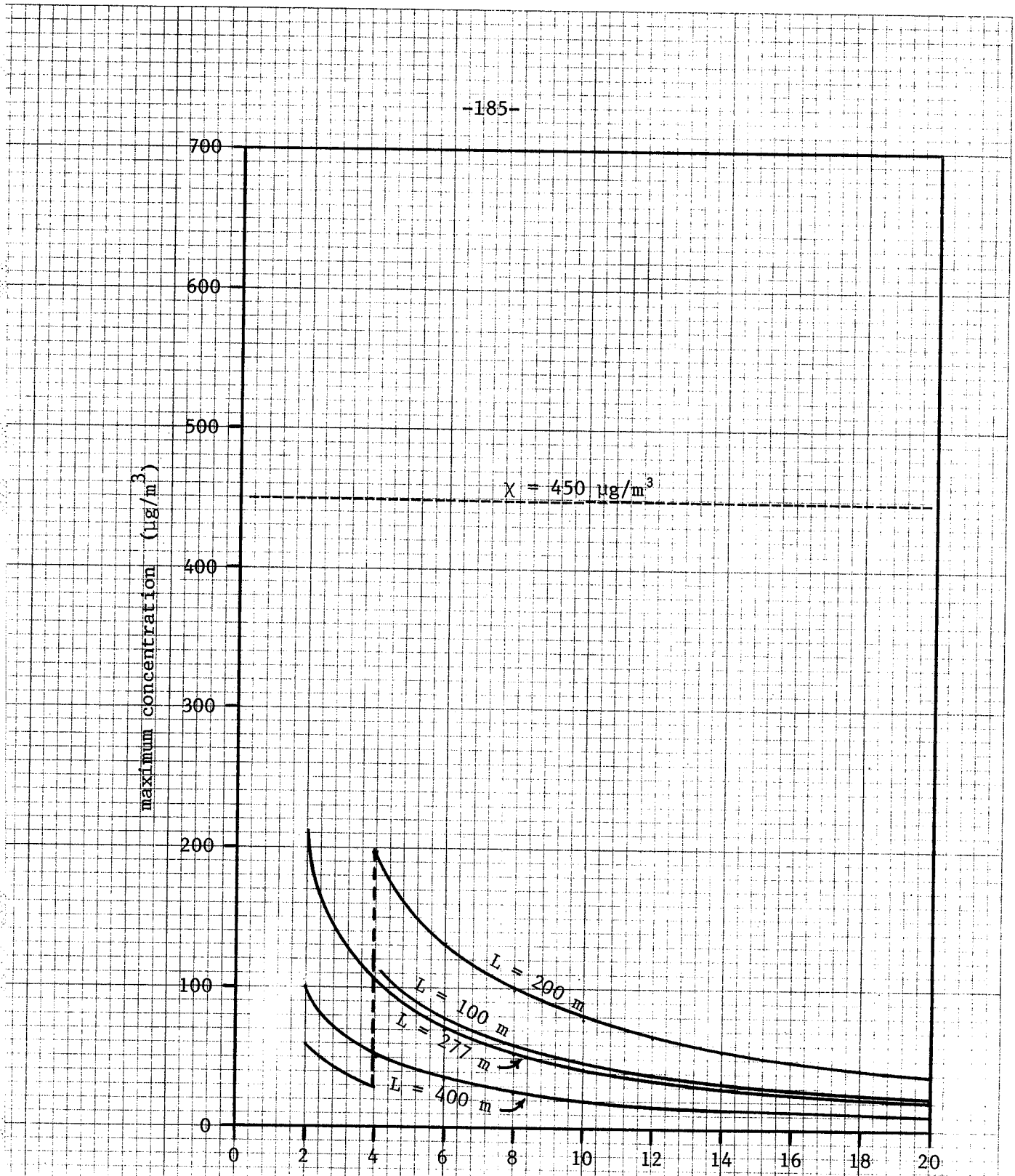

Figure 5.11. Limited Mixing Conditions. Maximum 1-hour ground-level SO_2 concentrations. Stability class C. January mean emission rate.

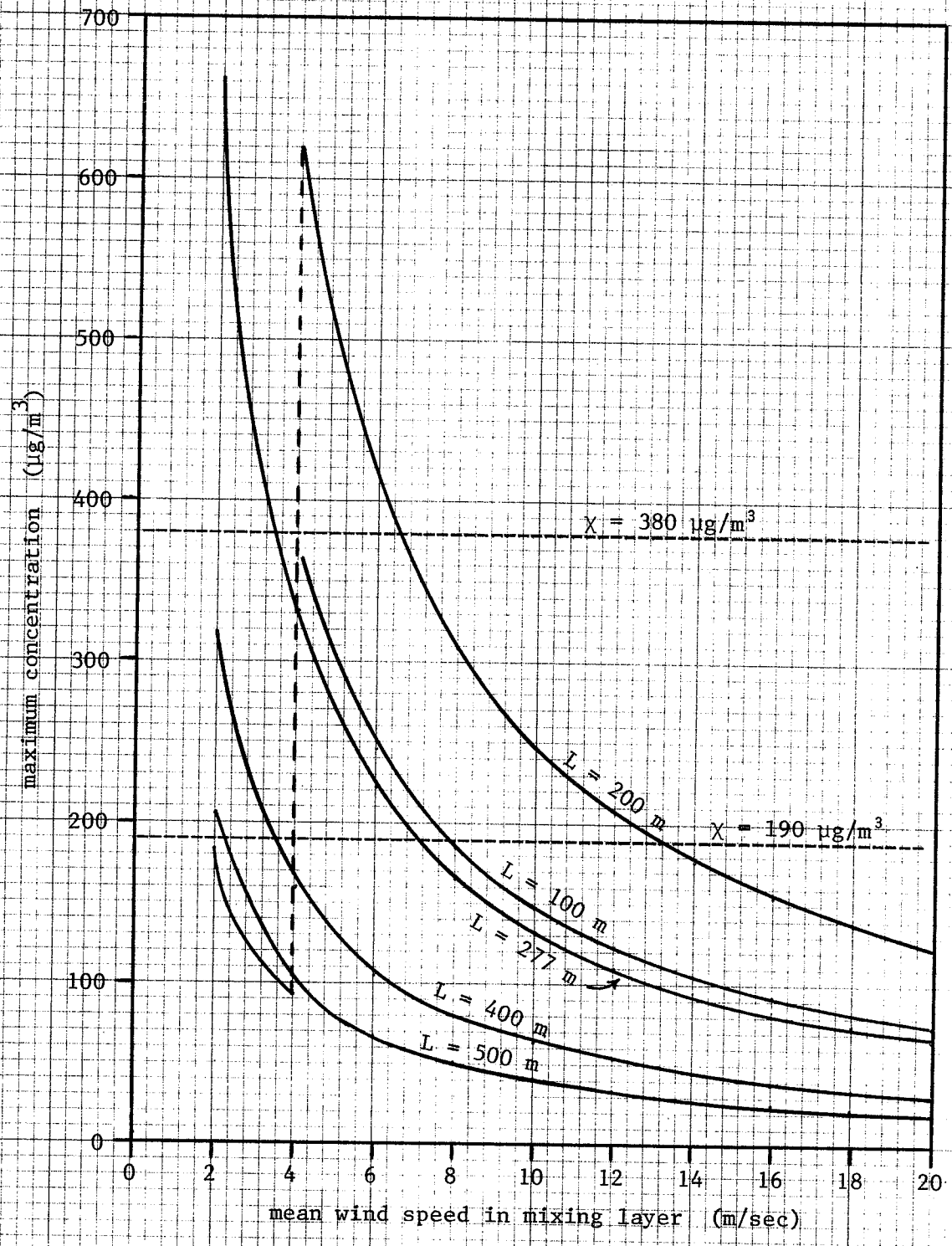

Figure 5.12. Limited Mixing Conditions. Maximum 1-hour ground-level NO_x concentrations. Stability class C. January mean emission rate.

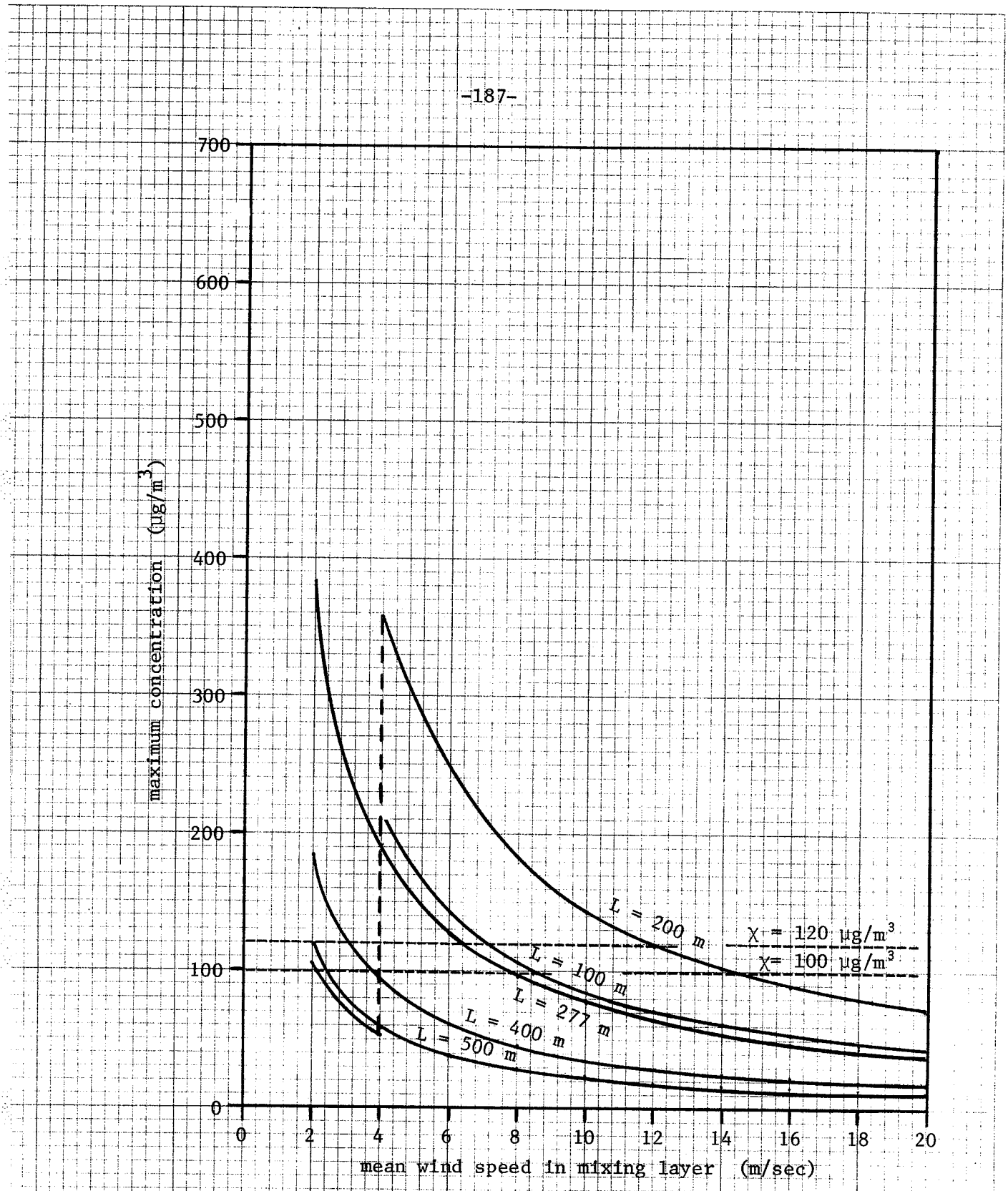

Figure 5.13. Limited Mixing Conditions. Maximum 24-hour ground-level Particulate concentrations. Stability class C. January mean emission rate.

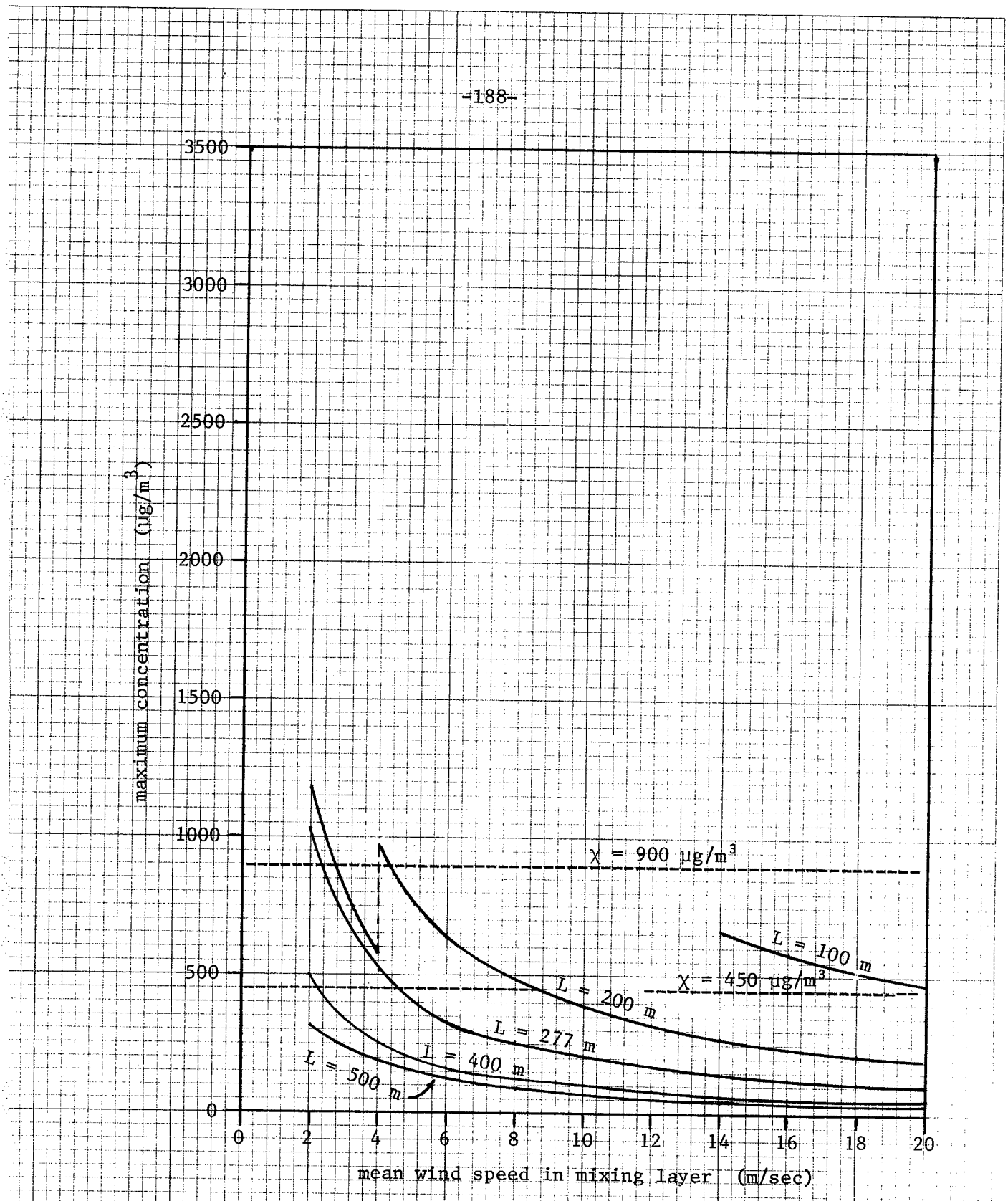

Figure 5.14. Limited Mixing Conditions. Maximum 1-hour ground-level SO_2 concentrations. Stability class C. Maximum emission rate.

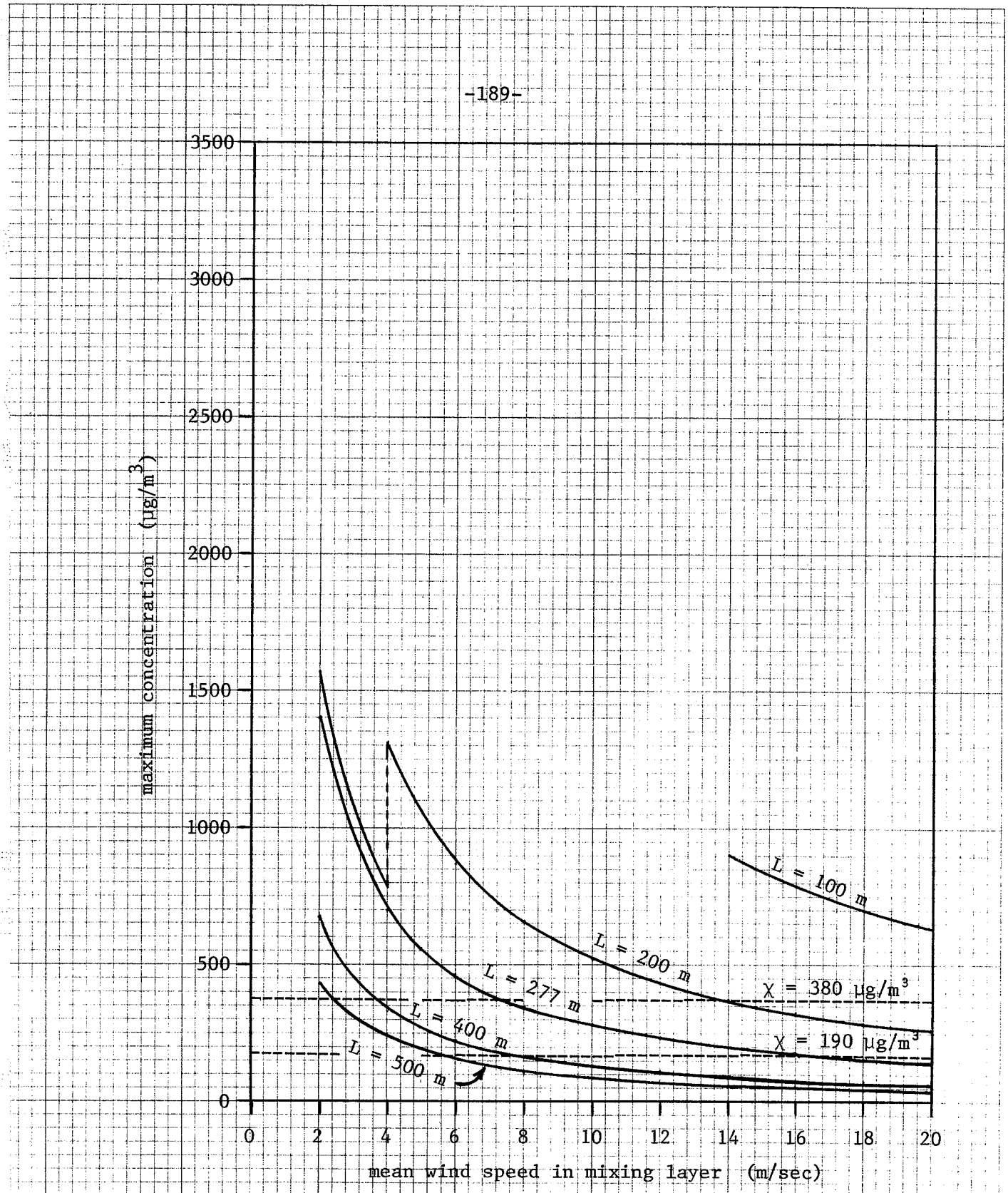

Figure 5.15. Limited Mixing Conditions. Maximum 1-hour ground-level NO_x concentrations. Stability class C. Maximum emission rate.

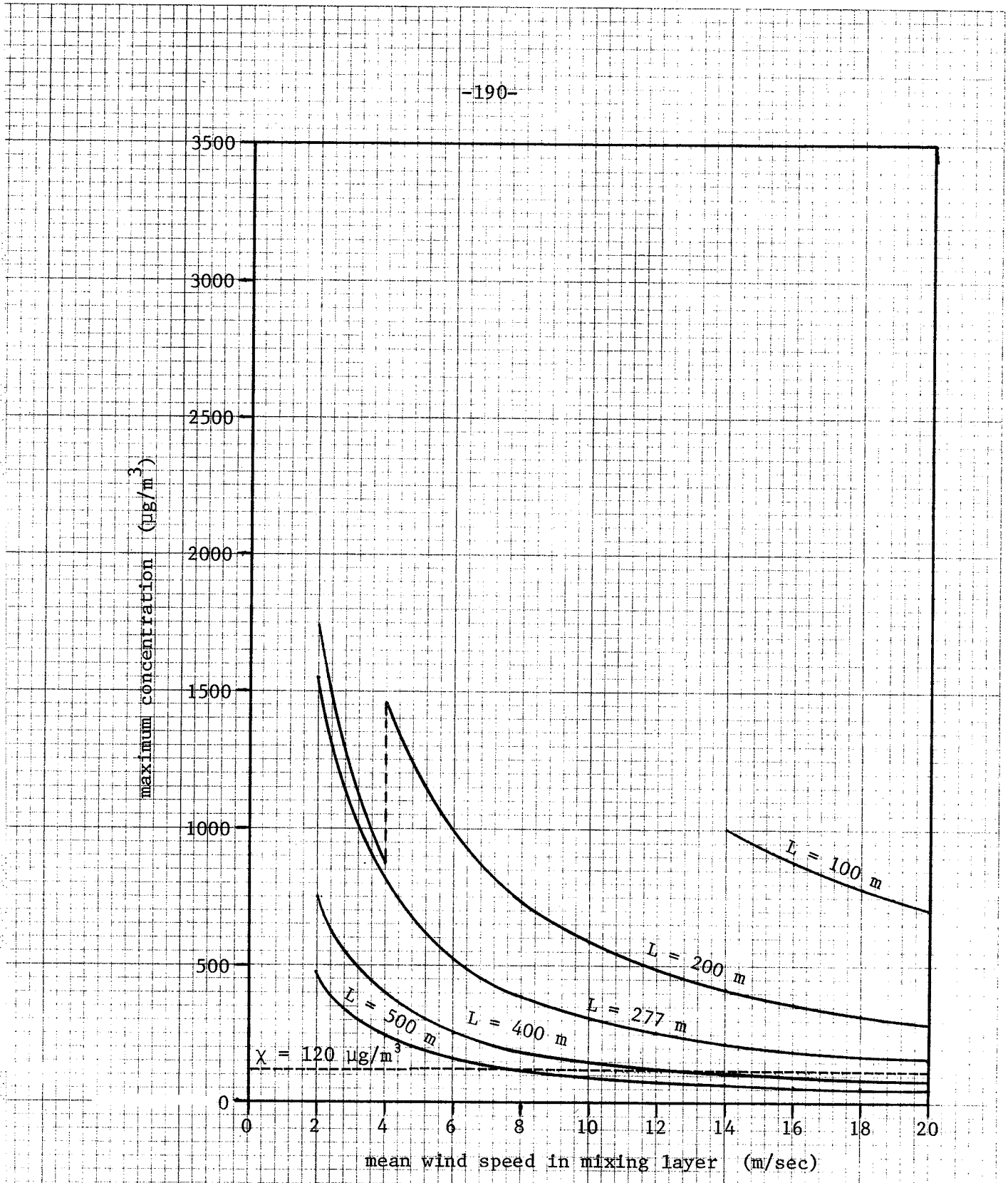

Figure 5.16. Limited Mixing Conditions. Maximum 24-hour ground-level Particulate concentrations. Stability class C. Maximum emission rate.

5.2.6 Concentration Variation with Downwind Distance

Figures 5.17, 5.18 and 5.19 illustrate the variation of the 1-hour SO_2, 1-hour NO_x and 24-hour suspended particulate ground-level concentrations, respectively, with downwind distance. These curves are based on the January mean emission rates and meteorological conditions.

Figures 5.20, 5.21 and 5.22 show the same variation of concentration with distance for the maximum emission rates and critical windspeed u_{cr} = 11.0 m/sec.

Figures 5.23, 5.24 and 5.25 show this variation for the maximum emission rates and the mean windspeed for the peak generating season.

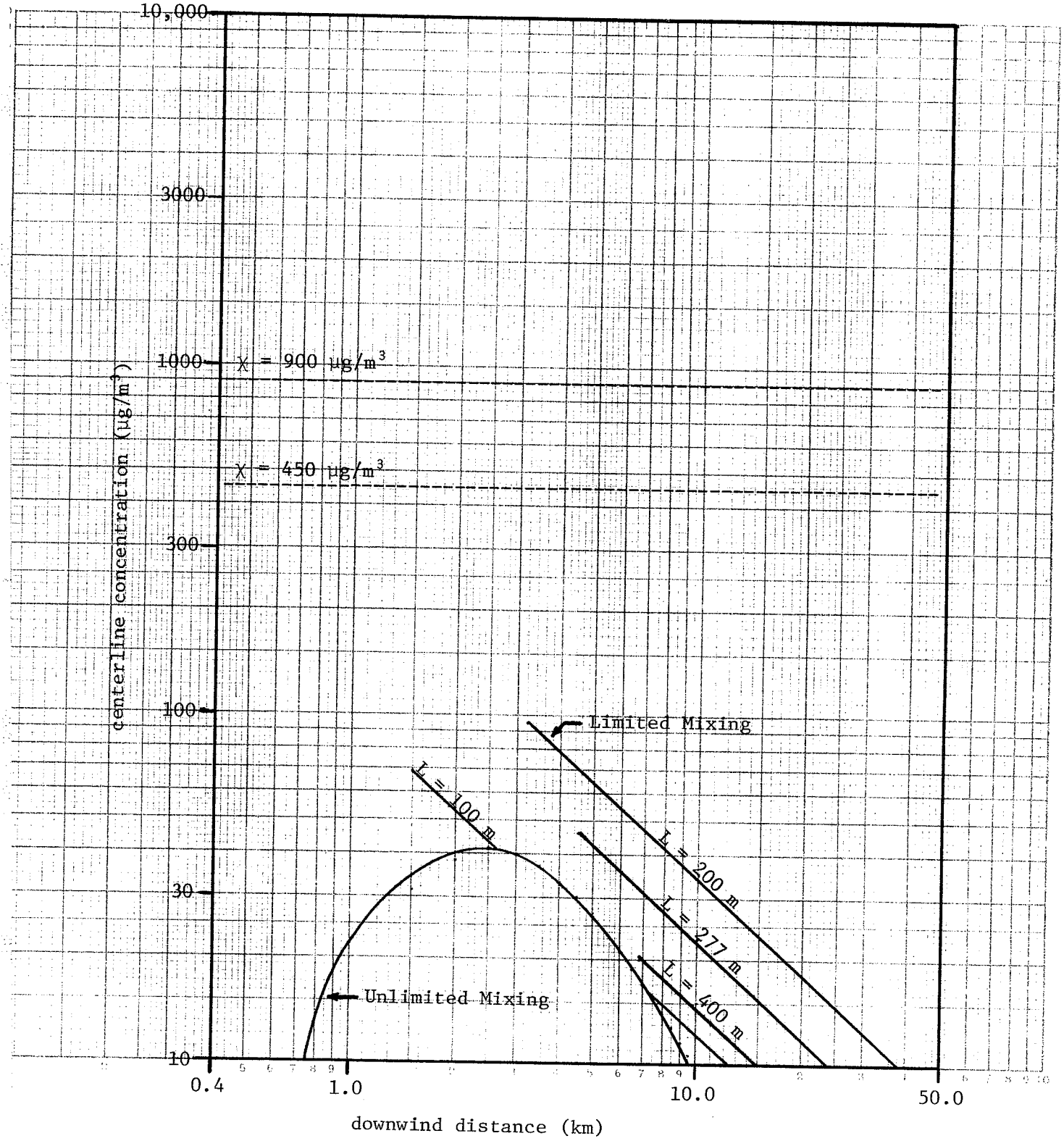

Figure 5.17. Ground-level 1-hour SO_2 concentrations along plume centerline. January emission rate. Windspeed = 4.7 m/sec. Stability class C.

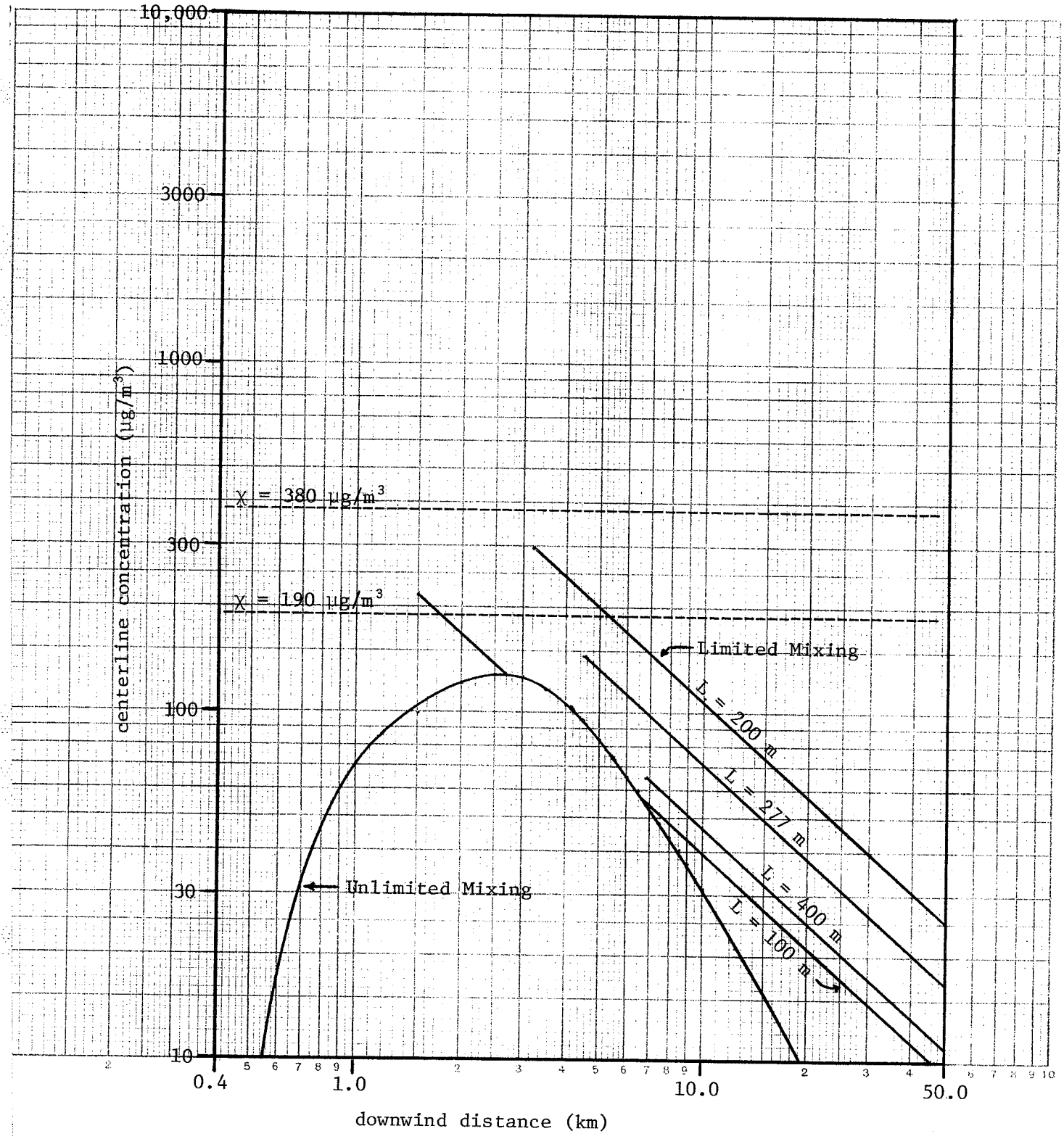

Figure 5.18. Ground-level 1-hour NO_x concentrations along plume centerline. January emission rate. Windspeed = 4.7 m/sec. Stability class C.

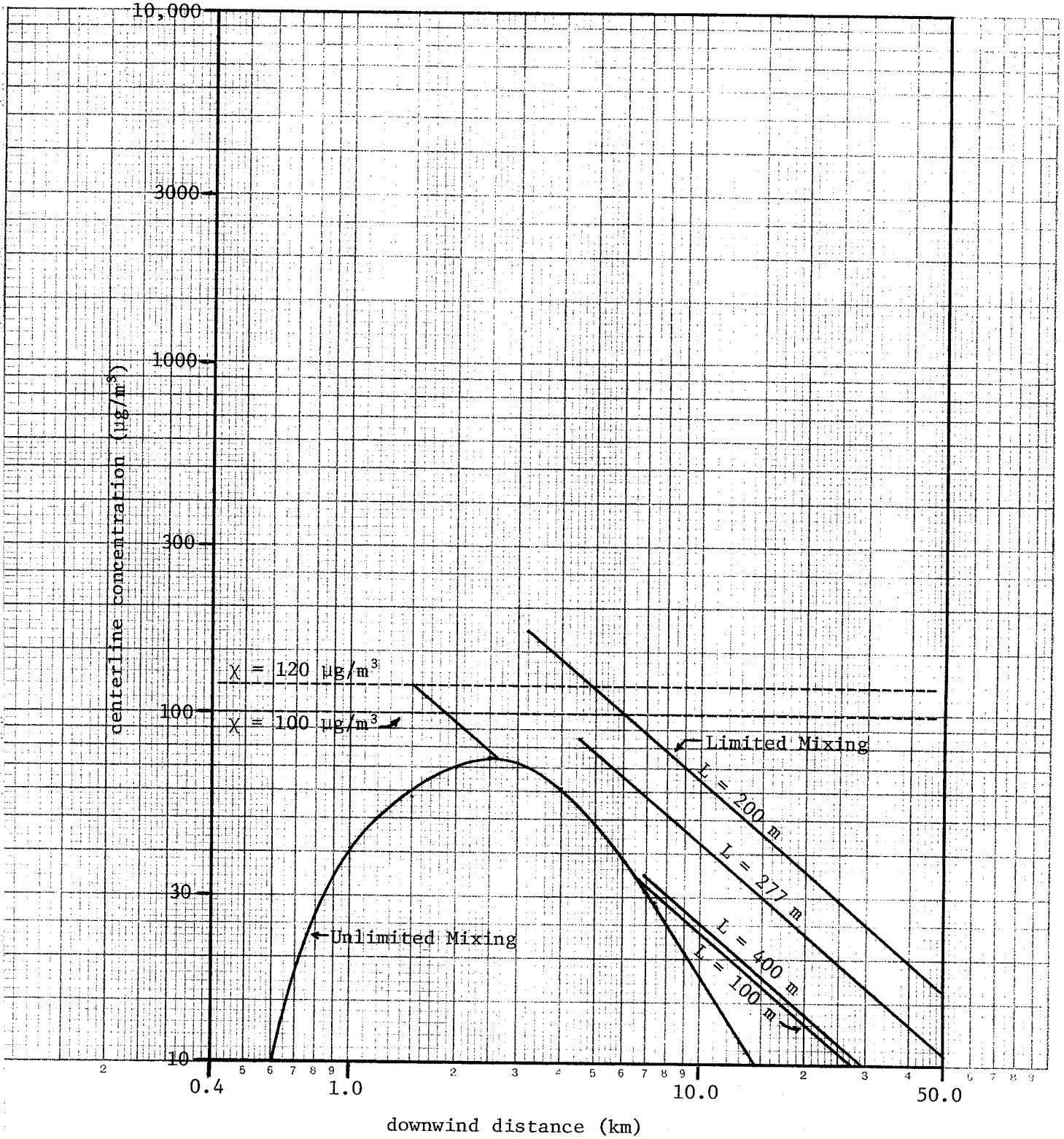

Figure 5.19. Ground-level 24-hour suspended particulate concentrations along plume centerline. January emission rate. Windspeed = 4.7 m/sec. Stability class C.

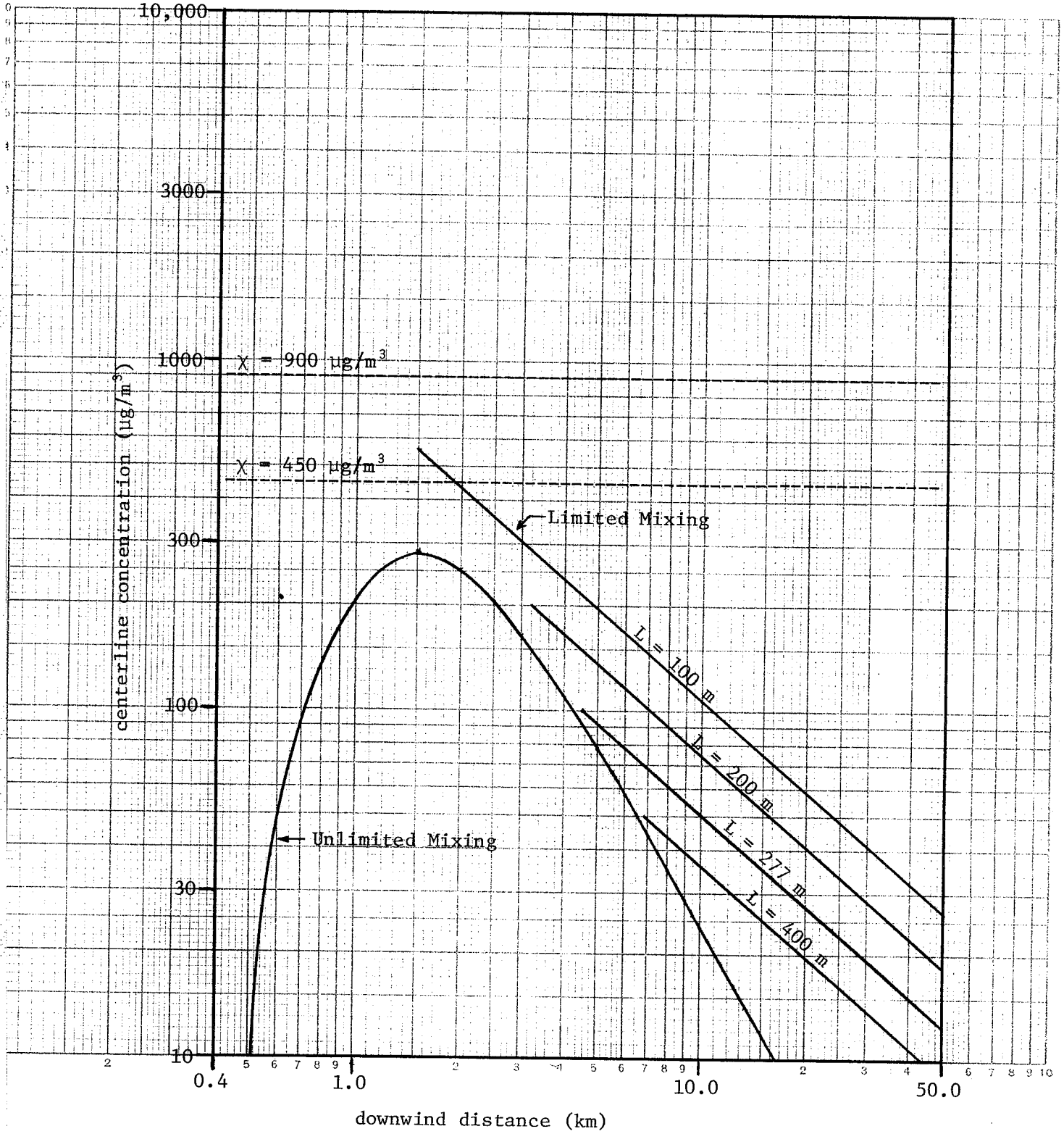

Figure 5.20. Ground-level 1-hour SO_2 concentrations along plume centerline. Maximum emission rate. Critical windspeed = 11.0 m/sec. Stability class C.

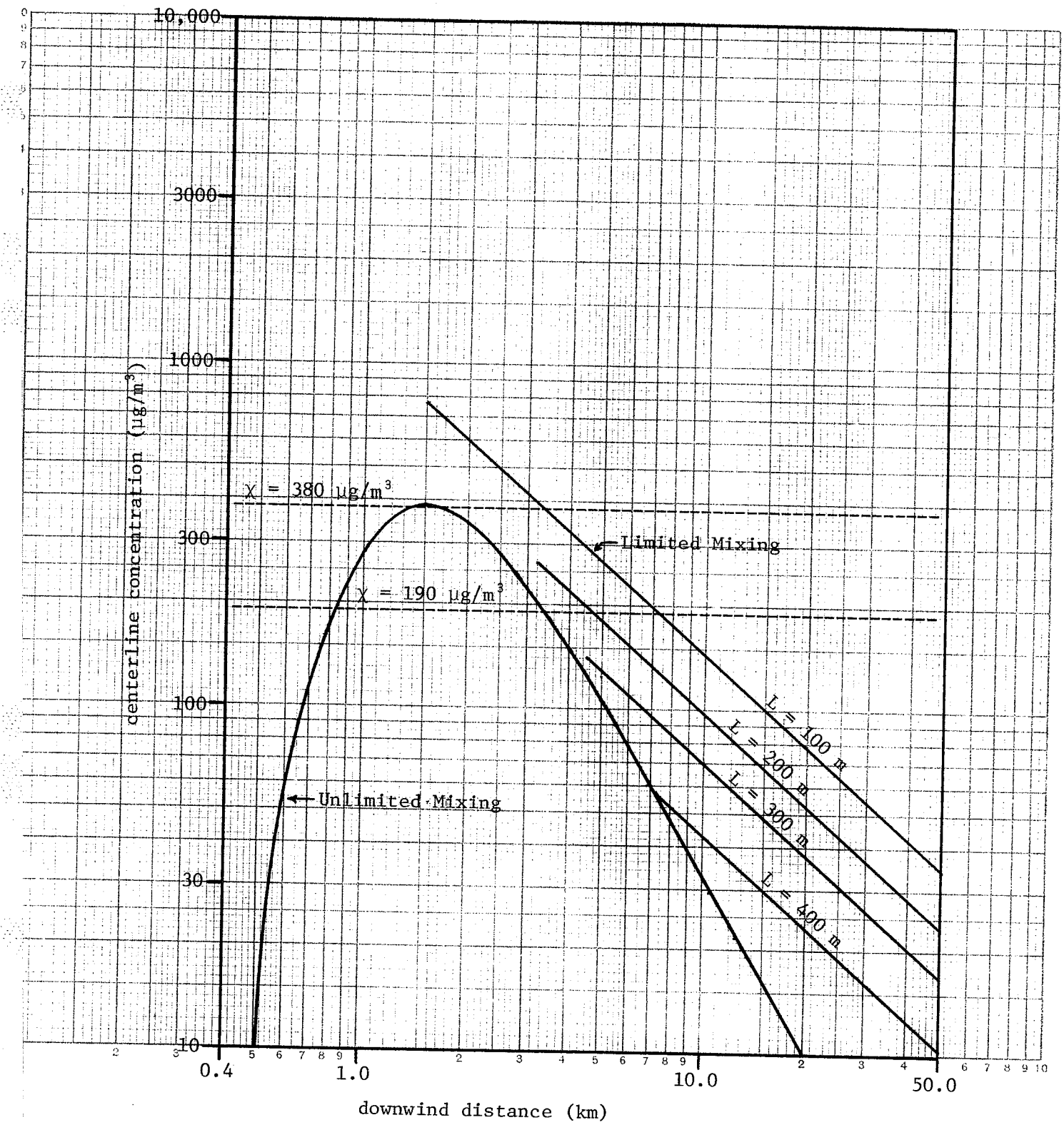

Figure 5.21. Ground-level 1-hour NO_x concentrations along plume centerline. Maximum emission rate. Critical windspeed = 11.0 m/sec. Stability class C.

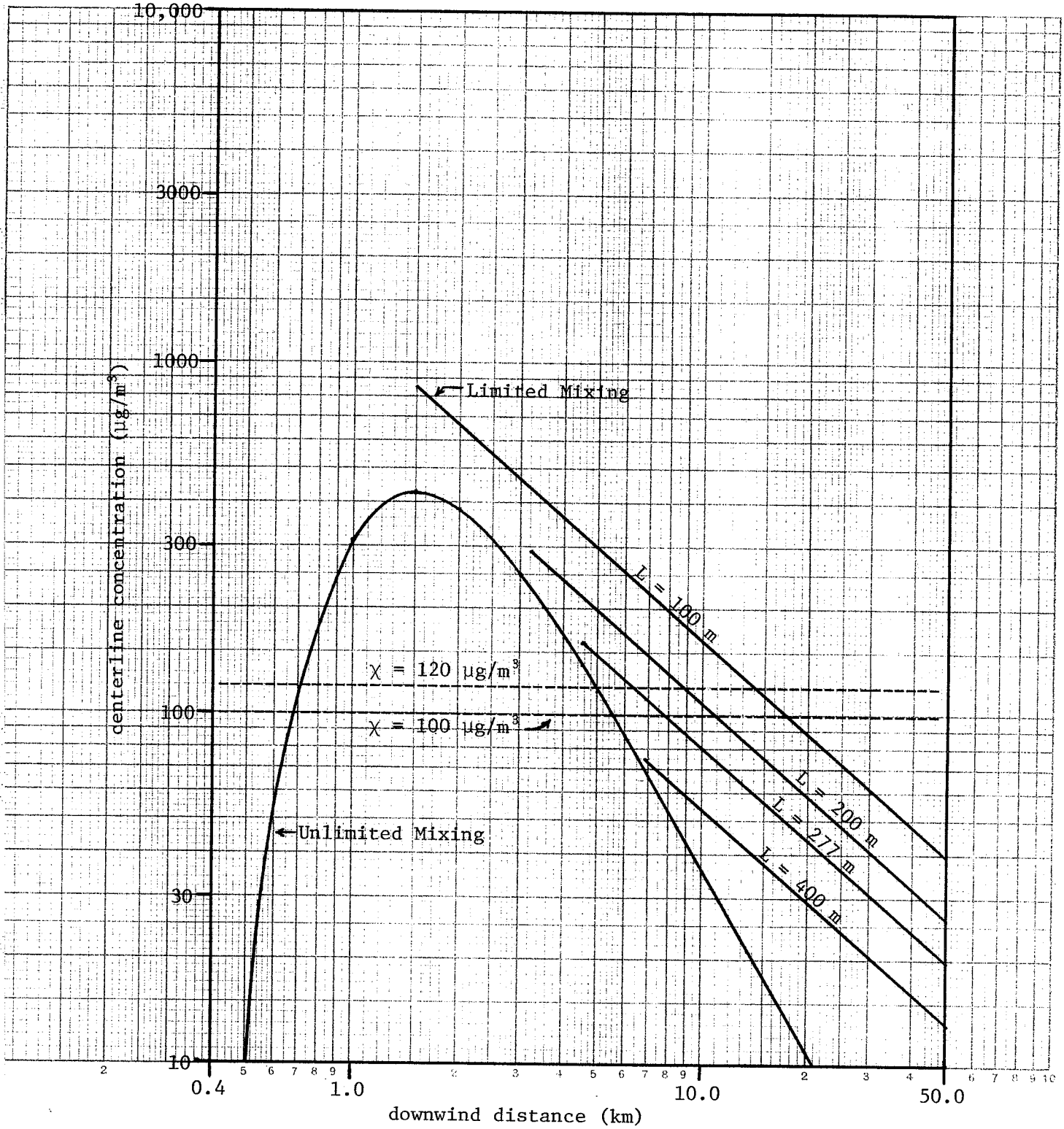

Figure 5.22. Ground-level 24-hour suspended particulate concentrations along plume centerline. Maximum emission rate. Critical windspeed = 11.0 m/sec. Stability class C.

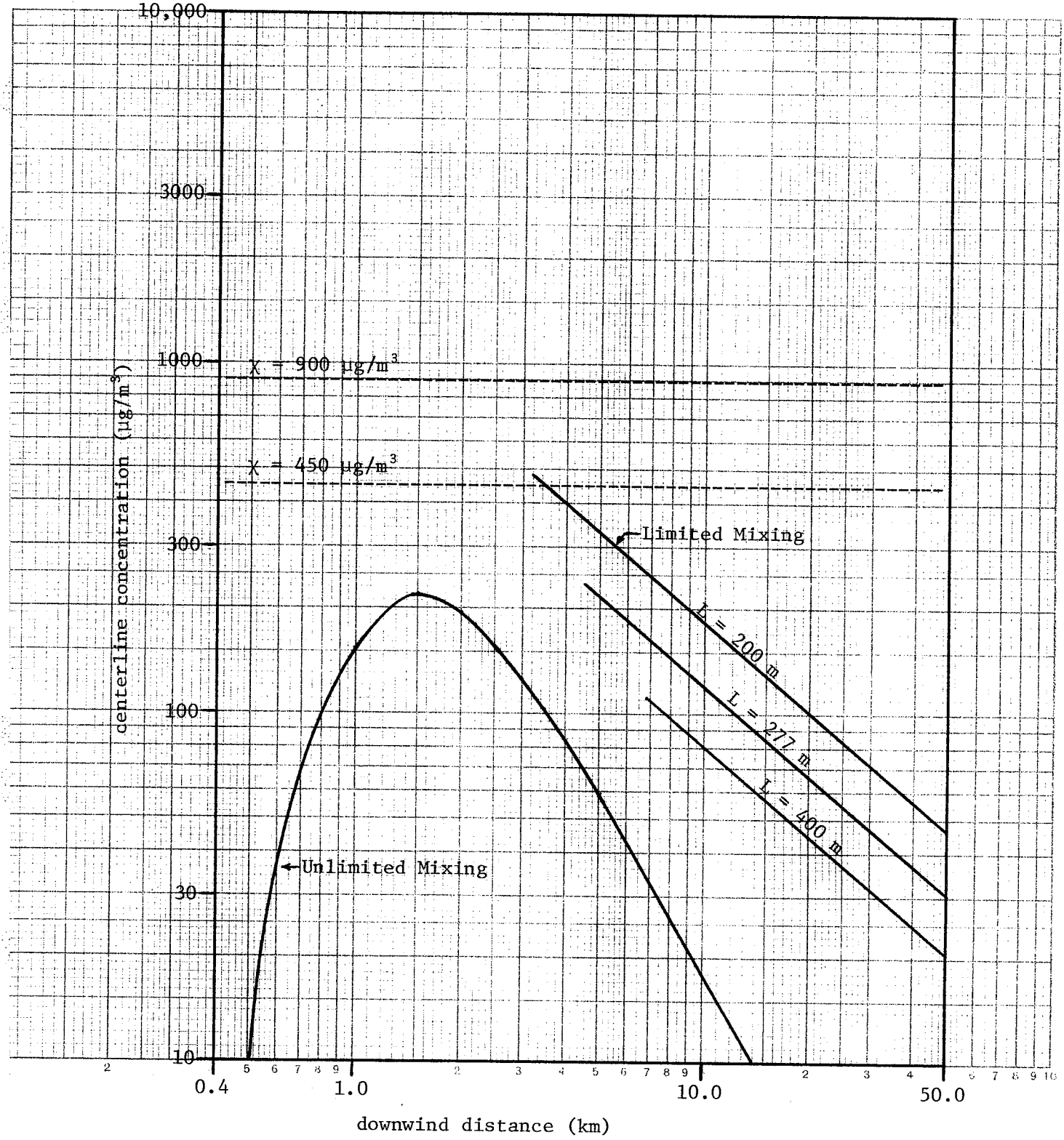

Figure 5.23. Ground-level 1-hour SO_2 concentrations along plume centerline. Maximum emission rate. Windspeed = 4.5 m/sec. Stability class C.

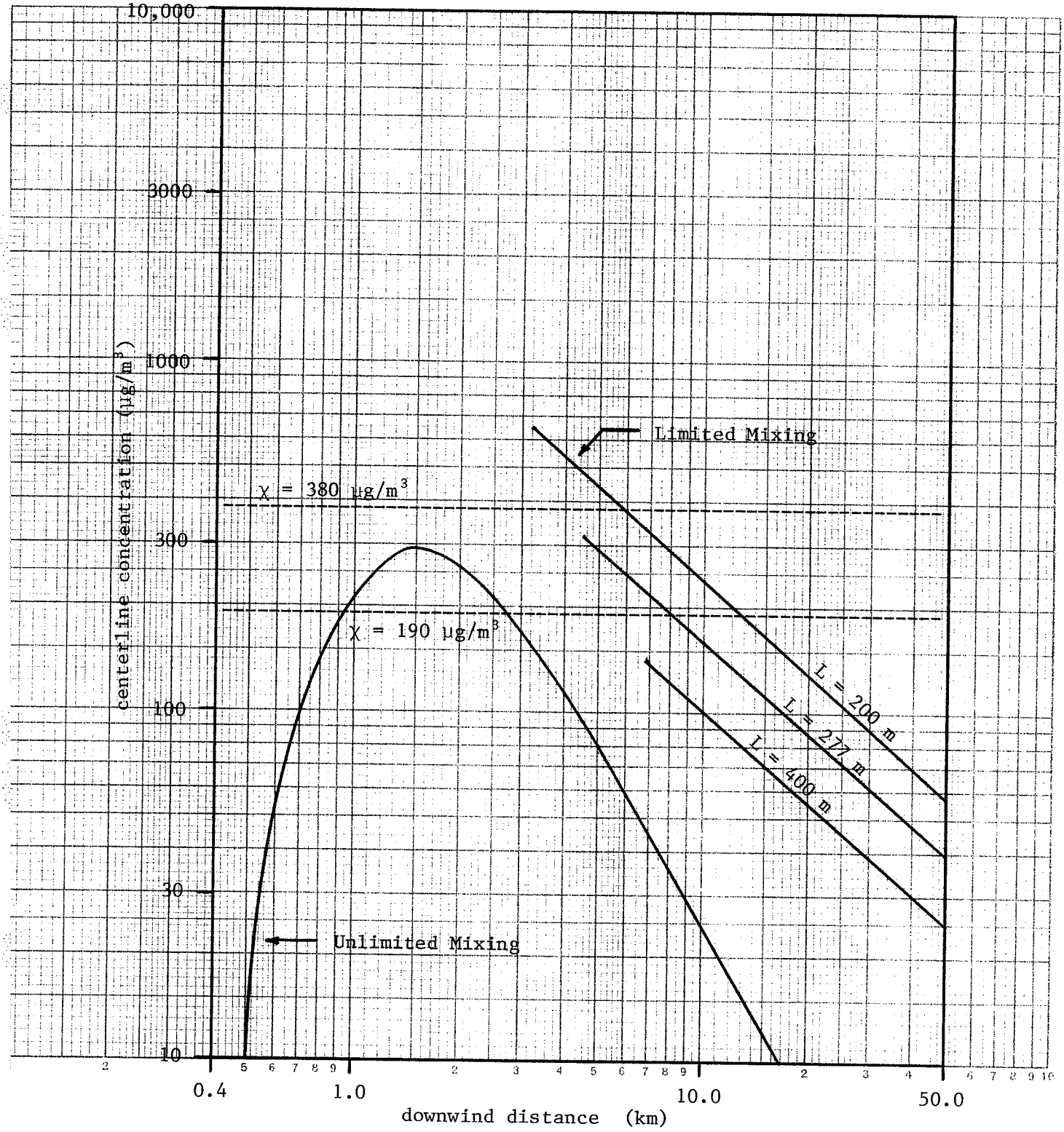

Figure 5.24. Ground-level 1-hour NO_x concentrations along plume centerline. Maximum emission rate. Windspeed = 4.5 m/sec. Stability class C.

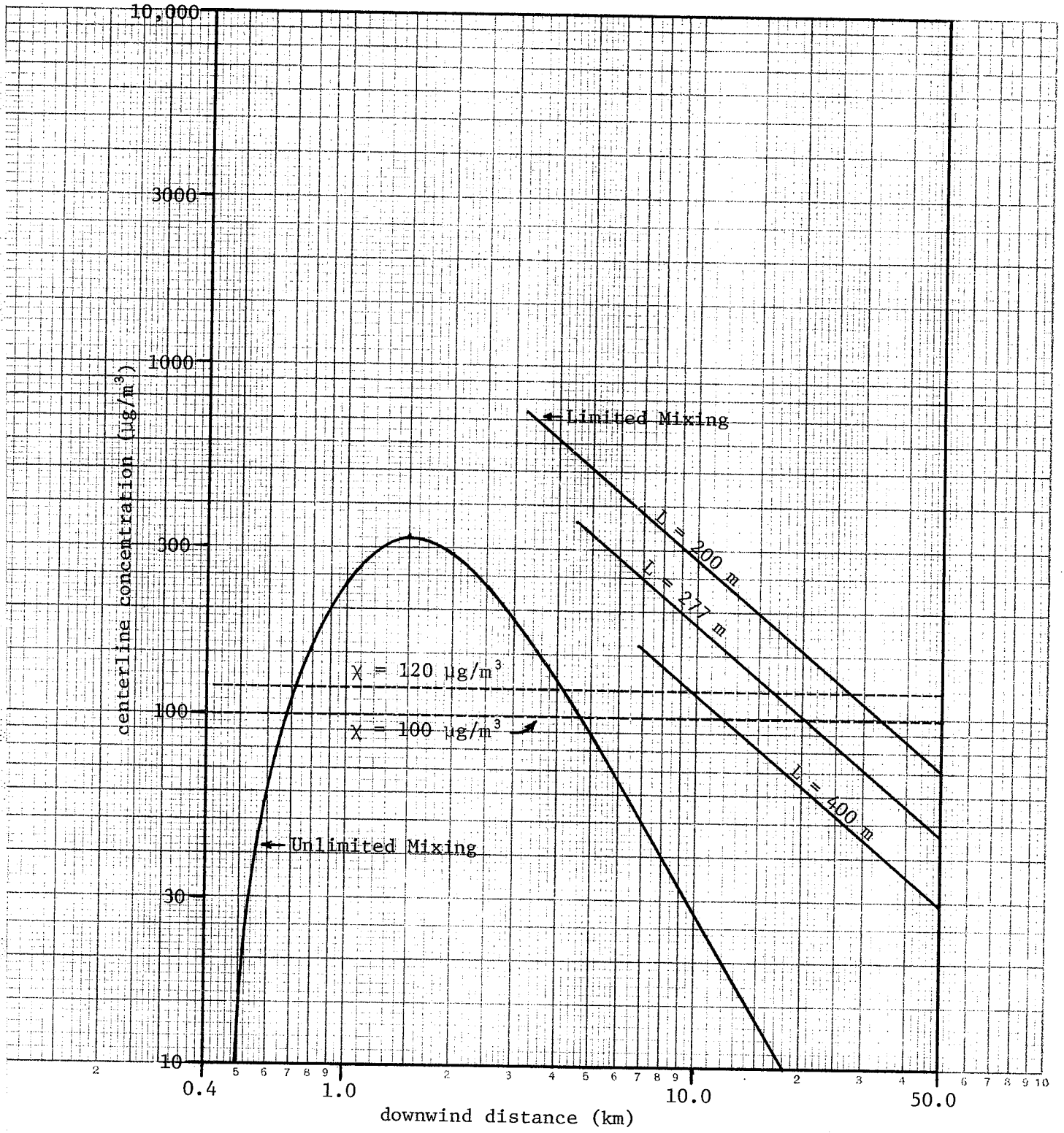

Figure 5.25. Ground-level 24-hour suspended particulate concentrations along plume centerline. Maximum emission rate. Windspeed = 4.5 m/sec. Stability class C.

5.2.7 Monthly Mean Concentrations

Table 5.4 compares the maximum monthly mean concentrations of SO_2, NO_x and suspended particulates for the three months of maximum power generation. The concentrations are based on the monthly mean emission rates and meteorological conditions, stability class C, and unlimited mixing conditions.

TABLE 5.4

MAXIMUM MONTHLY MEAN GROUND-LEVEL CONCENTRATIONS

MONTH	MAXIMUM MONTHLY MEAN CONCENTRATION ($\mu g/m^3$)		
	SO_2	NO_x	SUSPENDED PARTICULATES
December	4	13	13
January	4	13	14
February	2	6	6

5.2.8 Fumigation Concentrations

Table 5.5 lists the ground-level fumigation concentrations for the maximum emission rates, January windspeed, and stability class E. The approximate distance at which the maximum fumigation concentration occurs is 10 km.

TABLE 5.5

GROUND-LEVEL FUMIGATION CONCENTRATIONS

ON PLUME CENTERLINE AT x = 10 km

POLLUTANT	FUMIGATION CONCENTRATION (ug/m^3)
SO_2 (1-hour concentration)	72
NO_x (1-hour concentration)	98
PARTICULATES (24-hour concentration)	108

5.3 EMISSION CONCENTRATIONS

The following standardized emission concentrations were determined for Brandon Generating Station:

SO_2 emissions @ 68°F, 30" hg, 12% CO_2:

at January mean emission rate, χ = 0.015% SO_2 by volume

at Maximum mean emission rate, χ = 0.036% SO_2 by volume

Particulate Emissions @ 68°F, 30" Hg:

January mean emission rate, χ = 0.59 gr/scf

Maximum mean emission rate, χ = 1.13 gr/scf

6. DISCUSSION

6.1 JUSTIFICATION OF METHOD

6.1.1 Briggs' Plume Rise Equation

Briggs' plume rise equations (32) consistently give the best numerical agreement with plume rises observed under a variety of meteorological conditions. They also produce the least percentage of scatter of the plume rise formulas examined in the literature review.

Briggs' equations were developed using data from power plants covering a wide size range, including plants similar in size to the Brandon installation. In his analyses, Briggs was careful to exclude those data rendered inapplicable or unreliable by very small source size, underestimated windspeed, insufficient data, evidence of lakeshore circulation effects, or evidence of downwash of the plume due to terrain discontinuities.

In view of the care taken in their development and their demonstrated agreement with observed data, Briggs' plume rise equations were selected for use in this research. This choice is further supported by the fact that Briggs' equations are those normally used by the Air Pollution Control Directorate of Environment Canada in performing dispersion analyses.

6.1.2 Dispersion Equations

6.1.2.1 Unlimited Mixing Calculations

The Pasquill-Gifford dispersion equation has the advantages of simplicity, acceptable accuracy, and widespread application. Only two

dispersion parameters, σ_y, and σ_z, are required, and the results of most diffusion experiments are now being reported in terms of these variables (22). In addition, the Pasquill-Gifford method is currently being used by several government departments:

i) Manitoba Department of Mines, Resources and Environmental Management (87),

ii) Environment Canada (78,81),

iii) United States Department of Health, Education and Welfare - National Air Pollution Control Administration (22).

The Pasquill-Gifford method has therefore been used in the unlimited mixing calculations for Brandon Generating Station.

It should be noted that in Turner's original workbook (22) the averaging time for the Pasquill-Gifford diffusion coefficients is given as 10 minutes. In an address given at an EPA training course in 1972, Turner stated that in fact the given coefficients correspond more closely to averaging times of 30 minutes to 1 hour. For this reason no corrections for averaging time were required in computing the 1-hour concentrations using the σ_y and σ_z values from Figures 2.13 and 2.14, respectively.

6.1.2.2 Limited Mixing and Fumigation Calculations

The choice of Turner's simplified forms (22) of the Bierly and Hewson equations (57) for limited mixing and fumigation conditions was based on the same rationale as that given for the Pasquill-Gifford equations. Turner's equations have been applied as recently as January 1975 by the Atmospheric Environment Service (AES) of Canada in a study

of air pollution in Thompson, Manitoba (78), and are recommended by the Atmospheric Environment Service for first-order dispersion estimates.

The absence of afternoon upper air data for Brandon required that the monthly mean maximum mixing heights for Brandon be obtained by extrapolation of mixing height data for The Pas, Manitoba. Consultation with Mr. H. Fraser of the Atmospheric Environment Service in Winnipeg revealed that the inversion and mixing height characteristics of Brandon and The Pas are very similar, and that the above extrapolation is valid within the accuracy limits of the Brandon study (88). Mr. Fraser indicated that upper air variations from one area to another are much more conservative than surface air variations, allowing the inversion climatology for The Pas to be legitimately applied to Brandon.

A relatively weak inversion layer was assumed for the inversion penetration calculations (Appendix 8.5.4.5) in order that the limited mixing curves be representative of winter conditions. Examination of the upper air data for Shilo indicated that a value of $2^{o}C$ for ΔT_i would be approximately correct at or near the maximum daily mixing height on most days.

The frequency of nocturnal ground-based inversions in the Brandon area was determined through an analysis of the temperatures at the surface and at the first significant level above the surface (950 mb) for Shilo, Manitoba. Determination of the existence of a ground-based inversion from significant level data rather than from the complete temperature profile for each radiosonde ascent is considered satisfactory. Since significant level measurements must produce the temperature profile

to within $1^{o}C$ of the actual observed value, only those radiosonde ascents with near isothermal conditions off the surface might receive an incorrect classification, and it is unlikely that a significant bias would be introduced (74). This method was used by Munn (74) in his study of inversion climatology in Canada. Mr.H. Fraser of Atmospheric Environment Service indicated that due to the relatively short distance between Shilo and Brandon ($\simeq$ 21 kilometers), the Shilo data could be used without modification to determine the nocturnal inversion frequencies for Brandon (88).

6.1.2.3 Monthly Mean Concentrations

The long-term concentration equations of Gifford (51) and Turner (22) are essentially the same. Turner's equations were selected on the basis of their adaptability to use with the National Oceanic and Atmospheric Administration (NOAA) computer program. Both Turner's equations and the NOAA model are used extensively by Environment Canada and the United States Department of Health, Education and Welfare.

6.1.3 Computer Programs

The multiple source programs used in calculating the ground-level concentrations were selected primarily because of their availability and their applicability to the given operating parameters. The programs provide outputs in a form which facilitates the analysis of the results. Both the 1-hour and long-term multiple source programs are used by Environment Canada.

6.1.4 Selection of Operating Parameters and Meteorological Data

Operating parameters and meteorological data for the preceding dispersion analyses were selected so as to be representative of typical conditions during the months of maximum power generation. In addition, a set of "worst case" conditions was synthesized i.e. those conditions favoring maximum ground-level concentrations (maximum emission rate, limited mixing depth, minimum plume rise, low wind speed, and turbulent mixing conditions within the mixing depth).

Examination of the fuel consumption data for the peak generating season (December, January and February) revealed that ≃ 98% of the energy used for power generation at Brandon is supplied by lignite coal. The small quantities of natural gas and No. 2 fuel oil used for light-off and flame stabilization were therefore neglected in the emission calculations in order to provide emission estimates for normal operating conditions.

Probability analyses were limited to examinations of inversion frequency and the wind frequency distribution for Brandon and its effect upon monthly mean ground level concentrations. No attempt was made to quantify the probability of occurrence of specific ground-level concentrations because of the complexity of the variables which would be involved and the preliminary nature of this assessment. Such an analysis would require the determination of a detailed joint frequency distribution involving monthly diurnal load factors, ambient temperature variations, atmospheric lapse rates and mixing heights, in addition to the frequency distribution of wind speed and direction mentioned above. This problem

would be further compounded by the dependence of the load factor at Brandon Generating Station upon the combined effects of the system load demand and the hydraulic generating capabilities of the system. An analysis of this complexity is beyond the scope of this assessment and is precluded by the constraints of time and manpower available. Furthermore, in view of the limited accuracy of the emission estimates a more detailed dispersion analysis would be virtually meaningless.

6.1.5 Wind Shear Calculations

Reference is made in the literature (11,20,44) to the phenomenon of wind shear, the frictional drag which retards wind flow close to the ground. The result of this effect is a variation of the horizontal wind speed and direction with height in the affected surface layer (usually up to 500-700 m), given approximately by:

$$\bar{u}_h = \bar{u}_1 (z/z_1)^p$$

where $\bar{u}_h$ = wind at some upper elevation, z, and $\bar{u}_1$ = wind at reference height, z_1. The exponent p is not constant, but varies from about 0.12 to 0.50, depending on the underlying terrain and the atmospheric stability.

Due to the unavailability of vertical wind profile data for the Brandon area, wind shear effects were approximated by using a mean value of 0.25 for the exponent p (11). In view of the accuracy of the methods being used here, this approximation of the wind shear factor is not expected to introduce significant error into the results (22).

The calculated wind speeds at the stack levels, h_s, were used in the stack downwash calculations. The calculated wind speeds at the preliminary

effective stack heights, h", were used in Briggs' plume rise equation. Dispersion calculations, with the exception of monthly mean concentration calculations, were performed using the calculated windspeeds at the overall effective stack heights, h_e. Monthly mean concentrations were based on calculated wind speeds at the weighted mean effective stack heights (weighted with respect to emission rates for each stack); this procedure was dictated by the capacity of the NOAA computer program for only one mean wind speed input.

Wind direction also varies with height, with bearings at the gradient wind level (500-700 m) about 15^{o}-30^{o} greater than those of the surface wind, depending on the terrain characteristics and the atmospheric stability (11). At the elevations examined in the Brandon study these effects are expected to be small and have therefore been omitted from the wind direction frequency calculations, with negligible anticipated loss of accuracy.

6.2 DISCUSSION OF RESULTS

6.2.1 Wind Frequency Distributions

The wind roses of Figures 5.1-5.3 indicate that the least prevalent winds are those from the south, with a mean monthly frequency of .7% during the peak generating season. The prevailing winds are from the west and west northwest sectors with a combined mean monthly frequency of 32%. The ideal location for the plant in terms of minimizing pollutant ground-level concentrations in Brandon would therefore be south of the city. Cooling water requirements, however, necessitate the plant's proximity to the Assiniboine River, and within this constraint Brandon

Generating Station is in fact acceptably located on the prevailing downwind side of the city.

Winds from the east northeast, east, east southeast and southeast directions do, however, direct the plumes from the power plant stacks towards Brandon about 21% of the time during the peak generating season. Significant air pollutant concentrations are thus likely to occur in Brandon 21% of the time during the daylight hours. Furthermore, these winds are usually associated with limited mixing conditions which generally produce higher ground-level concentrations than unlimited mixing conditions. The actual concentrations which may be expected under these conditions are discussed in section 6.2.3.

6.2.2 Inversion Frequency and Fumigation Concentrations

The Shilo upper air data indicate that nocturnal inversions occur an average of 60% of the time during the winter. The readings used were taken at altitudes of at least 500 m and thus indicate that the stacks will emit into the stable layer and not above it. During these inversions the stack emissions would be concentrated in a relatively shallow layer aloft and would not reach the ground in appreciable concentrations as shown in Figure 1.12a. Consequently ground-level concentrations will be low on most nights.

Shortly after sunrise inversion break-up fumigation occurs, causing the pollutants previously emitted into the stable layer to be mixed rapidly downward to the ground (see 2.3.4.2). In some cases this results in high ground-level concentrations. The maximum fumigation concentrations calculated for Brandon (72 $\mu g/m^3$ SO_2, 98 $\mu g/m^3$ NO_x and 108 $\mu g/m^3$ suspended

particulates), however, are all well below the maximum values specified in the National and/or Manitoba Air Quality Objectives (450 $\mu g/m^3$ maximum desirable SO_2, 190 $\mu g/m^3$ maximum desirable NO_x, and 120 $\mu g/m^3$ maximum acceptable suspended particulates). The suspended particulate concentration is given as a 24-hour average only for the purpose of comparison with the air quality objectives. In fact, a 24-hour fumigation concentration is meaningless because these fumigations are generally of short duration, persisting for 30-45 minutes at distances of up to 30 km (19 mi) from the power station. In this case, the maximum concentrations were found to occur at a distance of about 10 km (6 mi) from the stacks. The area fumigated is also likely to be long and narrow. The chances of detecting fumigations of this type are therefore very slight unless the same area is fumigated repeatedly.

6.2.3 Unlimited Mixing and Limited Mixing Concentrations

6.2.3.1 General

Unlimited and limited mixing are the two additional dispersion conditions which result in significant ground-level pollutant concentrations. Dispersion calculations were performed for several sets of boundary conditions using the unlimited and limited mixing dispersion models listed in section 4.3. The results of these analyses, shown in Tables 5.2 and 5.3 and Figures 5.5 to 5.25, indicate that in many cases the limited mixing model produces ground-level concentrations 1 to 2 times as high as the unlimited mixing model. Table 5.2 shows that for the monthly mean emission rates and meteorological conditions, the December and January mean maximum ground-level concentrations for limited mixing are about 28%

and 15% greater, respectively, than those for unlimited mixing. In February the increased mean maximum daily mixing height shifts the emphasis to the unlimited mixing model which yields monthly mean maximum concentrations about 60% greater than the limited mixing model.

Limited and unlimited mixing concentrations at the maximum emission rates are compared in Table 5.3 and Figures 5.20 to 5.25. The maximum unlimited mixing concentrations are produced at the critical windspeed u_{cr} = 11.0 m/sec, as shown in Figure 5.4. These concentrations are several times greater than the limited mixing concentrations for 200-400 m mixing heights, but at a mixing height of 100 m the limited mixing maximum values are twice as high as the unlimited mixing values.

The maximum limited mixing concentrations occur at much lower windspeeds as shown by Figures 5.11 to 5.16. At the mean winter windspeed $\bar{u}$ = 4.5 m/sec, the limited mixing model predicts maximum concentrations 2 times higher than the unlimited mixing model for a 200 m mixing height. At L = 277 m, the mean mixing height for December and January, the unlimited and limited mixing maximum concentrations are approximately equal. As the mixing height increases further, the criticality shifts to the unlimited mixing model; at L = 400 m the limited mixing maximum is only half as great as that for unlimited mixing.

The criticality of a particular plume dispersion model is not necessarily established by the magnitude of the peak ground-level concentrations. The frequency of the model and duration of the resulting concentrations must also be considered. Surface windspeeds near u_{cr} (8.5 - 13.9 m/sec) have a frequency of only 11% as opposed to windspeeds near the winter mean (3.5 - 5.5 m/sec) which occur with a frequency of

about 30% (77), lending more importance to the latter case. Furthermore, windspeeds less than 3.5 m/sec occur 21% of the time, and result in increased limited mixing concentrations and decreased unlimited mixing concentrations. Mixing heights of 0 - 300 m, at which the limited mixing model is critical for $u < 5$ m/sec, occur approximately 40% of the time during the winter months. (78). The limited mixing model is therefore critical at least 20% of the time, or about 6 days per month at Brandon.

Another important factor is the distances from the stack at which the maximum ground-level concentrations occur. These are shown in Figures 5.5 to 5.10 and 5.17 to 5.25. The Brandon east and west city limits are 2 and 6 km, respectively, from the stacks at Brandon Generating Station. The peak unlimited mixing concentrations occur 1.5 and 2.5 km from the stacks at the maximum and December/January mean emission rates, respectively. The peak limited mixing concentrations occur at 1.5, 3.2, 4.5 and 6.8 km downwind for mixing heights of 100, 200, 277 and 400 m, respectively, regardless of emission rate. The most frequently occurring of these are the 200 and 277 m mixing heights. The maximum limited mixing concentrations thus occur most frequently <u>within</u> Brandon when the plumes are directed towards the city.

In summary, the limited mixing model is significant for three reasons:

1) The resulting maximum ground-level concentrations may be several times that estimated using the unlimited mixing model.
2) The peak limited mixing concentrations most frequently occur within Brandon when the winds are from the east northeast to southeast directions.

3) The limited mixing model is the critical one at least 20% of the time during the peak generating season. Maximum limited mixing surface concentrations may persist for 2 - 4 hours, usually occurring from mid-morning to mid-afternoon (78,88).

6.2.3.2 Sulfur Dioxide Concentrations

Ground-level 1-hour SO_2 concentrations at the January mean emission rate do not exceed the National and Manitoba Air Quality Maximum Desirable Objective of 450 ug/m3, as shown by Figures 5.11 and 5.17.

At the maximum emission rate the 1-hour SO_2 concentrations for unlimited mixing do not exceed the 450 ug/m^3 limit. For mixing heights between 100 and 300 m there are several combinations of mixing height and windspeed (bounded by u = 2 m/sec in the mixing layer) which give rise to hourly limited mixing SO_2 concentrations in excess 450 ug/m^3, as shown in Figure 5.14. The Maximum Acceptable Objective of 900 ug/m^3 is exceeded only for a very narrow range of surface windspeeds (1.0 to 2.5 m/sec) and mixing heights of 200 to 300 m. The maximum amount by which the 900 ug/m^3 objective is exceeded is about 270 ug/m^3, or 30%.

The monthly mean SO_2 concentrations (Table 5.4) are all well below the National Air Quality Maximum Desirable annual mean concentration of 30 ug/m^3.

6.2.3.3 Nitrogen Dioxide Concentrations

Hourly NO_x concentrations at the January mean emission rate not exceed the Manitoba Maximum Desirable Objective of 190 ug/m^3 for unlimited mixing conditions (Figure 5.18). The Maximum Acceptable Objective of 380 ug/m^3 is exceeded under limited mixing conditions for several combinations

of windspeeds and mixing height for u < 3.5 m/sec and mixing height values between 200 and 300 m (Figure 5.12). The NO_x concentrations under these conditions range from 380 to 660 ug/m^3.

At the maximum emission rate the maximum unlimited mixing concentration is 389 ug/m^3, approximately equal to the Maximum Acceptable Objective. The maximum limited mixing concentrations are several times higher than the 380 ug/m^3 limit for several mixing height/windspeed combinations (see Figure 5.15). The 380 ug/m^3 objective is exceeded for mixing heights of 100, 200, 277 and 400 m at windspeeds of 10 to 15, < 8, < 4, and < 2 m/sec, respectively, with resultant concentrations as high as 1000-1500 ug/m^3 at low windspeeds (< 2 m/sec).

The monthly mean NO_x concentrations (Table 5.4) are very low (6 to 13 ug/m^3) relative to the National Air Quality Maximum Desirable annual mean concentration of 60 ug/m^3.

6.2.3.4 Suspended Particulate Matter Concentrations

The maximum 24-hour suspended particulate unlimited mixing concentrations at the January mean emission rate do not exceed the Manitoba Maximum Desirable Objective of 100 ug/m^3 (see Figure 5.19). Under limited mixing conditions, however, the National and Manitoba Air Quality Maximum Acceptable Objective of 120 ug/m^3 (24-hour average) is exceeded for a wide range of mixing height and windspeed combinations. Twenty-four hour particulate concentrations greater than 120 ug/m^3 occur at the January mean emission rate for mixing heights of 100, 200, 277 and 400 m at surface windspeeds of < 4.7, < 6.7, < 3.3 and < 1.5 m/sec, respectively.

At the maximum emission rate, the 24-hour ground-level suspended

particulate concentrations exceed the Maximum Acceptable Objective for almost all limited and unlimited mixing conditions (Figures 5.16, 5.22, and 5.25). Under unlimited mixing conditions the maximum 24-hour concentrations reach 180 to 430 ug/m^3 for windspeeds > 2 m/sec. Limited mixing concentrations range from 120 to 1750 ug/m^3 for mixing heights of 200 to 400 m and windspeeds < 6 m/sec.

The monthly mean suspended particulate concentrations (6 to 13 ug/m^3) are below the National Air Quality Maximum Desirable annual mean concentration of 60 ug/m^3.

6.2.4 Emission Concentrations

The sulfur dioxide emission concentrations for the January mean and maximum emission rates do not exceed the Manitoba limit of 0.2% by volume at 68°F, 12% CO_2. (90)

Particulate emissions at both the mean emission rate (0.59 gr/scf) and the maximum emission rate (1.13 gr/scf) are in excess of the Manitoba limit of 0.4 gr/scf at 68°F, 30 inches mercury, and 12% CO_2, (90) by approximately 50% and 280%, respectively.

6.3 EMISSION ESTIMATES

The ground-level concentrations predicted by the foregoing dispersion analyses can be no more accurate than the estimated emission quantities. The most important variables in this case are the amount of retained in the boilers and the amount of flyash collected in the dust collectors. Information provided by Manitoba Hydro (84,85) and consultation with plant personnel indicated approximate values of 25% and 70%, respectively, for these parameters. Errors in these assumed values will be reflected

directly in the results of this study.

6.4 ACCURACY OF DISPERSION ANALYSES

The dispersion analyses performed in this study represent the best available methods of estimating pollutant concentrations downwind of an elevated source. For the boundary conditions examined, the values of σ_z used may be expected to be correct within a factor of 2. Uncertainties in the estimates of σ_y are generally less than those of σ_z. The predicted ground-level concentrations at the specified emission rates and conditions should be correct within a factor of 3, including errors in σ_y and u. (22).

7. CONCLUSIONS AND RECOMMENDATIONS

7.1 SIGNIFICANCE OF AIR POLLUTANT EMISSIONS FROM BRANDON GENERATING STATION

The major air pollution problem caused by the Brandon Generating Station is the occurrence of high daytime ground-level concentrations of suspended particulate matter for almost all limited and unlimited mixing conditions at full plant loading. These concentrations are 1 to 15 times higher than the Manitoba Maximum Acceptable Air Quality Objective of 120 ug/m^3, and are likely to result in reduced visibility, increased soiling, and increased cleaning requirements. (3). Detrimental health effects are also possible (2,3). These effects are especially of concern during the 21% of the time when the wind blows towards Brandon from the generating station.

The concentrations of nitrogen oxides due to Brandon Generating Station are not expected to cause any detrimental effects, even though they do exceed the maximum acceptable air quality levels by up to 3 times. At the predicted peak concentrations leaf damage occurs in some species of plants, (3), but since these high concentrations occur only in winter at Brandon this potential effect is of little concern. Photochemical smog, another possible result of excessive ambient NO_x concentrations, is similarly unlikely to pose a problem in the Brandon area as the hydrocarbons necessary for the smog to development are not expected to occur in significant concentrations.

The predicted sulfur dioxide concentrations are below the maximum acceptable levels under virtually all conditions and are not likely to have any detrimental effects upon the environment.

7.2 AIR POLLUTION CONTROL REQUIREMENTS

The only air pollution control requirement evident from this study is a reduction of the particulate emissions. A reduction of 90-95% would effectively bring the suspended particulate matter concentrations into compliance with the 120 ug/m^3 standard for virtually all mixing conditions experienced at Brandon.

7.3 FUTURE INVESTIGATION

7.3.1 Stack Sampling

The accuracy of a dispersion analysis depends greatly on the accuracy of the emission parameters. It is therefore recommended that further study be undertaken to verify the calculated emission rates used in this study. This would be best accomplished through the development of a stack sampling program for all stacks at varying load conditions.

7.3.2 Ambient Air Monitoring

Ambient air monitoring provides the best system for verifying the ground-level concentrations predicted by dispersion modelling, since it measures the actual concentrations which do occur. If continuous particulate concentration monitoring were carried out at several locations along the prevalent wind directions, representative hourly, daily, monthly and annual values could be obtained. In addition, averaging this data for each hour of the day and presenting it in a monthly format would allow positive identification of the months and times of day of highest ground-level suspended particulate concentrations. This data could then be compared with the dispersion estimates presented here.

8. APPENDICES

8.1 APPENDIX:SYMBOLS - PLUME RISE AND DOWNWASH EQUATIONS

Dimensions of each term are given in brackets: L = length, t = time, τ = temperature, m = mass.

A	a quantity of the dimensions of time (t), a function of the waste gas buoyancy and wind velocity; see Equation 2.12 and 2.13, Bosanquet (28)
C	mean dilution coefficient (dimensionless), Bosanquet (28)
C_p	specific heat of stack gas at constant temperature
C_{pa}	specific heat of air at constant pressure
D,d	stack diameter (internal) (L)
F	buoyancy flux parameter (L^4/t^3), Briggs (32)
F_m	momentum flux parameter (L^4/t^2), Briggs (32)
g	acceleration due to gravity (L/t^2)
h, h_s	stack height (L)
h'	effective stack height after accounting for stack aerodynamics (L)
h"	effective stack height after building and stack aerodynamics are accounted for (L)
h_e	effective source height after accounting for effects of plume rise and building and stack aerodynamics = h" + Δh (L)
h_b	height of building (L)
Δh	plume rise (L)
Δh_b	buoyancy rise (L), Bosanquet et al. (24)
Δh_v	momentum rise (L), Bosanquet et al. (24)
$\Delta h_{v_{max}}$	maximum momentum rise (L), Bosanquet et al. (24)
L	characteristic length for buoyant plume in a crosswind = F/u^3 (L), Briggs (32)
L_b	lesser of building height, h_b, or building width normal to wind direction, w_b (L)

Q, Q	mass emission rate of stack gas (m/t)
Q_h	heat emission rate of stack gas relative to ambient atmosphere (mL^2/t^3)
Q_{v1}	volume emission rate of stack gas at temperature T_1 (L^3/t); Bosanquet et al. (24, Bosanquet (28)
r	radius of stack (internal ((L)
s	restoring acceleration per unit vertical displacement for adiabatic motion in the atmosphere (t^{-2}), Briggs (32)
T	average absolute temperature of ambient air (τ)
T_s	average absolute temperature of gases emitted from stack (τ)
T_1	absolute temperature at which density of stack gas is equal to that of the ambient atmosphere (τ)
ΔT	temperature excess of stack gases relative to ambient air = $T_s = T$ (τ)
ΔT_1	$T_s - T_1$
t	time elapsed after waste gas leaves stack (t)
t_o	time required for waste gas to attain its exit momentum under the influence of buoyancy alone (t)
u	average wind speed at stack level (L/t)
V_s	stack gas exit velocity (L/t)
X	non-dimensional variable used by Bosanquet et al. (24); see Equation 2.5
X'	non-dimensional varialbe = $(t + t_o)/A$, Bosanquet (28)
X'_o	non-dimensional varialbe = t_o/A, Bosanquet (28)
x	horizontal distance downwind of stack (L)
x*	distance downwind at which atmospheric turbulence begins to dominate entrainment of air into plume (L), Briggs (32)
Z	non-dimensional variable used by Bosanquet et al. (24)
α	numerical constant in plume rise formula of Lucas et al. (29) ($L^{3/2}/m^{1/4}t^{1/4}$)
ρ	average density of ambient air (m/L^3)
ρ_o	average density of stack gas (m/L^3)
$d\theta/dz$	atmospheric lapse rate (potential temperature gradient of ambient air) (τ/L)

8.2 APPENDIX: SYMBOLS - DISPERSION EQUATIONS

Dimensions of each term are given in brackets: L = length, t = time, τ = temperature, m = mass.

a	fraction of the year during which the wind direction falls within a specified angle measuring 1 radian; see Equation 2.40, Bosanquet and Pearson (42)
a	non-dimensional constant used in Cramer's σ_y power law equation (48); see Equation 2.81
b	non-dimensional constant used in Cramer's σ_z power law equation (48); see equation 2.82
C_y	lateral diffusion coefficient ($L^{n/2}$), Sutton (43)
C_z	vertical diffusion coefficient ($L^{n/2}$), Sutton (43)
C_p	specific heat of air at constant pressure, cal/g^{o}K; see Equation 2.69
exp x	$\equiv e^x$
f	free falling speed of a dust particle (L/t), Bosanquet and Pearson (42); see Equation 2.45
f(θ,S,N)	frequency during the period of interest that the wind is from the direction θ, for the stability condition, S, and wind speed class, N; Turner (22), see Equation 2.77
h	height of source above ground (L), Bosanquet and Pearson (42)
h	vertical plume spread (L), Pasquill (50)
h_e	effective stack height (L)
h_{eN}	effective height of release for the wind speed u_N (L), Turner (22); see Equation 2.77
h_i	height of the base of an elevated inversion sufficient to be above the plume = $h_e + 2\sigma_z$, see Equations 2.61, 2.64, 2.67, 2.69, 2.70; height of the base of an elevated inversion, see Equation 2.65; (L)
h_s	physical stack height (L)
L	height of base of elevated stable air layer, limited mixing height (L), Bierly and Hewson (57)
m	mass emission rate over a unit area of the earth's surface (m/L^2), Bosanquet and Pearson (42)

n	turbulence index (dimensionless), Sutton (43)
p	numerical constant for vertical diffusion, Bosanquet and Pearson (42); $p = (h_i - h_e)/\sigma_z$, Bierly and Hewson (57), see Equation 2.65; variable exponent used in sampling time calculations, Turner (22), see Equation 2.73
Q	mass emission rate (m/t)
q	numerical constant for lateral diffusion, Bosanquet and Pearson (42)
R	net rate of sensible heating of an air column by solar radiation (cal/m^2 sec), Pooler (58); see Equation 2.69
s	averaging time of the variance $\overline{v'^2}_{\tau,s} = t/\beta$, Hay and Pasquill (49)
t	time (t)
t_m	time required for the mising layer to develop from the top of the stack to the top of the plume (t), Pooler (58) and Hewson (60); see Equations 2.69 and 2.70
u	average wind speed at stack level (L/t)
u_N	representative wind speed for class N, Turner (22); see Equation 2.77
v'	eddy velocity in the crosswind direction (L/t), Sutton (43)
$\overline{v'^2}/u^2$	crosswind gustiness factor, Sutton (43)
$v'^2_{\tau,s}$	variance of the lateral component of eddy velocity, for the time parameters τ and s, Hay and Pasquill (49)
w'	eddy velocity in the vertical direction (L/t), Sutton (43)
x	distance downwind of stack (L)
x_L	downwind distance at which an elevated stable layer begins to affect the vertical distribution under limited mixing conditions (L), Bierly and Hewson (57)
x_{max}	distance downwind to point of maximum concentration (L)
y	crosswind distance (L)
$\overline{Y^2}$	variance of wind-direction fluctuation, Hay and Pasquill (49)
z	height above ground (L)
β	ratio of the Lagrangian time-scale of turbulence to the time-scale deduced from (Eulerian) measurements of the turbulent fluctuations at a fixed point, Hay and Pasquill (49)

θ	lateral plume spread (degrees), Pasquill (50); wind direction (degrees), Turner (22)
ν	kinematic viscosity of ambient air
ρ_a	ambient air density (m/L^3)
σ_e	standard deviation of the wind elevation angle, Hay and Pasquill (45)
σ_p	standard deviation of crosswind spread of emitted particles (degrees), Hay and Pasquill (49)
σ_y, σ	standard deviation of the crosswind distribution of material in a plume (L)
σ_{y_F}	value of σ_y for fumigation conditions = σ_y for stable conditions plus one-eighth the effective emission height (L)
σ_z	standard deviation of the vertical distribution of material in a plume (L)
σ_{zS}	value of σ_z evaluated at the distance x for the stability class S, Turner (22); see equation 2.77
σ_θ	standard deviation of crosswind spread of emitted particles (degrees), Hay and Pasquill (49)
$\sigma^2_{\theta_{\tau,s}}$	variance of the horizontal wind direction for sampling time τ and averaging time s
τ	sampling time = duration of release of particles, or = duration of the sampling of the distribution of particles, Hay and Pasquill (49)
χ	effluent concentration of plume at given location (x,y,z); (m/L^3)
χ_{avg}	average concentration (m/L^3)
χ_{max}	maximum ground-level concentration on plume centerline (m/L^3)

8.3 APPENDIX: OPERATING DATA - BRANDON GENERATION STATION

8.3.1 Gross Power Generation

TABLE 8.1

BRANDON GENERATING STATION

GROSS POWER GENERATION (KILOWATT-HOURS)

MONTH	1970	1971	1972	1973	1974
January	23,760,000	134,795,000	97,909,000	73,278,000	74,618,000
February	34,954,800	97,626,000	63,860,000	55,386,000	26,378,000
March	15,751,000	40,929,000	31,704,000	23,528,000	9,605,000
April	89,547,200	25,401,000	24,972,000	76,080,000	8,774,000
May	38,017,000	4,440,000	13,423,000	65,293,000	9,663,000
June	15,502,000	3,200,000	3,432,000	46,380,000	1,260,000
July	5,288,000	-	1,937,000	18,682,000	2,074,000
August	11,252,000	1,660,000	5,474,000	49,691,000	2,096,000
September	3,372,000	18,041,000	9,460,000	91,454,000	946,000
October	37,476,000	45,926,000	40,050,000	42,998,000	-
November	83,551,000	36,209,000	59,186,000	39,611,000	-
December	108,801,000	77,343,000	88,116,000	40,868,000	-
TOTAL	476,272,000	485,570,000	439,343,000	623,249,000	-

8.3.2 Design and Operating Data for Boilers and Auxiliary Systems

TABLE 8.2

BRANDON GENERATING STATION

STACK DATA

Units No. 1-4, Stacks No. 1S and 2N

Stack No. 1S: serves units no. 1 and no. 2

Stack No. 2N: serves units no. 3 and no. 4

Stacks No. 1S and 2N:

Height	250 ft (76.2m)
Inside diameter, bottom	13.7 ft (4.17m)
Inside diameter, top	13.0 ft (3.96m)
Temperature range	295-375°F (145-190°C)
Typical temperature	300-320°F (150-160°C)
Velocity of gases* (at maximum rating)	3375 ft/min (17.1 m/sec)

Stack No. 3:

Height	350 ft (106.6m)
Inside diameter, bottom	15.5 ft (4.72m)
Inside diameter, top	12.0 ft (3.66m)
Temperature range	250-350°F (120-175°C)
Typical temperature	300-350°F (150-175°C)
Velocity of gases* (at maximum rating)	5010 ft/min (25.4 m/sec)

*calculated

TABLE 8.3

BRANDON GENERATING STATION

PERFORMANCE DATA - UNIT NO. 1: BOILER AND AUXILIARIES

OPERATING PARAMETER	GENERATOR OUTPUT (MEGAWATT)			
	33	30	24	15
General				
Fuel	lignite	lignite	lignite	lignite
Fuel firing rate, lbs/hr	58,872	54,288	43,895	27,997
Steam flow, lbs/hr	304,252	278,389	226,907	143,042
Forced Draft Fan				
Dry air, lbs/lb fuel	6.329	6.091	6.285	6.343
Air flow, lbs/hr	375,644	334,242	277,373	178,481
Induced Draft Fan				
Dry gas, lbs/lb fuel	6.660	6.432	6.631	6.693
Moisture in exhaust gas, lb/ft^3	0.642	0.617	0.623	0.620
Density of exhaust gas, lb/ft^3	0.03743	0.03814	0.03900	0.04060
Gas flow, ft^3/min	191,767	168,173	136,074	84,059

TABLE 8.4

BRANDON GENERATING STATION

DESIGN DATA - UNIT NO. 1: BOILER AND AUXILIARIES

OPERATING PARAMETERS	BOILER LOADING (% CAPACITY)		
	100%	50%	10%
Steam flow, lbs/hr	325,000	162,500	32,500
Fuel firing rate, lbs/hr	62,250	32,000	6,820
Excess air, %	22	22	50
Air to preheater, lbs/hr	365,000	173,000	24,000
Flue gas leaving boiler, lbs/hr	479,000	248,000	62,000
Temperatures, ^{o}F			
Flue gas leaving boiler	680	595	525
Flue gas leaving air preheater	320	295	275
Air entering air preheater	80	80	80
Air leaving air preheater	590	540	505
Air to coal pulverizers	590	540	505
Fan Capacities, cfm			
Forced draft fan, at 8.1" H_2O and $100^{o}F$		115,000	
Induced draft fan, at 9.7" H_2O and $340^{o}F$		236,500	

TABLE 8.5

BRANDON GENERATING STATION

DESIGN DATA - UNIT NO. 5: BOILER AND AUXILIARIES

OPERATING PARAMETERS	BOILER LOADING (% CAPACITY)	
	100	50
Steam flow, lbs/hr	875,000	437,500
Fuel firing rate, lbs/hr	161,000	84,800
Excess air, %	17	25
Air to Preheaters, lbs/hr	1,000,000	563,300
Flue gas leaving boiler, lbs/hr	1,159,000	649,500
Temperatures, ^{o}F		
Flue gas leaving boiler	-	-
Flue gas leaving air preheater	305	258
Air entering air preheater	80	80
Air leaving air preheater	484	441
Air to coal pulverizers	-	-
Fan Capacities, lbs/hr (total)		
2 Forced draft fans, at 5.1" H_2O and $80^{o}F$	855,000	
2 Induced draft fans, at 9.6" H_2O and $100^{o}F$	1,263,000	

8.3.3 Typical Analyses of Lignite Coal, Natural Gas, and No. 2 Fuel Oil

TABLE 8.6

ANALYSIS OF SASKATCHEWAN (BIENFAIT) LIGNITE

ANALYSIS	% by weight as received	
	Range	Typical
Proximate Analysis		
Moisture	28.5-40	35
Volatile Matter	23.5-32	26
Fixed Carbon	26.5-33	32
Ash	4.5-13.5	7
Sulfur	0.4-0.7	0.5
Calorific Value, Btu/lb	5900-8000	7200
Ultimate Analysis		
Carbon	42-46	42.0
Hydrogen	2.2-4.2	3.1
Sulfur	0.4-0.7	0.5
Nitrogen	0.6-0.8	0.7
Ash	4.5-13.5	7.0
Oxygen	10.9-12.3	11.0
Moisture	34-37	35.7
TOTAL		100.0

TABLE 8.7

ANALYSIS OF TYPICAL NATURAL GAS*

CONSTITUENT	% BY VOLUME**
N_2	2.35
CO_2	0.41
CH_4 (methane)	91.70
C_2H_6 (ethane)	4.91
C_3H_8 (propane)	0.54
C_4H_{10} (iso-butane)	0.03
C_4H_{10} (butane)	0.04
C_5H_{12} (iso-pentane)	0.01
C_5H_{12} (pentane)	0.01
C_6H_{14} (hexane)	nil
TOTAL	100.00
Sulfur	0.13 grains/100 cu ft
Calorific Value	1015 Btu/cu ft
Specific Gravity	0.593 S.G.

*Greater Winnipeg Gas Company

**unless otherwise specified

TABLE 8.8

ANALYSIS OF NO. 2 FUEL OIL*

CONSTITUENT	% BY VOLUME**
Carbon	86.1
Hydrogen	13.6
Nitrogen	trace
Oxygen	trace
Sulfur	0.27
Ash	0.001
Water	nil
TOTAL	99.971
Calorific Value	20,003 Btu/lb
Specific Gravity	0.89 S.G.

*Imperial Esso Diesel Fuel

**unless otherwise specified

8.3.4 Fuel Cycle and Discharges for Generating Units

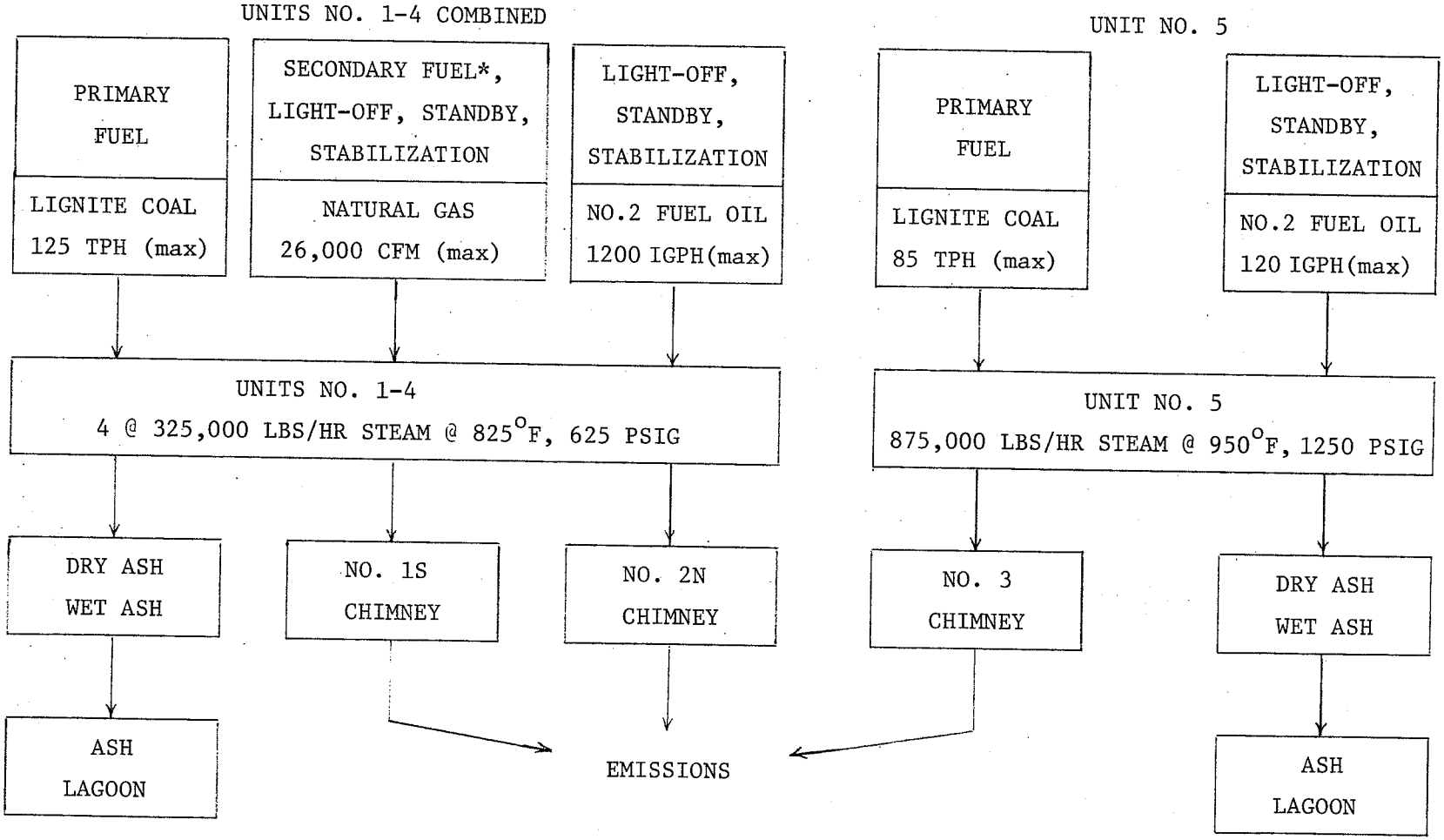

Figure 8.1. Fuel cycle and discharges for generating units (83).

8.3.5 Fuel Cycle and Discharges for Heating Boiler

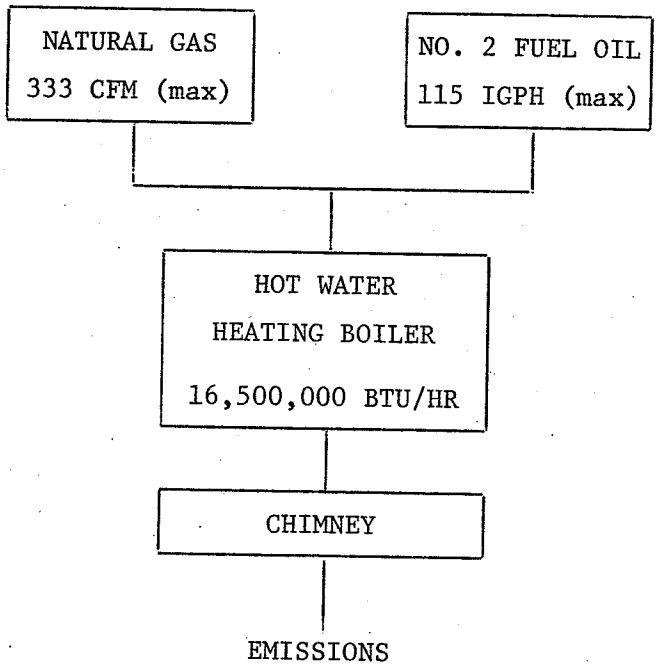

N.B. Natural gas and No. 2 fuel oil may be fired separately or in combination.

Figure 8.2. Fuel cycle and discharges for heating boiler.

TPH = tons per hour

CFM = cubic feet per minute

IGPH = imperial gallons per hour

8.3.6 Fuel Consumption for Power Generation

TABLE 8.9

BRANDON GENERATING STATION

MONTHLY FUEL CONSUMPTION (1970-1974) - COAL (TONS)

MONTH	1970	1971	1972	1973	1974
January	21,082	127,095	94,787	66,201	62,051
February	30,568	89,722	60,147	47,564	23,373
March	14,205	32,455	29,627	21,262	8,862
April	30,443	20,277	21,757	30,078	7,162
May	13,667	2,243	11,862	18,202	8,148
June	3,107	2,167	1,876	11,920	1,093
July	5,379	39	78	8,700	1,656
August	2,698	1,145	114	17,340	1,498
September	24,214	2,531	2,380	35,050	974
October	59,524	2,170	23,161	18,126	-
November	84,318	32,332	50,307	34,234	-
December	116,928	72,196	75,581	32,671	-
TOTAL	406,133	384,372	371,677	341,348	-

TABLE 8.10

BRANDON GENERATING STATION

MONTHLY FUEL CONSUMPTION (1970-1974) - NATURAL GAS (THOUSANDS OF CUBIC FEET)

MONTH	1970	1971	1972	1973	1974
January	11,810	29,831	6,724	25,683	5,250
February	9,520	50,990	7,759	24,497	5,981
March	4,811	77,777	4,104	11,448	10,081
April	58,256	24,275	5,084	500,551	3,387
May	8,463	27,896	2,512	591,778	5,477
June	27,821	15,022	19,810	439,392	0
July	69,850	339	26,134	125,739	1,227
August	4,063	3,629	77,618	386,976	1,348
September	116,657	196,636	88,240	635,411	1,146
October	194,579	540,646	194,126	270,326	-
November	161,285	15,457	29,971	8,744	-
December	4,891	10,049	37,076	14,060	-
TOTAL	672,006	992,097	499,158	3,034,605	-

TABLE 8.11

BRANDON GENERATING STATION

MONTHLY FUEL CONSUMPTION (1970-1974) - NO. 2 FUEL OIL (IMPERIAL GALLONS)

MONTH	1970	1971	1972	1973	1974
January	36,450	15,750	29,625	24,050	30,493
February	25,200	41,643	28,200	28,500	40,406
March	2,427	20,528	31,750	22,800	18,703
April	512	19,900	20,600	22,990	29,401
May	271	2,191	16,800	17,636	47,163
June	19,065	17,609	4,300	20,119	5,350
July	12,147	4,183	48	45,183	9.326
August	18,903	6,500	1,852	49,260	7,286
September	59,641	11,007	9.450	27,607	12,056
October	42,500	15,550	23,900	29,361	-
November	29,951	39,843	35,850	27,103	-
December	29,000	20,225	39,851	20,357	-
TOTAL	276,067	214,929	242,226	334,966	-

8.3.7 Analysis of Coal Ash

TABLE 8.12

ANALYSIS OF SASKATCHEWAN (BIENFAIT) LIGNITE ASH

ANALYSIS OF SASKATCHEWAN (BIENFAIT) LIGNITE ASH	% BY WEIGHT OF ASH	
	RANGE	LATEST ANALYSIS*
SiO_2	14-40	31.88
Al_2O_3	11-23	15.47
Fe_2O_3	3-8	3.56
TiO_2	0.4-1.1	1.05
P_2O_5	0.2-2	1.81
CaO	16-27	18.56
MgO	3-7	4.45
Na_2O	2-10	8.14
K_2O	0.2-1.3	0.18
SO_3	2.7-16.1	10.13
MnO_2	0.06-0.51	0.57
BaO	-	2.32
$CaSO_4$	-	-
Cl	-	0.2
Combustibles	-	1.53
TOTAL	-	99.83

*National Testing Laboratories Limited Report No. 4968 - Jan. 3/72.

8.3.8 Performance Data for Dust Collectors

TABLE 8.13

UNITS NO. 1,2, AND 3 - DUST COLLECTOR PERFORMANCE DATA

DESIGN GMPHT #24-720 PRAT-DANIEL DUST COLLECTORS

OPERATING PARAMETER	BOILER OUTPUT (lbs steam/hr)			
	32,500	162,500	325,000	325,000
Flue gas volume, cfm	25,000	87,500	180,500	197,000
Flue gas temperature, ^{o}F	375	295	320	340
Resistance, inches w.g.				
720 tubes operating	-	0.50	2.13	2.50
480 tubes operating	-	1.10	-	-
240 tubes operating	0.35	-	-	-
Efficiency-anticipated (%)	-	75.1	79.3	80.3
*Efficiency-guaranteed (%)	-	-	78.0	79.0

*Based on efficiency curves in Figure 8.3 and dust analysis in Table 8.13

TABLE 8.14

PARTICULATE COLLECTION EFFICIENCY FOR NORMAL LIGNITE FIRING

DESIGN GMPHT #24-720 PRAT-DANIEL TUBULAR DUST COLLECTORS

Particle Size Range (microns)	Average Size (microns)	Percent in Flue Gas	Collection Efficiency (%)		Weight Collected (%)	
			2.13" w.g.* pressure drop	2.5" w.g.* pressure drop	2.13" w.g.* pressure drop	2.5" w.g.* pressure drop
>60	60	4	99.5	99.6	3.98	3.98
40-60	50	7	99.5	99.6	6.96	6.97
30-40	35	11	99.3	99.5	10.92	10.95
20-30	25	6	98.0	98.2	5.88	5.89
15-20	17.5	13	97.0	98.0	12.60	12.74
10-15	12.5	13	94.0	95.0	12.22	12.35
7.5-10	8.75	16	87.0	88.2	13.92	14.11
<7.5	3.75	30	41.0	43.0	12.30	12.90
TOTAL	-	100	-	-	78.78	79.89
Correction factor from curve temperature (400°F) to operating temperature					+ .50	+ .37
Anticipated Efficiency					79.3	80.3
Guaranteed Efficiency					78.0	79.0

*w.g. = water guage

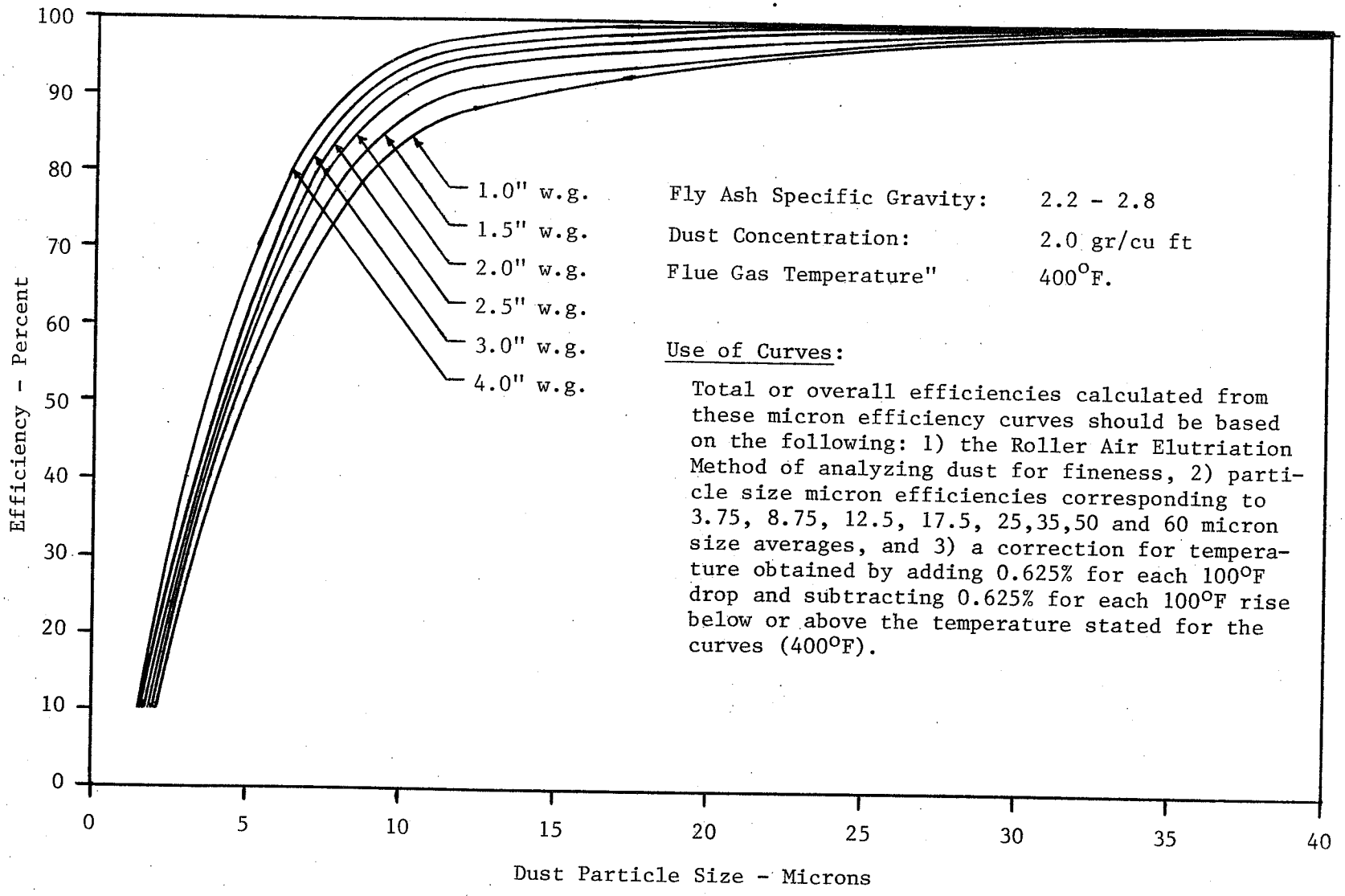

Figure 8.3 Prat-Daniel Design 6MIC Dust Collector Micron Efficiency Curves.

8.4 APPENDIX: METEOROLOGICAL DATA - BRANDON, MANITOBA

8.4.1 Temperature Data

TABLE 8.15

MEAN TEMPERATURES - BRANDON AIRPORT (76)

(LATITUDE 49°55'N, LONGITUDE 99°57'W, ELEVATION 1337 FT ASL)

PERIOD	MEAN DAILY TEMPERATURE (°F)	MEAN DAILY MAXIMUM TEMPERATURE (°F)	MEAN DAILY MINIMUM TEMPERATURE (°F)
January	-1.4	8.1	-10.7
February	4.5	15.5	-6.5
March	16.3	26.5	5.6
April	36.7	47.1	26.2
May	49.8	62.1	37.5
June	60.3	72.0	48.5
July	66.0	78.5	53.5
August	63.9	76.8	51.0
September	53.0	65.2	40.8
October	42.1	53.9	30.2
November	22.4	30.9	13.8
December	7.2	16.4	-2.0
Year	35.1	46.1	24.0

8.4.2 Sample Upper Air Data

TABLE 8.16

SHILO, MANITOBA - DECEMBER 1967

CONSTANT PRESSURE DATA - 12 GMT. (80)

STATION INSTRUMENTATION

USWB type radiosonde, GMD RDF tracking equipment

INDEX NO. LATITUDE LONGITUDE ELEVATION

72853 49°49'N 99°39'W 382 Meters

Day	SURFACE					1000 MBS					950 MBS					900 MBS				
	Altitude (Pres. on Sfc.)	Temp. °C	Humidity	Wind deg.	Wind mps.	Altitude gpm.	Temp. °C	Humidity	Wind deg.	Wind mps.	Altitude gpm.	Temp. °C	Humidity	Wind deg.	Wind mps.	Altitude gpm.	Temp. °C	Humidity	Wind deg.	Wind mps.
01	963	- 3.1	27	290	06	80					480	- 4.3	26	291	08	699	- 7.7	23	293	10
02	970	-12.3	13	290	04	156					550	- 5.6	26	284	07	970	- 2.3	21	279	11
03	959	- 2.1	28	250	06	51					445	- 1.0	28	263	09	898	5.1	27	289	22
04	959	0.4	30	090	06	45					450	1.5	29	109	07	897	5.9	15	170	11
05	966	- 7.6	19	140	02	110					505	2.7	28	166	03	956	5.8	31	200	04
06	965	- 4.0	27	090	02	101					500	- 4.7	27	098	04	935	- 2.4	23	120	09
07	968	- 1.6	34	045	02	120					520	- 2.8	32	055	04	956	- 4.6	30	079	06
08	968	- 1.7	32	135	02	123					530	- 3.2	29	125	04	959	- 3.7	32	129	07
09	976	- 2.7	30	200	02	192					600	- 4.0	26	248	04	1021	- 6.7	21	253	07
10	963	- 5.3	24	160	07	82					495	- 6.E		156	06	911	- 3.9	32	194	12
11	940	0.6	41	135	03	-114					295					733	0.9	44	230	04
12	954	- 4.8	22	340	06	14					420	- 5.2	22	338	07	842	- 8.7	20	332	12
13	970	-17.6	9	290	05	151					520	-17.0	9	302	09	964	-16.9	9	317	10
14	988	-20.1	7	290	04	291					670	-16.0	9	299	07	1077	-16.9	10	300	10
15	978	-10.4	12	250	09	210					610	-11.5	11	267	16	1027	- 2.9	9	268	26
16	960	- 9.6	15	270	03	63					460	- 8.6	12	271	04	891	- 4.6	15	261	09
17	941	- 1.7	27	110	03	-107					280					732	- 4.3	30	165	04
18	938	- 9.2	17	290	10	-122					270					699	-11.4	15	301	15
19	964	-15.2	9	270	07	99					480	-15.4	9	273	09	920	-17.6	8	286	16
20	974	-18.4	7	290	04	184					570	-18.4	7	323	06	982	-13.4	9	305	06
21	967	-17.4	7	350	05	131					515	-18.6	7	341	07	914	-22.8	6	339	10
22	978	-23.5	4	290	05	222					600	-23.4	4	321	11	997	-18.7	5	348	16
23	971	-13.3	12	175	04	161					550	-16.8	7	219	05	956	-13.7	14	281	10
24	964	-14.4	11	260	02	101					506	-11.8	15	273	06	915	2.7	27	293	14
25	977	-21.1	6	270	04	210					590	-18.2	7	317	12	996	-21.0	6	328	13
26	972	-17.9	7	040	02	161					540	-18.4	8	035	07	949	-18.6	9	009	07
27	976	-22.8	4	270	03	202					585	-20.4	5	303	09	979	-19.2	5	302	06
28	979	-27.9	3	360	01	226					610	-20.3	5	M		1003	-17.4	6	M	
29	967	- 9.3	14	300	08	119					510	-10.3	13	314	11	929	-13.5	12	330	18
30	974	-25.3	4	020	03	151					560	-27.0	3	025	08	980	-29.5	2	006	07
31	978	-36.1		270	01	228					590	-34.7	1	260	06	965	-30.3	2	269	05
MN	967	-12.1	17	280	.02	119					510	-12.2	15	300	04	929	- 9.8	17	295	06

8.4.3 Sample Wind Data

TABLE 8.17

MEAN MONTHLY WIND FREQUENCY DISTRIBUTION

JANUARY; 1963-1972 - BRANDON AIRPORT (77)

Wind Direction	Wind Speed Class (Miles per Hour)									Total Hours	Mean Speed
	1-3	4-7	8-12	13-18	19-24	25-31	32-38	39-46	47-54		
Calm										97.2	0.0
NNE	1.1	3.1	1.1	1.8	0.2	0.2				7.5	8.9
NE	1.1	8.5	11.3	8.7	3.3	1.4	0.2	0.1		34.7	12.1
ENE	2.0	13.4	23.3	25.9	6.4	1.3	0.2			72.6	12.3
E	2.8	17.1	18.2	14.4	3.2	0.3				56.1	10.3
ESE	0.4	4.6	4.2	3.4	0.7					13.3	10.0
SE	0.9	2.1	1.7	1.4						6.1	8.5
SSE	0.2	1.3	1.6	0.9						4.0	8.9
S	0.8	0.7	1.3	0.9	0.2					3.9	8.9
SSW	0.5	1.9	1.3	0.5	0.4	0.1				4.7	8.8
SW	1.3	5.6	6.4	2.8	0.7					16.8	9.1
WSW	2.2	13.6	23.1	11.9	1.9					52.8	10.0
W	3.4	26.4	53.8	41.2	11.2	3.3	0.4			139.7	11.9
WNW	2.3	15.2	37.8	43.5	23.5	9.9	1.0	0.1		133.3	14.6
NW	1.2	10.2	17.1	24.2	11.6	3.8				68.2	14.0
NNW	2.0	3.9	6.4	5.2	1.3	0.9				19.7	11.2
N	1.4	3.6	4.6	3.2	0.3	0.2				13.3	9.7
TOTAL	23.6	131.2	213.2	189.9	64.9	21.4	1.8	0.2		744.0	10.6

8.4.4 Mixing Height Data

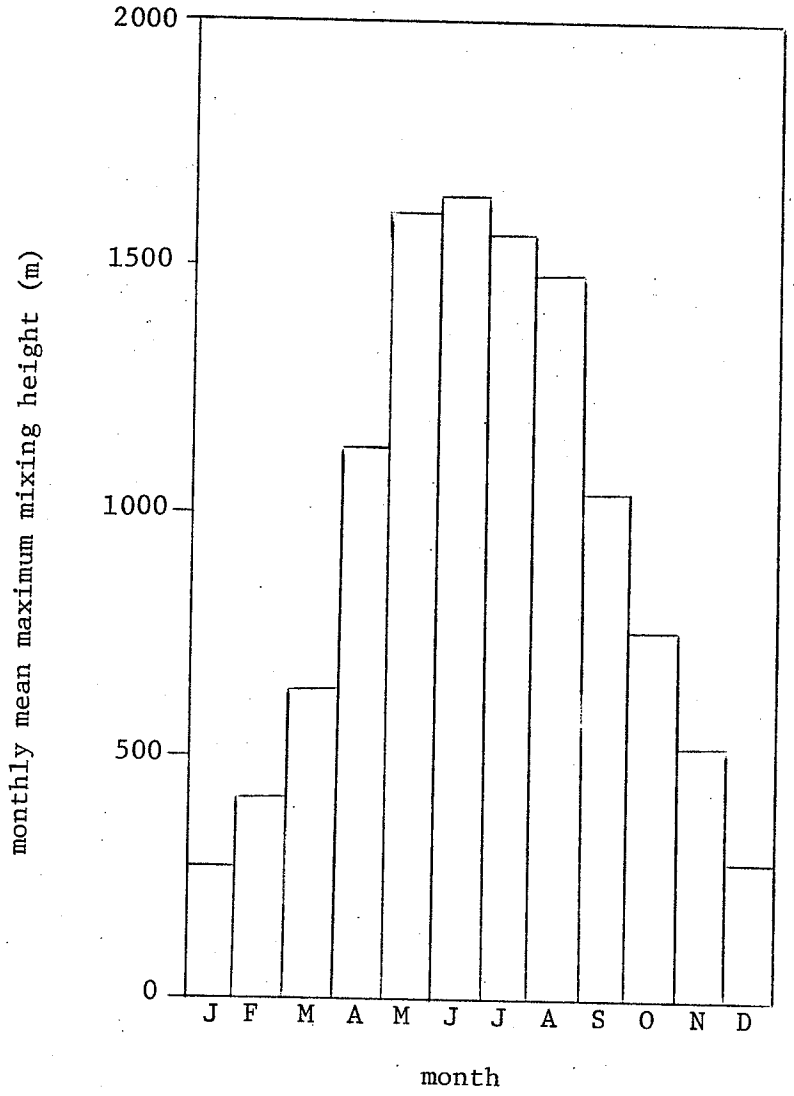

Figure 8.4. Brandon monthly mean maximum heights (extrapolated), (78).

8.5 APPENDIX: SAMPLE CALCULATIONS

8.5.1 Emission Rates

8.5.1.1 Monthly Mean Emission Rates:

SO_2 emission rate (monthly mean):

$$SO_2 \text{ produced} = \text{weight of coal burned} \times \%\text{Sulfur in coal (avg.)} \times \frac{\text{M.W. } SO_2}{\text{M.W. S}}$$

$$= 1 \text{ ton} \times 2000 \text{ lbs/T} \times 0.5\% \times \frac{64}{32}$$

$$= 20.0 \frac{\text{lbs } SO_2}{\text{Ton coal burned}}$$

$$SO_2 \text{ fixed in ash (as } SO_3) = \text{weight of coal burned} \times \%\text{Ash in coal (avg.)} \times \%SO_3 \text{ in Ash (avg.)} \times \frac{\text{M.W. } SO_2}{\text{M.W. } SO_3}$$

$$= 1 \text{ ton} \times 2000 \text{ lbs/T} \times 7\% \times 9.4\% \times \frac{64}{80}$$

$$= 10.5 \frac{\text{lbs } SO_2}{\text{Ton coal burned}}$$

$$SO_2 \text{ emitted} = 20.0 - 10.5 = 9.5 \frac{\text{lbs } SO_2}{\text{Ton coal burned}}$$

$$\text{Monthly mean coal consumption (January)} = \frac{\sum_{i=1}^{n} \text{January coal consumption}}{n}$$

where n = number of years of available data (see Table 8.9)

Monthly mean coal consumption (January)

$$= \frac{(21{,}082 + 127{,}095 + 94{,}787 + 66{,}201 + 62{,}051)}{5}$$

$$= 74{,}243 \text{ Tons}$$

$$\text{Mean hourly firing rate} = \frac{\text{Monthly mean coal consumption}}{\text{Hours in month}}$$

$$= \frac{74{,}243 \text{ T}}{31 \text{ days} \times 24 \text{ hrs/day}}$$

$$= 99.8 \text{ Tons/hour}$$

Unit No. 5 is loaded to full capacity before any of Units No. 1-4 are brought on line, provided the total load is greater than 45% of the maximum continuous rating for Unit No. 5, i.e. > 47 megawatts (equivalent to a firing rate of 38 Tons/hr of lignite).

Unit No. 5 mean hourly coal consumption = 8.5 Tons/hr

Balance burned in one of the 33 MW units, say Unit No. 1 = 99.8 - 85.0 = 14.8 Tons/hr

Unit No. 5 emissions are released through Stack No. 3.

Unit No. 1 emissions are released through Stack No. 1S.

Stack No. 3 mean SO_2 emission rate (January)

= 85 Tons/hr x 9.5 lbs SO_2/Ton coal burned

= 808 lbs/hr SO_2

= $\underline{1.02 \times 10^8 \text{ µg/sec } SO_2}$

Stack No. 1S mean SO_2 emission rate (January)

= 14.8 Tons/hr x 9.5 lbs SO_2/Ton coal burned

= 141 lbs/hr SO_2

= $\underline{1.77 \times 10^7 \text{ µg/sec } SO_2}$

NO_x emission rate (monthly mean):

NO_x emitted = 30 lbs/Ton coal burned*

Stack No. 3 emission rate (January) = 85 T/hr x 30 lbs NO_x/T

= 2550 lbs/hr NO_x

= 3.21×10^8 µg/sec NO_x

*EPA emission factor (7).

similarly: Stack No. 1S emission rate (January) = 444 lbs/hr NO_x

= 5.59×10^7 µg/sec NO_x

Particulate emission rate (monthly mean):

Particulates produced = coal burned x % Ash in coal (avg.)

= 1 ton x 2000 lbs/T x 7%

= 140 lbs Ash/Ton coal burned

Fly ash collected in ash hopper ≃ 25% of total ash

Fly ash dust collectors ≃ 75% of total

Estimated removal efficiency of dust collectors ≃ 70%

Estimated fly ash emission = 140 x (1-.25) x (1-.70)

= 31.50 lbs fly ash/Ton coal burned

Stack No. 3 mean particulate emission rate (January)

= 85 T/hr coal x 31.5 lbs/T coal

= 2678 lbs/hr particulates

= 3.37×10^8 µg/sec particulates

similarly: Stack No. 1S mean particle emission rate (January)

= 466 lbs/hr particulates

= 5.87×10^7 µg/sec particulates

TABLE 8.18

TABULATION OF MONTHLY MEAN EMISSION RATES

FOR THE THREE MONTHS OF MAXIMUM POWER GENERATION

(MICROGRAMS PER SECOND)

MONTH/SOURCE	SO_2	NO_x	PARTICULATES
December			
Stack No. 1S or 2N	1.78×10^7	5.63×10^7	5.91×10^7
Stack No. 3	1.02×10^8	3.21×10^8	3.37×10^8
Total	1.20×10^8	3.77×10^8	3.96×10^8
January			
Stack No. 1S or 2N	1.77×10^7	5.59×10^7	5.87×10^7
Stack No. 3	1.02×10^8	3.21×10^8	3.37×10^8
Total	1.20×10^8	3.77×10^8	3.96×10^8
February			
Stack No. 1S or 2N	0	0	0
Stack No. 3	8.89×10^7	2.81×10^8	2.95×10^8
Total	8.89×10^7	2.18×10^8	2.95×10^8

8.5.1.2 Maximum Emission Rates (Worst Case Conditions)

Assumptions: - maximum fuel sulfur content = 0.7%S

- maximum fuel ash content = 13.5%

- minimum SO_3 fixed in ash = 2.7%

- all units at maximum loading

SO_2 emitted = 1 ton x 2000 lbs/T x $\left((.7\% \times \frac{64}{32}) - (13.5\% \times 2.7\% \times \frac{64}{80}) \right)$

= 22.2 lbs SO_2/Ton coal burned

NO_x emitted = 30 lbs/Ton coal fired

Particulates emitted = 1 ton x 2000 lbs x 13.5% x (1-.25) x (1-.70)

= 60.8 lbs particulates/Ton coal burned

Unit No. 5 emissions are released through Stack No. 3.

Units No. 1 and 2 emissions are released through Stack No. 1S.

Units No. 3 and 4 emissions are released through Stack No. 2N.

Stack No. 1 emission rates:

SO_2 emission rate = $\frac{125 \text{ Tons/hr}}{4 \text{ units}}$ x 2 units x 22.2 lbs SO_2/Ton

= 1387.5 lbs/hr SO_2

= $\underline{1.75 \times 10^8 \text{ µg/sec } SO_2}$

similarly: NO_x emission rate = 1875 lbs/hr NO_x

= $\underline{2.36 \times 10^8 \text{ µg/sec } NO_x}$

Particulate emission rate = 3800 lbs/hr particulates

= $\underline{4.79 \times 10^8 \text{ µg/sec particulates}}$

TABLE 8.19

MAXIMUM EMISSION RATES - "WORST CASE" CONDITIONS

(MICROGRAMS PER SECOND)

EMISSION SOURCE	SO_2	NO_x	PARTICULATES
STACK NO. 1S	1.75×10^8	2.36×10^8	4.79×10^8
STACK NO. 2N	1.75×10^8	2.36×10^8	4.79×10^8
STACK NO. 3	2.38×10^8	3.21×10^8	6.51×10^8
TOTAL EMISSIONS	5.88×10^8	7.93×10^8	16.09×10^8

8.5.2 Wind Frequency Distributions - Wind Roses

$$\text{Frequency} = \frac{\text{no. of hours wind is from given direction}}{\text{average total hours in month}}$$

for January: total hours WNW wind = 133.3 hours

total hours - January = 744.0

(see Appendix 8.4.3)

$$\text{wind frequency - WNW, January} = \frac{133.3}{744.0} = 0.179$$

$$= \underline{17.9\%}$$

8.5.3 Plume Rise Calculations

Heat Emission:

Total heat emission for all units at full load $\simeq 3 \times 10^8$ Btu/hr

Heat emission for Stack No. 3 at full load

$$= 3 \times 10^8 \text{ Btu/hr} \times \frac{85 \text{ T/hr (coal burned in Unit No.5)}}{210 \text{ T/hr (total coal burned)}}$$

similarly:

TABLE 8.20

WIND FREQUENCY DISTRIBUTIONS FOR THE THREE MONTHS OF MAXIMUM POWER GENERATION

Wind Direction	December		January		February	
	Frequency %	$\bar{u}$ m/sec	Frequency %	$\bar{u}$ m/sec	Frequency %	$\bar{u}$ m/sec
Calm	12.7	-	13.1	-	14.1	-
NNE	1.8	4.0	1.0	4.0	1.7	4.7
NE	4.4	4.8	4.7	5.4	5.6	5.0
ENE	8.1	5.7	9.8	5.5	9.6	4.9
E	7.8	4.3	7.5	4.6	8.2	4.2
ESE	2.2	4.2	1.8	4.5	2.6	4.2
SE	2.8	5.2	0.8	3.8	2.4	5.1
SSE	1.0	5.2	0.5	4.0	0.7	3.6
S	0.9	4.0	0.5	4.0	0.6	2.9
SSW	1.2	3.8	0.6	3.9	1.2	3.6
SW	3.4	3.9	2.3	4.1	3.4	4.6
WSW	7.4	4.4	7.1	4.5	6.9	4.9
W	18.5	5.0	18.8	5.3	15.5	5.1
WNW	13.6	5.9	17.9	6.5	12.8	6.3
NW	8.0	5.8	9.2	6.3	7.5	5.8
NNW	3.3	5.8	2.6	5.0	4.0	5.5
N	2.8	4.2	1.8	4.3	3.2	5.3
TOTAL	100.0	4.4	100.0	4.7	100.0	4.4

$= 1.2 \times 10^8$ Btu/hr

= 35.6 MW

Applicable plume rise equations are as follows:

- for Stack No. 3, all cases, and Stacks No. 1S and SN at full load, use Briggs' Equation 2.37'.
- for Stack No. 1S (or 2N) at monthly mean load, use Briggs' Equation 2.36'.

similarly:

TABLE 8.21

HEAT EMISSIONS FROM STACKS (MW)

OPERATING CONDITIONS	STACK NO. 1S	STACK NO. 2N	STACK NO. 3
Full Load	26.2	26.2	35.6
Monthly Mean Load			
December	6.2	-	35.6
January	6.2	-	35.6
February	-	-	31.3

For Stack No. 3 at 100% Maximum Continuous Rating; December

Exit Velocity:

Stack temperature = $305^{o}F$

Excess air temperature = 17%

Stack gas volume = 200 cu ft/lb coal fired (Ref. 86)

$$V_s = \frac{85 \text{ T/hr} \times 2000 \text{ lb/T} \times 200 \text{ cu ft/lb} \times .30^{m}/\text{ft}}{3600 \text{ sec/hr} \times \pi \times (12/2)^2} = \underline{25.4 \text{ m/sec}}$$

Stack aerodynamics:

$h = h_s + 2\ (V_s/u - 1.5)D$

$u_{h_s} = u_z \left(\frac{h}{z}\right)^p$ (wind shear effects, (11))

p = 0.25 for unstable conditions

z = 10 m (elevation at which surface wind measurements are taken)

at $h = h_s = 106.6$ m, $u_z = 4.4$ m/sec

$u = 4.4\ (106.6/10)^{.25}$

$$h' = 106.6 + 2\left(\frac{25.4}{8.0} - 1.5\right)\ 3.66 = \underline{118.9\ m}.$$

Building aerodynamics:

$h_b = 49.8$ m

$L_b = 49.8$ m

$h_b + 1.5\ L_b = 49.8 + 1.5\ (49.8) = \underline{124.5\ m}.$

for Stack No. 3, $h' < h_b + 1.5\ L_b$ (118.9 m < 124.5 m)

Downwash will occur due to building aerodynamics (see 2.2.2).

$h_b + 0.5\ L_b = 49.8 + 0.5\ (49.8) = \underline{74.7\ m}.$

$h' > h_b + 0.5\ L_b$ (118.9 m > 74.7 m)

$h'' = 2h' - (h_b + 1.5\ L_b) = 2(118.9) - (49.8 + 1.5\ (49.8))$

$= \underline{113.3\ m}.$

Plume rise calculation:

$$\Delta h = 1.6F^{1/3}u^{-1}(10h_s)^{2/3} \qquad \text{(Equation 2.36')}$$

$$F = \frac{g\Delta T V_s d^2}{4T_s} \qquad \text{(Equation 2.25')}$$

$h_s = h'' = 113.3$ m

$u = u_m = 4.4\ (113.3/10)^{.25} = 8.1$ m/sec

$g = 9.8\ m/sec^2$

$\Delta T = T_s - T_a = 425^oK - 259^oK = 166^oK$

$T_s = 425^oK$

$d = 3.66\ m$

$V_s = 25.4\ m/sec$

$$F = \frac{9.8 \times 166 \times 25.4 \times (3.66)^2}{4 \times 425} = \underline{325\ m^4/sec^3}$$

$$\Delta h = \frac{1.6 \times (325)^{1/3} (10 \times 113.3)^{2/3}}{8.1} = \underline{147.4\ m}$$

$$h_e = h'' + \Delta h = 113.3 + 147.4 = \underline{260.7\ m}$$

similarly:

TABLE 8.22

EFFECTIVE STACK HEIGHTS

OPERATING CONDITIONS	STACK NO. 1S	STACK NO. 2N	STACK NO. 3
Monthly Mean Load			
December	114.0 m	-	260.7 m
January	110.8 m	-	247.3 m
February	-	-	246.3 m
Full Load			
December	203.5	203.5	260.7
January	194.6	194.6	247.3
February	205.4	205.4	263.2

8.5.4 Dispersion Calculations

8.5.4.1 Pasquill-Gifford Diffusion Coefficients

The diffusion coefficients σ_y and σ_z are selected on the basis of atmospheric stability according to the wind speed and insolation parameters given by Pasquill (50) in Table 2.10. Turner (22) defines "strong" insolation as that corresponding to a solar altitude greater than 60^o with clear skies, and "slight" insolation as that corresponding to a solar altitude of 15^o-35^o with clear skies.

Brandon daytime insolation:

- from Table 170, Solar Altitude and Azimuth, in the Smithsonian Meteorological Tables (83):

  Solar altitude - mean daily maximum: December = 18^o

  January = 20^o

  February = 26^o

  Daytime insolation is "slight" in all cases.

Brandon mean wind speeds: December = 4.4 m/sec

January = 4.7 m/sec

February = 4.4 m/sec

Stability class:

- for "slight" insolation and $\bar{u}$ = 2 to 5 m/sec, use Stability Class C diffusion coefficients (Figures 2.13 and 2.14).

  (Atmospheric Environment Service confirms that stability class C is the most common in the Brandon area.)

8.5.4.2 Unlimited Mixing Calculation

Gaussian equation for ground-level concentration under unlimited mixing conditions (Equation 2.58):

$$\chi(x,y,o) = \frac{Q}{\pi\sigma_y\sigma_z u} \exp\left[-\tfrac{1}{2}\left(\frac{y}{\sigma_y}\right)^2\right] \exp\left[-\tfrac{1}{2}\left(\frac{h_e}{\sigma_z}\right)^2\right]$$

For a downwind distance of 2 kilometers, the 1-hour ground-level SO_2 concentration on the plume centerline for Stack No. 3 at full load is calculated as follows:

$Q = 2.38 \times 10^8$ µg/sec (Table 8.19)

$\sigma_y = 195$ m (Figure 2.13)

$\sigma_z = 115$ m (Figure 2.14)

$h_e = 260.7$ m (December) (Table 8.22)

$u = 4.4$ m/sec at $z = 10$ m (Table 8.20)

$$u = 4.4\left(\frac{260.7}{10}\right)^{.25} = 10.0 \text{ m/sec at } z = h_e$$ (Reference 11, p.55)

$y = 0$

$$\chi_3(2 \text{ km},0,0) = \underline{26 \text{ µg/m}^3}$$

Similarly, the concentrations at the same point (x = 2 km, on plume centerline of Stack No. 3) for Stacks No. 1S and 2N at full load, assuming that the wind is from the east, are:

$$\chi_{1S}(2 \text{ km},61 \text{ m},0) - 53 \text{ µg/m}^3$$

$$\chi_{2N}(2\text{ km},34\text{ m},0) = 54\ \mu g/m^3$$

Total concentration of SO_2 at χ=2 km on centerline of plume from Stack No. 3

$$= \chi_3 + \chi_{1S} + \chi_{2N} = \underline{133\ \mu g/m^3\ SO_2}$$

The maximum ground-level concentrations and the points at which they occur are determined by inspection of the x-y plots of cumulative ground-level concentrations. The 24-hour concentrations required for particulate emissions are determined by applying the correction factor given by Briggs (65) in Figure 2.5 to the 1-hour particulate concentrations.

8.5.4.3 Limited Mixing Calculations

Gaussian equation for ground-level concentration under limited mixing conditions (Equation 2.72):

$$\chi(x,y,z) = \frac{Q}{\sqrt{2\pi}\sigma_y Lu} \exp\left(-\tfrac{1}{2}\frac{y}{\sigma_y}^2\right)$$

The maximum limited mixing concentration occurs at the point where the plume has become uniformly distributed through the mixing depth L. This occurs at $x = 2x_L$; where x_L is the downwind distance at which $\sigma_z = 0.47L$.

For full load conditions and mean mixing conditions for the month of January, the maximum 1-hour limited mixing ground-level SO_2 concentration on the plume centerline is calculated as follows:

$Q = 5.88 \times 10^8$ µg/sec (total for all stacks) (Table 8.19)

$L = 277$ m (Figure 8.4)

$\sigma_z = 0.47L = 130$ m

$u = 4.7$ m/sec (at $z = 10$ m) (Table 8.20)

Mean wind in mixed layer $= 4.7\left(\frac{277/2}{10}\right)^{.25} = \underline{9.1 \text{ m/sec}}$

$x_L = x_{\sigma_z} = 130$ m $= 2.25$ km

$2x_L = 4.5$ km = point of maximum limited mixing concentration

σ_y at $2x_L = 410$ m (Figure 2.13)

$y = 0$

$\chi(2x_L,0,0) = \underline{227 \text{ µg/m}^3 \text{ SO}_2}$

8.5.4.4 Inversion Penetration Calculations for Limited Mixing Concentrations

This calculation is required to determine the critical wind speed below which a stack effluent can penetrate an elevated inversion at a distance z_i above the stack height (h"). The results are used in establishing the boundary conditions for the limited mixing curves. If the plume from a given stack is shown to penetrate the elevated inversion layer at the mixing height L, then the emissions from that stack will not contribute significantly to the mixing ground-level concentrations. In this case the emissions are excluded from the limited mixing calculations.

Assumptions:

A relatively weak inversion layer ($\Delta T = 2^{o}C$) is assumed for this calculation.

from Briggs (32); penetration will occur if:

$$z_i \leq 2.0\left(\frac{F}{ub_i}\right)^{\frac{1}{2}} \qquad \text{(buoyant plume, wind)}$$

where z_i = height of penetrable elevated inversion above stack height (h")

F = buoyancy flux

u = wind speed at h"

$$b_i = g\,\frac{\Delta T_i}{T}$$

ΔT_i = temperature difference between top and bottom of elevated inversion, ^{o}K

T = ambient temperature, ^{o}K

for Stack No. 3:

F @ maximum emission rate (Ta = $-8.7^{o}C$) = 315 m^4/sec^3

F @ January mean emission rate (Ta = $-18.6^{o}C$) = 334 m^4/sec^3

Ta, "worst case" conditions = $-8.7^{o}C$

Ta, January mean = $-18.6^{o}C$

$\Delta T_i = 2^{o}C = 2^{o}K$

$$z_i = 2.0\left(\frac{F}{u_{h''}b_i}\right)^{\frac{1}{2}}$$

$$b_i = \frac{9.8\ m/sec^2 \times 2^{o}K}{(-8.7^{o}C + 273)} = 0.074 \qquad \text{(worst case)}$$

similarly, $b_i = 0.077$ (January mean)

$$z_i = 2.0\left(\frac{315}{u_{h''} \times 0.074}\right)^{\frac{1}{2}} = \underline{130\ u_{h''}^{-\frac{1}{2}} m} \quad \text{(worst case)}$$

similarly, $z_i = \underline{132\ u_{h''}^{-\frac{1}{2}} m}$ (January mean)

$h'' = 147.1$ m

for u = 2 m/sec:

$$u_{h''} = 2\left(\frac{147.1}{10.0}\right)^{.25} = 3.9 \text{ m/sec}$$

$$z_i = 130\ (3.9)^{-\frac{1}{2}} = 66 \text{ m}$$

$L_{cr} = h'' + z_i = 147 + 66 = 213$ m (critical inversion height for plume penetration at u = 2m/sec)

$L/2 = 106.5$ m

$$u_{L/2} = 2\left(\frac{106.5}{10}\right)^{.25} = 3.6 \text{ m/sec}$$ (critical wind speed for plume penetration at L = 213 m)

Similar calculations are performed for a range of wind speeds for both "worst case" and January mean conditions. Curves of mixing height versus critical wind speed are plotted for all stacks (see Figures 8.5 and 8.6). These curves are used to determine, for each mixing height examined, the critical wind speed below which a given plume will penetrate the inversion. Limited mixing calculations are then adjusted to account for the exclusion of those emissions which penetrate the inversion.

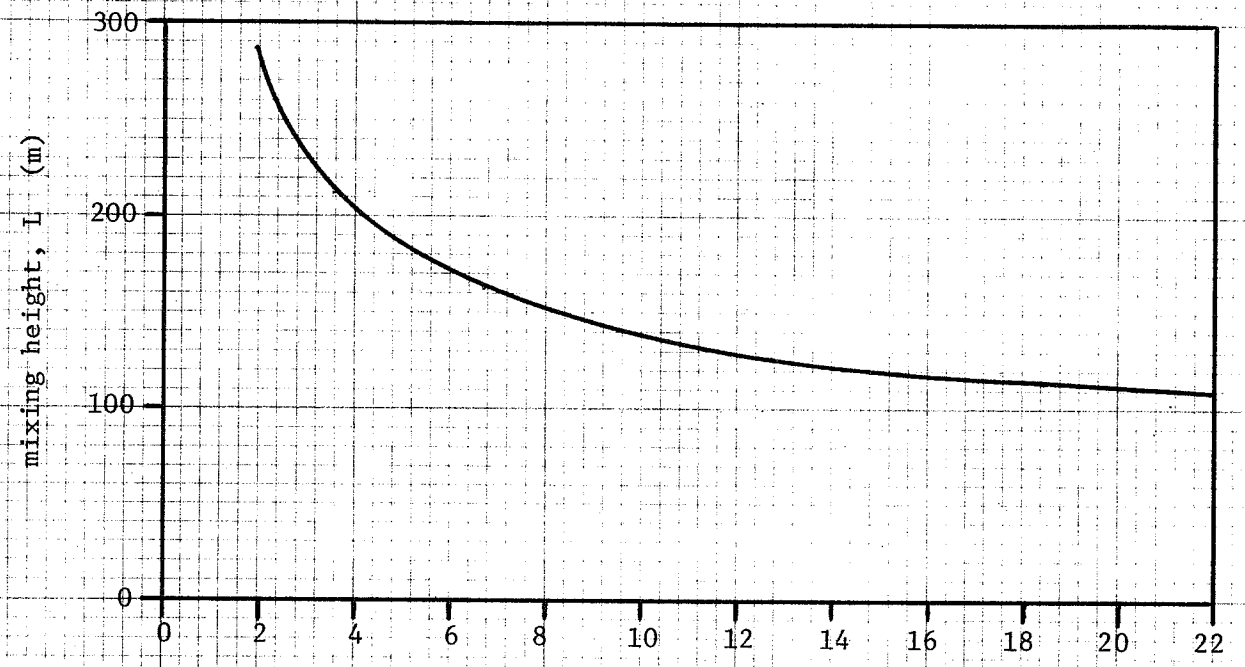

Figure 8.5. Inversion penetration curve - Stack No. 3

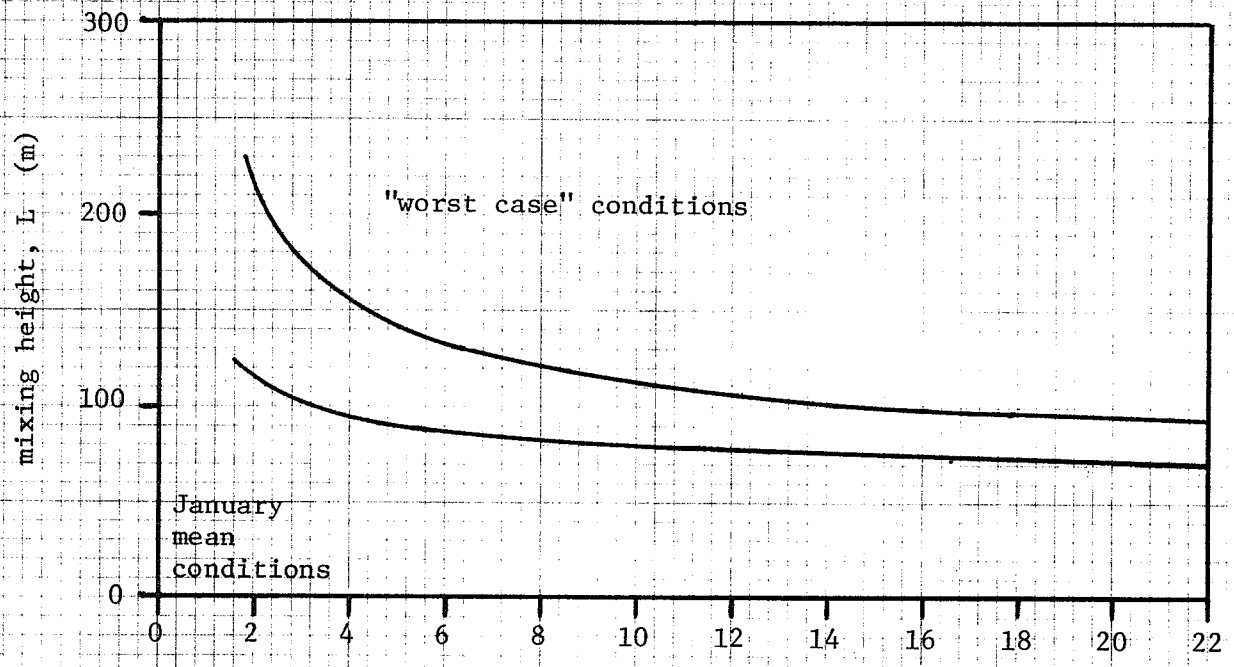

Figure 8.6. Inversion penetration curves - Stacks No. 1S and 2N

8.5.4.5 Inversion Break-Up Fumigation Calculations

Gaussian equation for ground-level concentrations under fumigation conditions (Equation 2.65):

$$\chi_F(x,y,o) = \frac{Q\int_{-\infty}^{p} \frac{1}{\sqrt{2\pi}} \exp(-0.5p^2)dp}{\sqrt{2\pi}\,\sigma_{y_F} u h_i} \exp\left[-\tfrac{1}{2}\left(\frac{y}{\sigma_{y_F}}\right)^2\right]$$

where $p = \frac{h_i - h_e}{\sigma_z}$ (Equation 2.65)

$\sigma_{y_F} = \sigma_y$ (stable) $+ h_e/8$ (Equation 2.68)

Nearest downwind distance to be considered for an estimate of fumigation concentrations must be great enough, based on the time required to eliminate the inversion, that the portion of the plume examined was initially emitted into stable air. This distance is given by:

$$x_F = ut_m$$ (Reference 22)

where u = mean wind speed in the stable layer

t_m = time required to eliminate inversion from $z = h_s$ to $z = h_i$

$$t_m = \frac{h_i^2 - h_s^2}{4K}$$ (Equation 2.70)

where $K = 3m^2/sec$ (Reference 60)

For full load conditions and January mean windspeed, the ground-level SO_2 concentration on the plume-centerline during an inversion break-up fumigation is calculated as follows:

$Q_{1S} = 1.75 \times 10^8$ µg/sec SO_2 (Table 8.19)

$Q_{2N} = 1.75 \times 10^8$ µg/sec SO_2 (Table 8.19)

$Q_3 = 2.38 \times 10^8$ µg/sec SO_2 (Table 8.19)

$h_{e_{1S,2N}} = 194.6$ m $h''_{1S,2N} = 66.5$ m (Table 8.22)

$h_{e_3} = 247.3$ m (Table 8.22)

$u = 4.7$ m/sec (Table 8.20)

let $x = 10$ km

$u_{h_i} \simeq 9$ m/sec

$$h_i = (t_m(4K) + (h'')^2)^{\frac{1}{2}}$$

$$t_m = \frac{x}{u_{h_i}} = \frac{10{,}000 \text{ m}}{9 \text{ m/sec}} = 1111 \text{ sec.}$$

$$h_i = ((1111)(12) + (66.5)^2)^{\frac{1}{2}} = 133 \text{ m.}$$

$$u_{h_i} = 4.7 \left(\frac{133}{10}\right)^{.25} = 8.98 \quad \therefore \text{ windspeed is O.K.}$$

σ_z (E stability, $x = 10$ km) $= 80$ m.

σ_y (E stability, $x = 10$ km) $= 410$

$$\sigma_{y_F} = 410 + \frac{194.6}{8} = 434 \text{ m.}$$

$$p = \frac{133 - 194.6}{80} = -0.77$$

$$\int = .22$$

$$\chi_{F_{1S+2N}} = \frac{1.75 \times 10^8 \ \mu g/sec \times (2 \text{ stacks}) \times .22}{\sqrt{2\pi}\ (434 \text{ m})(9 \text{ m/sec})(133 \text{ m})} = 59 \ \mu g/m^3$$

similarly $\chi_{F_3} = 13 \ \mu g/m^3$

$$\chi_{F_{total}} = \underline{\underline{72 \ \mu g/m^3 \ SO_2}}$$

similarly $\chi_F = \underline{\underline{98 \ \mu g/m^3 \ NO_x}}$

$\chi_F = 197 \ \mu g/m^3$ suspended particulates (1-hour concentration)

8.5.5 Emission Concentrations

Particulates:

January mean emission rate = 31.5 lbs particulates/Ton coal fired

Maximum emission rate = 60.8 lbs particulates/Ton coal fired

Flue gas volume @ $68^{o}F$, 12% CO_2 = $272 \times \frac{(68 + 460)}{(305 + 460)}$ = 188 cuft/lb coal fired

$\therefore$ mean particulate concentration of stack gas for Stack No. 3 =

$$\frac{31.5 \text{ lbs/Ton coal} \times 7000 \text{ grains/lb}}{188 \text{ cuft/lb coal} \times 2000 \text{ lbs/Ton}} = \underline{0.59 \text{ gr/scf}}$$

similarly, maximum particulate concentration of stack gas

for Stack No. 3 = 1.13 gr/scf

SO_2

January mean emission rate = 9.5 lbs SO_2/Ton coal fired

Maximum emission rate =22.2 lbs SO_2/Ton coal fired

mean volume of SO_2 @ $68^{o}F$ (Stack No. 3) =

$$9.5 \times \frac{359}{64.01} \times \frac{68 + 460}{32 + 460} = 57.2 \text{ cuft/Ton coal fired}$$

similarly, maximum volume of SO_2 @ $68^{o}F$ (Stack No. 3) = 133.6 cuft/Ton coal fired

$\therefore$ mean SO_2 emission concentration = $\frac{57.2}{188 \times 2000} \times 100\% = \underline{0.015\% \text{ by volume}}$

similarly, maximum SO_2 emission concentration = 0.036% by volume

9. ACKNOWLEDGEMENTS

The author wishes to thank Manitoba Hydro and the Atmospheric Environment Service of Canada for their kind assistance in the preparation of this report.

10. BIBLIOGRAPHY

1. Stern, A.C., Wohlers, H.C., Boubel, R.W., Lowry, W.P.
FUNDAMENTALS OF AIR POLLUTION
Academic Press, New York (1973)

2. Danielson, J.A. (editor)
AIR POLLUTION ENGINEERING MANUAL - 2nd edition
United States Environmental Protection Agency
Research Triangle Park, N.C. 27711
Publication No. AP-40 (1973)

3. Sawyer, R.F.
CENTRAL POWER PLANTS
- published in COMBUSTION-GENERATED AIR POLLUTION
Starkman, E.S. (editor)
Plenum Press, New York (1971)

4. Air Pollution Control Directorate
Environmental Protection Service
Environment Canada
A NATIONWIDE INVENTORY OF AIR POLLUTANT EMISSIONS - SUMMARY OF EMISSIONS FOR 1970
Technical Appraisal Report EPS 3-AP-73-1
Air Pollution Control Directorate, January 1973

5. Engdahl, R.B.
STATIONARY COMBUSTION SOURCES
- in AIR POLLUTION - VOLUME III
Stern, A.C. (editor)

6. Chapter 130 - Clean Environment Act of Canada

7. United States Environmental Protection Agency
COMPILATION OF AIR POLLUTANT EMISSION FACTORS
April 1973 Publication No. AP-42

8. Friedrich, F.D. and Hayden, A.C.S.
Department of Energy, Mines, and Resources - Canada
A COMBUSTION HANDBOOK FOR CANADIAN FUELS - 1973: VOL.2 - GASEOUS FUELS

9. Friedrich, F.D. - Department of Energy, Mines, and Resources - Canada
A COMBUSTION HANDBOOK FOR CANADIAN FUELS - 1969
VOLUME 1 - FUEL OIL

10. Edinger, J.G.
METEOROLOGY
in COMBUSTION-GENERATED AIR POLLUTION
Starkman, E.S. (editor)
Plenum Press, New York (1971)

11. American Society of Mechanical Engineers
RECOMMENDED GUIDE FOR THE PREDICTION OF THE DISPERSION OF AIRBORNE EFFLUENTS - 2nd edition

12. Department of the Environment - Canada
CLEAN AIR ACT - ANNUAL REPORT 1973-1974

13. Falkenberry, H.L., Slack, A.V., Gartrell, F.E.
CONTROL OF FOSSIL FUEL POWER PLANT STACK GAS EFFLUENTS
Combustion, October 1972, pp. 9-16

14. Rosenberg, H.S., Engdahl, R.B., Oxley, J.H., Genco, J.M.
STATUS OF SULFUR DIOXIDE CONTROL FOR FOSSIL FUEL COMBUSTION
paper presented to the 67th annual meeting of the American Institute of Chemical Engineering, December 1-5, 1974

15. Jonke, A.A.
FLUIDIZED-BED COMBUSTION RELATED TO AIR POLLUTION
National Engineer/Sept. 1972
pp. 6-12

16. Blakeslee, C.E. and Burbach, H.E.
CONTROLLING NOx EMISSIONS FROM STEAM GENERATORS
Journal - Air Pollution Control Association
Vol. 23, No. 1 - January 1973

17. Lee, G.K.
EMISSIONS FROM STATIONARY SOURCES
paper presented at Environment Canada Industrial Gas Cleaning Course - May 1, 1975

18. Bartok, W., Crawford, A.R., Skopp, A.
CONTROL OF NOx EMISSIONS FROM STATIONARY SOURCES
Chemical Engineering Progress
Vol. 67, No. 2

19. Harrison, D.
SOURCES OF AIR POLLUTION IN THE POWER GENERATION INDUSTRY AND THE VARIETY OF TECHNOLOGIES TO CONTAIN THESE POLLUTANTS
paper presented at Environment Canada Industrial Gas Cleaning Course - April 28, 1975

20. Strom, G.H.
ATMOSPHERIC DISPERSION OF STACK EFFLUENTS
- in AIR POLLUTION - VOL. I, pp. 227-274 (1968)
Stern, A.C. (editor)

21. Moses, H., Strom, G.H., and Carson, J.E.
EFFECTS OF METEOROLOGICAL AND ENGINEERING FACTORS ON STACK PLUME RISE
Nuclear Safety, Vol. 6 - No. 1, pp. 1-17 (1964)

22. Turner, D.B.
WORKBOOK OF ATMOSPHERIC DISPERSION ESTIMATES
U.S. Public Health Service
Publication #999-AP-26 (1969)

23. Davidson, W.F.
THE DISPERSION AND SPREADING OF GASES AND DUST FROM CHIMNEYS
Transactions of the Conference on Industrial Wastes - 14th Annual Meeting
Journal - Industrial Hygiene Foundation of America, pp. 38-55 (1949)

24. Bosanquet, C.H., Carey, W.F., and Halton, E.M.
DUST DEPOSITION FROM CHIMNEY STACKS
Proceedings of the Institute of Mechanical Engineers (London)
Vol. 162, pp. 355-367 (1950)

25. Holland, J.Z.
A METEOROLOGICAL SURVEY OF THE OAK RIDGE AREA
U.S. Atomic Energy Commission
Report No. ORO-99
Washington, D.C., pp. 554-559 (1953)

26. Hawkins, J.E., and Nonhebel, G.
CHIMNEYS AND THE DISPERSAL OF SMOKE
Journal - Institute of Fuel
Vol. 28, pp. 530-546 (1955)

27. Rupp, A.F., Beall, S.E., Bornwasser, L.P., and Johnson, D.F.
DILUTION OF STACK GASES IN CROSS WINDS
U.S. Atomic Energy Commission
Report No. AECD-1811
Washington, D.C. (1944)

28. Bosanquet, C.H.
THE RISE OF A HOT WASTE GAS PLUME
Journal - Institute of Fuel, Vol. 30, No. 197, pp. 322-328 (1957)

29. Lucas, D.H., Moore, D.J., and Spurr, G.
THE RISE OF HOT PLUMES FROM CHIMNEYS
International Journal of Air and Water Pollution
Vol. 7, pp. 473-500 (1963)

30. Lucas, D.H.
APPLICATION AND EVALUATION OF RESULTS OF THE TILBURY PLUME RISE AND DISPERSION EXPERIMENT
Atmospheric Environment
Vol. 1, No. 4, pp. 421-424 (July, 1964)

31. Briggs, G.A.
A PLUME RISE MODEL COMPARED WITH OBSERVATIONS
Journal - Air Pollution Control Association
Vol. 15, No. 9, pp. 433-438 (1965)

32. Briggs, G.A.
PLUME RISE
AEC Critical Review Serivs
USAEC Report TID-25075
November, 1969

33. Thomas, F.W., Carpenter, S.B., and Gartrell, F.E.
STACKS - HOW HIGH
Journal - Air Pollution Control Association
Vol. 13, No. pp. 198-204 (1963)

34. Briggs, G.A.
PLUME RISE: A RECENT CRITICAL REVIEW
Nuclear Safety, Vol. 12, No. 1, pp. 15-24
(Jan.-Feb. 1971)

35. Moses, H., and Strom, G.H.
A COMPARISON OF OBSERVED PLUME RISES WITH VALUES OBTAINED FROM WELL-KNOWN FORMULAS
Journal - Air Pollution Control Association
Vol. 11, No. 10, pp. 455-466 (1961)

36. Thomas, F.W., Carpenter, S.B., and Colbaugh, W.C.
PLUME RISE ESTIMATES FOR ELECTRIC GENERATING STATIONS
Journal - Air Pollution Control Association
Vol. 20, No. 3, pp. 170-177 (1970)

37. Sherlock, R.H., and Stalker, E.A.
A STUDY OF FLOW PHENOMENA IN THE WAKE OF SMOKE STACKS
Engineering Research Bulletin 29
University of Michigan, Ann Arbor, Michigan
(1941)

38. Nonhebel, G.
RECOMMENDATIONS ON HEIGHTS FOR NEW INDUSTRIAL CHIMNEYS
Journal - Institute of Fuel
Vol. 33, pp. 479-511 (1960)

39. Scorer, R.S.
THE BEHAVIOUR OF CHIMNEY PLUMES
International Journal of Air Pollution
Vol. 1, pp. 198-220 (1959)

40. Sherlock, R.H., and Lesher, E.J.
DESIGN OF CHIMNEYS TO CONTROL DOWNWASH OF GASES
American Society of Mechanical Engineers
Vol. 77 (Transactions), pp. 1-9 (January, 1955)

41. Strom, G.H.
WIND TUNNEL SCALE MODEL STUDIES OF AIR POLLUTION FROM INDUSTRIAL PLANTS
Industrial Wastes
Sept.-Oct., Nov.-Dec., 1955; Jan.-Feb., 1956
pp. 1-4 pp. 55-59 pp. 104-109

42. Bosanquet, C.H., and Pearson, J.L.
THE SPREAD OF SMOKE AND GASES FROM CHIMNEYS
Transactions of the Faraday Society - Vol. 32 (1936)
pp. 1249-1263

43. Sutton, O.G.
THE THEORETICAL DISTRIBUTION OF AIRBORNE POLLUTION FROM FACTORY CHIMNEYS
Quarterly Journal of the Royal Meteorological Society
Vol. 73 (1947)
pp. 426-436

44. Slade, D.H. (editor)
METEOROLOGY AND ATOMIC ENERGY - 1968
United States Atomic Energy Commission
Publication No. TID-24190 (July, 1968)

45. Hay, J.S., and Pasquill, F.
DIFFUSION FROM A FIXED SOURCE AT A HEIGHT OF A FEW HUNDRED FEET IN THE ATMOSPHERE
Journal of Fluid Mechanics - Vol. 2, pp. 299-310 (1957)

46. Cramer, H.E.
A PRACTICAL METHOD FOR ESTIMATING THE DISPERSAL OF ATMOSPHERIC CONTAMINANTS
Proceedings of the First National Conference on Applied Meteorology - American Meteorological Society, pp. C-33-C-55 (1957)

47. Cramer, H.E.
A BRIEF SURVEY OF THE METEOROLOGICAL ASPECTS OF ATMOSPHERIC POLLUTION
Bulletin of the American Meteorological Society
Vol. 40, No. 4, pp. 165-171 (1959)

48. Cramer, H.E.
ENGINEERING ESTIMATES OF ATMOSPHERIC DISPERSAL CAPACITY
Journal - American Industrial Hygiene Association
Vol. 20, No. 3, pp. 183-189 (1959)

49. Hay, J.S. and Pasquill, F.
DIFFUSION FROM A CONTINUOUS SOURCE IN RELATION TO THE SPECTRUM AND SCALE OF TURBULENCE
- in Advances in Geophysics - Vol. 6*
(Atmospheric Diffusion and Air Pollution)
Frenkiel and Sheppard (editors)
Academic Press, N.Y. (1959)
pp.345-365

50. Pasquill, F.
THE ESTIMATION OF THE DISPERSION OF WINDBORNE MATERIAL
Meteorological Magazine, Vol. 90, No. 1063, pp. 33-49 (1961)

51. Gifford, F.A.
ATMOSPHERIC DISPERSION CALCULATIONS USING THE GENERALIZED GAUSSIAN PLUME MODEL
Nuclear Safety - Vol. 2, No. 2, pp. 56-69 (1960)

52. Gifford, F.A.
USES OF ROUTINE METEOROLOGICAL OBSERVATIONS FOR ESTIMATING ATMOSPHERIC DISPERSION
Nuclear Safety, Vol. 2, No. 4, pp. 47-51 (1961)

53. Carpenter, S.B., Montgomery, T.L., Leavitt, J.M., Colbaugh, W.C., and Thomas, F.W.
PRINCIPAL PLUME DISPERSION MODELS: TVA POWER PLANTS
Journal - Air Pollution Control Association
Vol. 21, No. 8, pp. 491-495 (1971)

54. Montgomery, T.L., Norris, W.B., Thomas, F.W., and Carpenter, S.B.
A SIMPLIFIED TECHNIQUE USED TO EVALUATE ATMOSPHERIC DISPERSION OF EMISSIONS FROM LARGE POWER PLANTS
Journal - Air Pollution Control Association
Vol. 23, No. 5, pp. 388-394 (1973)

55. Hewson, E.W. and Gill, G.C.
METEOROLOGICAL INVESTIGATIONS IN COLUMBIA RIVER VALLEY NEAR TRAIL, B.C.
United States Bureau of Mines Bulletin 453
United States Government Printing Office
Washington, D.C. (1944)

56. Hewson, E.W.
STACK HEIGHTS REQUIRED TO MINIMIZE GROUND CONCENTRATIONS
Transactions of the American Society of Mechanical Engineers
Vol. 77, pp. 1163-1172 (1955)

57. Bierly, E.W. and Hewson, E.W.
SOME RESTRICTIVE METEOROLOGICAL CONDITIONS TO BE CONSIDERED IN THE DESIGN OF STACKS
Journal of Applied Meteorology, Vol. 1, No. 3, pp. 383-390 (1962)

58. Pooler, F.
POTENTIAL DISPERSION OF PLUMES FROM LARGE POWER PLANTS
United States Public Health Service
Publication No. 999-AP-16 (1965)

59. Smith, M.E.

Journal - Air Pollution Control Association
Vol. 6, No. , p.11- (1956)

60. Hewson, E.W.
THE METEOROLOGICAL CONTROL OF ATMOSPHERIC POLLUTION BY HEAVY INDUSTRY
Quarterly Journal - Royal Meteorological Society
Vol. 71, pp. 266-282

61. Stewart, N.G., Gale, H.J., Crooks, R.N.
THE ATMOSPHERIC DIFFUSION OF GASES DISCHARGED FROM THE CHIMNEY OF THE HARWELL REACTOR BEPQ.
International Journal of Air Pollution
Vol. 1, pp. 87-102.

62. Gifford, F.A.
PEAK TO AVERAGE CONCENTRATION RATIOS ACCORDING TO A FLUCTUATING PLUME DISPERSION MODEL
International Journal of Air Pollution
Vol. 3, No. 4, pp. 253-260 (1960)

63. Singer, I.A.
THE RELATION BETWEEN PEAK AND MEAN CONCENTRATIONS
Journal-Air Pollution Control Association
Vol. 11, pp. 336-341 (1961)

64. Singer, I.A., Imai, K., Del Campos, R.G. (1963)
PEAK TO MEAN POLLUTANT CONCENTRATION RATIOS FOR VARIOUS TERRAIN AND VEGETATION COVER
Journal-Air Pollution Control Association
Vol. 13, pp. 40-42

65. Briggs, G.A.
DIFFUSION ESTIMATION FOR SMALL EMISSIONS (DRAFT)
Air Resources Atmospheric Turbulence and Diffusion Laboratory
Oak Ridge, Tennessee
Contribution File No. (Draft) 79

66. Gifford, F.A.
COMPUTATION OF POLLUTION FROM SEVERAL SOURCES
International Journal of Air Pollution
Vol. 2, pp. 109-110

67. Barad, M.L. and Haugen, D.A.
A PRELIMINARY EVALUATION OF SUTTON'S HYPOTHESIS FOR DIFFUSION FROM A CONTINUOUS POINT SOURCE
Journal of Meteorology
Vol. 16, No. 1, pp. 12-20 (1959)

68. Pasquill, F.
ATMOSPHERIC DIFFUSION
D. Van Nostrand Co. Ltd. - London (1962)

69. Hilst, G.R. and Simpson, C.L.
OBSERVATIONS OF VERTICAL DIFFUSION RATES IN STABLE ATMOSPHERES
Journal of Meteorology
Vol. 15, No. 1, pp. 125-126 (1958)

70. Briggs, G.A.
DIFFUSION ESTIMATION FOR SMALL EMISSIONS
ATDL Contribution File No. 79 (Draft)
Air Resources Atmospheric Turbulence and Diffusion Laboratory - National Oceanic and Atmospheric Administration
Oak Ridge, Tennessee
May 1973

71. Statistics Canada
1971 Census

72. Brandon Chamber of Commerce

73. Surveys and Mapping Branch
Department of Energy, Mines and Resources - Canada
BRANDON, MANITOBA
Map No. 62G/13d, Edition 1 MCE, Series A 841 (1964)

74. Munn, R.E., and Tomlain, J., and Titus, R.L.
Canadian Meteorological Service, Toronto
A PRELIMINARY CLIMATOLOGY OF GROUND-BASED INVERSIONS IN CANADA
Atmosphere, Vol. 8, pp. 52-58 (1970)

75. THE ODYSSEY WORLD ATLAS
Golden Press, New York (1967)
pp. 37, 186

76. Atmospheric Environment Service - Department of the Environment - Canada
TEMPERATURE AND PRECIPITATION: 1941-1970, PRAIRIE PROVINCES
pp. 137, 138

77. Atmospheric Environment Service - Department of the Environment - Canada
MEAN MONTHLY WIND SPEED FREQUENCY - BRANDON (1963-1972)
Project No. 15073

78. Atmospheric Environment Service - Environment Canada
METEOROLOGICAL ASPECTS OF POLLUTANT DISPERSION FROM THE 500 FOOT SMELTER STACK AT THOMPSON, MANITOBA
January, 1975

79. Combustion Engineering - Superheater Ltd.
Montreal, Quebec
TYPE VU40S STEAM GENERATOR FOR THE MANITOBA HYDRO ELECTRIC BOARD - BRANDON, MANITOBA

80. Meteorological Branch - Department of Transport - Canada
MONTHLY BULLETIN - CANADIAN UPPER AIR DATA
Shilo, Manitoba; December-February/1967-1971

81. Conley, C.; Hutchison, D.J.; DiBartolo, A.B.
Abatement and Compliance Branch
Air Pollution Control Directorate
Environment Canada
SUGGESTED METHODS FOR THE DETERMINATION OF POLLUTION CONCENTRATIONS RESULTING FROM THE RELEASE OF EMISSIONS FROM SINGLE OR MULTIPLE POINT SOURCES (Draft) (1975)

82. Hanna, S.R.
Air Resources Atmospheric Turbulence and Diffusion Laboratory
National Oceanic and Atmospheric Administration
Oak Ridge, Tennessee
DESCRIPTION OF ATDL COMPUTER MODEL FOR DISPERSION FROM MULTIPLE SOURCES
Industrial Air Pollution Control (Noll, K. and Duncan, J. - editors)
Ann Arbor Science Publishers Inc. (1973)

83. List, R.J.
Smithsonian Meteorological Tables - 6th revised edition
Smithsonian Institute
Washington, D.C. (1951)
pp. 497-505

84. Drummond, G.R.
A BRIEF DESCRIPTION OF EMISSIONS TO ATMOSPHERE AT BRANDON GENERATING STATION
Manitoba Hydro
November 29, 1972

85. Biel, D.
Manitoba Hydro
BRANDON GENERATING STATION DESIGN AND OPERATING DATA RELATING TO AIR POLLUTION ASSESSMENT
September 1974

86. Friedrich, F.D., and Hayden, A.C.S.
Department of Energy, Mines & Resources - Canada
A COMBUSTION HANDBOOK FOR CANADIAN FUELS - 1974
VOLUME 3. COAL. PART 1
p. 320 (Figure 2)

87. Scouten Mitchell Sigurdson and Associates Ltd., and H.H. Angus & Associates Ltd.
AIR POLLUTION MODEL SINGLE SOURCE
Prepared for Environmental Health Laboratory Manitoba Department of Health and Social Development

88. Fraser, H.
Scientific Services Section
Atmoshperic Environment Service - Central Region
Winnipeg, Manitoba
- Private Consultation, June 19, 1975

89. Manitoba Department of Mines, Resources and Environmental Management
Air Pollution Control Division

90. Manitoba Public Health Reculations
Part III, Division 3
Atmospheric Pollution
Paragraphs 17a and 17b